

AD-A174 585

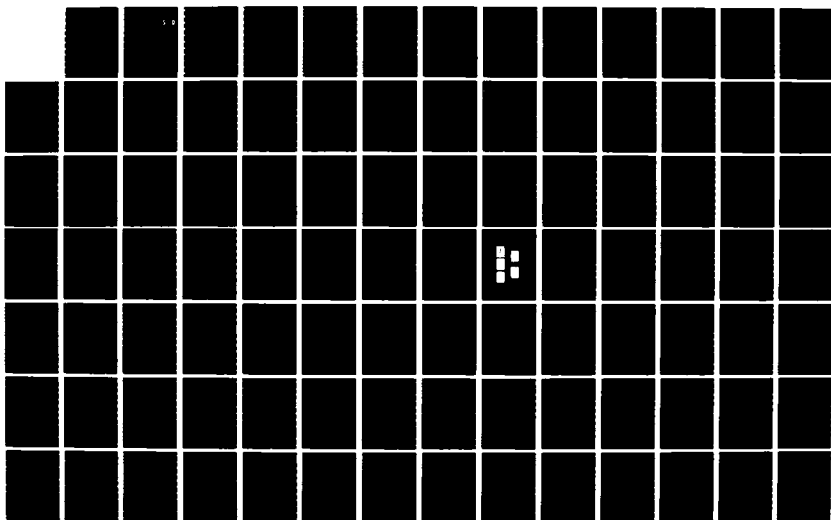
COMPUTATIONAL METHODS FOR NONLINEAR DYNAMICS PROBLEMS  
IN SOLID AND STRUCT (U) COMPUTATIONAL MECHANICS CO INC  
AUSTIN TX J T ODEN 31 MAR 86 TR-86-02 AFOSR-TR-86-2015  
F49620-84-C-0024

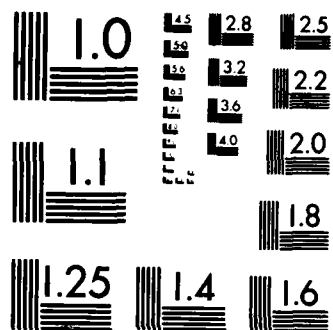
1/4

UNCLASSIFIED

F/G 20/11

NL





MICROCOPY RESOLUTION TEST CHART  
NATIONAL BUREAU OF STANDARDS-1963-A

AD-A174 585

AFOSR-TR. 86-2015

2

## FINAL REPORT

DTIC  
ELECTE  
NOV 26 1986  
S D

COMPUTATIONAL METHODS FOR NONLINEAR  
DYNAMICS PROBLEMS IN SOLID AND  
STRUCTURAL MECHANICS:

Approved for public release;  
distribution unlimited.

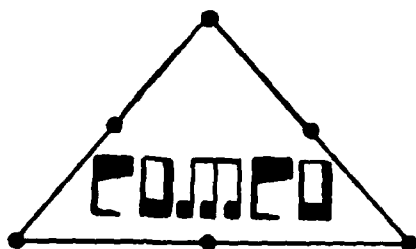
MODELS OF DYNAMIC FRICTIONAL  
PHENOMENA IN METALLIC STRUCTURES

CONTRACT F49620-84-C-0024

AIR FORCE OFFICE OF SCIENTIFIC RESEARCH

AIR FORCE OFFICE OF SCIENTIFIC RESEARCH (AFSC)  
NOTICE OF TRANSMITTAL TO DTIC  
This technical report has been reviewed and is  
approved for public release IAW AFR 190-12.  
Distribution is unlimited.  
MATTHEW J. KEEFER  
Chief, Technical Information Division

DTIC FILE COPY



THE COMPUTATIONAL MECHANICS COMPANY, INC.

COMPUTATIONAL MECHANICS  
COMPANY, INC.  
AUSTIN, TEXAS  
MARCH, 1986

DISTRIBUTION STATE

Approved for public release  
Distribution Unlimited

86 11 25 369

UNCLASSIFIED

SECURITY CLASSIFICATION OF THIS PAGE

## REPORT DOCUMENTATION PAGE

1. REPORT SECURITY CLASSIFICATION unclassified		16. RESTRICTIVE MARKINGS NONE	
2. SECURITY CLASSIFICATION AUTHORITY		3. DISTRIBUTION/AVAILABILITY OF REPORT Approved for public release; distribution unlimited.	
20. DECLASSIFICATION/DOWNGRADING SCHEDULE			
4. PERFORMING ORGANIZATION REPORT NUMBER(S) TR-86-02		5. MONITORING ORGANIZATION REPORT NUMBER(S) AFOSR-TR- 86 - 2015	
6. NAME OF PERFORMING ORGANIZATION Computational Mechanics Company, Inc.	8. OFFICE SYMBOL (If applicable) NA	7. NAME OF MONITORING ORGANIZATION AFOSR	
9. ADDRESS (City, State and ZIP Code) 4804 Avenue B, Austin, TX 78751		7. ADDRESS (City, State and ZIP Code) Bolling AFB DC 20332-6448	
10. NAME OF FUNDING/SPONSORING ORGANIZATION Air Force Office of Scien. Rsch.	8. OFFICE SYMBOL (If applicable) NA	9. PROCUREMENT INSTRUMENT IDENTIFICATION NUMBER F49620-84-C-0024	
10. ADDRESS (City, State and ZIP Code) Bolling Air Force Base D.C., 20332		10. SOURCE OF FUNDING NO. PROGRAM ELEMENT NO. 61102F PROJECT NO. 2302 TASK NO. B1 WORK UNIT NO.	
11. TITLE (Include Security Classification) Computational Methods for Nonlinear Dynamics Problems in Solid & Structural Mechanics			
12. PERSONAL AUTHOR(S) J. Tinsley Oden			
13. TYPE OF REPORT FINAL	13. TIME COVERED FROM 02-01-84 TO 02-01-86	14. DATE OF REPORT (Yr, Mo, Day) March 31, 1986	15. PAGE COUNT 327
16. SUPPLEMENTARY NOTATION NONE			
17. COSATI CODES FIELD GROUP SUB GR		18. SUBJECT TERMS (Continue on reverse if necessary and identify by block number) Dynamic friction, interface models, structural damping	
19. ABSTRACT (Continue on reverse if necessary and identify by block number) In this report the dynamic behavior of metallic bodies subjected to dry frictional contacts is studied. A simple model of interface response which incorporates a constitutive equation for the normal deformability of the interface and the Coulomb law of friction is developed. This interface model is incorporated in the formulation of problems in continuum mechanics that involve the contact of linearly elastic or viscoelastic bodies. Variational formulations for these problems are established and existence and uniqueness results are proved for steady-sliding and dynamic frictionless or frictional contact problems. The same interface model is also incorporated in finite dimensional models for contact problems: a simple rigid body model and finite element space discretizations of the continuum models. Numerical studies of steady sliding and its dynamic stability are presented, as well as numerical studies of friction-induced oscillations. In the latter case, the Newmark method and the central-difference technique are used to integrate numerically the equations of motion. In the numerical studies particular emphasis is given to the role played by normal			
20. DISTRIBUTION/AVAILABILITY OF ABSTRACT UNCLASSIFIED/UNLIMITED <input checked="" type="checkbox"/> SAME AS RPT <input type="checkbox"/> DTIC USERS <input type="checkbox"/>		21. ABSTRACT SECURITY CLASSIFICATION Unclassified	
22. NAME OF RESPONSIBLE INDIVIDUAL Dr. Anthony K. Amos		23. TELEPHONE NUMBER (Include Area Code) (912) 918-4530	
24. FORM 1473, 83 APR		25. OFFICE SYMBOL DERT/68CL52 NA Unclassified	

EDITION OF 1 JAN 73 IS OBSOLETE

SECURITY CLASSIFICATION OF THIS PAGE



19. (continued:)

degrees-of-freedom in frictional sliding. It is found that the inherent nonsymmetry of the coupling between normal and tangential degrees of freedom on the interface may lead to unstable steady sliding equilibria. It is also found that such instabilities and consequent high-frequency normal oscillations may lead to low-frequency stick-slip motions or to apparently smooth sliding motions at apparent values of the coefficient of kinetic friction that are lower than the coefficient of static friction. Numerical studies on the influence of various governing parameters on these behaviors are presented.

19. (continued:)

degrees-of-freedom in frictional sliding. It is found that the inherent nonsymmetry of the coupling between normal and tangential degrees of freedom on the interface may lead to unstable steady sliding equilibria. It is also found that such instabilities and consequent high-frequency normal oscillations may lead to low-frequency stick-slip motions or to apparently smooth sliding motions at apparent values of the coefficient of kinetic friction that are lower than the coefficient of static friction. Numerical studies on the influence of various governing parameters on these behaviors are presented.



Accession For	
NTIS CRA&I	<input checked="checked" type="checkbox"/>
DTIC TAB	<input type="checkbox"/>
Unannounced	<input type="checkbox"/>
Justification	
By	
Distribution /	
Availability Codes	
Dist	Availability or Special
A-1	

(11)

**COMPUTATIONAL METHODS FOR NONLINEAR  
DYNAMICS PROBLEMS IN SOLIC AND  
STRUCTURAL MECHANICS:**

**MODELS OF DYNAMIC FRICTIONAL  
PHENOMENA IN METALLIC STRUCTURES**

**PRINCIPAL INVESTIGATOR: J. TINSLEY ODEN**

**MARCH, 1986**

## FOREWORD

This report summarizes research obtained on Contract F-49620 84-C-0024 on Computational Methods for Nonlinear Dynamics Problems in Solid and Structural Mechanics. The report particularly focuses on Models of Dynamic Frictional Phenomena in Metallic Structures. The original research objectives of this project were:

- 1.) Develop analytical models for contact mechanics problems involving large deformations, rotations, large strains, and thermomechanical interactions, with due consideration of frictional resistance.
- 2.) Conduct preliminary studies of simple quasi-static problems with the characteristics listed above.
- 3.) Investigate dynamic friction mechanisms, their role in heat generation, and the resulting thermomechanical response. Examine role of thermomechanical effects in damage processes such as fatigue and wear.
- 4.) Conduct preliminary modeling studies of lubrication effects in structural dynamics.
- 5.) Conduct parameter studies of new static and dynamic friction models of large amplitude structural dynamics problems.
- 6.) Apply new static and dynamic models to the study of the mechanics of structural damping, metal forming, dynamic contact (impact problems) and elasto-plasticity. Correlate results with available experimental data wherever feasible.

All of these objectives have been accomplished.

The work led to the following technical articles:

1. Oden, J.T. and Martins, J.A.C. [1984], "Models and Computational Methods for Dynamic Friction Phenomena", Comp. Meth. Appl'd Mech. Engrg., vol. 52, pp. 527-634
2. Martins, J.A.C. and Oden, T.L. [1983], "A Numerical Analysis of a Class of Problems in Elastodynamics with Friction", Comp. Meth. Appl'd. Mech. Engrg., vol. 40, pp. 327-360
3. Oden, J.T. and Martins, J.A.C. [1984], "New Inteface Models of Dynamic Friction Effects in Nonlinear Structural Dynamics", Proceedings of AIAA 25th Structures, Structural Dynamics & Materials Conference and AIAA Dynamics Specialists Conference, Palm Springs, California, May, 1984

4. Rabier, P.J., Oden, J.T., Martins, J.A.C. and Campos, L.T. [1986], "Existence and Local Uniqueness of Solutions to Contact Problems in Elasticity with Nonlinear Friction Laws", Int. J. Eng. Sc. [to appear]
5. Martins, J.A.C. and Oden, J.T. [1986], "Existence and Uniqueness Results for Dynamic Contact Problems with Nonlinear Normal and Friction Interface Laws", J. Nonlin. Analysis [to appear]
6. Rabier, P.J. and Oden, J.T. [1986], "Part I. Preliminaries and Formulation of a Variation Inequality, J. Nonlin. Analysis [in review]
7. Rabier, P.J. and Oden, J.T. [1986], "Part II. Existence and Uniqueness Theorem", J. Nonlin. Analysis [in review]
8. Oden, J.T. and Martins, J.A.C. [1985], "New Models and Theories of Dynamic Friction", Developments in Mechanics, Vol. 13, Proceedings of the 19th Midwestern Mechanics Conference, Columbus, Ohio, Ed. Popelar, C.H.
9. Martins, J.A.C. and Oden, J.T. [1985], "Interface Models, Variational Principles and Numerical Solutions for Dynamic Friction Problems, In: Mechanics of Material Interfaces, Ed. Selvadurai, A.P.S. and Voyiadjis, G., Elsevier Science Publishers, Amsterdam, NL

The following personnel worked on the project:

Principal Investigator and Project Manager: Dr. J. Tinsley Oden

Senior Research Engineers: Dr. J.M. Bass, Dr. T.H. Miller

Graduate Research Engineers: Mr. C. Berry, Mr. J.A.C. Martins, Mr. K.T. Hsieh, Mr. P. Devloo

Senior Scientific Consultants: Dr. E.B. Becker, Dr. N. Kikuchi, Dr. P.J. Rabier.

## TABLE OF CONTENTS

CHAPTER		PAGE
1.	INTRODUCTION	
1.1	Motivation . . . . .	1
1.2	Objectives, outline and major contributions . . . . .	5
2.	PHYSICAL ASPECTS OF DYNAMIC FRICTION. A MODEL OF INTERFACE BEHAVIOR	
2.1	The classic laws of friction and the origin of frictional resistance - A brief review . . . . .	12
2.2	Static and kinetic friction. Stick-slip motion . . . . .	17
2.2.1	Introduction. Historical background . . . . .	17
2.2.2	Time dependence or rate dependence of the coefficient of static friction . . . . .	25
2.2.3	The steady-state coefficient of kinetic friction . . . . .	30
2.2.4	The coefficient of kinetic friction during the slip phase of stick-slip motions . . . . .	31
2.2.5	Memory-dependent friction . . . . .	34
2.3	The importance of the normal degree-of-freedom in sliding friction . . . . .	35
2.4	The normal stiffness of metallic surfaces . . . . .	41
2.5	A model of interface response . . . . .	44
3.	CONTINUUM MECHANICS MODELS	
3.1	Preliminary remarks. Orientation . . . . .	53
3.2	Formal statement of the dynamic contact problems . . . . .	57
3.3	Variational formulations for the dynamic contact problems . . . . .	50
3.4	Existence and uniqueness results for dynamic contact problems . . . . .	67

CHAPTER	PAGE
3.5 Formal statement of the steady-sliding problem . . . . .	90
3.6 Variational formulation for the steady-sliding problem	91
3.7 Existence and uniqueness of steady-sliding equilibrium solutions . . . . .	96
3.8 An eigenvalue problem . . . . .	109
4. A RIGID BODY MODEL	
4.1 Governing Equations . . . . .	112
4.2 Steady-sliding equilibrium and linear stability analysis . . . . .	117
4.2.1 Nondimensional form of the equations . . . . .	117
4.2.2 Numerical results . . . . .	119
4.2.3 Discussion . . . . .	130
4.3 Low-frequency stick-slip motion and apparent reduc- tions of kinetic friction . . . . .	133
4.3.1 Nondimensional form of the equations of motion	133
4.3.2 Numerical results and discussion . . . . .	135
4.4 Apparent reductions of static friction due to normal perturbations . . . . .	174
4.4.1 Introduction . . . . .	174
4.4.2 Numerical results . . . . .	175
4.4.3 Discussion . . . . .	181
4.5 Some remarks on the numerical results . . . . .	183
5. FINITE ELEMENT MODELS	
5.1 Finite element approximations . . . . .	191
5.2 A regularization of the Coulomb law of friction . . .	192

CHAPTER	PAGE
5.3. Algorithms for transient analysis .....	196
5.4 Algorithm for steady-sliding and linear stability analysis .....	202
5.5 Numerical results .....	202
6. CONCLUSIONS AND SUGGESTIONS FOR FURTHER RESEARCH	231
REFERENCES	
APPENDIX: SOLUTION TO SIGNORINI-LIKE PROBLEMS THROUGH INTERFACE MODELS	248
A.1 Introduction .....	249
A.2 Technical preliminaries .....	258
A.3 Variational formulation .....	273
A.4 Existence and uniqueness of solutions to the contact problem .....	294
A.5 Concluding remarks.....	310



## LIST OF FIGURES

FIGURE	CAPTION	PAGE
1.1.1	Models of two (equivalent) sliding systems which may have stick-slip oscillations . . . . .	2
1.1.2	Typical traces of stick-slip motion for systems (a) and (b) in Figure 1.1.1 . . . . .	3
2.2.1	Relation between amplitude of the stick-slip motion and driving velocity for various spring stiffnesses (K) . . . . .	22
2.2.2	Variation of stick-slip frequency with driving velocity for various normal loads . . . . .	23
2.2.3	Variation of stick-slip frequency with driving velocity for various lubrication conditions . . . . .	24
2.2.4	Models of the variation of the friction coefficient . . . . .	26
2.2.5	Rate dependence of the static coefficient of friction . . . . .	27
2.2.6	Friction force - sliding velocity characteristics for various driving velocities and natural frequencies of the system . . . . .	33
2.3.1	Simultaneous tangential ( $u_T$ vs. $t$ ) and normal ( $h$ vs. $t$ ) jumps of the slider during stick-slip motion . . . . .	36
2.3.2	Oscillogram of free normal oscillations in stages of tangential jumps of a slider in the course of self-excited friction oscillations . . . . .	38
2.5.1	Initial gap, normal displacement and penetrating approach at the contact surface $\Gamma_C$ . . . . .	45
2.5.2	Hysteresis loops for the normal deformation of the interface (schematic) . . . . .	49
3.2.1	Geometry and notation for the continuum mechanics models of contact and sliding phenomena . . . . .	58
3.7.1	Geometric interpretation of the sufficient conditions on $A$ and $B$ for $T(K) \subset K$ , when $m_T = 1$ . . . . .	104

FIGURE	CAPTION	PAGE
4.1.1	Geometry and degrees of freedom of a rigid block sliding with friction on a moving foundation . . . .	113
4.2.1	Steady-sliding normal displacement ( $u_{y0}$ ) of a rigid block as a function of the friction parameter ( $f \in [0,1]$ ) for $m_n = m_T = 2.5$ and three values of the geometric parameter $h$ ( $h=H/L$ ). . . . .	121
4.2.2	Steady-sliding rotational displacement ( $u_{\theta 0}$ ) of a rigid block as a function of the friction parameter ( $f \in [0,1]$ ) for $m_n = m_T = 2.5$ and three values of the geometric parameter $h$ ( $h=H/L$ ) . . . . .	122
4.2.3	Orthographic projections (a,b,c) and perspective (d) of the root curves of the characteristic equation (4.2.13) for the admissible range of the friction parameter $f \in [0,1/0.45)$ with $m_n = m_T = 2.5$ , $h=0.45$ and $\hat{z}=0.00$ fixed . . . . .	123-125
4.2.4	Orthographic projections of the root curves of the characteristic equation (4.2.13) for the admissible range of the friction parameter $f \in [0,1/0.45)$ with $m_n = m_T = 2.5$ , $h=0.45$ and $\hat{z}=0.02$ fixed . . . . .	126-127
4.2.5	Effect of the normal interface damping on the stability of the steady-sliding equilibrium of a rigid block . . . . .	128
4.2.6	Effect of the value of the powers $m_n = m_T$ on the stability of the steady-sliding equilibrium of a rigid block . . . . .	129
4.3.1	Phase plane plot for the normal motion of the center of mass. Small friction case: $(h,f)=(0.625,0.15)$ . . . . .	138
4.3.2	Phase plane plot for the rotation of the block. Small friction case: $(h,f)=(0.625,0.15)$ . . . . .	139
4.3.3	Phase plane plot of the growing portion of the normal oscillation of the center of mass in the course of low-frequency stick-slip motion . . . . .	141
4.3.4	Phase plane plot of the tangential motion of the points of the block on the contact surface during the "slip" phase of the low-frequency stick-slip motion . . . . .	143

FIGURE	CAPTION	PAGE
4.3.5	Apparently smooth sliding for small $s$ , small $z_x$ , large $u'_x$ . . . . .	144
4.3.6	Low-frequency stick-slip motions for various small driving velocities . . . . .	145
4.3.7	Phase plane plots for the rotation degree-of-freedom	146
4.3.8	Phase plane plots for the tangential motion of the points of the block on the contact surface . . . . .	147
4.3.9	Evolution of the normal contact force ( $\Sigma_{ny}$ ), the friction force ( $\Sigma_{Tx}$ ) and the ratio friction force/absolute value of the normal force, for one cycle of oscillation . . . . .	148
4.3.10	The decrease of the time of stick with the increase of the driving velocity . . . . .	149
4.3.11	Phase plane plot of the decaying portion of the normal oscillation of the center of mass in the course of low-frequency stick-slip motion . . . . .	151
4.3.12	Effect of the normal interface damping on the tangential trace . . . . .	152
4.3.13	Effect of the normal interface damping on the normal oscillations . . . . .	153
4.3.14	Phase plane plot of the steady normal oscillation of the center of mass for $\dot{z}=0.0$ . . . . .	155
4.3.15	Phase plane plot of the steady tangential oscillation of the points of the block on the contact surface for $\dot{z}=0.0$ . . . . .	156
4.3.16	Amplitude of the low-frequency stick-slip motion ( $\Delta u_x$ ) vs. driving velocity ( $u'_x$ ) . . . . .	158
4.3.17	Amplitude of the low frequency stick-slip motion ( $\Delta u_x/s=\Delta u_x/Y$ ) vs. driving velocity ( $u'_x/\sqrt{s} = u'_x/\sqrt{gY}$ ) . . . . .	159
4.3.18	Frequency of the low-frequency stick-slip motion vs. driving velocity . . . . .	162
4.3.19	Tangential displacement traces for large $s$ , small	

FIGURE	CAPTION	PAGE
	$z_x$ and various $u_x^C$ . . . . .	164
4.3.20	Tangential displacement traces for for small $s$ , large $z_x$ and various $u_x^C$ . . . . .	165
4.3.21	Apparent coefficient of kinetic friction vs. average sliding velocity (log scale) . . . . .	166
4.3.22	Apparent coefficient of kinetic friction vs. average sliding velocity (linear scale) . . . . .	167
4.3.23	Phase plane plots for the rotational motion . . . . .	169
4.3.24	Phase plane plots for the tangential motion of the center of mass (G) and the points of the block on the contact surface (C) . . . . .	170
4.3.25	Evolution of the normal contact force ( $\Sigma_{N_y}$ ), the friction force ( $\Sigma_{T_x}$ ) and the ratio friction force/ absolute value of the normal force, for two cycles of oscillation . . . . .	171
4.4.1	Unperturbed and perturbed tangential displacements for a normal perturbation $p_{u_{y_j}} = -0.05$ at $u_{x_i} = 0.575$ . . . . .	177
4.4.2	Unperturbed and perturbed tangential displacements for a normal perturbation $p_{u_{y_j}} = -0.10$ at $u_{x_i} = 0.55$ . . . . .	178
4.4.3	Minimum tangential displacement $u_{x_i}$ along the "stick" loading path at which a normal perturbation $p_{u_{y_j}}$ pro- duces "premature" sliding, when the driving velocity is $u_{x_k}^C$ . . . . .	180
4.5.1	Effect of the regularization parameter on the com- puted stick-slip motion . . . . .	185
4.5.2	Effect of the maximum time step size ( $\Delta\tau_{\max}$ ) on the computed stick-slip motion . . . . .	186
4.5.3	"Irregular" tangential displacement traces obtained numerically with three different time step sizes . . . . .	189
5.2.1	Graphs of $ \cdot $ , $\text{sgn}(\cdot)$ and of their regularized approximations $\mathcal{P}_\epsilon(\cdot)$ and $\mathcal{P}'_\epsilon(\cdot)$ . . . . .	195
5.5.1	Dimensions and finite element discretization of a	

FIGURE	CAPTION	PAGE
	deformable slab . . . . .	203
5.5.2	Distribution of normal stresses on $\Gamma_C$ at several time instants due to periodic loading on $\Gamma_F$ . . . . .	206
5.5.3	Distribution of tangential stresses on $\Gamma_C$ at several time instants due to periodic loading on $\Gamma_F$ . . . . .	207
5.5.4	Tangential displacements at Node 55 using different values of $\epsilon$ . . . . .	209
5.5.5	Tangential velocities at Node 55, using different values of $\epsilon$ . . . . .	210
5.5.6	Friction stress at Node 55, using different values of $\epsilon$ . . . . .	211
5.5.7	Undeformed (x) and deformed mesh configurations of a compressed slab in steady sliding equilibrium for $\mu=0(*)$ , $\mu=0.5(\square)$ , and $\mu=1.0(\triangle)$ . . . . .	213
5.5.8	Distribution of normal stresses on $\Gamma_C$ for the steady sliding equilibrium of a compressed slab at various values of $\mu$ . . . . .	214
5.5.9	Effect of increasing the compression on the eigenvalues with positive real part of a compressed slab . . . . .	215
5.5.10	Deformed configurations of a linearly elastic block for the steady sliding equilibrium configurations at several values of $\mu$ . . . . .	217
5.5.11	Eigenvalues with positive real parts for a finite element discretization of a block in steady sliding on a moving belt . . . . .	219
5.5.12	Comparison of the eigenvalues associated with 'normal and rotational modes' obtained with the rigid body and the finite element models (first quadrant of the complex plane) . . . . .	220
5.5.13	Evolution of the spring elongation for different velocities $U_x^C$ . . . . .	222
5.5.14	Phase plane plots of the normal oscillation of the contact node 29 during the "sliding" portion of the low-frequency stick-slip motion. . . . .	223

FIGURE	CAPTION	PAGE
5.5.15	Evolution of the normal stresses on the contact Node 29 ( $U_x^C = 0.01 \text{ cm s}^{-1}$ ) . . . . .	225
5.5.16	Evolution of the friction stresses on the contact Node 29 ( $U_x^C = 0.01 \text{ cm s}^{-1}$ ) . . . . .	225
5.5.17	Evolution of the normal contact stress at Node 29 during the contact portion of a cycle of normal oscillation ( $U_x^C = 0.08 \text{ cm s}^{-1}$ ) . . . . .	226
5.5.18	Evolution of the friction stress at Node 29 during the contact portion of a cycle of normal oscillation ( $U_x^C = 0.08 \text{ cm s}^{-1}$ ) . . . . .	227
5.5.19	Evolution of the ratio friction/normal stresses at Node 29 during the contact portion of a cycle of normal oscillation ( $U_x^C = 0.08 \text{ cm s}^{-1}$ ) . . . . .	228
5.5.20	Phase plane plot of the normal oscillation of Node 29 for $U_x^C = 0.80 \text{ cm s}^{-1}$ . . . . .	230

## CHAPTER 1

### INTRODUCTION

#### 1.1 Motivation

*Relative sliding motion between dry or poorly lubricated bodies is frequently accompanied by noisy and troublesome vibrations.* If the sound generated by the friction-induced oscillations of violin strings may be the delight of all music lovers, the sound of a long piece of chalk sliding on a board, the ringing of a wine glass when a moistened finger is run around its rim, the squeak of the ill-lubricated hinges of a slowly opening door or the squealing of vehicle brakes give a better idea of how undesirable the noise generated by frictional oscillations may be. In industrial environments, friction-induced oscillations may be a serious problem. The precise positioning of tables of machine tools is fundamental for the accuracy of the work performed with them. However, it may be severely prejudiced by the intermittency of its sliding motion, particularly at the low speeds employed during final positioning adjustments. Such stick-slip motions (a designation coined by Bowden and Leben [1939]) have a saw-tooth wave form consisting of successive periods of repose and sudden sliding (see Figs. 1.1.1 and 1.1.2) and are the typical friction-induced oscillations observed at small sliding speeds. In other applications, violent friction-induced oscillations may lead to surface damage and failure of machine components.

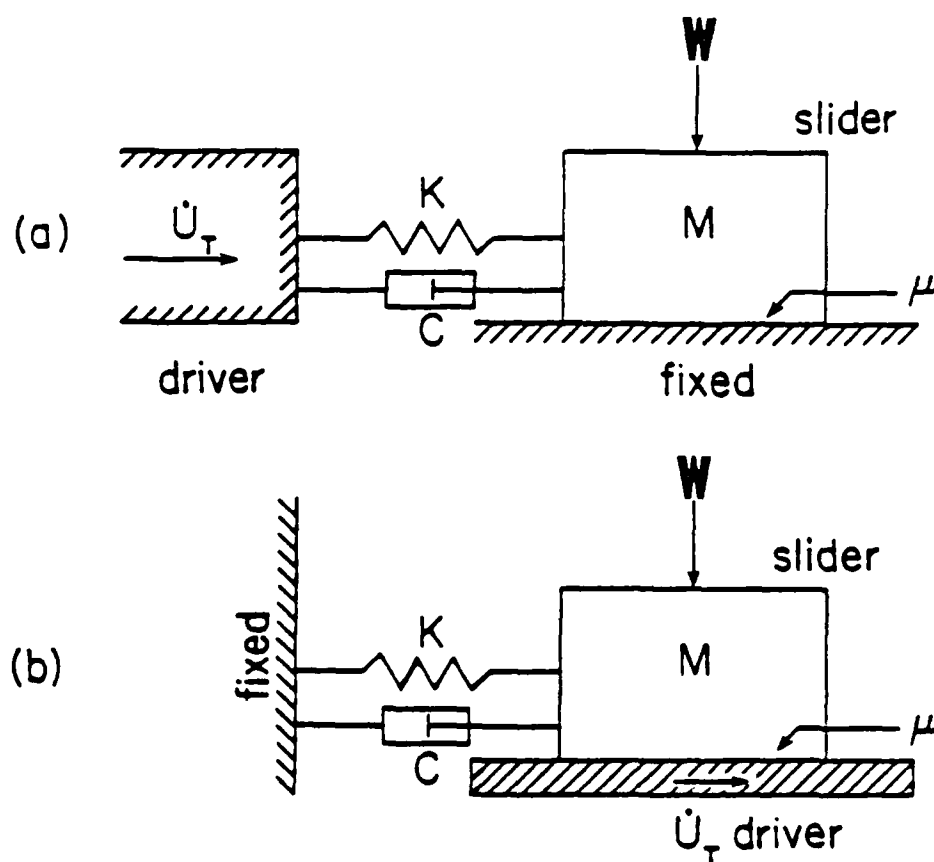


Figure 1.1.1. Models of two (equivalent) sliding systems which may have stick-slip oscillations.  
 $K$  = linear stiffness;  $C$  = linear damping;  $M$  = mass of the slider;  $W$  = normal load;  $\dot{U}_T$  = driving velocity;  $\mu$  = friction coefficient.



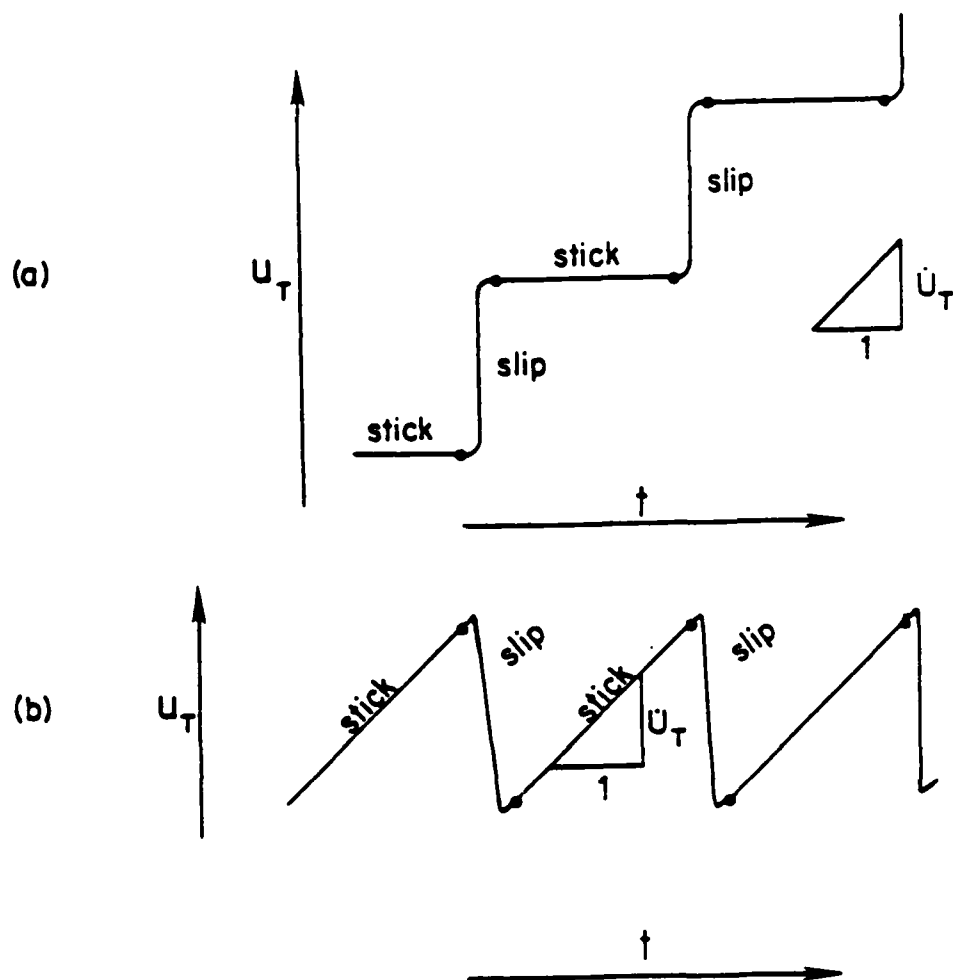


Figure 1.1.2. Typical traces of stick-slip motion for systems (a) and (b) in Figure 1.1.1.

$u_T$  = displacement of the slider;  $t$  = time;

$\dot{u}_T$  = driving velocity.

Most experimental studies on friction and wear have been concerned with finding qualitative and/or quantitative relationships between friction and wear data and various governing parameters and conditions, namely: the properties of bulk and surface layer materials, the roughness of the surfaces in contact, the stress levels, the sliding speed, the temperature, the environment, the properties of the lubricants and the lubrication conditions. The correlations found in those experimental works are usually assumed to be intrinsic characteristics of the interfaces tested for the ranges of parameters and conditions considered and, frequently, they are used in the design of operating machinery. Difficulties on the reproducibility of friction data with different experimental apparati under otherwise similar conditions, and dependence of the results of wear tests on the dynamic properties of the equipment have been occasionally mentioned in the literature (Barwell [1959], Soda et al [1975], Kato et al [1982], Madakson [1983]). However, these effects have received comparatively little attention. Recent experimental results by Rice et al [1982] and Aronov et al [1983, 1984] show, in a striking manner, the effect that the change of stiffness properties of an experimental apparatus may have on the wear results. It should be noted that, for some experimental apparati and with appropriate vibration measurement instrumentation, the correlation between stiffness changes, friction-induced oscillations and wear results may be clear (Aronov et al [1984]); in other circumstances, particularly when the oscillations do not produce an audible noise

(Rice *et al.* [1982]), it may be rather difficult even to suspect of those effects. Equally striking are the observations reported by Tolstoi [1967] on the effect of external normal damping on the measurable values of the coefficients of static and kinetic friction: sufficiently strong normal damping of the free normal microvibrations of a slider can increase significantly the static friction, eliminate apparent decreases of kinetic friction with the increase in sliding velocity, i.e., it can eliminate all the frequently observed or assumed distinctions between static and kinetic friction. It is thus clear that *no correct interpretation of experimental friction and wear data is possible, no reliable prediction of friction and wear in operating machinery can be done, without a good knowledge on the dynamic properties of the equipment involved and a good understanding of the oscillations that are likely to accompany most sliding motions.*

## 1.2 Objectives, outline and major contributions

*The objective of the research summarized in this report is the development of models and computational methods for the study of dynamic friction phenomena involving the dry contact of metallic bodies. Special emphasis is given here to the following topics:*

- (1) The study of phenomenological interface constitutive laws capable of modelling realistic normal and tangential contact conditions.

(ii) The formulation of dynamic contact problems incorporating appropriate interface laws.

(iii) The numerical study of friction-induced oscillations at small sliding speeds, in particular the occurrence of stick-slip oscillations.

It is well known that no engineering surfaces are perfectly flat, no matter how precise the machining process used to produce an apparently flat finish. Under magnification one observes that all polished surfaces have undulations that form hills and valleys, the dimensions of which are large in comparison with molecular dimensions. Furthermore, the surface layers (contaminants, adsorbed materials, oxides, work-hardened layers) which cover most exposed metallic surfaces and which meet in actual contact processes, do not have the same mechanical properties as the underlying bulk materials. *It is therefore natural in developing continuum mechanics models for contact problems, to assign to the interface a separate structure characterized by phenomenological laws independent of the constitutive equations that characterize the parent bulk materials.*

Toward assessing what features these interface models should exhibit, a review and critique of a substantial body of experimental literature on this subject has been done and is presented elsewhere (Oden and Martins [1985]). In Chapter 2 of this report the major conclusions of that study are summarized as a basis for the interface model introduced in the final section of the same chapter. *That interface model incorporates a constitutive law for the normal*

*deformability of the interface and Coulomb's law of friction. Contrary to classical assumptions used in the study of friction-induced oscillations, no distinction between coefficients of static and kinetic friction and no dependence of the latter on the sliding speed is considered in this work.*

The use of separate constitutive assumptions for the interface behavior has not been frequent in continuum mechanics formulations involving the dry contact between solid bodies (for a recent interesting exception and related topics see Felder [1985] and the references therein). Usually, unilateral contact conditions are adopted which simply assert that, when two deformable bodies are pressed together, no mutual penetration of the bodies occurs. In other words, the compressed interface is assumed to have no normal compliance.

This approach has led to serious mathematical difficulties, particularly in the formulation of dynamic contact problems. To date, no general theory of existence is available for these problems even in the frictionless case. Many of the unresolved mathematical difficulties can be traced to the requirement of an unilateral (non-compliant) contact constraint. In fact, these unilateral dynamic contact problems are a particular case of general classes of evolution problems governed by second-order (in time) partial differential equations and subjected to unilateral constraints on the unknown displacement field itself as opposed to constraints on the time derivative of the displacement. Regularization (penalization) techniques and monotonicity arguments, used successfully in the

case of constraints on the time derivative of the unknown function, do not, in general, yield the desired results when the constraint is on the function itself because, in this case, the corresponding multi-valued operator is not monotone. Perhaps not surprisingly, *it will be shown, in the initial sections of Chapter 3, that, by taking into account the normal compliance of the interface, the essential difficulty in the formulation of physically realistic and mathematically well posed dynamic contact problems is removed.*

Throughout most of this work, one question will be central: what conditions may determine the occurrence of a smooth steady-sliding or an intermittent stick-slip motion? By steady-sliding it is meant, (recall Fig. 1.1.1(b)) the preservation of the static equilibrium position of the body (slider) in frictional contact with the moving foundation. When stick-slip oscillations occur, the body does not stay in such an equilibrium position, although, at the conclusion of the stick portion of each cycle, one would expect it to be in a state very close to equilibrium. It is therefore natural to ask if such steady-sliding equilibrium positions exist, if they are unique and if they are dynamically stable. In an attempt to answer these questions, the elastostatics problem corresponding to the steady-sliding configuration and an appropriate eigenvalue problem are formulated in the final sections of Chapter 3. *There it is proved that, for sufficiently small coefficients of friction or applied forces, the steady-sliding problem has locally unique solutions.*

The continuum mechanics problems formulated in Chapter 3 are not easy to solve. The use of numerical techniques to obtain approximate solutions will certainly be the only alternative available to study the complex situations of interest. However, the number of degrees-of-freedom required to produce acceptable finite-dimensional models and the associated computational effort appear to be excessive for the preliminary, essentially qualitative studies that are needed to evaluate the interface laws adopted in Chapter 2. A simple mechanical system, not unlike many seen in friction experiments, that has sufficient degrees-of-freedom to capture qualitatively the dynamic friction behavior observed experimentally at low speeds, is a simple rigid body in plane motion. In Chapter 4, the same interface laws adopted in the continuum case are also assumed to hold on the contact interface of the rigid body. The influence of various physical and geometric parameters on the dynamic behavior of the rigid body is studied in the same chapter. There it is shown that, for sufficiently large coefficients of friction and appropriate values of the other parameters involved, steady-sliding is dynamically unstable. The dynamic instability of steady-sliding equilibrium is a consequence of the inherent non-symmetry of the friction contributions to the governing equations and it may occur even when the coefficient of kinetic friction is assumed to be equal to the coefficient of static friction. In the same chapter it is also numerically shown that, for sufficiently small driving velocity, tangential stiffness and damping (recall Fig. 1.1.1) the instability of the steady sliding may lead to

low-frequency stick-slip oscillations; for sufficiently large driving velocity, or for sufficiently large tangential stiffness or damping, "apparently smooth" sliding motions at average apparent values of the coefficient of kinetic friction smaller than the static one can be observed; and, again, all this may happen when the true coefficient of kinetic friction is equal to the coefficient of static friction.

In Chapter 5, numerical techniques for the study of dynamic friction phenomena are presented. Standard finite element methods are used to obtain finite-dimensional approximations to the continuum mechanics problems formulated in Chapter 3. The multivalued Coulomb friction law is approximated by using a regularization technique. It is an immediate consequence of the theorems proved in Chapter 3 that the semi-discrete finite-element approximations of the regularized dynamic friction problems converge, in appropriately weak topologies, to the solution of the continuum non-regularized dynamic friction problem, when the regularization parameter tends to zero and the dimension of the finite-element space tends to infinity. Full discretization of the governing equations is achieved by employing techniques commonly used in structural dynamics computations: the Newmark method and the central-difference technique. The same time-discretization techniques are also used in the computations of Chapter 4 with the rigid-body models. In the final sections of Chapter 5, various numerical examples demonstrate the feasibility of the techniques proposed and show that instability of steady



*sliding and stick-slip motions may also occur and be numerically studied in the case of deformable bodies.*

In Chapter 6, a summary and the major conclusions of this work are presented. Suggestions for further research are also advanced. It has also been noted that the mathematical theory of contact and friction with Coulomb's law of friction is incomplete and unsatisfactory. The details of a mathematical theory of dynamic friction have now been established, and these are discussed in Chapter 4. There remains the study of open questions of existence and uniqueness of solutions of the Signorini problem for elastostatics with friction and the associated mathematical details needed to make such a theory complete and self consistent. Some particular results that are not readily reduced from the dynamics theory of Chapter 3 are developed in an Appendix to this report. In particular, the Signorini problem of contact of an elastic body with friction is resolved by special methods in this Appendix.

Major contributions to this study are the following:

- (i) A model of interface response for the study of dynamic friction problems involving the dry contact of metallic bodies;
- (ii) Formulation of dynamic contact problems and proof of existence and uniqueness of solutions to these problems;
- (iii) Formulation of a steady sliding equilibrium problem and proof of existence and local uniqueness of the solution to this problem;
- (iv) Numerical techniques and algorithms for the study of dynamic friction problems;
- (v) Numerical results and parametric studies on the stability of steady-sliding, on the occurrence of stick-slip oscillations and on apparent reductions of the coefficient of kinetic friction.

## CHAPTER 2

### PHYSICAL ASPECTS OF DYNAMIC FRICTION

#### A MODEL OF INTERFACE BEHAVIOR

#### 2.1 The classic laws of friction and the origin of frictional resistance - A brief review

When two metallic bodies in contact are subjected to applied forces which tend to produce relative sliding motion, friction stresses develop on the interface that tend to oppose that motion.

In the following only the resultants of the stresses on the contact surface will be considered:  $\sum_n$ , the normal force and  $\sum_T$ , the friction force. The metallic bodies are considered essentially as rigid bodies with a well-defined tangential relative velocity  $v_T$ . For consistency with usual continuum mechanics conventions employed later, a negative normal force  $\sum_n$  is associated with the compression of the interface.

According to Moore [1975], the classic laws of friction, as they evolved from early studies in the past centuries, are the following:

(i) The friction force (at the onset of sliding and during sliding) is proportional to the normal contact force,

$$|\sum_T| = \mu |\sum_n| . \quad (2.1.1)$$

The coefficient of proportionality,  $\mu$ , is known as the coefficient of friction. Often two values of  $\mu$  are quoted: the coefficient of static friction,  $\mu_s$ , which applies to the

onset of sliding and the coefficient of kinetic friction,  $\mu_k$ , which prevails during sliding motion.

(ii) The coefficient of friction is independent of the apparent area of contact.

(iii) The static coefficient is greater than the kinetic coefficient.

(iv) The coefficient of kinetic friction is independent of the sliding velocity.

Another important characteristic of the friction force is the following (Rabinowicz [1965]):

(v) When tangential motion occurs, the friction force acts in the same direction of the relative velocity but in opposite sense,

$$\sum \vec{T} = -\mu |\sum \vec{n}| \frac{\vec{v}_T}{|\vec{v}_T|} . \quad (2.1.2)$$

The first two laws, usually known as the Amontons laws of friction, are generally observed to hold for gross motions of effectively rigid bodies. However, we notice that deviations from the first law have been reported at various circumstances: an increase of the coefficient of friction for light loads (Bowden and Tabor [1964]), or an increase of friction for loads greater than a fairly well defined value which corresponds to the breaking of the oxide films on the surface (Bowden and Tabor [1964]) or yet a decrease of the friction coefficient for very high loads when the true area of contact approaches the magnitude of the apparent area of contact and bulk plastic deformation of the bodies in

contact occurs (Bay and Wanheim [1976]).

The third and fourth laws deserve a more detailed discussion since they are intimately associated with the occurrence of stick-slip and other friction-induced oscillations. That discussion is postponed to Sections 2.2 and 2.3.

According to Rabinowicz [1965], the fifth property above has been essentially confirmed by experiment: for surfaces without pronounced directional properties, the instantaneous friction force may fluctuate by a degree or so from its assigned direction, changing direction continuously and in random fashion as sliding proceeds.

Detailed historical accounts and thorough discussions of the theories proposed by early researchers to explain the origins of frictional resistance can be found in the books of Bowden and Tabor [1964], Dowson [1979] and Kragelskii [1965, 1982].

The adhesion-plowing theory of Bowden and Tabor (reviewed in Bowden and Tabor [1950, 1964] and Tabor [1972, 1975, 1981]) has been the most widely accepted in recent decades among the researchers of solid contact phenomena.

In that theory, the interfacial friction between metallic bodies is attributed essentially to two causes: *the formation and shearing of metallic junctions between the surface asperities and the plastic deformation of the softer surface by hard asperities.* As a consequence, the friction coefficient can be given as the sum of two components resulting from each of the above effects,

$$\mu = \mu_a + \mu_p, \quad (2.1.3)$$

where  $\mu_a$  results from the adhesion (welding) and  $\mu_p$  results from the plastic deformation (plowing).

According to Bowden and Tabor [1964], when two clean metal bodies are put in contact, plastic flow at the tips of the asperities and local welding between opposing asperities occur. The true area of contact ( $A_r$ ) is then proportional to the normal load,

$$A_r = |\sum n|/H. \quad (2.1.4)$$

Here  $H$  is the hardness of the softer of the contacting materials. Under plausible assumptions on the relative strength of the interface and the undeformed material in the hinterland, it is shown that the adhesion component of the coefficient of friction is given by

$$\mu_a = \tau/H, \quad (2.1.5)$$

where  $\tau$  denotes the shear strength of the softer of the contacting materials.

The Amontons laws of friction are then verified: the friction force is proportional to the normal load and independent of the apparent area of contact.

For most materials,  $\tau$  is of the order of  $0.2H$  so that, for this simplified model,  $\mu_a \approx 0.2$ . However, for clean metals enormous values of  $\mu$  may be obtained and even for metals in air  $\mu$  may be of the order unity. According to the same authors, this discrepancy can be overcome if the plastic *junction growth* (the increase of true area of contact) due to combined normal and tangen-

tial loading of the asperities is considered. In the amended theory the junction growth is restricted by the presence of weak contaminant layers on the interface so that in the end: for *perfectly clean* surfaces of very ductile materials infinitely large values of  $\mu_a$  are predicted; a very small amount of weakening of the interface reduces  $\mu_a$  to reasonable values of the order unity; and for *very weak* (contaminated) surfaces, such as when a good lubricant or a thin layer of a softer material is present,  $\mu_a$  is given again by an expression of the form (2.1.5) with  $\tau$  denoting now the shear strength of the weak contaminant.

We wish to point out that this theory not only gives an explanation for the Amontons laws of friction, but also allows for interpretations of the other classic laws. Following arguments of Rabinowicz [1951, 1965] the static friction is often greater than the kinetic because the strength of the junctions would increase with the time of stationary contact (we will discuss this point in Section 2.2.2); the weak dependence of the friction force on the sliding velocity would be a consequence of the small rate dependence of the strengths of most solids; the opposite directions of friction and sliding velocity would be a consequence of the isotropy of the plastically deforming material on the contact.

We also point out that all the theory is based on the proportionality  $A_r \propto \tau_n$  (c.f. (2.1.4)). Archard [1957] and Greenwood and Williamson [1966], among others, have shown that the assumption of plastic deformation of the asperities is not essential to obtain

this proportionality. Consequently, the Amontons laws can also be explained in a similar manner when the deformation of the asperities is elastic. On the other hand, deviations from the proportionality  $A_r \propto |\Sigma_n|$  lead to deviations from the Amontons laws.

The plowing component ( $\mu_p$ ) of the friction can be estimated using, for example, the simplified model of a hard conical asperity grooving on a softer surface. It can be shown that, for the usually small slopes of the asperities, the plowing component of friction is negligible unless the adhesion is small.

Despite the wide acceptance of the adhesion-plowing theory and its effectiveness in explaining the basic laws of friction, several serious criticisms (e.g. Bikerman [1976]) have been offered and some alternative theories have been proposed, especially in recent years. These alternative theories have been developed by authors who are especially concerned with the *evolution of the friction force during prolonged sliding* and with the *interaction between friction and the wear damage of the surfaces*. The mechanisms advanced by these new theories to explain the origin of friction involve the interlocking effects of the roughness, adhesion effects, and plastic deformation effects - plowing by hard asperities and entrapped wear particles and deformation of the asperities and of the subsurface layers (see e.g. Rigney and Hirth [1979], Heilmann and Rigney [1981], Kuhlmann-Wilsdorf [1981], Suh and Sin [1981]).

## 2.2 Static and kinetic friction. Stick-slip motion.

### 2.2.1 Introduction. Historical Background.

The distinction between the coefficients of static and kinetic friction has been mentioned in the literature for centuries, at least since the work of Euler [1750]. That distinction was also a major topic of Coulomb's [1785] detailed experimental study. Coulomb's work is, in addition, the first major reference dealing with the increase of the coefficient of static friction with increasing times of repose (stationary contact before the initiation of sliding). Indeed, for certain combinations of materials and surface conditions, Coulomb observed distinctions between static and kinetic friction, dependence of the kinetic friction on the sliding velocity and dependence of the static friction on the time of repose. However, for dry metal-to-metal interfaces all those distinctions or variations were absent or negligible.

Shortly after Coulomb's work, Vince [1785] also observed that, for a variety of hard materials, the coefficient of kinetic friction was independent of sliding speeds. Through the nineteenth century, various authors confirmed the observations of Coulomb for dry metallic interfaces with regard to both the coefficients of static and kinetic friction: Rennie [1829], Morin [1832-35], Hirn [1854], Jenkin and Ewing [1877].

Other authors, however, had different views: Kimball [1877a,b] and Conti [1875] proposed, on the basis of their experiments with various dry or lubricated surfaces that, in general, the coefficient of kinetic friction would be small and increasing with sliding velocity at low velocities, then at some velocity (dependent on



the materials and the normal pressure) it would achieve a maximum after which it would decrease with the increase of speed. But also, from Conti's experiments, it was clear that such variations were smaller for the case of dry interfaces.

As noted by Kragelskii [1965], the early experiments on kinetic friction were done at relatively small sliding speeds: Coulomb did not exceed 2.5 m/s; Rennie, 2.56 m/s, Morin, 4 m/s and Jenkin and Ewing 0.003 m/s. The application of dry friction in the brakes of railway carriages prompted the study of frictional sliding at higher velocities. For sliding speeds in the range 1 - 25 m/s, approximately, Poirée [1852], Bochet [1861] and Galton [1878] observed decreases of the coefficient of friction with the increase of sliding velocity, consistent with the results of Kimball and Conti. For sufficiently high sliding speeds it is thus clear that decreases of kinetic friction with increasing speeds may indeed occur in the dry sliding of metallic bodies. Kragelskii [1965, 1982] provides various practical formulae for this situation and explains it as being the result of material softening due to the high temperatures generated on the contact neighborhood.

However, for the small velocity range that we are mostly interested in, the situation is not so clear. Conflicting results obtained with various lubrication conditions and the absence of a clear understanding on the distinction between dry and lubricated sliding added much to the confusion established during the second

half of the past century on the velocity dependence of the coefficient of friction. Unfortunately, the fundamental advances on the theory and applications of lubrication by the turn of the century (1880's to 1910's - see Dowson [1979]) apparently were not accompanied by corresponding advances on the knowledge of dry friction at small velocities.

Well into the twentieth century Bowden and Leben [1939] and Bowden and Tabor [1939], while studying the nature of kinetic friction between dry metallic surfaces, observed that the friction force was not constant during sliding: typical saw-tooth stick-slip oscillations occurred when the metals in contact were not similar; large very irregular but more slow fluctuations occurred when the surfaces in contact were of the same metal.

The need to eliminate or attenuate stick-slip motions in various practical applications has originated the publication of a large number of studies on the subject during the past fifty years. These studies have provided most of the recent information on dry sliding friction at small speeds. The papers by Bell and Burdekin [1969-70], Antoniou, Cameron and Gentle [1976], Richardson and Nolle [1976] and Oden and Martins [1985] provide surveys of related aspects of the friction literature and additional references.

Soon it was realized that the stick-slip motion was a relaxation oscillation which was influenced not only by the nature of the surfaces in contact but also, in a fundamental manner, by the dynamic properties (stiffness, inertia, damping ...) of the

experimental apparatus.

In experiments carried out, using either especially designed apparatus or slightly modified machine tool tables and slideways, it has been observed that the amplitude of the stick-slip motion decreases when:

- (a) the driving velocity  $\dot{U}_T$  increases (see Fig. 2.2.1)
- (b) the damping coefficient  $C$  increases (Brockley et al [1967])
- (c) the spring stiffness  $K$  increases (see Fig. 2.2.1)
- (d) the mass  $M$  of the slider decreases (Kato and Matsubayashi [1970]).

It has also been observed that the frequency of the stick-slip motion increases with the increase of the driving velocity and that the maximum value of this frequency approaches the undamped natural frequency of the system (Figs. 2.2.2 and 2.2.3) although in some cases the oscillation stops at a level well below that natural frequency.

Kaidanovskii and Khaikin [1933] and Blok [1940] pointed out that such oscillations might occur if the friction force decreased when the sliding velocity increases, a condition that may lead to an overall negative damping in the sliding system. The decrease of the coefficient of friction with the increase of sliding velocity according to some continuous or discontinuous law, has been thus one of the most common assumptions in the studies of stick-slip motion. The other major assumption used in the literature is the

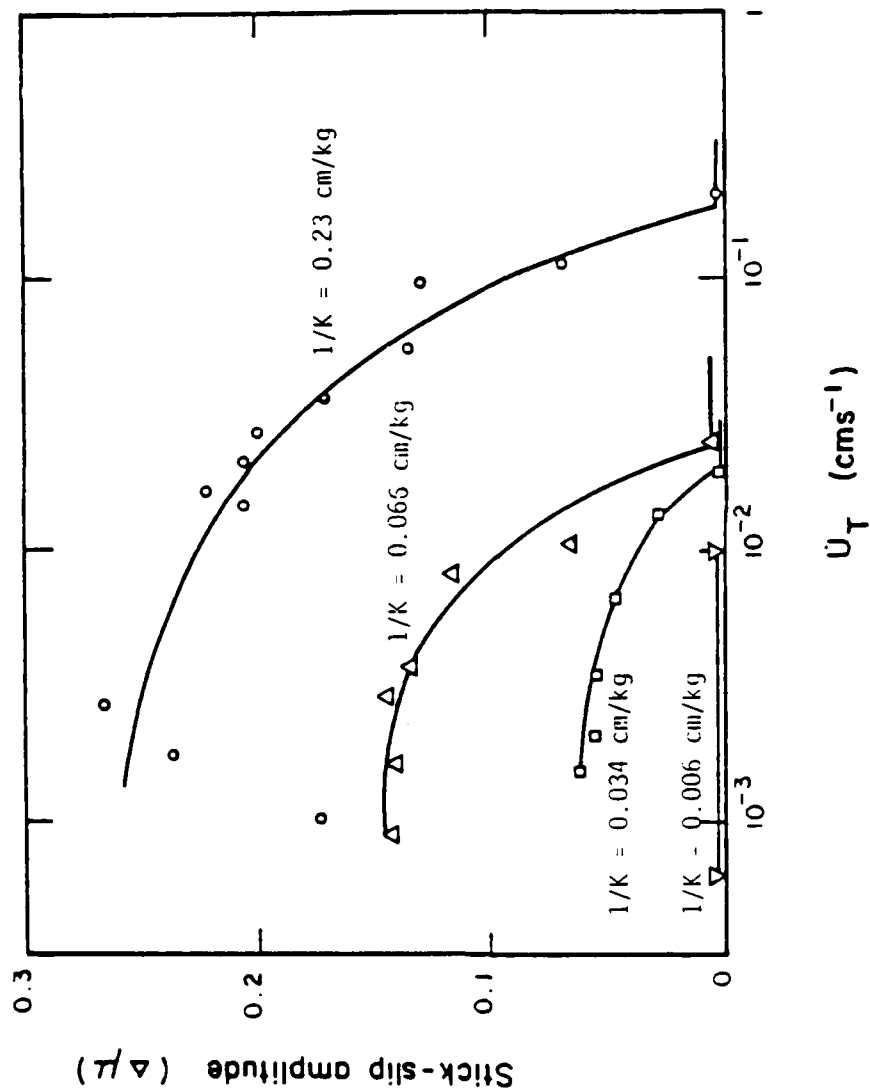


Figure 2.2.1. Relation between amplitude of the stick-slip motion and driving velocity for various spring stiffnesses ( $K$ ). Steel on steel unlubricated. Normal load = 1750 g. (Rabinowicz [1965]).

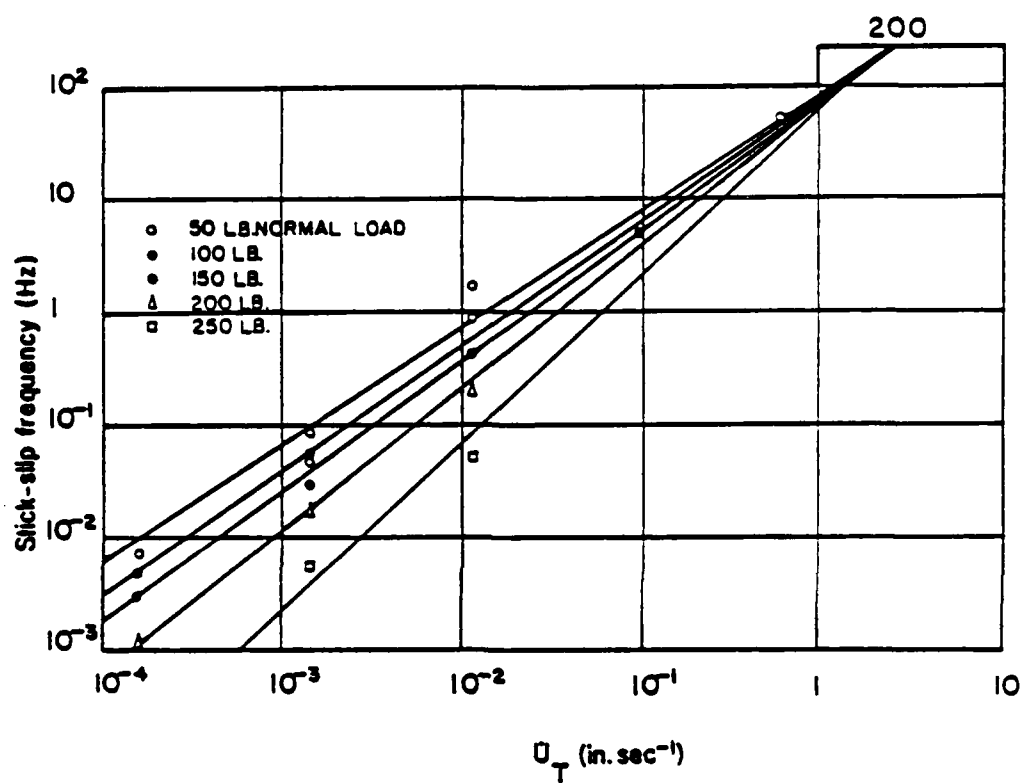


Figure 2.2.2. Variation of stick-slip frequency with driving velocity for various normal loads. Natural frequencies of the system: tangential mode ~150 Hz; normal mode ~200 Hz. Unlubricated. (Dokos [1946]).

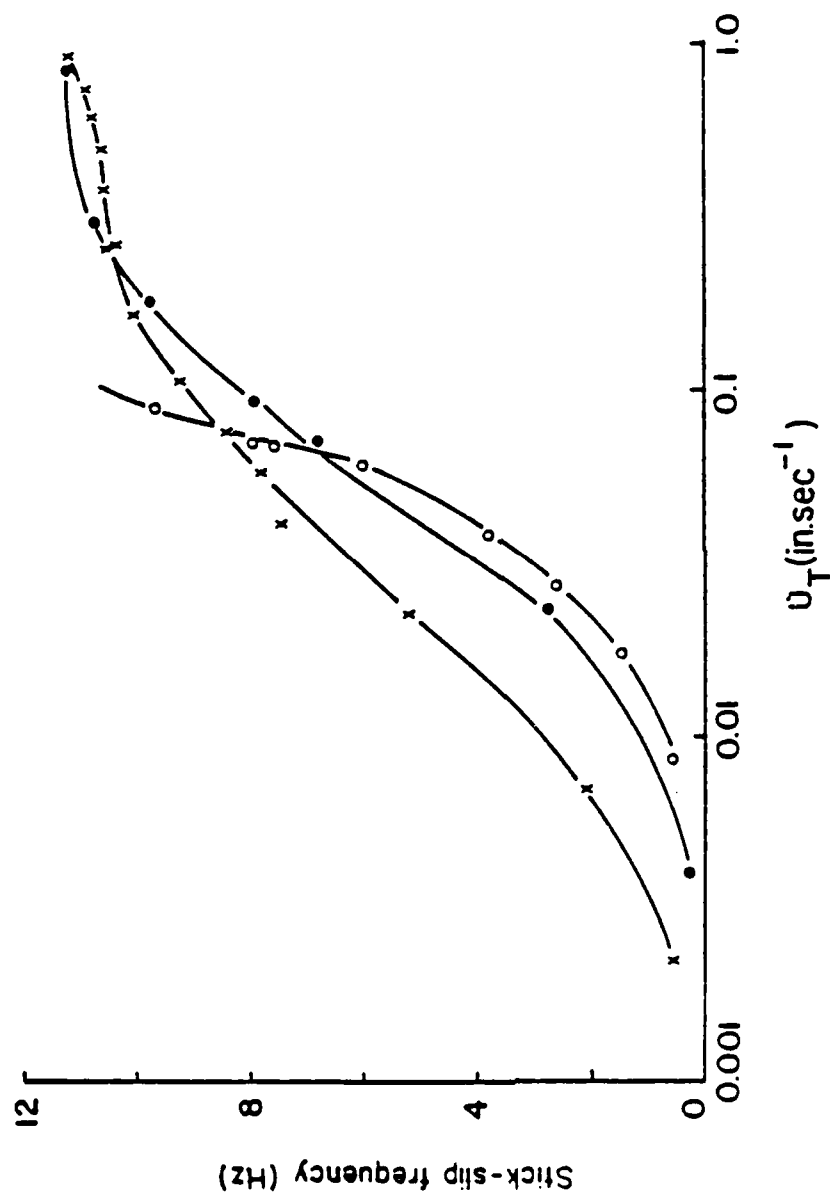


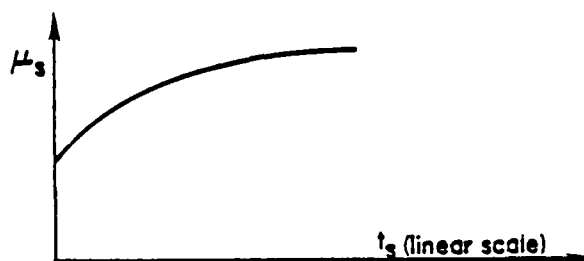
Figure 2.2.3. Variation of stick-slip frequency with driving velocity for various lubrication conditions. Natural frequency of the system (tangential motion): 11.5 Hz. Lubrication conditions: • unlubricated; x lubricant 1; o lubricant 2. (Bell and Burdett [1969-70])

increase of the coefficient of static friction with the time of stationary contact (Ishlinskii and Kragelskii [1944]). In Fig. 2.2.4, we summarize some of the most representative assumptions used in the study of stick-slip oscillations.

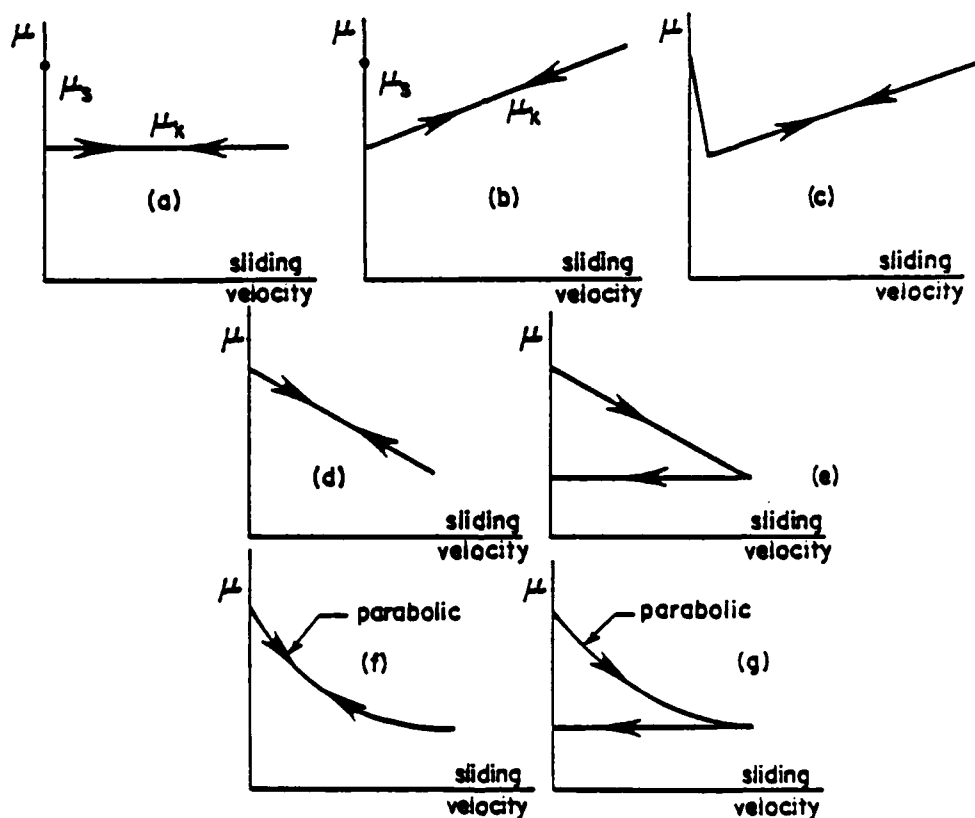
At this point a question arises: if, as noted previously, most early researchers of frictional sliding with dry metallic bodies could not find significant dependence of the kinetic friction on the sliding speed at small speeds, or significant dependence of the static friction on the time of stationary contact, then what are the additional experimental results that support the use of such assumptions in the analyses of stick-slip motions?

### 2.2.2 Time dependence or rate dependence of the coefficient of static friction.

Consider a slider resting on a surface with no macroscopic sliding motion relative to the surface and the friction force  $\sum_T$  increasing at a constant rate  $\dot{\varphi} = \dot{\sum_T} / |\sum_n|$  until gross sliding occurs. Under these conditions it can be observed that the value  $\mu_s$  of  $\varphi = \sum_T / |\sum_n|$  at which the macroscopic sliding occurs increases with the decrease of the rate ( $\dot{\varphi}$ ) of application of the tangential force (see Fig. 2.2.5). Observations of this kind can be done in the course of stick-slip oscillations: smaller driving velocities imply smaller rates of application of the tangential force and, consequently, the friction force at the onset of sliding becomes larger.



(I) Variation of  $\mu_s$  with time of stationary contact ( $t_s$ ). (For a survey of the various analytical expressions used in the literature see Richardson and Nolle [1976]).



(II) Variation of  $\mu_k$  with sliding velocity.

Figure 2.2.4. Models of the variation of the friction coefficient.  
 (IIa) Blok [1940]; (I) & (IIa) Ishlinskii and Kragelskii [1944]; (I) & (IIb) Derjaguin et al [1957]; (I) & (IIc) Brockley et al [1967]; (IIId) Bell et al [1969-70]; (IIe) Bell et al [1969-70]; (IIIf) Banerjee [1969]; (IIg) Go and Pavelescu [1982].



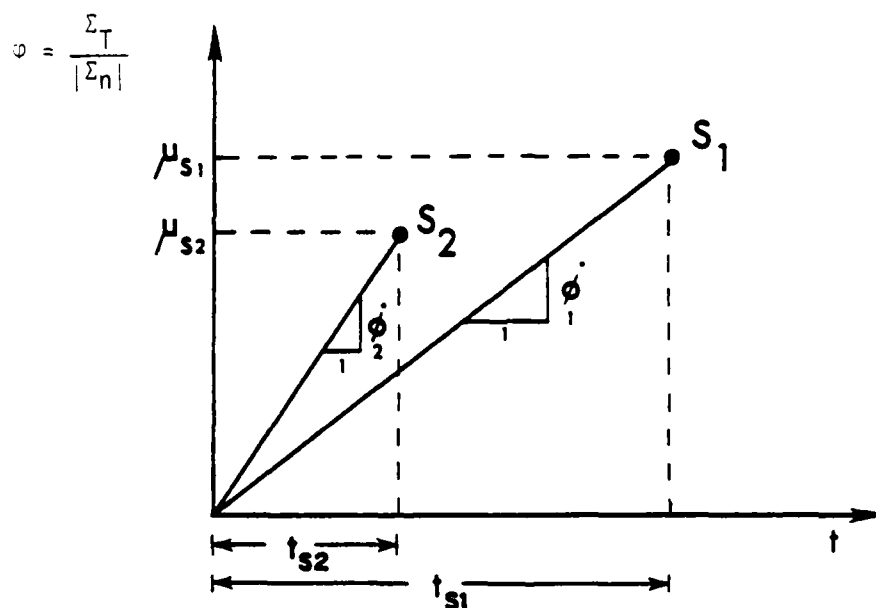


Figure 2.2.5. Rate dependence of the static coefficient of friction.  $S_1$  and  $S_2$  are the points at which gross sliding initiates;  $\dot{\phi}_1$  and  $\dot{\phi}_2$  are the rates of increase of the tangential force coefficients  $\phi_1$  and  $\phi_2$ ;  $t_{s1}$  and  $t_{s2}$  are the times of stationary contact;  $\mu_{s1}$  and  $\mu_{s2}$  are the static coefficients of friction.

$$\dot{\phi}_1 < \dot{\phi}_2 \Rightarrow \mu_{s1} > \mu_{s2}$$

As seen in Fig. 2.2.5, smaller rates  $\dot{v}$  correspond also to larger times of stationary contact ( $t_s$ ). This led to the classical statement: the coefficient of static friction ( $\mu_s$ ) increases with the time of stationary contact ( $t_s$ ). And this also led to a physical interpretation analogous to the one used to explain coefficients of static friction larger than coefficients of kinetic friction (recall Section 2.1): the strength of the contact junctions would increase with the time of stationary contact. Expressions proposed by several authors for this "time dependence of the coefficient of static friction" can be found in a survey paper by Richardson and Nolle [1976] and have been used in the analysis of stick-slip motions. See also Brockley and Davis [1968] and Kato and Matsubayashi [1970] for specific mechanisms proposed to explain the contact strengthening.

However, the experimental work of several authors suggests that these interpretations were not correct.

Simkins [1967] carried out experiments to observe the micro-displacements of a slider before gross-sliding. He found that higher rates of loading inevitably led to macroscopic sliding at lower force levels. However, in other experiments designed to assess the influence of the time of stationary contact on the value of the static coefficient of friction, he could not find any correlation between the time of stationary contact and the value obtained for that coefficient.

Johannes, Green and Brockley [1973] (working with lubricated

surfaces) and Richardson and Nolle 1976 (with "quite dry but not grease free" surfaces) carried out experiments in such a manner that they could vary independently the rate of application of the tangential force and the time of stationary contact. In those circumstances they found that the governing variable was the rate of increase of the tangential force and not the time of stationary contact.

The dependence of  $\mu_s$  on  $\dot{\phi}$  obtained by Richardson and Nolle is such that, for sufficiently small load rates, the coefficient of static friction is constant and equal to a value which is the usually quoted coefficient of static friction. For large loading rates the coefficient of static friction tends to be constant and equal to a value which is usually interpreted as the coefficient of kinetic friction, although comparative measurements have rarely been made.

As a consequence of their observations, Richardson and Nolle [1976] suggest that empirical expressions of  $\mu_s$  as a function of  $t_s$  should be recast as  $\mu_s$  as a function of  $\dot{\phi}$ . Although such a program appears feasible, the implications of those experimental findings are more profound than that solution suggests: if the coefficient of static friction is not affected by the time of stationary contact, all the classical interpretations in terms of an increase of the strength of the junctions with time will no longer be valid. What is then the mechanism responsible for the "rate dependence" of the static friction? Although it has been suggested (Bhushan [1980]) that the strain rate dependence

of the metal strengths should be taken into account in this context, to our knowledge no detailed explanation has been advanced and the whole subject appears to be far from settled (in this respect see also Tudor and Bo [1982]).

### 2.2.3. The steady -state coefficient of kinetic friction.

For hard on soft metal combinations (steel on indium and steel on lead) coefficients of friction increasing with sliding velocity in the ranges  $10^{-10}$  to  $10^{-4}$  cm/s and  $10^{-10}$  to  $10^{-8}$  cm/s, respectively, were obtained by Burwell and Rabinowicz [1953]. These increasing portions of the  $\mu - v_T$  curves are attributed by Rabinowicz [1965], Kragelskii [1965] and Tolstoi [1967] to the creep deformation of the interface asperities. Burwell and Rabinowicz [1953] point out that, for harder metals, such as aluminum copper, steel, etc., it is probable that an initial increasing branch of the  $\mu - v_T$  curve also exists. The difficulty to provide additional experimental evidence of this, at velocities of the order  $10^{-9}$  cm/s, is obviously extraordinary. In any case, since those velocities are so small, it can be concluded, following Bowden and Tabor [1964], that the frictional behavior of ordinary engineering metals at room temperature is reasonably well explained in terms of their plastic properties without introducing the part played by creep.

On the other hand, despite the frequent allusions to coefficients of friction decreasing with sliding velocity, most of the experimental steady-sliding results of that type available in

the literature apply to lubricated surfaces. A reason for this, in addition to the obvious importance of the lubricated case, is the difficulty in obtaining, with dry metallic interfaces and most of the experimental apparatus, a smooth steady-sliding (without stick-slip oscillations) at low sliding speeds (Heyman, Rabinowicz and Rightmire [1955]). Despite these difficulties some steady-state decreasing friction-velocity curves are reported in the works of Rabinowicz [1965] (a small negative slope for titanium on titanium in the range  $10^{-7}$  to  $10^2$  cm/s, larger slopes for steel on steel in the range  $10^{-3}$  to  $10^2$  cm/s), Bell and Burdekin [1969-70b] (cast-iron on cast-iron for speeds smaller than 2.54 cm/s down to a non-specified speed). For the same hard on soft metal combinations mentioned above, but for larger speeds ( $> 10^{-3}$  cm/s), Burwell and Rabinowicz [1953] also obtained  $\mu - v_T$  decreasing curves. In another paper, Heyman, Rabinowicz and Rightmire [1955] concluded that the limited data obtained by them at that time suggested that, for most metals, the coefficient of friction was affected very little as the speed varied in the range  $10^{-4}$  to  $10^{-6}$  cm/s. Rabinowicz [1965] states that for hard metal combinations decreasing  $\mu - v_T$  curves are typically found but he emphasizes the smallness of the slopes of those curves when  $\mu$  is plotted against the logarithm of the speed.

#### 2.2.4. The coefficient of kinetic friction during the slip phase of stick-slip motions.

Whatever the steady-state friction-velocity curve is or

is believed to be, it soon became clear that during the slip portion of the stick-slip cycles the friction force would not follow the path predicted by such a curve. Instead, experimental results show that the friction force follows a loop - the friction force during the acceleration portion of the sliding is in general distinct from the friction force during the deceleration.

Unfortunately, the various experimental observations of these cycles are not conclusive: different material combinations and different experimental apparatus originate loops with distinct shapes and orientations (Sampson et al [1943], Hunt et al [1965], Bell and Burdekin [1969-70], Antoniou et al [1976] and, even for the same materials and the same experimental apparatus, changes on the driving velocity or dynamic properties of the apparatus affect radically the resulting loops (see the experimental results of Bell and Burdekin [1969-70] reproduced in Fig. 2.2.6).

Those experimental observations, particularly those in Fig. 2.2.6, suggest that the friction-velocity plots obtained in the course of stick-slip motions are not an intrinsic property of the surfaces in contact - they are greatly affected by all the dynamic variables involved in each particular experimental set up.

*Rather than assume a simplified relationship between the friction force and the sliding velocity, from which the experimental evidence will deviate often, an acceptable theory of stick-slip motion will have to explain, in a unified manner, the complex relationship between the friction force and the sliding velocity*

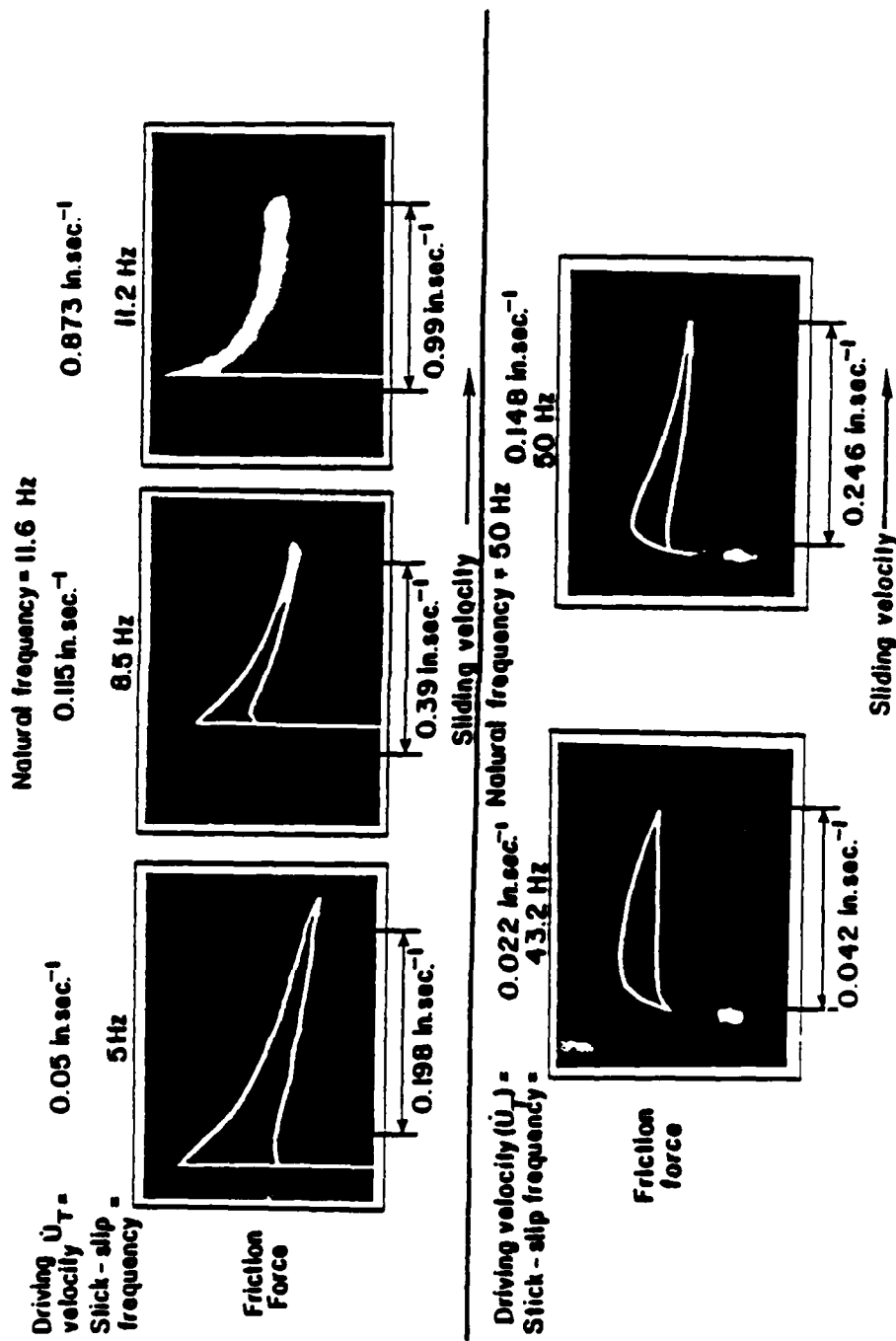


Figure 2.2.6. Friction force - sliding velocity characteristics for various driving velocities and natural frequencies of the system. Unlubricated. (Bell and Burdekin [1969-70]).

and also other factors that are associated with the stick-slip motion (e.g. the rate dependence of the static friction).

#### 2.2.5. Memory-dependent friction.

Some authors have attempted to give unified interpretations of various phenomena observed at low sliding speeds on the basis of friction laws that allow for a dependence of the friction stresses on the previous sliding history.

Various experimental observations with metals suggested to Rabinowicz [1958] that the friction force would be determined not only by the instantaneous sliding conditions but by the sliding history of a preceeding critical distance (of the order  $10^{-3}$  cm for various metallic surfaces). This critical distance concept was employed by the same author with the purpose of: explaining clockwise loops described by the friction force during the sliding portion of stick-slip cycles; correlating the steady-state friction-sliding speed curves [ $\mu_K = \mu_K(v_T)$ ] with the static friction-time of stationary contact curves [ $\mu_S = \mu_S(t_S)$ ]; explaining the transition from stick-slip motion to smooth steady-sliding.

Although Rabinowicz [1958] provided some promising comparisons between the predictions of his model and experimental results, the absence of a detailed analytical or numerical study on the behaviors predicted by his model precludes a definitive conclusion on its validity. Furthermore, experimental results published after Rabinowicz's paper raise some new difficulties: How to explain the counterclockwise loops of the friction coefficient observed



by Antoniou et al. [1976]? How to surmount the questions raised (recall Section 2.2.2) on the validity of the major physical basis for Rabinowicz's correlation between the  $u_s(t_s)$  and  $\mu_k(v_T)$  curves, i.e., the increase of the strength of the junctions with the time of contact?

More elaborate models which also take into account memory effects in frictional phenomena, have been advanced in recent years by Ruina [1980, 1983], Rice and Ruina [1983], Gu et al. [1983] and some promising results and simulations of geological fault slip phenomena based on these models have been presented (Tse and Rice [1984]). A brief summary and discussion of this current field of research can be found in Oden and Martins [1985]. To our knowledge, an experimental study on the applicability of these models to metal surfaces has not been done yet.

### 2.3. The importance of the normal degree of freedom in sliding friction.

Substantially different ideas were advanced mainly by some Russian authors: initially Kudinov [1958] for lubricated contacts and later Tolstoi [1967] for dry contacts. Tolstoi observed that the forward movements of a slider during stick-slip motion occur in strict synchronism with upward normal jumps (Fig. 2.3.1). Observed decreases of friction during the sliding portions of the stick-slip motion might be thus the result of a decrease of the average normal contact force during the sliding and jumping, without the need

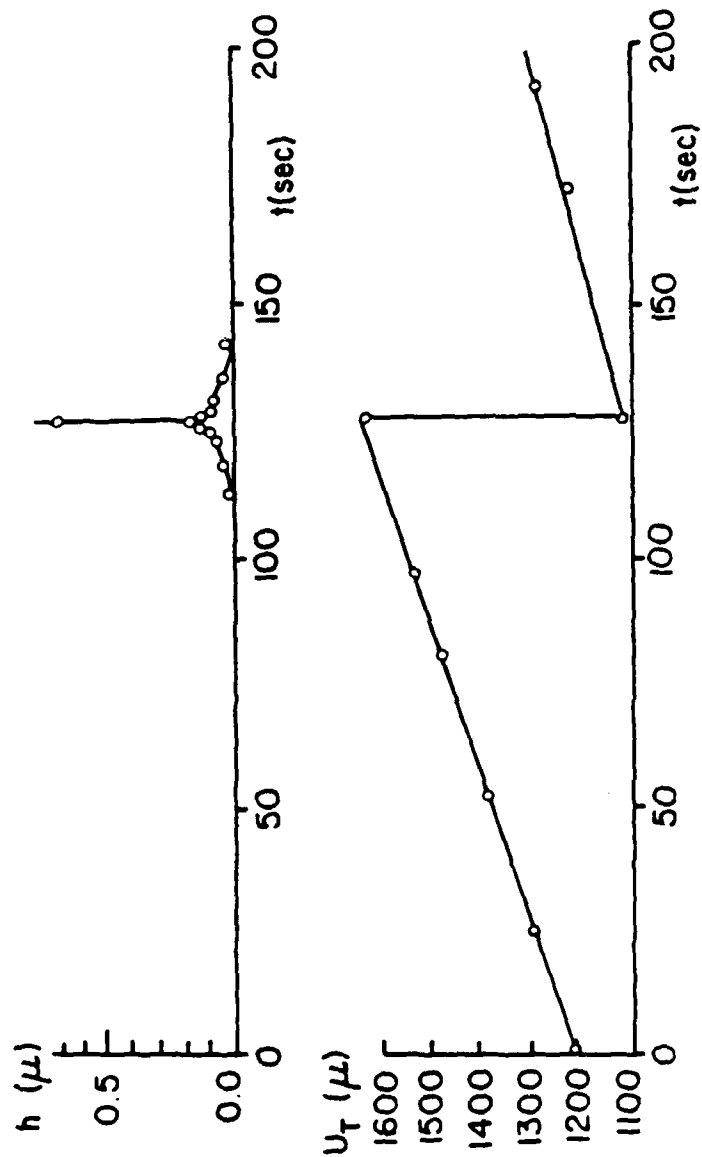


Figure 2.3.1. Simultaneous tangential ( $u_T$  vs.  $t$ ) and normal ( $h$  vs.  $t$ ) jumps of the slider during stick-slip motion. Unlubricated. (Tolstoi [1967]).

to consider any reduction on the real coefficient of friction. More detailed observation of these upward jumps revealed that, while sliding, the body undergoes a normal oscillation, the frequency of which (of the order of  $10^3$  Hz) is consistent with the normal interface stiffness properties (Fig. 2.3.2).

We note that several authors have also done observations analogous to these. In their early study Bowden and Tabor [1939] measured the interface electrical conductance during stick-slip motion and observed a marked fall of electrical conductance during the slip phase of the motion (see Figs. 9a and 9b, Plate 26, op. cit.). More detailed analysis also revealed that during those slips the conductance actually oscillated very rapidly with frequencies of the order  $10^5$  Hz (see Fig. 10a, Plate 26, op. cit.). These changes in conductance are attributed by those authors to corresponding changes in the true area of contact and this indeed suggests the occurrence of normal oscillations of the type observed by Tolstoi and co-workers. Of course, for clearly distinct experimental apparatus, contact geometries and loads, the frequencies observed are also very different. Sharp decreases of electrical conductance during the slip phase of (lubricated) stick-slip motions can also be found in the work of Johannes et al [1973]. Direct measurements of the separation of unlubricated and lubricated surfaces during stick-slip motion were also done by Bo and Pavelescu [1982] and by Tudor and Bo [1982], respectively. Other experimental evidence, although less conclusive, of the influence of the normal degree

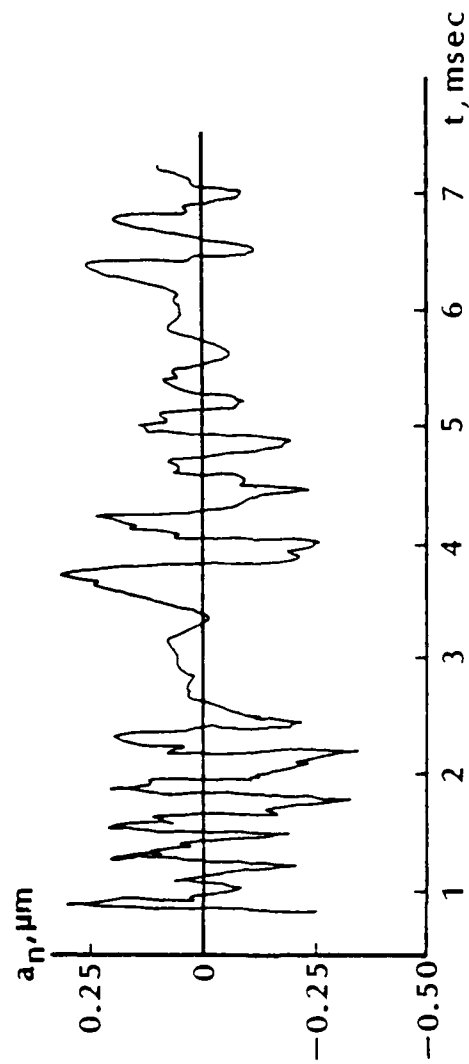


Figure 2.3.2. Oscillogram of free normal oscillations in stages of tangential jumps of a slider in the course of self-excited friction oscillations (reproduced from Budanov, Kudinov and Tolstoi [1980], after experimental results of Tolstoi, Borisova and Grigorova [1971])

of freedom on stick-slip motions was presented by Antoniou, Cameron and Gentle [1976] and by Elder and Eiss [1969].

Specially important was the experimental observation by Tolstoi that external damping of the normal free microvibrations of a slider could eliminate the decrease of friction force with the increase of sliding velocity. No quantitative distinction between static and kinetic friction could be observed in those circumstances. Furthermore, when normal damping was introduced, with no change on the driving velocity, during a run that showed stick-slip oscillations, it was observed that the oscillations ceased and that the value of the coefficient of friction for the subsequent smooth sliding was even greater than the maximum values obtained at the end of the stick periods of the stick-slip motion. The responsibility of the freedom of normal displacement for both the falling  $\sum_T - v_T$  relation and the stick-slip motion was corroborated in another manner: sufficiently heavy tangential damping alone could indeed suppress the stick-slip oscillations but it failed to affect the negative slope of the  $\sum_T - v_T$  curve.

From these (and other) observations Tolstoi concludes that oscillations normal to the contact surface play a key role in both "static" and "kinetic" friction.

With respect to *static friction*, apparent reductions of the measurable static coefficient at any rate of application of the tangential force, would be the result of microseisms of amplitudes 0.1 to 10  $\mu m$  commonly observed on the earth crust (cf. Coulomb

[1956])).

With respect to *kinetic friction*, Tolstoi and co-workers have proposed the following mechanisms to explain apparent coefficients of kinetic friction lower than the static one:

(I) *Asymmetry of normal contact oscillations* (Tolstoi [1967])

- An increase in the speed of the slider increases upward components of the impulses exerted on the slider asperities as they collide with those of the underlying surface; this increases the amplitude of the normal natural vibrations of the slider which are governed by the contact stiffness and mass of the slider; due to the nonlinearity of the normal force-penetration relationship (see Section 2.4), the normal vibrations of the slider are *highly asymmetric* and, consequently, an increase of the amplitude of the oscillation decreases the mean level of penetration during sliding; hence, the average area of contact decreases and, as a result, the friction force also decreases. This mechanism provides thus an explanation for *apparent decreases of kinetic friction with increasing sliding speeds*.

(II) *High-frequency stick-slip motions* (Budanov, Kudinov and Tolstoi [1980]) - Oscillations in normal contact force induce similar oscillations on the maximum instantaneously available friction force so that during each cycle of normal oscillation the slider will alternately stick and slide; since the frequency of the normal oscillation is high, its amplitude small and the average sliding velocity of the body also small, the motion of

the body will be recorded as an apparently smooth sliding; furthermore the ratio between friction and normal force for the short periods of sticking is smaller than the coefficient of static friction, so that, in average, an apparent coefficient of kinetic friction results which is smaller than the true static one; also, for larger average sliding speeds, the average time of stick of the successive stick-slip cycles will be smaller, so that *the average apparent coefficient of friction will increase with the average sliding velocity.*

As might be expected, the influence of normal oscillations on friction phenomena is not exclusive of the stick-slip motion. For various experimental observations on this respect we refer to the works of Tolstoi [1967], Godfrey [1967], Lenkiewicz [1969], Soom and Kim [1983a, b] and Aronov et al [1983, 1984].

The experimental evidence collected in this section leads us to the conclusion that *an appropriate model for sliding friction must incorporate physically reasonable normal contact interface conditions.*

The stiffness properties of compressed metallic surfaces are summarized in the next section.

#### 2.4. The normal stiffness of metallic interfaces.

Theoretical models and experimental results for the normal deformability of rough metallic surfaces are available in the literature. For the theoretical developments we refer to the survey papers of Archard [1974], Thomas [1975] and Whitehouse

[1980]. More recent references are the papers by Greenwood [1984] and by Greenwood, Johnson and Matsubara [1984]. For the experimental work we refer to the survey papers of Back, Burdekin and Cowley [1973] and Woo and Thomas [1980].

The more elaborate theoretical models are based on a statistical description of the surface topography and incorporate suitable assumptions on the mechanical behavior of the interface asperities: elastic, plastic, elasto-plastic, work-hardening, etc.

Comparing the predictions of the theoretical models with the available experimental results, some broad conclusions on the behavior of quasistatically compressed metallic surfaces can be drawn. We summarize them as follows (for additional details see Oden and Martins [1985]):

*On the mode of deformation of metal surfaces:*

(i) The essential factors affecting the mode of deformation of a rough surface are the material properties and the surface finish. The normal load is expected to have little effect on the mode of deformation of the surface.

(ii) For most engineering materials and surface finishes, the initial contact of the surfaces is expected to be plastic even at light loads.

(iii) The repeated loading-unloading-reloading of the metal surfaces, as in normal sliding or in metallurgical polishing, produces changes in the shape of the asperities, which lead to a subsequent elastic deformation, provided that severe wear is



prevented during the process of sliding.

*On the stiffness of compressed rough surfaces:*

(iv) At small penetrating approaches (large separations) the stiffness of rough surfaces becomes vanishingly small.

(v) The stiffness of a surface is inversely proportional to its roughness.

(vi) The normal load increases roughly as an exponential function of the penetrating approach (the separation decreases proportionally to the increase of the logarithm of the load).

(vii) For light loads, because of (iv), the normal load is closely proportional to a power, in the range  $1/0.5$  to  $1/0.3$ , of the penetrating approach.

Andrew, Cockburn and Waring [1967-68] studied the dynamic response of the annular interfaces of several mild steel discs compressed together with some preload when subjected to a normal harmonic force. They observed that the interface normal stiffness depended linearly on the normal preload, which is consistent with (vi) above. This and other more qualitative information collected in Oden and Martins [1985] suggests that the normal stiffness properties summarized above also hold in dynamic situations which do not involve significant sliding. The experimental observations of Tolstoi and co-workers mentioned earlier also suggest that the same happens for situations involving frictional sliding.

## 2.5. A model of interface response

The interface between contacting bodies is a hypothetical medium of vanishing thickness, the mechanical response of which depends upon the various geometrical and physical properties of the surfaces in contact. For the class of problems addressed here, we wish to characterize the response of such an interface to normal and tangential deformations in a way consistent with the experimental observations summarized above.

Consider a continuous material body  $B$ , in contact with another material body  $B_1$  over a contact surface  $\Gamma_C \subset \partial B$ . The contact surface  $\Gamma_C$  represents the boundary of the parent bulk material of which the body  $B$  is composed. One can regard it as parallel to a surface representing the average surface height of the asperities of the physical body  $B$ . We suppose that  $\Gamma_C$  has a well defined exterior normal vector  $\underline{n}$ .

For simplicity of presentation, but with easy generalization, we assume that the body  $B_1$  is rigid and ideally flat. In the spirit of Fig. 1.1.1(b), we also assume that the body  $B_1$  does not move on the direction of  $\underline{n}$ , but that it can move with some prescribed velocity  $\dot{\underline{u}}_T^C$  parallel to  $\Gamma_C$ .

We suppose that the actual interface (asperities, oxide film, adsorbed gas, work-hardened material, etc.) is initially of thickness  $t_0$  as shown in Fig. 2.5.1. The initial gap  $g$  between  $B$  and  $B_1$  is defined as the distance, along the direction of the normal vector  $\underline{n}$ , between the highest asperities of the body  $B$



and the flat surface of  $B_1$  in the reference (undeformed) configuration. The interface thickness after deformation is denoted by  $t$  in Fig. 2.5.1 and the actual displacement of  $\Gamma_C$  in the direction of  $\underline{n}$  is  $u_n = \underline{u} \cdot \underline{n}$ . Thus, the approach of the material contact surfaces is

$$a = t_0 - t = (u_n - g)_+ \quad (2.5.1)$$

where  $(\cdot)_+ = \max\{0, \cdot\}$ .

On the other hand, if  $\dot{\underline{u}}_T = \dot{\underline{u}} - \dot{u}_n \underline{n}$  denotes the tangential velocity of the points on  $\Gamma_C$ , then the relative sliding velocity between bodies  $B$  and  $B_1$  is equal to  $\dot{\underline{u}}_T - \dot{\underline{u}}_T^C$ . Here  $(\cdot)$  denotes partial differentiation with respect to time  $\frac{\partial}{\partial t}(\cdot)$ .

Denoting by  $\sigma_n$  and  $\underline{\sigma}_T$  the normal and tangential (frictional) stresses on  $\Gamma_C$ , respectively, the constitutive relations for the interface adopted here are the following:

#### Normal interface response

$$-\sigma_n = c_n[(u_n - g)_+]^{m_n} + b_n[(u_n - g)_+]^{l_n} \dot{u}_n \quad (2.5.2)$$

#### Friction conditions

$$\left. \begin{aligned} u_n \leq g &\Rightarrow \underline{\sigma}_T = \underline{0} \\ u_n > g &\Rightarrow \left\{ \begin{array}{l} |\underline{\sigma}_T| \leq c_T[(u_n - g)_+]^{m_T} \\ \text{and} \\ |\underline{\sigma}_T| < c_T[(u_n - g)_+]^{m_T} \Rightarrow \dot{\underline{u}}_T - \dot{\underline{u}}_T^C = \underline{0} \\ \text{and} \\ |\underline{\sigma}_T| = c_T[(u_n - g)_+]^{m_T} \Rightarrow \exists \lambda \geq 0, \dot{\underline{u}}_T - \dot{\underline{u}}_T^C = -\lambda \underline{\sigma}_T \end{array} \right\} \end{aligned} \right\} \quad (2.5.3)$$

Here  $c_n$ ,  $m_n$ ,  $b_n$ ,  $l_n$ ,  $c_T$ ,  $m_T$  are material parameters characterizing

the interface and are to be determined experimentally.

The following remarks provide an explanation and interpretation of these relations:

1. The interface constitutive equation (2.5.2) combines a nonlinear power-law elastic contribution,  $\sigma_n^e = -c_n [(u_n - g)_+]^{m_n}$ , with a nonlinear dissipative component given by  $\sigma_n^d = -b_n [(u_n - g)_+]^{c_n} \dot{u}_n$ . We incorporate these nonlinear boundary effects in our model instead of a classical non-penetration unilateral contact condition because:

(i) For metallic bodies the deformation of the contact interface may be of an order of magnitude comparable with the bulk linear elastic deformation of the contacting bodies (Back, Burdekin and Cowley [1974], Villanueva-Leal and Hinduja [1984]).

(ii) The experimental results of Andrew, Cockburn and Waring [1967-68] (Section 2.4) and those of Tolstoi and other authors (Section 2.3) strongly suggest that physically reasonable normal contact conditions have to be used in dynamic problems.

2. The form of the nonlinearly elastic contribution  $\sigma_n^e$  is consistent with the experimental observations outlined earlier for the case of interfaces subjected to low nominal pressures ( $|\sigma_n| < 5$  MPa) characteristic of sliding interfaces (recall (iv) and (vii) in Section 2.4):

$$\begin{aligned} \text{a)} \quad \frac{d\sigma_n^e}{da} \Big|_{a=0} &= 0 \quad (a = (u_n - g)_+) \\ \text{b)} \quad -\sigma_n^e &\propto a^{m_n} \quad \text{with } 2 \leq m_n \leq 3.33. \end{aligned}$$

Tables with experimental values of the constants  $c_n$  and

$m_n$  for several combinations of materials and surface finishes can be found in Back, Burdekin and Cowley [1973]. Finite element computations of *static* contact problems using such power-law normal interface constitutive equations have been done earlier by Back, Burdekin and Cowley [1974] and Villanueva-Leal and Hinduja [1984].

3. The nonlinear dissipative term  $\sigma_n^d$  is designed to model, only in an approximate manner, the hysteresis loops that result from the actual elasto-plastic behavior of the interface asperities. Indeed, the constitutive equation (2.5.2) allows for the approximation of loading paths of the form presented in Fig. 2.5.2(a) by loops of the form in Fig. 2.5.2(b). Thornley et al [1965] obtained experimentally loops of the type depicted in Fig. 2.5.2(a) when the surfaces were allowed to unload completely, that is to say, when some, even small, tangential reorientation of the surfaces was allowed. The idea of a similar approximation was proposed by Hunt and Crossley [1975] for vibroimpact phenomena involving macroscopic Hertzian contacts. For small energy losses, the correlation between the damping coefficient  $b_n$  and the energy loss per cycle of contact is readily obtainable (Hunt and Crossley [1975]).

4. The friction law (2.5.3) is a slightly generalized local form of the classical dry friction laws (recall 2.1.1, 2). That law allows for possible deviations from the Amontons laws (recall Section 2.1), i.e., a possible dependence of the coefficient of friction ( $\mu$ ) on the normal stress according to

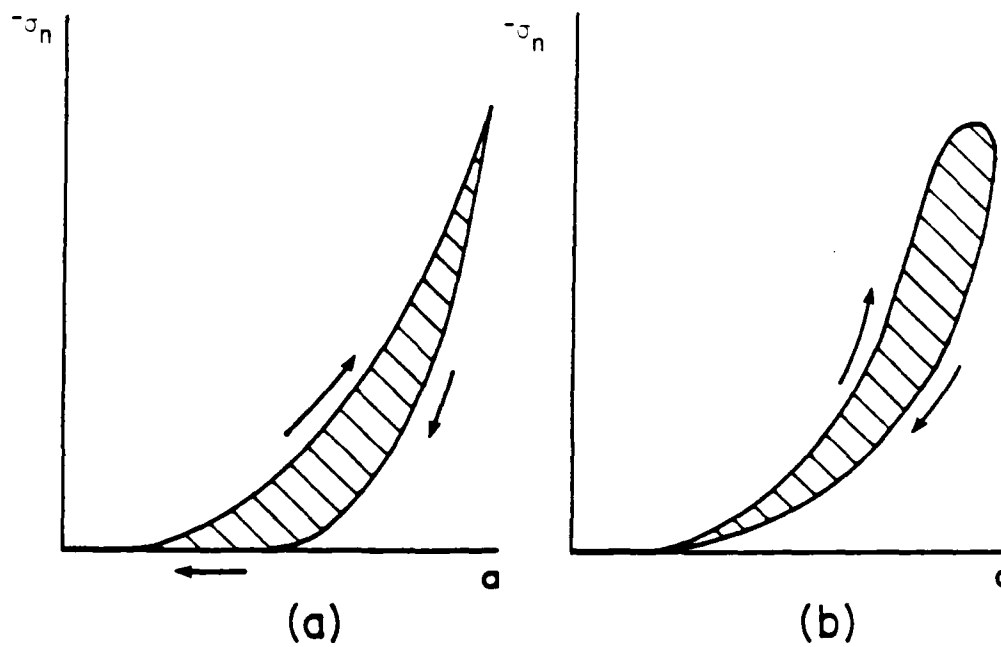


Figure 2.5.2. Hysteresis loops for the normal deformation of the interface (schematic). (a) Experimentally observed loop, under quasi-static loading conditions. (b) Hysteresis loop modelled by the constitutive equation (2.5.2) under dynamic loading conditions.

$$\mu = C |\sigma_n|^\alpha \text{ with } \alpha = m_T/m_n - 1 \text{ and } C = c_T/c_n^{m_T/m_n}$$

if the normal dissipative effects are negligible ( $b_n \approx 0$ ). If  $m_T = m_n$  (and again  $b_n \approx 0$ ) the usual Coulomb's law of friction is recovered with  $\mu = c_T/c_n$ .

5. In using the friction law (2.5.3) we assume that there exists no distinction between coefficients of static and kinetic friction and no variation of the latter with the sliding speed. This means that creep or thermal softening effects will not be taken into account in the present study. We do these assumptions because:

(i) The experimental observations of Tolstoi and co-workers summarized in Section 2.3 clearly suggest that at small sliding speeds those distinctions or variations are not intrinsic properties of the interfaces.

(ii) Occurrence of friction-induced oscillations even for sliding speeds in regions where the slope of the  $\mu - v_T$  curve is positive have already been observed (Yokoi and Nakai [1979]). Furthermore, instability of steady-sliding and occurrence of self-excited oscillations with some systems that have two or more degrees-of-freedom and particular geometric configurations have been explained without recourse to the classical assumption of a decreasing  $\mu - v_T$  curve (Shobert [1957], Spurr [1961-62], Jarvis [1963-64], Earles and Lee [1976], Earles and Badi [1984], Aronov et al [1984]).

We wish thus to study how much of the frictional behaviors observed at low speeds can be explained and numerically simulated



without those classical assumptions.

6. Dissipative effects on a metallic interface are associated with plastic deformation of the interface asperities. Of course, such plastic deformation involves both tangential and normal motions coupled in a complex manner (recall Section 2.1) which we cannot expect to reproduce in detail with the dissipative terms in (2.5.2, 3). Related to this is also the fact that the friction law (2.5.3) does not take into account preliminary (plastic) tangential micro-displacements known to occur before gross-sliding (Courtney-Pratt and Eisner [1957]). We believe however that these approximations are acceptable because we are not interested in studying the details of small quasistatic evolutions of the bodies involved, but rather gross motions and oscillations for which the major contributions of the interface are its nonlinear elasticity and its tangential frictional dissipation, with a comparatively much smaller contribution of the normal dissipation. In this context we remark that in all the calculations done by Tolstoi and co-workers to analyze their experimental results, only the two major contributions mentioned above were taken into account, although, of course, those authors were perfectly aware of the existence of the normal dissipation.

7. The constitutive assumptions (2.5.2, 3) are not completely consistent with some aspects of the work of Tolstoi and co-workers:

(i) The nonlinearly elastic contribution in (2.5.2) is not of the form experimentally observed by those authors for the surfaces and loads they worked with, but it can be shown (see

Martins and Oden [1986]) that, within the range of validity of our model, (2.5.2) leads to normal microvibrations with frequencies close to those considered by Tolstoi as typical:  $10^3$  Hz.

(ii) *In their work, these authors did not propose a deterministic constitutive law for frictional sliding.* Instead they postulated a time-averaged behavior consistent with their observations and the asymmetry mechanism (I) in Section 2.3. Our phenomenological law (2.5.3) is not consistent with that mechanism (see Martins and Oden [1986]). However (see Chapter 4), we will be able to model their high-frequency stick-slip mechanism (II) and also other effects that are attributed by those authors to their mechanism (I).

8. Finally, we observe that no time or rate dependence of the static friction are considered with the law (2.5.3). Consequences of this on our results will be analyzed and, much in the spirit of Tolstoi's ideas on the apparent reductions of static friction, a preliminary study on the effect of external perturbations on the measurable static friction will be done in Chapter 4.

## CHAPTER 3

### CONTINUUM MECHANICS MODELS

#### 3.1 Preliminary remarks. Orientation.

In Chapter 1 we observed that no general theory of existence is available to date for continuum mechanics problems involving the unilateral (non-compliant) dynamic contact of deformable bodies, even in the frictionless case. Furthermore, in finite-dimensional situations, examples of non-existence and non-uniqueness of solutions are known for both frictionless and frictional cases (see, e.g., Schatzman [1978], Carriero and Pascali [1980], Lötstedt [1984] and Jean and Pratt [1985]). Sufficient conditions for existence and/or uniqueness in finite dimensional problems have been proved for frictionless situations by Schatzman [1978], Carriero and Pascali [1980, 1982], Lötstedt [1982], Buttazo and Percivale [1981, 1983], Degiovani [1984], Percivale [1985], and for frictional situations by Lötstedt [1984] and Jean and Pratt [1985]. For the reasons indicated in Chapter 1, easy extensions of these results to infinite dimensions have not been possible. However, several works have been published that provide important results for particular cases or related problems: the unilateral contact of strings with continuous or discrete obstacles (Amerio and Prouse [1975], Amerio [1976, 1977], Citrini [1975a, 1975b, 1977], Schatzman [1980a, 1980b], Bamberger and Schatzman [1983], Burridge et al [1982]), a wave problem in a half-space with a unilateral constraint at

the boundary (Lebeau and Schatzman [1984]) and, recently, the unilateral contact of an axially deforming rod with an obstacle at one of its ends (Schatzman and Bercovier [1985]); and the important work of Duvaut and Lions [1976] on dynamic or quasistatic evolution problems involving linearly elastic or viscoelastic bodies subjected to Coulomb's friction on a part of the boundary where the normal stresses are prescribed.

It is our objective in Sections 3.2 to 3.4 to formulate dynamic problems in continuum mechanics involving the contact interface laws adopted in Chapter 2 and to show that these problems do have a unique solution. In Section 3.2, we present formal statements of the problems to be studied. In Section 3.3 we establish the variational statements which govern a class of dynamic frictionless contact problems involving linearly elastic bodies and a class of dynamic frictional contact problems involving linearly viscoelastic bodies. In Section 3.4 we prove the existence and uniqueness of solutions for these classes of problems.

The techniques used in the proofs are now classical: Faedo-Galerkin approximations, regularization technique, compactness and monotonicity arguments. Indeed, in the frictionless case, we encounter a second order hyperbolic semilinear differential equation, the essential distinguishing feature relatively to other equations treated in the literature (e.g., Lions [1969], Reed [1976]) being the fact that the nonlinearity arises on the boundary. The existence proof given here employs essentially the strategy

of the proof of Theorem 1.1 in Lions [1969, pp. 8-14]. When friction is taken into account, we are led to a variational inequality which is similar in several respects to those studied earlier by Duvaut and Lions [1976]. Here we extend their results to a case in which the normal and frictional stresses on the contact boundary depend nonlinearly on the normal interface deformation.

In Sections 3.5 to 3.7 we study a steady-sliding problem in elastostatics, again with the interface laws of Chapter 2 holding on the contact boundary. With the applied forces and the (non-zero) driving velocity (recall Fig. 1.1.1(b)) both given independent of time, the steady-sliding positions are the singular points for the autonomous case of the dynamic friction problem studied in Sections 3.2 to 3.4.

The static friction problem that has received most attention in the mathematics and continuum mechanics literature is the Signorini problem with friction. In both the Signorini and the steady-sliding problems the actual contact surface is unknown a priori. But, while in the Signorini problem the actual regions of stick and slip and the direction of the tangential stresses are also unknown, in the steady-sliding problem it is a priori known that all the contact region must be sliding and that the direction of the tangential stresses must be opposite to the known direction of relative sliding.

The question of the existence of solutions to the general Signorini problem with friction was put forth as an open problem

by Duvaut and Lions [1976]. Duvaut [1982] pointed out that a mollification of the contact pressure would provide sufficient regularity for the establishment of existence of solutions to Signorini-type problems, and this led to several studies of non-local friction laws and the establishment of a mathematical theory for these problems: Demkowicz and Oden [1982], Oden and Pires [1983], Pires [1982], Pires and Oden [1983]. Recently, Nečas, Jarušek and Haslinger [1980] and Jarušek [1983] have shown that even without mollification and without the regularity needed to write a variational statement, existence of solutions to Signorini's problems with friction could also be proved. In all the developments, uniqueness of solutions has been proved only for sufficiently small coefficients of friction.

In Section 3.5 a formal statement of the steady-sliding problem is presented and in Section 3.6 the equivalence between classical and variational statements of the problem is proved. The existence and uniqueness of solutions to the problem are studied in Section 3.7. There, both existence and uniqueness are proved only for sufficiently small data: small applied forces or small coefficients of friction.

The technique used in the proof of existence for the steady-sliding problem is similar to the one used by Oden and Pires [1983] to prove existence of solution to a Signorini problem with non-local friction. Both proofs are based on some version of the Schauder fixed point theorem: if  $T$  is a compact mapping of a nonempty closed

bounded convex set  $K$  of a Banach space  $V$  into itself then  $T$  has a fixed point in  $K$ . The essential difference is that in Oden and Pires [1983] the compactness of  $T$  results from the compactness of a smoothing operator used in the non-local friction law adopted, while here the compactness of  $T$  results from the compactness of the trace operator.

Finally, in Section 3.8 an eigenvalue problem is formulated which is intended to give information on the stability of the small (formally) linearized oscillations of the body about the steady-sliding equilibrium position.

### 3.2. Formal statement of the dynamic contact problems.

Let  $\Omega \subset \mathbb{R}^N$  ( $N = 2$  or  $3$ ) be an open bounded domain representing the interior of the body. The sufficiently smooth (e.g. Lipschitz continuous) boundary  $\Gamma$  of  $\Omega$  contains three open subsets  $\Gamma_D$ ,  $\Gamma_F$  and  $\Gamma_C$  (see Fig. 3.2.1) such that,

$$\Gamma = \bigcup_{\alpha} \bar{\Gamma}_{\alpha} \quad , \quad \Gamma_{\alpha} \cap \Gamma_{\beta} = \emptyset \text{ if } \alpha \neq \beta$$

$$\text{meas} (\bar{\Gamma}_{\alpha} - \Gamma_{\alpha}) = 0$$

$$\alpha, \beta \in \{D, F, C\} \quad .$$

Points (particles) in  $\Omega$  with cartesian coordinates  $x_i$ ,  $1 \leq i \leq N$ , relative to a fixed coordinate frame are denoted by  $\underline{x} = (x_1, x_2, \dots, x_N)$  and the volume measure by  $dx$ . Points on  $\Gamma$  with cartesian coordinates  $s_i$ ,  $1 \leq i \leq N$ , relative to the same coordinate frame, are denoted by  $\underline{s}$  and the surface measure by  $ds$ .

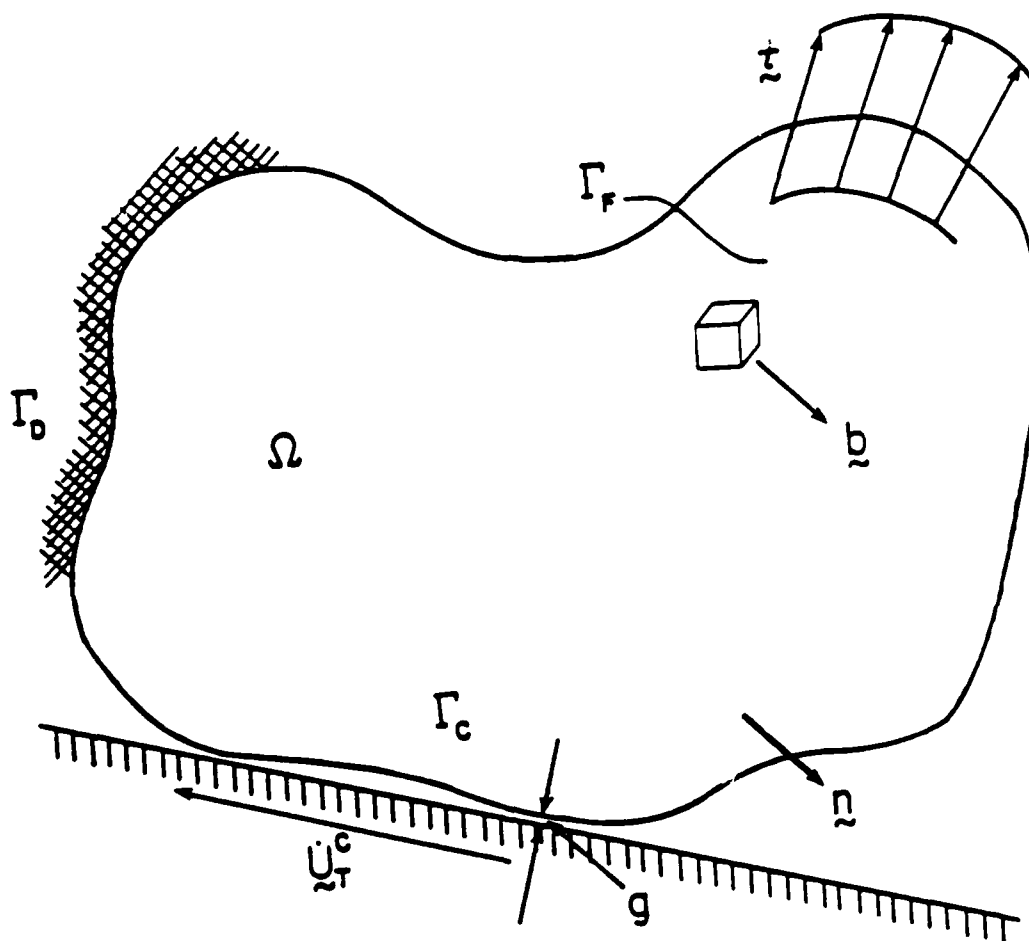


Figure 3.2.1. Geometry and notation for the continuum mechanics models of contact and sliding phenomena.



We assume that the components  $\sigma_{ij}$ ,  $1 \leq i, j \leq N$ , of the Cauchy stress tensor depend linearly on the gradients of the displacements and their time derivatives according to the following viscoelastic constitutive equation:

$$\sigma_{ij}(\underline{u}) = A_{ijkl} u_{k,1} + C_{ijkl} \dot{u}_{k,1}, \quad 1 \leq i, j, k, l \leq N. \quad (3.2.1)$$

Here  $\underline{u} = (u_1, u_2, \dots, u_N) = \underline{u}(\underline{x}, t)$  is the vector field of displacements, the components of which are sufficiently smooth functions of position ( $\underline{x}$ ) and time ( $t$ ) and  $A_{ijkl} = A_{ijkl}(\underline{x})$  and  $C_{ijkl} = C_{ijkl}(\underline{x})$  denote the usual elasticity and viscosity coefficients, respectively. In (3.2.1) and throughout this work,  $(\ )_{,1}$  denotes partial differentiation with respect to  $x_1$  and the usual summation convention is used.

We suppose that body forces with components of force per unit volume  $b_i = b_i(\underline{x}, t)$ ,  $1 \leq i \leq N$ , act in the body. Displacements  $u_i^D = u_i^D(\underline{s}, t)$ ,  $1 \leq i \leq N$ , are prescribed on  $\Gamma_D$  and tractions  $t_i = t_i(\underline{s}, t)$ ,  $1 \leq i \leq N$ , are prescribed on  $\Gamma_F$ . We also suppose that the body may come in contact along the (candidate) contact surface  $\Gamma_C$  with a foundation which slides by the material contact surface with a velocity  $\dot{\underline{u}}_T^C = \dot{\underline{u}}_T^C(\underline{s}, t)$  (the driving velocity) tangent to  $\Gamma_C$ ;  $g = g(\underline{s})$  denotes the normal gap between the body and the foundation measured in the undeformed configuration  $\underline{u} = 0$ ;  $c_n = c_n(\underline{s})$ ,  $c_T = c_T(\underline{s})$ ,  $b_n = b_n(\underline{s})$ ,  $m_n$ ,  $m_T$  and  $\lambda_n$  denote the material parameters in the interface constitutive equations (2.5.2,3); in those equations the normal stress on  $\Gamma_C$  is given by  $\sigma_n = \sigma_n(\underline{u}) = \sigma_{ij}(\underline{u}) n_i n_j$  and

the components of the tangential stress vector  $\underline{\sigma}_T$  on  $\Gamma_C$  are given by  $\sigma_{Ti} = \sigma_{Ti}(\underline{u}) = \sigma_{ij}(\underline{u})n_j - \sigma_n(\underline{u})n_i$ ,  $1 \leq i, j \leq N$ .  $\rho = \rho(\underline{x})$  denotes the mass density of the material of which the body is composed.

With the above notations, the class of dynamics problems studied here is governed, for a time interval  $[0, T]$  by the following system of equations and conditions:

#### Linear Momentum Equations

$$\rho \underline{u}_i - \sigma_{ij}(\underline{u})_{,j} = b_i \quad \text{in } \Omega \times (0, T) \quad (3.2.2)$$

where the  $\sigma_{ij}$  satisfy the constitutive equations (3.2.1).

#### Boundary Conditions

$$u_i = u_i^D \quad \text{on } \Gamma_D \times (0, T) \quad (3.2.3)$$

$$\sigma_{ij}(\underline{u})n_j = t_i \quad \text{on } \Gamma_F \times (0, T) \quad (3.2.4)$$

The contact interface conditions (2.5.2,3) hold

$$\text{on } \Gamma_C \times (0, T) \quad (3.2.5)$$

#### Initial Conditions

$$\left. \begin{aligned} \underline{u}(\underline{x}, 0) &= \underline{\bar{u}}_0(\underline{x}) \\ \underline{\dot{u}}(\underline{x}, 0) &= \underline{\bar{u}}_1(\underline{x}) \end{aligned} \right\} \quad \underline{x} \in \Omega. \quad (3.2.6)$$

### 3.3. Variational formulations for the dynamic contact problems.

In Section 3.4 we study questions of existence and uniqueness of solution for the general class of problems (3.2.2-6) in the following cases:

- $$\left. \begin{array}{l} (1) \text{ with no viscous damping and no friction;} \\ (2) \text{ with viscous damping and friction.} \end{array} \right\} \quad (3.3.1)$$

In the present section, we specify minimum regularity requirements for the dependence of various functions on the space variables, we indicate various assumptions on the data, and we introduce the definitions of various spaces and forms which will be used in the variational statements to be established in the end of the section. Further restrictions on the functions involved (in particular, the regularity of their time dependence) will be needed later and will be specified in the statements of the Theorems in Section 3.4.

For simplicity of presentation, we shall assume hereafter that,

$$\text{meas } (\Gamma_D) > 0 \quad (3.3.2)$$

$$u_i^D \equiv 0, \quad 1 \leq i \leq N \quad (3.3.3)$$

$$\rho \equiv 1 \quad (3.3.4)$$

$$b_n \equiv 0. \quad (3.3.5)$$

Denoting by  $H^1(\Omega)$  the usual Sobolev space of functions with  $L^2$ -derivatives in  $\Omega$ , it is well known that values on  $\Gamma$  for a function in  $H^1(\Omega)$  can be interpreted as the values of its  $H^{\frac{1}{2}}(\Gamma)$  image through the linear, continuous, surjective trace map (cf. Kufner et al [1977]). With such interpretation holding hereafter, we define the Hilbert space

$$V = \{v \in (H^1(\Omega))^N: v = 0 \text{ a.e. on } \Gamma_D\}$$

endowed with the usual  $(H^1(\Omega))^N$ -norm denoted by  $\|\cdot\|$ . The topological dual of  $V$  is denoted by  $V'$ ,  $\langle \cdot, \cdot \rangle$  denotes duality pairing on  $V' \times V$  and  $\|\cdot\|_*$  denotes the  $V'$ -norm.

We denote by  $H$  the usual  $(L^2(\Omega))^N$ -Hilbert space and  $(\cdot, \cdot)$  and  $|\cdot|$  will denote the usual  $(L^2(\Omega))^N$ -inner product and norm, respectively.

We assume that the elasticity coefficients satisfy the following conditions (with  $1 \leq i, j, k, l \leq N$ ),

$$A_{ijkl} \in L^\infty(\Omega)$$

$$A_{ijkl}(x) = A_{jikl}(x) = A_{ijlk}(x) = A_{klij}(x) \quad \text{a.e. } x \in \Omega \quad (3.3.6)$$

$$\exists \alpha_A > 0, \quad A_{ijkl}(x) A_{kl} A_{ij} \geq \alpha_A A_{ij} A_{ij} \quad \text{a.e. } x \in \Omega,$$

for every symmetric matrix  $[A_{ij}] \in \mathbb{R}^{N \times N}$ .

In case (2) of (3.3.1), the coefficients  $C_{ijkl}$  are assumed to satisfy the following conditions (also with  $1 \leq i, j, k, l \leq N$ ),

$$C_{ijkl} \in L^\infty(\Omega)$$

$$C_{ijkl}(x) = C_{jikl}(x) = C_{ijlk}(x) = C_{klij}(x) \quad \text{a.e. } x \in \Omega \quad (3.3.7)$$

$$\exists \alpha_C > 0, \quad C_{ijkl}(x) A_{kl} A_{ij} \geq \alpha_C A_{ij} A_{ij} \quad \text{a.e. } x \in \Omega,$$

for every symmetric matrix  $[A_{ij}] \in \mathbb{R}^{N \times N}$ .

It follows from these assumptions that the bilinear forms,  $a: V \times V \rightarrow \mathbb{R}, c: V \times V \rightarrow \mathbb{R}$  defined by,

$$a(\underline{w}, \underline{v}) = \int_{\Omega} A_{ijkl} w_{k,l} v_{i,j} dx, \quad \underline{w}, \underline{v} \in V$$

$$c(\underline{w}, \underline{v}) = \int_{\Omega} C_{ijkl} w_{k,l} v_{i,j} dx, \quad \underline{w}, \underline{v} \in V$$

are continuous and V-elliptic, i.e.,

$$\exists M_a, M_c, \alpha_a, \alpha_c > 0 \text{ such that } \forall \underline{w}, \underline{v} \in V$$

$$|a(\underline{w}, \underline{v})| \leq M_a \|\underline{w}\| \|\underline{v}\|, \quad |c(\underline{w}, \underline{v})| \leq M_c \|\underline{w}\| \|\underline{v}\| \quad (3.3.8)$$

$$a(\underline{v}, \underline{v}) \geq \alpha_a \|\underline{v}\|^2, \quad c(\underline{v}, \underline{v}) \geq \alpha_c \|\underline{v}\|^2 \quad (3.3.9)$$

We assume that

$$1 \leq m_n, m_T \begin{cases} < +\infty & \text{if } N=2 \\ \leq 3 & \text{if } N=3 \end{cases}$$

and we denote by  $q$  the number  $q=1+m_n$ , in case (1) of (3.3.1), or  $q = 1 + \max\{m_n, m_T\}$ , in case (2) of (3.3.1). It follows that, for these values of  $q$ , the space  $H^{\frac{1}{2}}(\Gamma)$  is continuously embedded in  $L^q(\Gamma)$  (c.f. Kufner et al [1977]);  $q'$  denotes the Hölder conjugate exponent of  $q$ , i.e.,  $q' = q/(q-1)$ .

Following standard notations, we denote by  $\underline{b}(t)$  and  $\underline{t}(t)$  the functions  $\underline{x} \mapsto \underline{b}(\underline{x}, t)$  and  $\underline{s} \mapsto \underline{t}(\underline{s}, t)$ , respectively, and we assume that  $\underline{b}(t) \in H$ , and  $\underline{t}(t) \in (L^{q'}(\Gamma_C))^N$ . We can thus define  $\underline{f}(t) \in V'$  such that,

$$\langle \underline{f}(t), \underline{v} \rangle = \int_{\Omega} \underline{b}(t) \cdot \underline{v} \, dx + \int_{\Gamma_F} \underline{t}(t) \cdot \underline{v} \, ds, \quad \underline{v} \in V.$$

We further assume that

$$c_n, c_T \in L^\infty(\Gamma_C), \quad c_n, c_T \geq 0 \text{ a.e. on } \Gamma_C, \quad g \in L^q(\Gamma_C),$$

and that there exists a function  $\underline{\phi}(t)$  such that

$$\underline{\phi}(t), \dot{\underline{\phi}}(t) \in V$$

$$\underline{\phi}_n(t) = 0, \dot{\underline{\phi}}_T(t) = \dot{\underline{U}}_T^C(t) \text{ a.e. on } \Gamma_C.$$

Finally, we define nonlinear maps  $P: V \rightarrow V'$  and  $j: V \times V \rightarrow \mathbb{R}$  such that

$$\langle P(\underline{w}), \underline{v} \rangle = \int_{\Gamma_C} c_n[(w_n - g)_+]^m v_n \, ds, \quad \underline{w}, \underline{v} \in V$$

$$j(\underline{w}, \underline{v}) = \int_{\Gamma_C} c_T[(w_n - g)_+]^m |\underline{v}_T| \, ds, \quad \underline{w}, \underline{v} \in V.$$

From a mechanical point of view, the space  $V$  denotes the space of admissible displacements (and velocities in case (2) of (3.3.1)) at all times  $t \in [0, T]$ . The bilinear forms  $a(.,.)$  and  $c(.,.)$  represent virtual work (or power) due to elastic and viscous deformation, respectively;  $\langle \underline{f}(t), \cdot \rangle$  represents virtual work (or power) of the external applied forces;  $\langle P(\cdot), \cdot \rangle$  represents virtual work (or power) due to the normal compliance of the interface and  $j(.,.)$  represents virtual power due to frictional sliding.

**Remark 3.3.1.** Assumptions (3.3.2-4) are by no means essential and are used only to simplify the proofs in Section 3.4.

If  $\Gamma_D = \emptyset$ , assumptions (3.3.6,7) lead to the following estimates

$$\forall \lambda > 0, \exists \alpha_a, \alpha_c > 0 \text{ such that,}$$

$$a(\underline{v}, \underline{v}) + \lambda |\underline{v}|_{\alpha_a}^2 \geq \alpha_a \|\underline{v}\|^2, \quad c(\underline{v}, \underline{v}) + \lambda |\underline{v}|_{\alpha_c}^2 \geq \alpha_c \|\underline{v}\|^2 \quad (3.3.10)$$

which should replace (3.3.9). All the estimates derived from (3.3.9) in the proofs below can be derived also from (3.3.10), although the details are lengthier.

If  $\underline{u}^D \neq \underline{0}$ , in particular, if the prescribed displacements are time dependent, the regularity of such dependence requires special attention. The treatment of the prescribed velocities  $\dot{\underline{u}}_T^C$  and the assumptions on  $\underline{\phi}$  in Theorem 3.4.2 are typical of this.

If  $\rho \neq 1$  but  $\rho \in L^\infty(\Omega)$  with  $\rho(\underline{x}) \geq \rho_0 (= \text{constant}) > 0$  a.e.  $\underline{x} \in \Omega$ , the usual  $(L^2(\Omega))^N$ -inner product should be replaced by the equivalent weighted inner product  $\int_{\Omega} \rho(\underline{x}) w_j v_j \, dx$ ,  $\underline{w}, \underline{v} \in H$ .  $\square$

**Remark 3.3.2.** Additional boundary terms corresponding to the deformation of linear springs on a part of  $\Gamma$  could also be easily incorporated in the formulation. See Oden and Martins [1985] and Rabier, Martins, Oden and Campos [1986].  $\square$

It is now simple to show, in a *formal* manner, that, for each of the cases in (3.3.1) any solution of (3.2.2-5) satisfies a variational statement which we shall use in the definitions<sup>1</sup> of the problems below:

**Problem 1** (no viscous damping and no friction). Find a function  $t \rightarrow \underline{u}(t)$  of  $[0, T] \rightarrow V$  such that

$$\langle \ddot{\underline{u}}(t), \underline{v} \rangle + a(\underline{u}(t), \underline{v}) + \langle P(\underline{u}(t)), \underline{v} \rangle = \langle \underline{f}(t), \underline{v} \rangle \quad \forall \underline{v} \in V, \quad (3.3.11)$$

with the initial conditions,

<sup>1</sup>These definitions are obviously still incomplete since regularity with respect to time and regularity of the initial conditions has not yet been specified.

$$\left. \begin{aligned} \underline{u}(0) &= \underline{u}_0 \\ \dot{\underline{u}}(0) &= \underline{u}_1 \end{aligned} \right\} \quad (3.3.12)$$

**Problem 2** (viscous damping and friction). Find a function  $t \mapsto \underline{u}(t)$  of  $[0, T] \rightarrow V$  such that

$$\begin{aligned} & \langle \ddot{\underline{u}}(t), \underline{v} - \dot{\underline{u}}(t) \rangle + a(\underline{u}(t), \underline{v} - \dot{\underline{u}}(t)) + c(\dot{\underline{u}}(t), \underline{v} - \dot{\underline{u}}(t)) \\ & + \langle P(\underline{u}(t)), \underline{v} - \dot{\underline{u}}(t) \rangle + j(\underline{u}(t), \underline{v} - \dot{\underline{u}}(t)) - j(\underline{u}(t), \dot{\underline{u}}(t) - \dot{\underline{u}}(t)) \\ & \geq \langle \underline{f}(t), \underline{v} - \dot{\underline{u}}(t) \rangle \quad \forall \underline{v} \in V, \end{aligned} \quad (3.3.13)$$

with the initial conditions (3.3.12).

**Remark 3.3.3.** Details of the calculations leading to the variational statements (3.3.11) and (3.3.13) are well known and we refer the reader to, e.g., Duvaut and Lions [1976] or Demkowicz and Oden [1982] for similar calculations. Here we only observe that the variational inequality (3.3.13) is a result of the nondifferentiability of the frictional functional  $j(\cdot, \cdot)$  with respect to the second argument (velocity). In this context we observe that the friction conditions (2.5.3) on  $\Gamma_C$  imply that, for every  $\underline{v} \in V$ ,

$$\begin{aligned} & \sigma_T \cdot (\underline{v}_T - \dot{\underline{u}}_T) + c_T [(u_n - g)_+]^{m_T} (|\underline{v}_T - \dot{\underline{u}}_T^C| + |\dot{\underline{u}}_T - \dot{\underline{u}}_T^C|) \geq 0 \\ & \text{on } \Gamma_C \times (0, T) \end{aligned}$$

and this produces the inequality sign in (3.3.13).  $\square$



**Remark 3.3.4.** Denoting by  $A \in L(V, V')$  and  $C \in L(V, V')$ , the operators

$$\langle \tilde{A}w, \tilde{v} \rangle = a(\tilde{w}, \tilde{v}), \quad \langle \tilde{C}w, \tilde{v} \rangle = c(\tilde{w}, \tilde{v}), \quad \forall \tilde{w}, \tilde{v} \in V$$

the statements (3.3.11) and (3.3.13) can be expressed, respectively, in the equivalent operator forms,

$$\begin{aligned} \tilde{u}(t) + \tilde{A}u(t) + P(\tilde{u}(t)) &= \tilde{f}(t) \text{ in } V' \\ \tilde{u}(t) + \tilde{A}u(t) + \tilde{C}\dot{u}(t) + P(\tilde{u}(t)) + \partial_2 j(\tilde{u}(t), \dot{\tilde{u}}(t) - \dot{\tilde{\phi}}(t)) &\ni \\ &\tilde{f}(t) \text{ in } V' \end{aligned}$$

where  $\partial_2 j(\tilde{u}(t), \dot{\tilde{u}}(t) - \dot{\tilde{\phi}}(t))$  denotes the partial subdifferential of  $j$  with respect to the second argument (velocity) at  $(\tilde{u}(t), \dot{\tilde{u}}(t) - \dot{\tilde{\phi}}(t)) \in V \times V$  (note that  $j$  is convex with respect to the velocity argument).  $\square$

### 3.4. Existence and uniqueness results for dynamic contact problems

**Theorem 3.4.1:** In addition to the assumptions listed in the preceding sections, let

$$\left. \begin{aligned} 1 \leq m_n &\begin{cases} < +\infty & \text{if } N=2 \\ \leq 3 & \text{if } N=3 \end{cases} \\ q &= 1 + m_n \end{aligned} \right\} \quad (3.4.1)$$

$$\left. \begin{aligned} \underline{b}, \dot{\underline{b}} &\in L^2(0, T; H) \\ \underline{t}, \dot{\underline{t}} &\in L^2(0, T; (L^{q'}(\Gamma_F))^N) \\ [\text{hence } \underline{f}, \dot{\underline{f}} &\in L^2(0, T; V')] \end{aligned} \right\} \quad (3.4.2)$$

$$\left. \begin{aligned} \underline{u}_0 &\in V \\ \underline{u}_1 &\in H. \end{aligned} \right\} \quad (3.4.3)$$

Then, there exists a unique solution for Problem 1 such that

$$\left. \begin{aligned} \underline{u} &\in L^\infty(0, T; V) \\ \dot{\underline{u}} &\in L^\infty(0, T; H) \\ \ddot{\underline{u}} &\in L^\infty(0, T; V') \end{aligned} \right\} \quad (3.4.4)$$

**Proof:** We first prove the existence of solutions. Let  $\{\underline{w}_i\}_{i=1}^\infty$  be a sequence of functions such that,

$$\underline{w}_i \in V \quad \forall i; \quad (3.4.5)$$

$$\begin{aligned} \underline{w}_1, \dots, \underline{w}_m &\text{ are linearly independent } \forall m, \\ &\text{and span the subspace } V_m \text{ of } V; \end{aligned} \quad (3.4.6)$$

$$V = \overline{\bigcup_{m \geq 1} V_m}. \quad (3.4.7)$$

Let us consider the following Faedo-Galerkin approximation of Problem 1:

Find a function  $\underline{u}^m : \Omega \times [0, T] \rightarrow \mathbb{R}^N$  in the form

$$\underline{u}^m(\underline{x}, t) = \sum_{i=1}^m U_i^m(t) \underline{w}_i(\underline{x}) \quad (3.4.8)$$

such that

$$(\dot{u}^m(t), \underline{v}) + a(\underline{u}^m(t), \underline{v}) + \langle P(\underline{u}^m(t)), \underline{v} \rangle = \langle f(t), \underline{v} \rangle \quad \forall \underline{v} \in V_m \quad (3.4.9)$$

with the initial conditions

$$\left. \begin{aligned} \underline{u}^m(0) = \underline{u}_0^m &= \sum_{i=1}^m \alpha_i^m \underline{w}_i \rightarrow \underline{u}_0 \text{ in } V \text{ as } m \rightarrow \infty \\ \dot{\underline{u}}^m(0) = \dot{\underline{u}}_1^m &= \sum_{i=1}^m \beta_i^m \underline{w}_i \rightarrow \underline{u}_1 \text{ in } H \text{ as } m \rightarrow \infty \end{aligned} \right\} \quad (3.4.10)$$

From the theory of systems of ordinary differential equations, it is known that a solution for (3.4.9,10) exists in an interval  $[0, t_m]$ . We proceed to obtain *a priori estimates* on the solution that ultimately will show that  $t_m = T$ .

Letting  $\underline{v} = \dot{\underline{u}}^m(t)$  in (3.4.9), it follows that

$$\begin{aligned} \frac{d}{dt} \left[ \frac{1}{2} |\dot{\underline{u}}^m(t)|^2 + \frac{1}{2} a(\underline{u}^m(t), \underline{u}^m(t)) + p(\underline{u}^m(t)) \right] &= \\ &= \langle f(t), \dot{\underline{u}}^m(t) \rangle \end{aligned} \quad (3.4.11)$$

where  $p: V \rightarrow \mathbb{R}$  denotes the energy associated with the normal deformation of the interface,

$$p(\underline{v}) = \frac{1}{m_n+1} \int_{\Gamma_C} c_n [(v_n - g)_+]^{m_n+1} ds, \quad \underline{v} \in V.$$

Integrating (3.4.11) in time from 0 to  $t$ , integrating by parts its right-hand side, using the continuity and  $V$ -ellipticity properties (3.3.8,9) of  $a(\cdot, \cdot)$  and Young's inequality, we obtain

$$\begin{aligned}
& |\dot{\tilde{u}}^m(t)|^2 + \alpha_a \|\tilde{u}^m(t)\|^2 \\
& \leq |\dot{\tilde{u}}^m(0)|^2 + M_a \|\tilde{u}^m(0)\|^2 + C_1 \|c_n\|_{\infty, \Gamma_C} \|u_n^m(0) - g\|_{q, \Gamma_C}^q \\
& + \frac{1}{\delta_1} \|f(t)\|_*^2 + \delta_1 \|\tilde{u}^m(t)\|^2 + \int_0^t \|f(\tau)\|_*^2 d\tau + \int_0^t \|\tilde{u}^m(\tau)\|^2 d\tau
\end{aligned}$$

where the  $\delta_i (i=1, 2, \dots)$  denote arbitrary positive constants and the  $C_i (i=1, 2, \dots)$  denote positive constants independent of  $m$ . Now, choosing  $\delta_1$  such that  $\delta_1 < \alpha_a$ , observing that  $\tilde{f}, \dot{\tilde{f}} \in L^2(0, T; V')$  implies that  $\tilde{f} \in C^0([0, T]; V')$ , and taking into account the boundedness of  $\tilde{u}^m(0)$  and  $\dot{\tilde{u}}^m(0)$  implied by the initial conditions (3.4.10), it follows that

$$|\dot{\tilde{u}}^m(t)|^2 + \|\tilde{u}^m(t)\|^2 \leq C_2 + C_3 \int_0^t (|\dot{\tilde{u}}^m(\tau)|^2 + \|\tilde{u}^m(\tau)\|^2) d\tau$$

Application of the Gronwall inequality then leads to the desired estimate,

$$|\dot{\tilde{u}}^m(t)|^2 + \|\tilde{u}^m(t)\|^2 \leq C_4$$

i.e.,

$$\tilde{u}^m \in \text{bounded set of } L^\infty(0, T; V); \quad (3.4.12)$$

$$\dot{\tilde{u}}^m \in \text{bounded set of } L^\infty(0, T; H); \quad (3.4.13)$$

and also,

$$c_n[(u_n^m - g)_+]^{m_n} \in \text{bounded set of } L^\infty(0, T; L^{q'}(\Gamma_C)). \quad (3.4.14)$$

With these estimates, we are now in position to take the limit as  $m \rightarrow \infty$ .

First we observe that (3.4.12-14) imply that there exists a

subsequence of  $\underline{u}^m$ , also denoted  $\underline{u}^m$ , such that

$$\underline{u}^m \rightharpoonup \underline{u} \text{ weak star in } L^\infty(0,T;V), \quad (3.4.15)$$

$$\dot{\underline{u}}^m \rightharpoonup \dot{\underline{u}} \text{ weak star in } L^\infty(0,T;H), \quad (3.4.16)$$

$$c_n[(u_n^m - g)_+]^{m_n} \rightharpoonup \chi \text{ weak star in } L^\infty(0,T;L^{q'}(\Gamma_C)). \quad (3.4.17)$$

In order to show that  $\chi = c_n[(u_n - g)_+]^{m_n}$ , we first observe that (3.4.12, 13) imply that

$$\underline{u}^m \in \text{bounded set of } \left( H^1(\Omega \times (0,T)) \right)^N.$$

Since the trace map is compact from  $H^1(\Omega \times (0,T))$  to  $L^2(\Gamma \times (0,T))$ , it follows that (by extracting a subsequence of  $\underline{u}^m$  again denoted by  $\underline{u}^m$ ),

$$\underline{u}^m \rightarrow \underline{u} \text{ strongly in } \left( L^2(\Gamma \times (0,T)) \right)^N \text{ and a.e. on } \Gamma \times (0,T)$$

and then,

$$c_n[(u_n^m - g)_+]^{m_n} \rightarrow c_n[(u_n - g)_+]^{m_n} \text{ a.e. on } \Gamma_C \times (0,T). \quad (3.4.18)$$

On the other hand, (3.4.14) implies that

$$c_n[(u_n^m - g)_+]^{m_n} \in \text{bounded set of } L^{q'}(\Gamma_C \times (0,T)). \quad (3.4.19)$$

From (3.4.18) and (3.4.19) it follows (c.f. Lions [1969], Lemma 1.3, pp.12, 13]) that  $c_n[(u_n^m - g)_+]^{m_n} \rightarrow c_n[(u_n - g)_+]^{m_n}$  weakly in  $L^{q'}(\Gamma_C \times (0,T))$ .

Since (3.4.17) also implies that  $c_n[(u_n^m - g)_+]^{m_n} \rightharpoonup \chi$  weakly in  $L^{q'}(\Gamma_C \times (0,T))$ , the uniqueness of weak limits implies that, in fact,  $\chi = c_n[(u_n - g)_+]^{m_n}$  and

$$c_n[(u_n^m - g)_+]^{m_n} \rightharpoonup c_n[(u_n - g)_+]^{m_n} \text{ weak star in } L^\infty(0,T;L^{q'}(\Gamma_C)). \quad (3.4.20)$$

Let now  $v$  in (3.4.9) be equal to  $\underline{w}_j$ , with  $j$  fixed and  $m > j$ , i.e.

$$(\underline{u}^m, \underline{w}_j) + a(\underline{u}^m, \underline{w}_j) + \langle P(\underline{u}^m), \underline{w}_j \rangle = \langle \underline{f}, \underline{w}_j \rangle \quad (3.4.21)$$

From (3.4.15) and (3.4.16) it follows that, as  $m \rightarrow \infty$ ,

$$a(\underline{u}^m, \underline{w}_j) \rightarrow a(\underline{u}, \underline{w}_j) \text{ weak star in } L^\infty(0, T) \quad (3.4.22)$$

$$(\dot{\underline{u}}^m, \underline{w}_j) \rightarrow (\dot{\underline{u}}, \underline{w}_j) \text{ weak star in } L^\infty(0, T) \quad (3.4.23)$$

and then

$$\begin{aligned} (\ddot{\underline{u}}^m, \underline{w}_j) &= \frac{d}{dt} (\dot{\underline{u}}^m, \underline{w}_j) \rightarrow \frac{d}{dt} (\dot{\underline{u}}, \underline{w}_j) = \frac{d}{dt} \langle \dot{\underline{u}}, \underline{w}_j \rangle = \\ &= \langle \ddot{\underline{u}}, \underline{w}_j \rangle \text{ in } \mathcal{D}'(0, T) \end{aligned} \quad (3.4.24)$$

and, from (3.4.20),

$$\langle P(\underline{u}^m), \underline{w}_j \rangle \rightarrow \langle P(\underline{u}), \underline{w}_j \rangle \text{ weak star in } L^\infty(0, T).$$

We can conclude from (3.4.21) that

$$\langle \ddot{\underline{u}}, \underline{w}_j \rangle + a(\underline{u}, \underline{w}_j) + \langle P(\underline{u}), \underline{w}_j \rangle = \langle \underline{f}, \underline{w}_j \rangle \text{ in } \mathcal{D}'(0, T) \quad \forall j \geq 1.$$

It follows from (3.4.7) that (3.3.11) holds in  $\mathcal{D}'(0, T)$ . Furthermore, since  $\underline{u} \in L^\infty(0, T; V)$ , we have  $A\underline{u} \in L^\infty(0, T; V')$  and  $P(\underline{u}) \in L^\infty(0, T; V')$  and, since  $\underline{f}, \dot{\underline{f}} \in L^2(0, T; V')$ , we also have  $\underline{f} \in L^\infty(0, T; V')$ . We can thus conclude that  $\ddot{\underline{u}} \in L^\infty(0, T; V')$  and that (3.3.11) holds for a.e.  $t \in [0, T]$ .

Finally, we have to prove that  $\underline{u}$  and  $\dot{\underline{u}}$  satisfy the initial conditions (3.3.12).

From (3.4.15) and (3.4.16) it follows that,  $\underline{u}^m(0) \rightarrow \underline{u}(0)$  weakly in  $H$  and from (3.4.10) it follows that also  $\underline{u}^m(0) \rightarrow \underline{u}_0$  weakly

in  $H$ . The uniqueness of weak limits implies then that  $(3.3.12)_1$  is satisfied.

On the other hand, from  $(3.4.24)$  and  $(3.4.4)_3$  it follows that  $\langle \underline{\dot{u}}^m, \underline{w}_j \rangle \rightarrow \langle \underline{\dot{u}}, \underline{w}_j \rangle$  weak star in  $L^\infty(0,T)$ . This, together with  $(3.4.23)$  implies that  $\langle \underline{\dot{u}}^m(0), \underline{w}_j \rangle \rightarrow \langle \underline{\dot{u}}(0), \underline{w}_j \rangle$  and, since from  $(3.4.10)$ ,  $\langle \underline{\dot{u}}^m(0), \underline{w}_j \rangle \rightarrow \langle \underline{\bar{u}}_1, \underline{w}_j \rangle$ , it follows that  $\langle \underline{\dot{u}}(0), \underline{w}_j \rangle = \langle \underline{\bar{u}}_1, \underline{w}_j \rangle \quad \forall j \geq 1$ . The density property  $(3.4.7)$  finally implies that  $(3.3.12)_2$  holds. This concludes the existence proof.

We now prove the uniqueness of solution. Let  $\underline{u}$  and  $\underline{u+w}$ , both satisfying  $(3.4.4)$ , be two solutions of Problem 1, for the same data and with assumptions  $(3.4.1-3)$  in force. Writing the variational statement  $(3.3.11)$  for  $\underline{u+w}$  and  $\underline{u}$  and subtracting the resulting equations, we obtain

$$\langle \underline{\ddot{w}}(t), \underline{v} \rangle + a(\underline{w}(t), \underline{v}) + \langle P(\underline{u}(t) + \underline{w}(t)) - P(\underline{u}(t)), \underline{v} \rangle = 0$$

$$\forall \underline{v} \in V$$

i.e.,

$$\underline{\ddot{w}} + A\underline{w} + P(\underline{u+w}) - P(\underline{u}) = \underline{0} \text{ in } L^\infty(0,T;V') \quad (3.4.25)$$

with the initial conditions

$$\underline{w}(0) = \underline{\dot{w}}(0) = \underline{0} \quad (3.4.26)$$

Alternatively, we can put  $(3.4.25,26)$  in the form of a first order differential equation:

$$\left. \begin{aligned} \underline{\dot{X}} &\stackrel{\text{def}}{=} [\underline{w}, \underline{z}] \in L^\infty(0,T;V \times H) \\ \underline{\dot{X}}(\cdot) &= F(\underline{X}(\cdot), \cdot) \text{ in } L^\infty(0,T;H \times V') \\ \underline{X}(0) &= \underline{0} \text{ in } V \times H \end{aligned} \right\} \quad (3.4.27)$$

where  $F : (V \times H) \times [0, T] \rightarrow H \times V'$  is given by,

$$F(\underline{w}, \underline{z}, t) = [\underline{z}, -A\underline{w} + P(\underline{u}(t)) - P(\underline{u}(t) + \underline{w})],$$

$$\forall [\underline{w}, \underline{z}] \in V \times H, \text{ for a.e.t. } \in [0, T].$$

We then need to show that for any given  $\underline{u} \in L^\infty(0, T; V)$  the only solution of (3.4.27) is the trivial solution  $[0, 0]$ .

We can also put (3.4.27) in the integral equation form,

$$\underline{X}(t) = \int_0^t F(\underline{X}(\tau), \tau) d\tau. \quad (3.4.28)$$

Since  $\underline{X}(t) \in V \times H \subset H \times V'$  we can compute  $\|\underline{X}(t)\|_{H \times V'}$  and we have,

$$\|\underline{X}(t)\|_{H \times V'} \leq \int_0^t \|F(\underline{X}(\tau), \tau)\|_{H \times V'} d\tau.$$

But,

$$\begin{aligned} & \|F(\underline{X}(\tau), \tau)\|_{H \times V'} \\ &= \|\underline{z}(\tau)\| + \|-A\underline{w}(\tau) - P(\underline{u}(\tau) + \underline{w}(\tau)) + P(\underline{u}(\tau))\|_* \\ &\leq \|\underline{z}(\tau)\| + C_1 \|\underline{w}(\tau)\| \end{aligned}$$

$$+ \sup_{\substack{\underline{y} \in V \\ \underline{y} \neq 0}} \left\{ \frac{\|c_n\|_{\infty, \Gamma_C}}{\|\underline{y}\|} \int_{\Gamma_C} |[(u_n(\tau) - g)_+]^{m_n} - [(u_n(\tau) + w_n(\tau) - g)_+]^{m_n}| |\underline{v}_n| ds \right\}$$

and

$$\begin{aligned} & |[(u_n(\tau) - g)_+]^{m_n} - [(u_n(\tau) + w_n(\tau) - g)_+]^{m_n}| \\ &\leq m_n (|u_n(\tau) - g|^{m_n-1} + |u_n(\tau) + w_n(\tau) - g|^{m_n-1}) |w_n(\tau)|. \end{aligned}$$

Since both  $\underline{u}$  and  $\underline{u} + \underline{w}$  exist in  $L^\infty(0, T; V)$ , we have

$$\int_{\Gamma_C} |[(u_n(\tau) - g)_+]^{m_n} - [(u_n(\tau) + w_n(\tau) - g)_+]^{m_n}| |\underline{v}_n| ds$$



$$\begin{aligned}
&\leq m_n \| |u_n(\tau) - g|^{m_n-1} + |u_n(\tau) + w_n(\tau) - g|^{m_n-1} \|_{\frac{q}{q-2}, \Gamma_C} \|w_n(\tau)\|_{q, \Gamma_C} \|v_n\|_{q, \Gamma_C} \\
&\leq C_2 \|w(\tau)\| \|v\|
\end{aligned} \tag{3.4.29}$$

and then

$$\|F(\underline{X}(\tau), \tau)\|_{H \times V'} \leq |z(\tau)| + C_1 \|\underline{w}(\tau)\| + C_2 \|\underline{w}(\tau)\| \leq C_3 \|\underline{X}(\tau)\|_{H \times V'}.$$

We have thus

$$\|\underline{X}(t)\|_{H \times V'} \leq C_3 \int_0^t \|\underline{X}(\tau)\|_{H \times V'} d\tau$$

which, when we apply Gronwall's inequality, allows us to conclude that

$$\underline{X} \approx 0 \text{ in } L^\infty(0, T; H \times V'), \text{ hence in } L^\infty(0, T; V \times H).$$

This concludes the proof of the theorem.  $\square$

**Remark 3.4.1.** The uniqueness of solutions obtained in Theorem 3.4.1 implies (by using a simple contradiction argument) that the whole sequence  $\underline{u}^m$  of the solutions of the finite dimensional problem (3.4.8-10) (and not only some subsequence of it) converges, in the weak sense of (3.4.15,16) to the solution  $\underline{u}$  of Problem 1.  $\square$

Turning now to Problem 2, we have:

**Theorem 3.4.2.<sup>2</sup>** In addition to the assumptions listed in Sections 3.2 and 3.3, let

$$\left. \begin{aligned} 1 \leq m_n, m_T &\begin{cases} < +\infty & \text{if } N=2 \\ < 3 & \text{if } N=3 \end{cases} \\ q &= 1 + \max\{m_n, m_T\} \end{aligned} \right\} \tag{3.4.30}$$

$$\left. \begin{aligned} \underline{b} &\in L^2(0,T;H) \\ \underline{t} &\in L^2(0,T;(L^{q'}(\Gamma_C))^N) \\ [\text{hence } \underline{f} &\in L^2(0,T;V')] \end{aligned} \right\} \quad (3.4.31)$$

$$\begin{aligned} \exists \underline{\Phi} \in V, \exists \Theta \in H^2(0,T) \text{ such that } \underline{\phi}(\underline{x},t) &= \underline{\Phi}(\underline{x}) \cdot \Theta(t) \\ \text{a.e. } (\underline{x},t) &\in \Omega \times (0,T) \end{aligned} \quad (3.4.32)$$

$$\left. \begin{aligned} \underline{u}_0 &\in V \\ \underline{u}_1 &\in H \end{aligned} \right\} \quad (3.4.33)$$

Then, there exists a unique solution to Problem 2, such that

$$\left. \begin{aligned} \underline{u} &\in L^\infty(0,T;V) \\ \dot{\underline{u}} &\in L^\infty(0,T;H) \cap L^2(0,T;V) \\ \ddot{\underline{u}} &\in L^2(0,T;V') \end{aligned} \right\} \quad (3.4.34)$$

**Proof:** We start by proving *uniqueness*. Let  $\underline{u}^1$  and  $\underline{u}^2$  be two solutions of Problem 2, both satisfying (3.4.34), for the same data and with hypotheses (3.4.30-3.4.33) in force. Writing the variational statement (3.3.13), successively for  $\underline{u}^1$  and  $\underline{u}^2$ , taking  $\underline{v}$  equal to  $\dot{\underline{u}}^2(t)$  in the first statement and equal to  $\dot{\underline{u}}^1(t)$  in the second and adding the resulting inequalities, we obtain,

$$\begin{aligned} &\frac{1}{2} \frac{d}{dt} [|\dot{\underline{w}}(t)|^2 + a(\underline{w}(t), \underline{w}(t))] + c(\dot{\underline{w}}(t), \dot{\underline{w}}(t)) \\ &\leq \langle P(\underline{u}^2(t)) - P(\underline{u}^1(t)), \dot{\underline{w}}(t) \rangle \end{aligned}$$

<sup>2</sup>Assumptions (3.4.31-33) and conclusions (3.4.34) are very similar to those in Duvaut and Lions [1976, Theorem 6.1 bis, p. 167]. Assumption (3.4.32), together with previous assumptions on  $\underline{\phi}$  in Section 3.3, requires  $\underline{\Phi}_n = 0$  a.e. on  $\Gamma_C$  and  $\underline{\Phi}_T \cdot \dot{\underline{\Theta}} = \dot{\underline{U}}_T^C$  a.e. on  $\Gamma_C \times (0,T)$ .

$$\begin{aligned}
& + j(\underline{u}^1(t), \underline{\dot{u}}^2(t) - \dot{\underline{\phi}}(t)) - j(\underline{u}^1(t), \underline{\dot{u}}^1(t) - \dot{\underline{\phi}}(t)) \\
& + j(\underline{u}^2(t), \underline{\dot{u}}^1(t) - \dot{\underline{\phi}}(t)) - j(\underline{u}^2(t), \underline{\dot{u}}^2(t) - \dot{\underline{\phi}}(t))
\end{aligned}$$

where  $\underline{w} = \underline{u}^1 - \underline{u}^2$  and  $\underline{w}(0) = \dot{\underline{w}}(0) = 0$ . Integration of this equation in time from 0 to  $t$  leads to the estimate

$$\begin{aligned}
& |\dot{\underline{w}}(t)|^2 + \alpha_a \|\underline{w}(t)\|^2 + 2\alpha_c \int_0^t \|\dot{\underline{w}}(\tau)\|^2 d\tau \\
& \leq 2 \int_0^t \int_{\Gamma_c} c_n |[(u_n^2(\tau) - g)_+]^{m_n} - [(u_n^1(\tau) - g)_+]^{m_n}| \cdot |\dot{\underline{w}}_n(\tau)| ds d\tau \\
& + 2 \int_0^t \int_{\Gamma_c} c_T |[(u_n^2(\tau) - g)_+]^{m_T} - [(u_n^1(\tau) - g)_+]^{m_T}| \cdot |\dot{\underline{w}}_T(\tau)| ds d\tau .
\end{aligned}$$

Using an estimation of the type in (3.4.29) and Young's inequality we obtain

$$|\dot{\underline{w}}(t)|^2 + \|\underline{w}(t)\|^2 \leq c_1 \int_0^t (|\dot{\underline{w}}(\tau)|^2 + \|\underline{w}(\tau)\|^2) d\tau$$

from which the uniqueness follows.  $\square$

In order to prove the existence of a solution for Problem 2, we shall first introduce a family of (convex and Gâteaux differentiable with respect to the velocity argument) approximations of the friction functional  $j$ , depending on a real parameter  $\varepsilon > 0$ . Accordingly, a regularized version of Problem 2 will be introduced and the questions of existence and uniqueness for this auxiliary problem will be studied. Only after this we shall complete the

proof of Theorem 3.4.2 by showing that, as the regularization parameter  $\epsilon \rightarrow 0$ , the solutions of the approximate problems converge, in an appropriate sense, to the solution of the original Problem 2.

Let us first consider a family of functions  $\psi_\epsilon: \mathbb{R}^N \rightarrow \mathbb{R}$  depending on a real parameter  $\epsilon > 0$ , satisfying the following conditions (sufficient for our purposes),

$$(i) \quad \psi_\epsilon \in C^1(\mathbb{R}^N, \mathbb{R}) \quad \forall \epsilon > 0 \quad (3.4.35)$$

$$(ii) \quad 0 \leq \psi_\epsilon(\underline{v}) \leq |\underline{v}| \quad \forall \epsilon > 0, \quad \forall \underline{v} \in \mathbb{R}^N \quad (3.4.36)$$

$$(iii) \quad \psi_\epsilon(\theta \underline{w} + (1-\theta)\underline{v}) \leq \theta \psi_\epsilon(\underline{w}) + (1-\theta)\psi_\epsilon(\underline{v}) \quad (3.4.37)$$

$$\forall \epsilon > 0, \quad \forall (\underline{w}, \underline{v}) \in \mathbb{R}^N \times \mathbb{R}^N, \quad \forall \theta \in [0, 1]$$

$$(iv) \quad \exists D_1 > 0 \text{ such that } \forall \epsilon > 0, \quad \forall (\underline{w}, \underline{v}) \in \mathbb{R}^N \times \mathbb{R}^N$$

$$|\psi'_\epsilon(\underline{w})(\underline{v})| \leq D_1 |\underline{v}| \quad (3.4.38)$$

$$(v) \quad \exists D_2 > 0 \text{ such that } \forall \epsilon > 0, \quad \forall \underline{v} \in \mathbb{R}^N,$$

$$|\psi_\epsilon(\underline{v}) - |\underline{v}|| \leq D_2 \epsilon \quad (3.4.39)$$

where  $\psi'_\epsilon(\underline{w})(\underline{v})$  denotes the directional derivative of  $\psi_\epsilon$  at  $\underline{w}$  on the direction of  $\underline{v}$  and  $|\cdot|$  denotes here the euclidean norm of a vector in  $\mathbb{R}^N$ .

We now define a family of regularized friction functionals

$j_\epsilon: V \times V \rightarrow \mathbb{R}$ , depending on the parameter  $\epsilon > 0$

$$j_\epsilon(\underline{w}, \underline{v}) = \int_C c_T[(\underline{w}_n - \underline{g})_+]^m \psi'_\epsilon(\underline{v}_T) ds, \quad \underline{w}, \underline{v} \in V$$

which, as a result of (3.4.35-38), are well-defined, and convex and Gâteaux-differentiable with respect to the second argument. The partial Gâteaux-derivative of  $j_\epsilon$  with respect to the second argument at  $(\underline{w}, \underline{v}) \in V \times V$  in the direction of  $\underline{z} \in V$  is given by

$$\langle J_\epsilon(\underline{w}, \underline{v}), \underline{z} \rangle = \int_C c_T[(\underline{w}_n - \underline{g})_+]^m \psi'_\epsilon(\underline{v}_T)(\underline{z}_T) ds, \quad \underline{w}, \underline{v}, \underline{z} \in V.$$

With the above definitions we study now the regularized version of Problem 2.

**Problem 2 $_\epsilon$**  (viscous damping and regularized friction). Find a function  $t \mapsto \underline{u}_\epsilon(t)$  of  $[0, T] \rightarrow V$  such that,

$$\left. \begin{aligned} &\langle \ddot{\underline{u}}_\epsilon(t), \underline{v} \rangle + a(\underline{u}_\epsilon(t), \underline{v}) + c(\dot{\underline{u}}_\epsilon(t), \underline{v}) \\ &+ \langle P(\underline{u}_\epsilon(t)), \underline{v} \rangle + \langle J_\epsilon(\underline{u}_\epsilon(t), \dot{\underline{u}}_\epsilon(t) - \dot{\underline{\phi}}(t)), \underline{v} \rangle \\ &= \langle \underline{f}(t), \underline{v} \rangle \quad \forall \underline{v} \in V \end{aligned} \right\} \quad (3.4.40)$$

with the initial conditions,

$$\left. \begin{aligned} \underline{u}_\epsilon(0) &= \underline{\bar{u}}_0 \\ \dot{\underline{u}}_\epsilon(0) &= \underline{\bar{u}}_1 \end{aligned} \right\} \quad (3.4.41)$$

**Lemma 3.4.1.** Let the hypotheses of Theorem 3.4.2 hold. Then, there exists a unique solution to Problem 2 $_\epsilon$ , such that

$$\left. \begin{aligned} \underline{u}_\epsilon &\in L^\infty(0, T; V) \\ \dot{\underline{u}}_\epsilon &\in L^\infty(0, T; H) \cap L^2(0, T; V) \\ \ddot{\underline{u}}_\epsilon &\in L^2(0, T; V') \end{aligned} \right\} \quad (3.4.42)$$

**Proof.** Again with the assumptions (3.4.5-7), but choosing now  $w_1 = \bar{\phi}$  (recall (3.4.32)), we consider the Faedo-Galerkin approximations for Problem 2<sub>ε</sub>:

Find a function  $u_\varepsilon^m: \mathbb{R}_+ \times [0, T] \rightarrow \mathbb{R}^N$  in the form (3.4.8) such that,

$$\left. \begin{aligned} & (\ddot{u}_\varepsilon^m(t), v) + a(u_\varepsilon^m(t), v) + c(\dot{u}_\varepsilon^m(t), v) \\ & + \langle P(u_\varepsilon^m(t)), v \rangle + \langle J_\varepsilon(u_\varepsilon^m(t), \dot{u}_\varepsilon^m(t) - \dot{\bar{\phi}}(t)), v \rangle \\ & = \langle f(t), v \rangle \quad \forall v \in V_m \end{aligned} \right\} \quad (3.4.43)$$

with the initial conditions,

$$\left. \begin{aligned} u_\varepsilon^m(0) &= u_{\varepsilon 0}^m \rightarrow \bar{u}_0 \text{ strongly in } V \text{ as } m \rightarrow \infty; \\ \dot{u}_\varepsilon^m(0) &= u_{\varepsilon 1}^m \rightarrow \bar{u}_1 \text{ strongly in } H \text{ as } m \rightarrow \infty. \end{aligned} \right\} \quad (3.4.44)$$

Letting  $v = \dot{u}_\varepsilon^m(t) - \dot{\bar{\phi}}(t)$  in (3.4.43) we proceed to obtain *a priori estimates* on the solution  $u_\varepsilon^m$ . First we obtain,

$$\begin{aligned} & \frac{d}{dt} \left[ \frac{1}{2} |\dot{u}_\varepsilon^m(t)|^2 + \frac{1}{2} a(u_\varepsilon^m(t), u_\varepsilon^m(t)) + p(u_\varepsilon^m(t)) \right] \\ & + c(\dot{u}_\varepsilon^m(t), \dot{u}_\varepsilon^m(t)) + \langle J_\varepsilon(u_\varepsilon^m(t), \dot{u}_\varepsilon^m(t) - \dot{\bar{\phi}}(t)), \dot{u}_\varepsilon^m(t) - \dot{\bar{\phi}}(t) \rangle \\ & = \langle f(t), \dot{u}_\varepsilon^m(t) - \dot{\bar{\phi}}(t) \rangle + (\ddot{u}_\varepsilon^m(t), \dot{\bar{\phi}}(t)) + a(u_\varepsilon^m(t), \dot{\bar{\phi}}(t)) + \\ & \quad + c(\dot{u}_\varepsilon^m(t), \dot{\bar{\phi}}(t)). \end{aligned}$$

Integrating this equation from 0 to  $t$ , integrating by parts the term  $(\ddot{u}_\varepsilon^m(t), \dot{\bar{\phi}}(t))$ , observing that  $\langle J_\varepsilon(w, v), v \rangle \geq 0 \quad \forall w, v \in V$  and following steps similar to the previous proof, we finally obtain

AD-A174 585

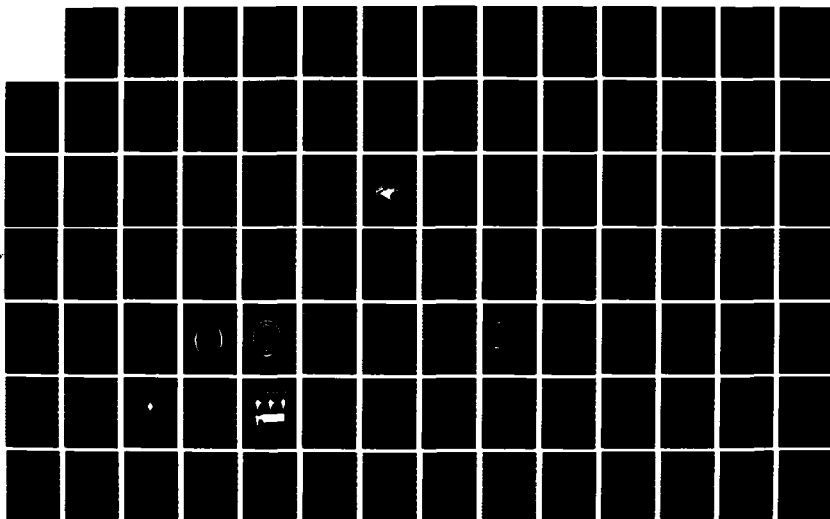
COMPUTATIONAL METHODS FOR NONLINEAR DYNAMICS PROBLEMS  
IN SOLID AND STRUCT (U) COMPUTATIONAL MECHANICS CO INC  
AUSTIN TX J T ODEN 31 MAR 86 TR-86-02 AFOSR-TR-86-2015  
F49620-84-C-0024

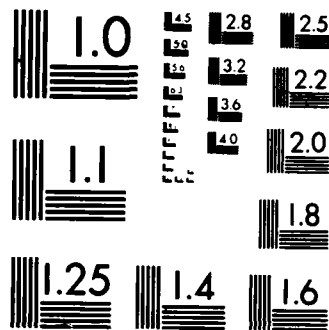
2/4

UNCLASSIFIED

F/G 20/11

NL





XEROCOPY RESOLUTION TEST CHART  
NATIONAL BUREAU OF STANDARDS-1963-A



$$\begin{aligned}
& \|\dot{u}_\epsilon^m(t)\|^2 + \|u_\epsilon^m(t)\|^2 + \int_0^t \|\dot{u}_\epsilon^m(\tau)\|^2 d\tau \\
& \leq C_1 + C_2 \int_0^t (\|\dot{u}_\epsilon^m(\tau)\|^2 + \|u_\epsilon^m(\tau)\|^2) d\tau
\end{aligned}$$

We have then

$$u_\epsilon^m \in \text{bounded set of } L^\infty(0, T; V) \quad (3.4.45)$$

$$\dot{u}_\epsilon^m \in \text{bounded set of } L^\infty(0, T; H) \cap L^2(0, T; V) \quad (3.4.46)$$

$$c_n[(u_{\epsilon n}^m - g)_+]^m \in \text{bounded set of } L^\infty(0, T; L^{q'}(\Gamma_C)) \quad (3.4.47)$$

$$c_T[(u_{\epsilon n}^m - g)_+]^{m_T} \in \text{bounded set of } L^\infty(0, T; L^{q'}(\Gamma_C)) , \quad (3.4.48)$$

with all the bounds independent of  $m$  and  $\epsilon$ . It follows that a subsequence of  $u_\epsilon^m$ , again denoted  $u_\epsilon^m$ , exists such that as  $m \rightarrow \infty$ ,

$$u_\epsilon^m \rightharpoonup u_\epsilon \text{ weak star in } L^\infty(0, T; V) \quad (3.4.49)$$

$$\dot{u}_\epsilon^m \rightharpoonup \dot{u}_\epsilon \text{ weak star in } L^\infty(0, T; H) \text{ and weakly in } L^2(0, T; V) \quad (3.4.50)$$

and, using the compactness arguments used earlier,

$$\left. \begin{aligned}
c_n[(u_{\epsilon n}^m - g)_+]^{m_n} &\rightarrow c_n[(u_{\epsilon n} - g)_+]^{m_n} \\
c_T[(u_{\epsilon n}^m - g)_+]^{m_T} &\rightarrow c_T[(u_{\epsilon n} - g)_+]^{m_T}
\end{aligned} \right\} \text{weak star in } L^\infty(0, T; L^{q'}(\Gamma_C)) \quad (3.4.51)$$

It turns out, however, that we can obtain, and we shall need later, stronger results. In fact, introducing the spaces,

$$W = \{v \in (H^{\frac{1}{2}}(\Gamma))^N : v = 0 \text{ a.e. on } \Gamma_D\}$$

$$G = \{v \in (L^q(\Gamma))^N : v = 0 \text{ a.e. on } \Gamma_D\}$$

it follows from (3.4.49,50) that, in particular,

$$\underline{u}_\epsilon^m \rightharpoonup \underline{u} \text{ weakly in } L^2(0,T;W)$$

$$\dot{\underline{u}}_\epsilon^m \rightharpoonup \dot{\underline{u}}_\epsilon \text{ weakly in } L^2(0,T;G).$$

Since  $W \subset G$  with compact injection, it follows from Lions [1969, Theorem 5.1, pp. 58-59] that  $\underline{u}_\epsilon^m \rightarrow \underline{u}_\epsilon$  strongly in  $L^2(0,T;G)$  and, consequently,

$$\underline{u}_{\epsilon n}^m \rightarrow \underline{u}_{\epsilon n} \text{ strongly in } L^2(0,T;L^q(\Gamma_C)).$$

From this and (3.4.47,48) it results that

$$\left. \begin{aligned} c_n[(\underline{u}_{\epsilon n}^m - g)_+]^m &\rightarrow c_n[(\underline{u}_{\epsilon n} - g)_+]^m \\ c_T[(\underline{u}_{\epsilon n}^m - g)_+]^m &\rightarrow c_T[(\underline{u}_{\epsilon n} - g)_+]^m \end{aligned} \right\} \text{strongly in } L^2(0,T;L^{q'}(\Gamma_C)) \quad (3.4.52)$$

Let now  $\underline{v}$  in (3.4.43) be equal to  $\underline{w}_j$ , with  $j$  fixed and  $m > j$ . From (3.4.49-51) it follows, after taking the limit as  $m \rightarrow \infty$  and using arguments similar to those in the proof of Theorem 3.4.1, that

$$\begin{aligned} \langle \ddot{\underline{u}}_\epsilon, \underline{v} \rangle + a(\underline{u}_\epsilon, \underline{v}) + c(\dot{\underline{u}}_\epsilon, \underline{v}) + \langle P(\underline{u}_\epsilon), \underline{v} \rangle + \langle \chi_\epsilon, \underline{v} \rangle &= \langle \underline{f}, \underline{v} \rangle \\ \text{in } L^2(0,T) \quad \forall \underline{v} \in V \end{aligned} \quad (3.4.53)$$

with  $\underline{u}_\epsilon, \dot{\underline{u}}_\epsilon$  satisfying the initial conditions (3.4.41) and  $\ddot{\underline{u}}_\epsilon$  satisfying (3.4.42)<sub>3</sub>.

In order to conclude the existence proof, we have to show that in fact  $\chi_\epsilon = J_\epsilon(\underline{u}_\epsilon, \dot{\underline{u}}_\epsilon - \dot{\underline{\phi}})$  in  $L^2(0,T;V')$ . We do this by using a *monotonicity* argument of the type, e.g., in Duvaut and Lions [1976, Theorems 5.1, 5.2, pp. 55,56] and Lions [1969, Theorem 6.1, pp. 222-226]. The monotonicity of  $J_\epsilon$  with respect to the second argument (velocity) implies that

$$0 \leq \chi^m = \int_0^T \langle J_\epsilon(\underline{u}_\epsilon^m, \dot{\underline{u}}_\epsilon^m - \dot{\underline{\phi}}) - J_\epsilon(\underline{u}_\epsilon^m, \varphi - \dot{\underline{\phi}}), \dot{\underline{u}}_\epsilon^m - \varphi \rangle dt \quad \forall \varphi \in L^2(0,T;V).$$

But, from (3.4.43) it follows that,

$$\begin{aligned}
 0 \leq \chi^m = & -\frac{1}{2} |\dot{\underline{u}}_e^m(T)|^2 - \frac{1}{2} a(\underline{u}_e^m(T), \underline{u}_e^m(T)) - p(\underline{u}_e^m(T)) \\
 & + \frac{1}{2} |\dot{\underline{u}}_e^m(0)|^2 + \frac{1}{2} a(\underline{u}_e^m(0), \underline{u}_e^m(0)) + p(\underline{u}_e^m(0)) \\
 & + \int_0^T [\langle \underline{f}, \dot{\underline{u}}_e^m \rangle - c(\dot{\underline{u}}_e^m, \dot{\underline{u}}_e^m)] dt \\
 & - \int_0^T \langle J_\epsilon(\underline{u}_e^m, \dot{\underline{u}}_e^m - \dot{\underline{\phi}}), \underline{\varphi} \rangle dt \\
 & - \int_0^T \langle J_\epsilon(\underline{u}_e^m, \underline{\varphi} - \dot{\underline{\phi}}), \dot{\underline{u}}_e^m - \underline{\varphi} \rangle dt
 \end{aligned} \tag{3.4.54}$$

Since  $\dot{\underline{u}}_e^m(T) \rightharpoonup \dot{\underline{u}}_e(T)$  weakly in  $H$  and  $\underline{u}_e^m(T) \rightharpoonup \underline{u}_e(T)$  weakly in  $V$ , and taking into account the initial conditions (3.4.44), the strong convergence property (3.4.52) and the weak upper semi-continuity of various terms, we obtain

$$\begin{aligned}
 0 \leq \limsup_{m \rightarrow \infty} \chi^m \\
 \leq & -\frac{1}{2} |\dot{\underline{u}}_e(T)|^2 - \frac{1}{2} a(\underline{u}_e(T), \underline{u}_e(T)) - p(\underline{u}_e(T)) \\
 & + \frac{1}{2} |\dot{\underline{u}}_1|^2 + \frac{1}{2} a(\underline{u}_0, \underline{u}_0) + p(\underline{u}_0) \\
 & + \int_0^T [\langle \underline{f}, \dot{\underline{u}}_e \rangle - c(\dot{\underline{u}}_e, \dot{\underline{u}}_e)] dt \\
 & - \int_0^T \langle \underline{\chi}_e, \underline{\varphi} \rangle dt \\
 & - \int_0^T \langle J_\epsilon(\underline{u}_e, \underline{\varphi} - \dot{\underline{\phi}}), \dot{\underline{u}}_e - \underline{\varphi} \rangle dt
 \end{aligned} \tag{3.4.55}$$

On the other hand, integrating (3.4.53) from 0 to  $T$ , with  $\underline{v} = \dot{\underline{u}}_e(t)$ , we have

$$-\frac{1}{2} |\dot{\underline{u}}_e(T)|^2 - \frac{1}{2} a(\underline{u}_e(T), \underline{u}_e(T)) - p(\underline{u}_e(T))$$

$$\begin{aligned}
& + \frac{1}{2} |\bar{u}_1|^2 + \frac{1}{2} a(\bar{u}_0, \bar{u}_0) + p(\bar{u}_0) \\
& + \int_0^T [\langle f, \dot{u}_{\epsilon} \rangle - c(\dot{u}_{\epsilon}, \dot{u}_{\epsilon})] dt \\
& = \int_0^T \langle \chi_{\epsilon}, \dot{u}_{\epsilon} \rangle dt
\end{aligned}$$

and then,  $\forall \varphi \in L^2(0, T; V)$

$$0 \leq \int_0^T \langle \chi_{\epsilon} - J_{\epsilon}(u_{\epsilon}, \varphi - \dot{\phi}), \dot{u}_{\epsilon} - \varphi \rangle dt.$$

We can conclude (cf. Duvaut and Lions [1976, p. 56]) that  $\chi_{\epsilon} = J_{\epsilon}(u_{\epsilon}, \dot{u}_{\epsilon} - \dot{\phi})$  in  $L^2(0, T; V')$ , as desired. This concludes the proof of existence.

The uniqueness proof follows steps similar to those in Theorem (3.4.2) and is omitted.  $\square$

**Remark 3.4.2.** The step in the above proof that extends earlier results in Duvaut and Lions [1976, Theorem 6.1 bis, p.167] applicable for viscoelastic bodies with *prescribed normal stresses* on the frictional (regularized Coulomb's law) contact surface to the present situation, in which the *normal interface law* (2.5.2) holds, is precisely the one that requires the strong convergence (3.4.52). In fact, the passage from (3.4.54) to (3.4.55) relies on the fact that

$$\begin{aligned}
& \lim_{m \rightarrow \infty} \int_0^T \langle J_{\epsilon}(u_{\epsilon}^m, \varphi - \dot{\phi}), \dot{u}_{\epsilon}^m - \varphi \rangle dt \\
& = \lim_{m \rightarrow \infty} \int_0^T \int_{\Gamma_C} c_T [(u_{\epsilon}^m - g)_+]^m [\psi'_{\epsilon}(\varphi_T - \dot{u}_T^C)] (\dot{u}_{\epsilon}^m - \varphi_T) ds dt
\end{aligned}$$

$$\begin{aligned}
&= \int_0^T \int_{\Gamma_C} c_T[(u_{\epsilon n} - g)_+]^{m_T} [\psi'_\epsilon(\varphi_T - \dot{u}_T^C)(\dot{u}_{\epsilon T} - \varphi_T)] ds \, dt \\
&= \int_0^T \langle J_\epsilon(u_{\epsilon n}, \varphi - \dot{\phi}), \dot{u}_{\epsilon T} - \varphi \rangle dt
\end{aligned}$$

because  $c_T[(u_{\epsilon n}^m - g)_+]^{m_T} \rightarrow c_T[(u_{\epsilon n} - g)_+]^{m_T}$  strongly in  $L^2(0, T; L^{q'}(\Gamma_C))$

and  $\psi'_\epsilon(\varphi_T - \dot{u}_T^C)(\dot{u}_{\epsilon T}^m - \varphi_T) \rightarrow \psi'_\epsilon(\varphi_T - \dot{u}_T^C)(\dot{u}_{\epsilon T} - \varphi_T)$  weakly in  $L^2(0, T; L^q(\Gamma_C))$ .

□

**Continuation of the Proof of Theorem 3.4.2. (Existence of solution).**

Applying to the regularized equation (3.4.40) the same procedures used earlier with its finite dimensional approximation (3.4.43), we conclude that the bounds (3.4.45-48) also hold for  $\underline{u}_\epsilon$ . In addition, since

$$\begin{aligned}
\ddot{\underline{u}}_\epsilon(t) &= -A\underline{u}_\epsilon(t) - C\dot{\underline{u}}_\epsilon(t) - P(\underline{u}_\epsilon(t)) - J_\epsilon(\underline{u}_\epsilon(t), \dot{\underline{u}}_\epsilon(t) - \dot{\phi}(t)) \\
&\quad + f(t) \text{ in } V',
\end{aligned}$$

it follows that

$$\ddot{\underline{u}}_\epsilon \in \text{bounded set of } L^2(0, T; V')$$

We can conclude that a subsequence of  $\underline{u}_\epsilon$  again denoted by  $\underline{u}_\epsilon$  exists such that, as  $\epsilon \rightarrow 0$ ,

$$\left. \begin{aligned}
\underline{u}_\epsilon &\rightarrow \underline{u} \text{ weak star in } L^\infty(0, T; V) \\
\dot{\underline{u}}_\epsilon &\rightarrow \dot{\underline{u}} \text{ weak star in } L^\infty(0, T; H) \text{ and weakly in } L^2(0, T; V) \\
\ddot{\underline{u}}_\epsilon &\rightarrow \ddot{\underline{u}} \text{ weakly in } L^2(0, T; V')
\end{aligned} \right\} (3.4.56)$$

$u_{\epsilon n} \rightarrow u_n$  strongly in  $L^2(0, T; L^q(\Gamma_C))$

$$\left. \begin{aligned} c_n[(u_{\epsilon n} - g)_+]^{m_n} &\rightarrow c_n[(u_n - g)_+]^{m_n} \\ c_T[(u_{\epsilon n} - g)_+]^{m_T} &\rightarrow c_T[(u_n - g)_+]^{m_T} \end{aligned} \right\} \begin{array}{l} \text{weak star in} \\ L^\infty(0, T; L^{q'}(\Gamma_C)) \text{ and} \\ \text{strongly in} \\ L^2(0, T; L^{q'}(\Gamma_C)). \end{array} \quad (3.4.57)$$

We shall now take the limit as  $\epsilon \rightarrow 0$ . Taking  $\underline{v}$  in (3.4.40) equal to  $\underline{v}(t) - \dot{\underline{u}}_\epsilon(t)$ , with  $\underline{v} \in L^2(0, T; V)$  arbitrary, and integrating from 0 to T, it follows that

$$\begin{aligned} & \int_0^T [\langle \ddot{\underline{u}}_\epsilon, \underline{v} \rangle + a(\underline{u}_\epsilon, \underline{v}) + c(\dot{\underline{u}}_\epsilon, \underline{v}) + \\ & \quad + \langle P(\underline{u}_\epsilon), \underline{v} \rangle + j_\epsilon(\underline{u}_\epsilon, \underline{v} - \dot{\underline{\phi}}) - \langle \underline{f}, \underline{v} \rangle] dt \\ & \geq \int_0^T [\langle \ddot{\underline{u}}_\epsilon, \dot{\underline{u}}_\epsilon \rangle + a(\underline{u}_\epsilon, \dot{\underline{u}}_\epsilon) + c(\dot{\underline{u}}_\epsilon, \dot{\underline{u}}_\epsilon) + \langle P(\underline{u}_\epsilon), \dot{\underline{u}}_\epsilon \rangle + j_\epsilon(\underline{u}_\epsilon, \dot{\underline{u}}_\epsilon - \dot{\underline{\phi}})] dt \\ & = \frac{1}{2} |\underline{u}_\epsilon(T)|^2 + \frac{1}{2} a(\underline{u}_\epsilon(T), \underline{u}_\epsilon(T)) + p(\underline{u}_\epsilon(T)) \\ & \quad - \frac{1}{2} |\underline{u}_\epsilon(0)|^2 - \frac{1}{2} a(\underline{u}_\epsilon(0), \underline{u}_\epsilon(0)) - p(\underline{u}_\epsilon(0)) \\ & \quad + \int_0^T c(\dot{\underline{u}}_\epsilon, \dot{\underline{u}}_\epsilon) dt + \int_0^T j_\epsilon(\underline{u}_\epsilon, \dot{\underline{u}}_\epsilon - \dot{\underline{\phi}}) dt. \end{aligned} \quad (3.4.58)$$

Computing now  $\lim_{\epsilon \rightarrow 0}$  of the left-hand side of the above inequality and  $\liminf_{\epsilon \rightarrow 0}$  of the right-hand side, we obtain

$$\begin{aligned} & \int_0^T [\langle \ddot{\underline{u}}, \underline{v} \rangle + a(\underline{u}, \underline{v}) + c(\dot{\underline{u}}, \underline{v}) + \langle P(\underline{u}), \underline{v} \rangle + j(\underline{u}, \underline{v} - \dot{\underline{\phi}}) - \langle \underline{f}, \underline{v} \rangle] dt \\ & \geq \frac{1}{2} |\dot{\underline{u}}(T)|^2 + \frac{1}{2} a(\underline{u}(T), \underline{u}(T)) + p(\underline{u}(T)) \\ & \quad - \frac{1}{2} |\underline{u}_1|^2 - \frac{1}{2} a(\underline{u}_0, \underline{u}_0) - p(\underline{u}_0) \end{aligned}$$

$$+ \int_0^T c(\dot{\underline{u}}, \dot{\underline{u}}) dt + \int_0^T j(\underline{u}, \dot{\underline{u}} - \dot{\underline{\phi}}) dt$$

i.e.,

$$\begin{aligned} & \int_0^T [\langle \dot{\underline{u}}, \dot{\underline{v}} - \dot{\underline{u}} \rangle + a(\underline{u}, \dot{\underline{v}} - \dot{\underline{u}}) + c(\dot{\underline{u}}, \dot{\underline{v}} - \dot{\underline{u}}) \\ & + \langle P(\underline{u}), \dot{\underline{v}} - \dot{\underline{u}} \rangle + j(\underline{u}, \dot{\underline{v}} - \dot{\underline{\phi}}) - j(\underline{u}, \dot{\underline{u}} - \dot{\underline{\phi}})] dt \\ & \geq \int_0^T \langle \dot{\underline{f}}, \dot{\underline{v}} - \dot{\underline{u}} \rangle dt \quad \forall \underline{v} \in L^2(0, T; V) \end{aligned}$$

from which it follows that (3.3.13) holds for a.e.  $t \in [0, T]$ ,

$\forall \underline{v} \in V$  (cf. Duvaut and Lions [1976, pp. 57, 58]).  $\square$

**Remark 3.4.3.** In a manner similar to Remark 3.4.2, the passage to the limit on the right-hand side of (3.4.58) relies on the strong convergence property (3.4.57). In fact,

$$\begin{aligned} & \liminf_{\epsilon \rightarrow 0} \int_0^T j_{\epsilon}(\underline{u}_{\epsilon n}, \dot{\underline{u}}_{\epsilon} - \dot{\underline{\phi}}) dt \\ & = \lim_{\epsilon \rightarrow 0} \int_0^T \int_{\Gamma_C} \{c_T[(u_{\epsilon n} - g)_+]^{m_T} - c_T[(u_n - g)_+]^{m_T}\} \psi_{\epsilon}(\dot{\underline{u}}_{\epsilon T} - \dot{\underline{u}}_T^C) ds dt \\ & + \lim_{\epsilon \rightarrow 0} \int_0^T \int_{\Gamma_C} c_T[(u_n - g)_+]^{m_T} \{\psi_{\epsilon}(\dot{\underline{u}}_{\epsilon T} - \dot{\underline{u}}_T^C) - |\dot{\underline{u}}_{\epsilon T} - \dot{\underline{u}}_T^C|\} ds dt \\ & + \liminf_{\epsilon \rightarrow 0} \int_0^T \int_{\Gamma_C} c_T[(u_n - g)_+]^{m_T} |\dot{\underline{u}}_{\epsilon T} - \dot{\underline{u}}_T^C| ds dt \\ & \geq \int_0^T \int_{\Gamma_C} c_T[(u_n - g)_+]^{m_T} |\dot{\underline{u}}_T - \dot{\underline{u}}_T^C| ds dt \\ & = \int_0^T j(\underline{u}, \dot{\underline{u}} - \dot{\underline{\phi}}) dt \end{aligned}$$

because:  $c_T[(u_{\varepsilon n}-g)_+]^{m_T} \rightarrow c_T[(u_n-g)_+]^{m_T}$  strongly in  $L^2(0,T;L^{q'}(\Gamma_C))$

and due to (3.4.36),  $\psi_\varepsilon(\dot{u}_{\varepsilon T}-\dot{u}_T^C)$  is bounded in  $L^2(0,T;L^q(\Gamma_C))$ ;

$c_T[(u_n-g)_+]^{m_T} \in L^\infty(0,T;L^{q'}(\Gamma_C))$  and, due to (3.4.39),  $\psi_\varepsilon(\dot{u}_{\varepsilon T}-\dot{u}_T^C) \rightarrow$

$|\dot{u}_{\varepsilon T}-\dot{u}_T^C| \rightarrow 0$  in  $L^1(0,T;L^q(\Gamma_C))$ ; and, finally, the functional

$\tilde{v} \rightarrow \int_0^T \int_{\Gamma_C} \varphi(t) |\tilde{v}_T(t)| \, ds \, dt$  of  $L^2(0,T;V) \rightarrow \mathbb{R}$ , with  $\varphi = c_T[(u_n-g)_+]^{m_T}$

given in  $L^2(0,T;L^{q'}(\Gamma_C))$  is convex and continuous, hence weakly lower semicontinuous.

The passage to the limit on the left hand-side of (3.4.58) does not require the strong convergence property mentioned earlier:

$$\begin{aligned} & \lim_{\varepsilon \rightarrow 0} \int_0^T j_\varepsilon(u_\varepsilon, v - \dot{\phi}) \, dt \\ &= \lim_{\varepsilon \rightarrow 0} \int_0^T \int_{\Gamma_C} c_T[(u_{\varepsilon n}-g)_+]^{m_T} \psi_\varepsilon(v_T - \dot{u}_T^C) \, ds \, dt \\ &= \int_0^T \int_{\Gamma_C} c_T[(u_n-g)_+]^{m_T} |\tilde{v}_T - \dot{u}_T^C| \, ds \, dt \\ &= \int_0^T j(\tilde{u}, \tilde{v} - \dot{\phi}) \, dt \end{aligned}$$

because  $c_T[(u_{\varepsilon n}-g)_+]^{m_T} \rightarrow c_T[(u_n-g)_+]^{m_T}$  weak star in  $L^\infty(0,T;L^{q'}(\Gamma_C))$  and

due to (3.4.39),  $\psi_\varepsilon(v_T - \dot{u}_T^C) \rightarrow |\tilde{v}_T - \dot{u}_T^C|$  strongly in  $L^1(0,T;L^q(\Gamma_C))$ .  $\square$

**Remark 3.4.4.** We emphasize the key role played by the viscous damping in the proof of Theorem 3.4.2. It is the viscous



damping that guarantees the strong convergences (3.4.52) and (3.4.57). Such a situation should be expected from the beginning since our methods are the same of Duvaut and Lions [1976] and those authors exposed in Theorem 5.7, pp. 156-162 (op. cit.), the difficulties in obtaining a priori estimates in the presence of frictional contributions dependent on velocities on the boundary of the domain. Those authors were able to show existence and uniqueness of solution with *prescribed time dependent* normal forces on the contact boundary only when viscous damping effects were taken into account (Theorem 6.1 bis, p. 167, op. cit.). For a linearly elastic material, only the case of *prescribed time independent* normal forces on the contact surface was successfully studied (Theorem 5.7, pp. 156-162, op. cit.).

**Remark 3.4.5.** With the same arguments of Remark 3.4.1, it results that the whole sequence  $\underline{u}_\varepsilon^m$  (cf. Lemma 3.4.1) converges to  $\underline{u}_\varepsilon$  in the weak sense of (3.4.49,50) and the whole sequence  $\underline{u}_\varepsilon$  (cf. Theorem 3.4.2) converges to  $\underline{u}$  in the weak sense of (3.4.56). Without further effort (by just using the compactness results of Lions [1969, Theorem 5.1, pp. 58-59]), some additional strong convergence results for the finite dimensional regularized solutions  $\underline{u}_\varepsilon^m$  as  $m \rightarrow \infty$ ,  $\varepsilon \rightarrow 0$  can be stated. We have, in particular,

$$\underline{u}_\varepsilon^m(\dot{\underline{u}}_\varepsilon^m) \rightarrow \underline{u}(\dot{\underline{u}}) \text{ strongly in } L^p(0,T; (H^{1-\delta}(\Omega))^N)$$

with  $1 < p < \infty$  and  $0 < \delta \leq 1$  arbitrary.  $\square$

### 3.5. Formal statement of the steady-sliding problem.

Let us assume that the prescribed displacements  $(\underline{u}^D)$  and the forces  $(\underline{b}, \underline{t})$  applied to the body considered in the previous sections are independent of time and that the driving velocity  $(\dot{\underline{u}}_T^C)$  is also independent of time and different from zero everywhere on  $\Gamma_C$ . We denote by  $\underline{\eta}$  the unit vector field parallel to the driving velocity at each point of  $\Gamma_C$ . The equations governing the steady-sliding equilibrium positions  $(\underline{u}_0)$  are obtained from (3.2.2-5) by simply setting  $\dot{\underline{u}} = \ddot{\underline{u}} \equiv 0$ . We have thus:

#### Equilibrium Equations

$$\sigma_{ij}(\underline{u}_0)_{,j} + b_i = 0 \text{ in } \Omega \quad (3.5.1)$$

where the  $\sigma_{ij}$  satisfy the constitutive equations (3.2.1) with, of course,  $\dot{\underline{u}} \equiv 0$ .

#### Boundary Conditions

$$u_{0i} = u_i^D \quad \text{on } \Gamma_D \quad (3.5.2)$$

$$\sigma_{ij}(\underline{u}_0)n_j = t_i \quad \text{on } \Gamma_F \quad (3.5.3)$$

$$-\sigma_n(\underline{u}_0) = c_n[(u_{0n} - g)_+]^m \quad \text{on } \Gamma_C \quad (3.5.4)$$

$$\tau_T(\underline{u}_0) = c_T[(u_{0n} - g)_+]^m \tau_C \quad \text{on } \Gamma_C. \quad (3.5.5)$$

### 3.6. Variational formulation for the steady sliding problem.

All the assumptions, notations and definitions introduced in Sections 3.2 and 3.3 that are relevant for the present problem are kept in force hereafter. For clarity we enumerate them: the smoothness (Lipschitz continuity) of the domain  $\Omega$  and the decomposition of the boundary  $\Gamma$ ; the simplifying assumptions (3.3.2) and (3.3.3); the definitions and notations associated with the spaces  $V$  and  $H$ ; the assumptions (3.3.6) on the elasticity coefficients; the definition of the bilinear form  $a(\cdot, \cdot)$ ; the assumptions  $1 \leq m_n, m_T$  if  $N=2$ , and  $1 \leq m_n, m_T \leq 3$  if  $N=3$ ; the notations  $q=1+\max\{m_n, m_T\}$  and  $q' = q/(q-1)$ ; the assumptions on  $\underline{b}$  and  $\underline{t}$  and the definition of  $\underline{f}$  (eliminating, of course, their time dependence); the assumptions on  $c_n$ ,  $c_T$  and  $g$ ; and the definition of the nonlinear map  $P$ .

In addition, we denote by  $\Sigma$  the following open subset of  $\Gamma$

$$\Sigma = \text{int}(\Gamma - \Gamma_D) .$$

From Section 3.4 we recall the definitions of the spaces

$$W = \{ \underline{\xi} \in (H^{\frac{1}{2}}(\Gamma))^N : \underline{\xi} = 0 \text{ a.e. on } \Gamma_D \}$$

$$G = \{ \underline{\xi} \in (L^q(\Gamma))^N : \underline{\xi} = 0 \text{ a.e. on } \Gamma_D \} .$$

As a closed subspace of  $(H^{\frac{1}{2}}(\Gamma))^N$ , the space  $W$  is a Hilbert space.

A possible choice for the Hilbertian norm on  $W$  is

$$\| \underline{\xi} \|_W = \inf_{\underline{v} \in V} \{ \| \underline{v} \| : \underline{v} = \underline{\xi} \text{ on } \Gamma \}, \quad \underline{\xi} \in W .$$

The topological dual of  $W$  will be denoted by  $W'$  and the duality pairing in  $W' \times W$  will be denoted by  $\langle \cdot, \cdot \rangle_W$ . For the values of  $q$  indicated above the space  $W$  is *continuously embedded* in  $G$ , which in turn is canonically isomorphic to the space  $(L^q(\Sigma))^N$ , the topological dual of which is  $(L^{q'}(\Sigma))^N$ . It is also well-known that, for the above values of  $q$ , the space  $H^{\frac{1}{2}}(\Gamma)$  is dense in  $L^q(\Gamma)$ . Similarly, the space  $W$  is *dense* in  $(L^q(\Sigma))^N$ : a similar result obtained using a system of local charts is mentioned in Hünlich and Nauman [1978, Lemma 1.4, pp. 212-213] when  $q=2$ . The embedding of  $W$  in  $(L^q(\Sigma))^N$  is *compact* for all the values of  $q$  mentioned above except for the limit case  $q=4$ ,  $N=3$  (cf. Kufner et al. [1977]), i.e., except when  $\max\{m_n, m_T\} = 3$  and  $N=3$ . The compactness of this embedding was already used in the proof of Theorem 3.4.2.

Finally, we introduce the nonlinear operator  $J_n : V \rightarrow V'$  such that

$$\langle J_n(\underline{w}), \underline{v} \rangle = - \int_{\Gamma_C} c_T [(\underline{w}_n - \underline{g})_+]^{m_T} \underline{n} \cdot \underline{v}_T \, ds, \quad \underline{w}, \underline{v} \in V$$

Here  $\langle J_n(\cdot), \cdot \rangle$  represents virtual work of the friction stresses on  $\Gamma_C$ . The unitary tangential field  $\underline{n}$  is assumed to satisfy

$$\underline{n} \in (L^\infty(\Gamma_C))^N$$

$$\sum_{i=1}^N [n_i(\underline{s})]^2 = 1 \text{ a.e. } \underline{s} \in \Gamma_C$$

$$\sum_{i=1}^N n_i(\underline{s}) \, n_i(\underline{s}) = 0 \text{ a.e. } \underline{s} \in \Gamma_C.$$

With the above definitions and notations established, we can now state a weak formulation for the steady-sliding problem (3.5.1-5):

**Problem 3** (steady-sliding). Find a function  $\underline{u}_0 \in V$  such that

$$a(\underline{u}_0, \underline{v}) + \langle P(\underline{u}_0), \underline{v} \rangle + \langle J_\eta(\underline{u}_0), \underline{v} \rangle = \langle f, \underline{v} \rangle \quad \forall \underline{v} \in V. \quad (3.6.1)$$

We now show in what sense the solutions of the variational problem (3.6.1) can be interpreted for the solutions to problem (3.5.1-5). Our approach here relies on a generalized Green's formula, given below in Lemma 3.6.1. In what follows,  $\mathcal{D}(\Omega)$  denotes the space of indefinitely differentiable functions with compact support in  $\Omega$  equipped with the usual inductive limit topology and by  $\mathcal{D}'(\Omega)$  its topological dual, the space of distributions over  $\Omega$ . We introduce the operator

$$\begin{aligned} \text{div } \underline{\sigma} : V &\rightarrow (\mathcal{D}'(\Omega))^N \\ [\text{div } \underline{\sigma}(\underline{v})]_i &= \sigma_{ij}(\underline{v})_{,j} = (E_{ijkl} v_{k,l})_{,j}, \quad 1 \leq i, j, k, l \leq N. \end{aligned} \quad (3.6.2)$$

In addition, let  $V_\sigma$  denote the subspace of  $V$  defined by

$$V_\sigma = \{ \underline{v} \in V : \text{div } \underline{\sigma}(\underline{v}) \in H \}. \quad (3.6.3)$$

**Lemma 3.6.1.** (Generalized Green's formula). There is a unique linear mapping

$$\tau : V_\sigma \rightarrow W'$$

verifying

$$[\tau(\underline{w})]_i = \sigma_{ij}(\underline{w}) n_j \quad \text{on } \Sigma$$

for every  $\underline{w} \in V$  such that  $\sigma_{ij}(\underline{w}) = E_{ijk} w_{k,l} \in C^1(\bar{\Omega})$ ,  $1 \leq i, j, k, l \leq N$ ,  
and

$$a(\underline{w}, \underline{v}) + (\operatorname{div} \underline{\sigma}(\underline{w}), \underline{v}) = \langle \pi(\underline{w}), \underline{v} \rangle_W, \quad (3.6.4)$$

for every pair  $(\underline{w}, \underline{v}) \in V_\sigma \times V$ .

**Proof:** The proof of this result follows standard arguments and is omitted. See, e.g., Showalter [1979, Theorems III.2.C and III.3.A, pp. 55-58] or Kikuchi and Oden [1986, Theorems 5.8 and 5.9] for the proofs of similar or more general propositions.  $\square$

**Theorem 3.6.1.** An element  $\underline{u}_0 \in V$  is a solution of Problem 3, if and only if

$$(i) \quad \underline{u}_0 \in V \quad \text{and}$$

$$\operatorname{div} \underline{\sigma}(\underline{u}_0) + \underline{b} = \underline{0} \quad \text{a.e. in } \Omega \quad (3.6.5)$$

$$(ii) \quad \pi(\underline{u}_0) \in (L^{q'}(\Sigma))^N \quad \text{and}$$

$$\pi(\underline{u}_0) = \underline{t} \quad \text{a.e. on } \Gamma_F \quad (3.6.6)$$

$$(\pi(\underline{u}_0))_n = -c_n [(u_{0n} - g)_+]^m \quad \text{a.e. on } \Gamma_C \quad (3.6.7)$$

$$(\pi(\underline{u}_0))_T = c_T [(u_{0n} - g)_+]^{m_T} \quad \text{a.e. on } \Gamma_C. \quad (3.6.8)$$

**Proof:** Let  $\underline{u}_0 \in V$  be a solution of the variational problem (3.6.1) and let  $\underline{v} \in (\mathcal{D}(\Omega))^N \subset V$ . Since all the boundary terms vanish for such a choice of  $\underline{v}$ , we have

$$a(\underline{u}_0, \underline{v}) = \int_{\Omega} \underline{b} \cdot \underline{v} \, dx, \quad \text{i.e.,}$$

$$\int_{\Omega} \sigma_{ij}(\underline{u}_0) v_{i,j} dx = \int_{\Omega} b_i v_i dx.$$

As the above relation holds for every  $\underline{v} \in (\mathcal{D}(\Omega))^N$ , it is equivalent to

$$-\operatorname{div} \underline{\sigma}(\underline{u}_0) = \underline{b} \text{ in } (\mathcal{D}'(\Omega))^N,$$

which proves (i). Next, as we have just seen that  $\underline{u}_0 \in V_\sigma$ , the generalized Green's formula of Lemma 3.6.1, the definitions of  $\underline{f}$ ,  $P$  and  $J_n$  and the variational statement (3.6.1) yield

$$\begin{aligned} & -\int_{\Omega} (\operatorname{div} \underline{\sigma}(\underline{u}_0)) \cdot \underline{v} dx + \langle \pi(\underline{u}_0), \underline{v} \rangle_W \\ &= \int_{\Omega} \underline{b} \cdot \underline{v} dx + \int_{\Gamma_F} \underline{t} \cdot \underline{v} ds \\ &+ \int_{\Gamma_C} \{-c_n[(u_{0n}-g)_+]^m v_n + c_T[(u_{0n}-g)_+]^{m_T} n \cdot \underline{v}_T\} ds \end{aligned}$$

for every element  $\underline{v} \in V$ . With (3.6.5) and since the trace map is onto from  $V$  to  $W$ , this reduces to

$$\langle \pi(\underline{u}_0), \underline{\xi} \rangle_W = \int_{\Sigma} \underline{\psi} \cdot \underline{\xi} ds$$

for every  $\underline{\xi} \in W$ , where  $\underline{\psi} \in (L^{q'}(\Sigma))^N$  is (uniquely) defined by

$$\underline{\psi} = \begin{cases} \underline{t} & \text{on } \Gamma_F \\ -c_n[(u_{0n}-g)_+]^m \underline{n} + c_T[(u_{0n}-g)_+]^{m_T} \underline{n} & \text{on } \Gamma_C. \end{cases}$$

From the density of the space  $W$  in the space  $(L^q(\Sigma))^N$ , it follows that  $\pi(\underline{u}_0)$  can be uniquely extended (by  $\underline{\psi}$ ) as a linear continuous form on  $(L^q(\Sigma))^N$ . Hence,  $\pi(\underline{u}_0) = \underline{\psi} \in (L^{q'}(\Sigma))^N$ . Boundary conditions (3.6.6) - (3.6.8) are immediate from this result.

To prove that conditions (i) and (ii) of Theorem 3.6.1

imply  $\underline{u}_0 \in V$  and  $\underline{u}_0$  is a solution to the variational problem (3.6.1), we need only to reverse the steps of the above proof.  $\square$

### 3.7. Existence and uniqueness of steady-sliding equilibrium solutions.

Toward the study of the questions of existence and uniqueness of solutions to Problem 3, we first consider the following auxiliary problem:

**Problem 3.** Find a function  $\hat{u} \in V$  such that

$$a(\hat{u}, \underline{v}) + \langle P(\hat{u}), \underline{v} \rangle = \langle \underline{f}, \underline{v} \rangle + \int_{\Gamma_C} \hat{g}_T \cdot \underline{v}_T \, ds, \quad \forall \underline{v} \in V \quad (3.7.1)$$

where the data  $\hat{g}_T$  satisfies:

$$\hat{g}_T \in S_T = \{ \underline{\psi} \in (L^{q'}(\Gamma_C))^N : \underline{\psi} \cdot \underline{n} = 0 \text{ a.e. on } \Gamma_C \} \quad (3.7.2)$$

$S_T$  is the space of the tangential stresses on  $\Gamma_C$  and is a reflexive Banach space. The norm of a function in  $S_T$  is the  $(L^{q'}(\Gamma_C))^N$ -norm:

$$\| \underline{\psi} \|_{q', \Gamma_C} = \left\{ \sum_{i=1}^N \int_{\Gamma_C} |\psi_i|^{q'} \, ds \right\}^{1/q'}, \quad \underline{\psi} \in (L^{q'}(\Gamma_C))^N.$$

Sufficient conditions for existence and uniqueness of solution to Problem 3 are recorded in the following

**Lemma 3.7.1.** Let (3.7.2) and all the assumptions in Section 3.6 hold. Then:

- (i) There exists a unique solution to Problem 3.
- (ii) The map  $B: S_T \rightarrow V$  which associates with each  $\hat{g}_T \in S_T$



the solution  $\hat{u} \in V$  of (3.7.1) is Lipschitz continuous in the sense that, there exist  $L > 0$ , only dependent on the domain and the other (fixed) data for Problem  $\hat{3}$ , such that

$$\|B(\hat{g}_T) - B(\hat{g}_T)\| \leq L \|\hat{g}_T - \hat{g}_T\|_{q, \Gamma_C} \quad \forall (\hat{g}_T, \hat{g}_T) \in S_T \times S_T \quad (3.7.3)$$

**Proof:** Existence and uniqueness can be proved by using well-known results from the Theory of Optimization or the Theory of Monotone Operators. In order to apply a result of the latter, we recast the variational statement (3.7.1) in the equivalent operator form

$$\hat{A}(\hat{u}) = \hat{f} \quad \text{in } V' \quad (3.7.4)$$

where  $\hat{A} \stackrel{\text{def}}{=} A + P: V \rightarrow V'$  (recall Section 3.3), i.e.,

$$\langle \hat{A}(\underline{w}), \underline{v} \rangle = a(\underline{w}, \underline{v}) + \langle P(\underline{w}), \underline{v} \rangle \quad \forall (\underline{w}, \underline{v}) \in V \times V$$

and, for given  $\underline{f} \in V'$  and  $\hat{g}_T \in S_T$ ,  $\hat{f} \in V'$  is defined by

$$\langle \hat{f}, \underline{v} \rangle = \langle \underline{f}, \underline{v} \rangle + \int_{\Gamma_C} \hat{g}_T \cdot \underline{v}_T \, ds \quad \forall \underline{v} \in V.$$

Sufficient conditions for existence and uniqueness of solutions to the operator equation (3.7.4) are the following (cf. Lions [1969, pp. 171-173]): boundedness, hemicontinuity, coercivity and strict monotonicity of the operator  $\hat{A}$ .

In the present problem the boundedness of  $\hat{A}$  results from the boundedness of  $A$  and the estimate

$$\langle P(\underline{w}), \underline{v} \rangle \leq C \|c_n\|_{\infty, \Gamma_C} (\|\underline{w}\| + \|g\|_{q, \Gamma_C})^m \|\underline{v}\| \quad \forall (\underline{v}, \underline{w}) \in V \times V,$$

which implies the boundedness of  $P$ . In the above,  $C$  denotes a sufficiently large constant independent of  $\underline{w}$  and  $\underline{v}$ . The continuity (hence *hemicontinuity*) of  $A$  results from the continuity of  $A$  and the estimate

$$\begin{aligned} & \langle P(\underline{w}) - P(\underline{z}), \underline{v} \rangle \\ & \leq C \|c_n\|_{\infty, \Gamma_C} [\max\{\|\underline{w}\|, \|\underline{z}\|\} + \|g\|_{q, \Gamma_C}]^{m-1} \|\underline{w} - \underline{z}\| \|\underline{v}\| \\ & \quad \forall (\underline{v}, \underline{w}, \underline{z}) \in V^3, \end{aligned}$$

which implies the continuity of  $P$ . In the above,  $C$  is a constant independent of  $\underline{v}$ ,  $\underline{w}$  and  $\underline{z}$ . The strong monotonicity (hence *strict monotonicity* and *coercivity*) of  $\hat{A}$  results from the  $V$ -ellipticity property (3.3.9) of  $a(\cdot, \cdot)$  and the monotonicity of  $P$ , i.e.,

$$\begin{aligned} & \langle \hat{A}(\underline{w}) - \hat{A}(\underline{z}), \underline{w} - \underline{z} \rangle \\ & = a(\underline{w} - \underline{z}, \underline{w} - \underline{z}) + \int_{\Gamma_C} c_n \{ [(w_n - g)_+]^m - [(z_n - g)_+]^m \} (w_n - z_n) ds \\ & \geq \alpha_a \|\underline{w} - \underline{z}\|^2. \end{aligned}$$

This completes the proof of the assertion (i).

In order to prove the *Lipschitz continuity* (3.7.3) of the map  $B$ , let  $\hat{\underline{u}} = B(\hat{\underline{g}}_T)$  and  $\hat{\underline{z}} = B(\hat{\underline{r}}_T)$  be the solutions of Problem  $\hat{3}$  for  $\hat{\underline{g}}_T \in S_T$  and  $\hat{\underline{r}}_T \in S_T$ , respectively, and with the other data fixed. Writing the variational statement (3.7.1) successively for  $\hat{\underline{u}}$  and  $\hat{\underline{z}}$ , subtracting the resulting equations and choosing  $\underline{v} = \hat{\underline{u}} - \hat{\underline{z}}$ , we obtain

$$a(\hat{\underline{u}} - \hat{\underline{z}}, \hat{\underline{u}} - \hat{\underline{z}}) + \langle P(\hat{\underline{u}}) - P(\hat{\underline{z}}), \hat{\underline{u}} - \hat{\underline{z}} \rangle$$

$$= \int_{\Gamma_C} (\hat{g}_T - \hat{I}_T) \cdot (\hat{u}_T - \hat{z}_T) \, ds.$$

The monotonicity of the operator  $P$ , the  $V$ -ellipticity (3.3.9) of  $a(\cdot, \cdot)$  and the continuity of the trace map lead to desired result (3.7.3) with  $L = C/\alpha_a$ , where  $C$  denotes here the trace map continuity constant. This completes the proof of the lemma.  $\square$

**Theorem 3.7.1.** In addition to the assumptions listed in Section 3.6, let

$$\left. \begin{aligned} 1 \leq m_n & \begin{cases} < +\infty & \text{if } N=2 \\ < 3 & \text{if } N=3 \end{cases} \\ q &= 1 + \max\{m_n, m_T\} \end{aligned} \right\} \quad (3.7.5)$$

$$\exists \tilde{w}^* \in V \text{ such that } \tilde{w}^* \cdot \tilde{n} = g \text{ a.e. on } \Gamma_C. \quad (3.7.6)$$

Then there exists a constant  $C = C(\Omega, \Sigma, \Gamma_C, m_n, m_T)$  such that if, in addition,

$$\frac{\|c_T\|_{\infty, \Gamma_C}}{\alpha_a} \left( \frac{\|f\|_* + M_a \|\tilde{w}^*\|}{\alpha_a} \right)^{m_T-1} < C \quad (3.7.7)$$

then there exists a strictly positive number  $R = R(\Omega, \Sigma, \Gamma_C, m_n, m_T,$

$\|c_T\|_{\infty, \Gamma_C}, \|\tilde{w}^*\|, M_a, \alpha_a, \|f\|_*)$  such that, in the set

$$K = \{\tilde{v} \in V : \|\tilde{v} - \tilde{w}^*\| \leq R\}, \quad (3.7.8)$$

there exists a unique solution to Problem 3.

**Proof:** In order to prove existence of solutions we first define the map  $\varphi : (L^q(\Sigma))^N \rightarrow S_T$ , given by

$$\varphi(\underline{\xi}) = c_T [(\xi_n - g)_+]^{m_T} \underline{n}, \quad \underline{\xi} \in (L^q(\Sigma))^N,$$

where we have extended  $c_T$ ,  $g$  and  $\underline{n}$  by zero on  $\Sigma - \Gamma_C$ . This map assigns to each displacement field  $\underline{\xi}$  on the boundary the corresponding tangential stresses on  $\Gamma_C$ , according to (3.5.5). The continuity of the map  $\varphi$  follows from the estimate:

$$\begin{aligned} & \|\varphi(\underline{\xi}) - \varphi(\underline{\zeta})\|_{q', \Gamma_C} \\ &= \left\{ \sum_{i=1}^N \int_{\Gamma_C} |c_T \{[(\xi_n - g)_+]^{m_T} - [(\zeta_n - g)_+]^{m_T}\} n_i|^{q'} ds \right\}^{1/q'} \\ &\leq c \|c_T\|_{\infty, \Gamma_C} \|[(\xi_n - g)_+]^{m_T} - [(\zeta_n - g)_+]^{m_T}\|_{q/m_T, \Sigma} \\ &\leq c \|c_T\|_{\infty, \Gamma_C} \{ (\|\xi_n - g\|_{q, \Sigma}^{q-1} + \|\zeta_n - g\|_{q, \Sigma}^{q-1}) \|\xi_n - \zeta_n\|_{q, \Sigma} \}^{m_T/q} \\ &\leq c \|c_T\|_{\infty, \Gamma_C} \cdot \max\{ \|\xi_n - g\|_{q, \Sigma}^{m_T/q'}, \|\zeta_n - g\|_{q, \Sigma}^{m_T/q'} \} \cdot \|\xi_n - \zeta_n\|_{q, \Sigma}^{m_T/q} \end{aligned}$$

where  $\underline{\xi}$  and  $\underline{\zeta}$  are arbitrary elements of  $(L^q(\Sigma))^N$  and the  $c$ 's denote various constants independent of  $\underline{\xi}$  and  $\underline{\zeta}$ .

Let  $K$  be the bounded, closed, convex subset of the Banach space  $V$ , defined by (3.7.8). We denote by  $T$  the mapping  $T: K \rightarrow V$  which results from the following composition

$$T = \bar{B} \circ \bar{\varphi} \circ \bar{\gamma}$$

where  $\bar{\gamma} : K \rightarrow (L^q(\Sigma))^N$  is the restriction of the trace map  $\gamma$  to the

set  $K$ ;  $\bar{\varphi} : Rg(\bar{\gamma}) \rightarrow S_T$  is the restriction to the range of  $\bar{\gamma}$  of the map  $\varphi$  defined above; and  $\bar{B} : Rg(\bar{\varphi}) \rightarrow V$  is the restriction to the range of  $\bar{\varphi}$  of the map  $B$  defined in Lemma 3.7.1.

Since the maps  $B$  and  $\varphi$  are continuous and the trace map  $\gamma$  is compact (note that  $m_n, m_T < 3$  and  $q < 4$  if  $N=3$ ) then the map  $T$  is compact.

In order to apply the Schauder's fixed point theorem (see, e.g., Oden [1986]) in the existence proof, we need now to show that a constant  $C$  exists such that, if (3.7.7) holds, then we can find  $R > 0$  such that, with  $K$  given by (3.7.8),  $T(K) \subset K$ , i.e.,

$$\|T(\underline{u}^*) - \underline{w}^*\| \leq R \quad \forall \underline{u}^* \in K, \quad (3.7.9)$$

where  $\underline{w}^*$  is an element of  $V$  satisfying (3.7.6).

Let  $\underline{u}^*$  be an arbitrary element of  $K$  and let  $\underline{u} = T(\underline{u}^*) = B(\varphi(\gamma(\underline{u}^*))) \in V$ .

From the definition of the maps  $B$ ,  $\varphi$  and  $\gamma$  and from the variational statement (3.7.1), it follows that

$$a(\underline{u}, \underline{v}) + \langle P(\underline{u}), \underline{v} \rangle = \langle \underline{f}, \underline{v} \rangle + \int_{\Gamma_C} c_T [(u_n^* - g)_+]^{m_T} \underline{n} \cdot \underline{v}_T \, ds,$$

for every  $\underline{v} \in V$ . Letting  $\underline{v} = \underline{u} - \underline{w}^*$  and adding and subtracting  $a(\underline{w}^*, \underline{u} - \underline{w}^*)$  we obtain

$$\begin{aligned} a(\underline{u} - \underline{w}^*, \underline{u} - \underline{w}^*) &+ \int_{\Gamma_C} c_n [(u_n - g)_+]^{m_n} (u_n - g) \, ds \\ &= a(\underline{w}^*, \underline{u} - \underline{w}^*) + \langle \underline{f}, \underline{u} - \underline{w}^* \rangle \\ &+ \int_{\Gamma_C} c_T [(u_n^* - g)_+]^{m_T} \underline{n} \cdot (\underline{u}_T - \underline{w}_T^*) \, ds \end{aligned}$$

Using the V-ellipticity property (3.3.9) and continuity (3.3.8) of  $a(\cdot, \cdot)$  and the fact that  $[(y)_+]^{m_n} y \geq 0$  for every  $y \in \mathbb{R}$ , we obtain

$$\|\underline{u} - \underline{w}^*\| \leq C_1 A \|\underline{u}^* - \underline{w}^*\|^{m_T} + B \quad \forall \underline{u}^* \in K. \quad (3.7.10)$$

Here we used the notations

$$\left. \begin{aligned} A &= \frac{\|c_T\|_{\infty, \Gamma_C}}{\alpha_a} \\ B &= \frac{\|f\|_* + M_a \|\underline{w}^*\|}{\alpha_a} \end{aligned} \right\} \quad (3.7.11)$$

and  $C_1 = C_1(\Omega, \Sigma, \Gamma_C, m_n, m_T)$  is a constant.

For reasons that will become clear later, we introduce another constant  $C_0$  satisfying

$$C_1 \leq C_0. \quad (3.7.12)$$

Clearly, we also have

$$\|\underline{u} - \underline{w}^*\| \leq C_0 A \|\underline{u}^* - \underline{w}^*\|^{m_T} + B \quad \forall \underline{u}^* \in K. \quad (3.7.13)$$

Denoting  $x = \|\underline{u}^* - \underline{w}^*\|$ , a sufficient condition for (3.7.9) to hold, with some  $R > 0$ , is then

$$C_0 A x^{m_T} + B \leq R \quad \forall x \in [0, R]. \quad (3.7.14)$$

We study now what conditions on  $A$  and  $B$  are sufficient for this inequality to hold.

The trivial case  $A=0$  ( $\|c_T\|_{\infty, \Gamma_C} = 0$ ) leads to the condition  $R \geq B$  which can always be satisfied by some  $R > 0$ .

In the case  $A > 0$ , we consider first the particular case

$m_T = 1$ . In this case, a sufficient condition for (3.7.14) to hold is

$$A < 1/C_0.$$

The constant  $C$  in (3.7.7) can thus be chosen as

$$C = 1/C_0 \quad (3.7.15)$$

and the radius  $R$  in (3.7.8) can be any number satisfying

$$C_0 A R + B \leq R \quad (3.7.16)$$

i.e.,  $R \geq B/(1-C_0 A)$ . In the case  $m_T > 1$ , sufficient conditions for (3.7.14) to hold can be interpreted geometrically as follows (see Fig. 3.7.1): the curve  $y = C_0 A x^{m_T} + B$  must intersect the line  $y=x$ . The condition for the existence of such an intersection is

$$C_0 A x_0^{m_T} + B \leq x_0$$

$$\left. \frac{d}{dx} (C_0 A x^{m_T} + B) \right|_{x=x_0} = 1$$

i.e., the point  $(x_0, C_0 A x_0^{m_T} + B)$  at which the tangent to the curve  $y = C_0 A x^{m_T} + B$  is parallel to the line  $y=x$ , must be below or on the line  $y=x$ . An easy calculation leads to the following condition on  $A$  and  $B$

$$AB^{m_T-1} \leq \frac{(m_T-1)^{(m_T-1)}}{m_T^{m_T}} \cdot \frac{1}{C_0}$$

The constant  $C$  in (3.7.7) can thus be chosen as

$$C = [(m_T-1)^{(m_T-1)} / m_T^{m_T}] \cdot (1/C_0), \quad (3.7.17)$$

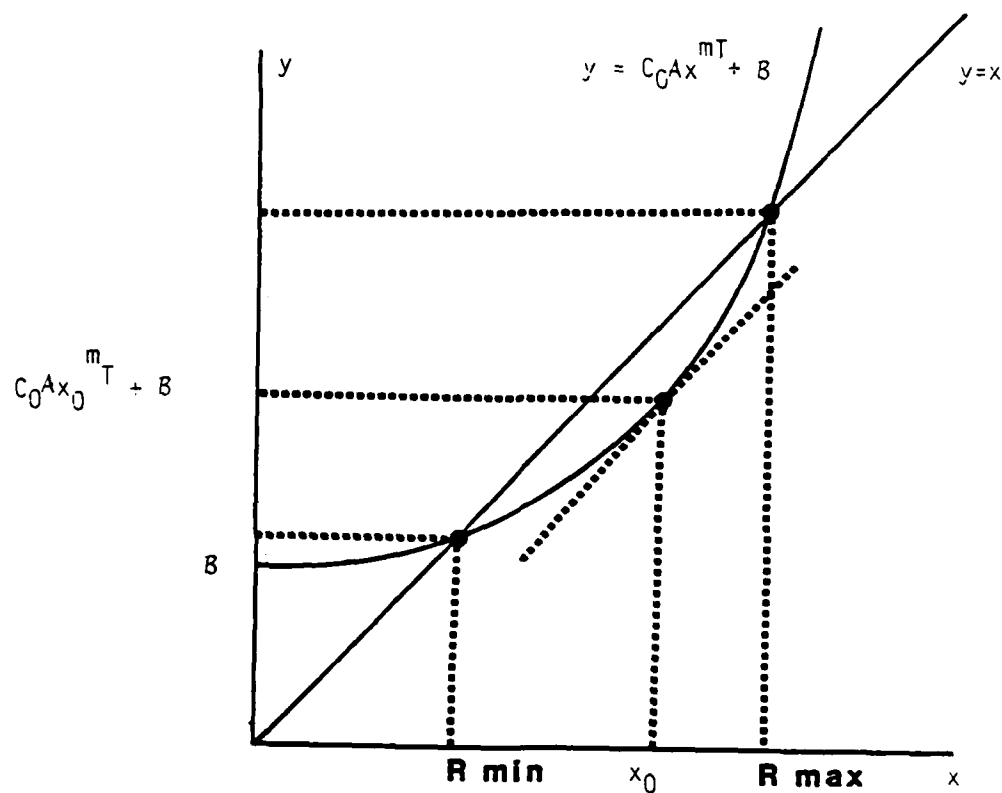


Figure 3.7.1. Geometric interpretation of the sufficient conditions on  $A$  and  $B$  for  $T(K) \subset K$ , when  $m_T > 1$ .



and the admissible values for  $R$  in (3.7.8) are  $R \in [R_{\min}, R_{\max}]$ , with  $R_{\min}$  and  $R_{\max}$  denoting the  $x$  (or  $y$ ) coordinates of the points of intersection (see Fig. 3.7.1), and  $R_{\max}$  being always strictly positive. Equivalently, the admissible values of  $R$  satisfy the inequality

$$C_0 A R^{m_T} + B \leq R. \quad (3.7.18)$$

We have thus proved that, if condition (3.7.7) is satisfied, there exists a set  $K$  that is *nonempty* and such that  $T(K) \subset K$ . The Schauder's fixed point theorem implies then that there exists a  $\underline{u}_0 \in K$  such that

$$\underline{u}_0 = T(\underline{u}_0) = B(\varphi(\gamma(\underline{u}_0)))$$

i.e., (3.6.1) holds. This completes the proof of existence.

We now prove that for sufficiently small data (condition (3.7.7) with an appropriate choice of the constant  $C$ ) the solutions to Problem 3 are *unique in the set  $K$*  where existence was just proved.

Let  $\underline{u}_1, \underline{u}_2 \in K$  be two solutions of Problem 3. Taking  $\underline{u}_0$  in (3.6.1) successively equal to  $\underline{u}_1$  and  $\underline{u}_2$ , subtracting the resulting equations and letting  $\underline{v} = \underline{u}_1 - \underline{u}_2$  we obtain

$$\begin{aligned} a(\underline{u}_1 - \underline{u}_2, \underline{u}_1 - \underline{u}_2) + \langle P(\underline{u}_1) - P(\underline{u}_2), \underline{u}_1 - \underline{u}_2 \rangle \\ + \langle J_n(\underline{u}_1) - J_n(\underline{u}_2), \underline{u}_1 - \underline{u}_2 \rangle = 0 \end{aligned}$$

Using the monotonicity of the operator  $P$ , the  $V$ -ellipticity of  $a(\cdot, \cdot)$ , the definition of the operator  $J_n$  and an estimation of

the type in (3.4.29), we obtain

$$\left. \begin{aligned} \|u_1 - u_2\|^2 &\leq C_2 \frac{\|c_T\|_{\infty, \Gamma_C}}{2\alpha_3} \\ &\cdot (\|u_1 - w^*\|^{m_T-1} + \|u_2 - w^*\|^{m_T-1}) \cdot \|u_1 - u_2\|^2, \end{aligned} \right\} \quad (3.7.19)$$

where  $C_2 = C_2(\Omega, \Sigma, \Gamma_C, m_n, m_T)$  is a constant. Since both  $u_1$  and  $u_2$  are elements of  $K$ , it results that

$$(1 - C_2 A R^{m_T-1}) \|u_1 - u_2\|^2 \leq 0.$$

In the trivial case  $A=0$  ( $\|c_T\|_{\infty, \Gamma_C} = 0$ ) this immediately implies uniqueness of solution (consistent with Lemma 3.7.1).

If  $A \neq 0$ , we have from (3.7.16) or (3.7.18)

$$R^{m_T-1} \leq \frac{1}{C_0 A} \left(1 - \frac{B}{R}\right) \leq \frac{1}{C_0 A},$$

and then,

$$\left(1 - \frac{C_2}{C_0}\right) \|u_1 - u_2\|^2 \leq 0,$$

from which the uniqueness follows if  $C_0$  satisfies:

$$C_2 < C_0 \quad (3.7.20)$$

We can thus conclude that the constant  $C$  in (3.7.7) sufficient to have existence and uniqueness of solution in the set  $K$  is

$$C = \begin{cases} 1/C_0 & \text{if } m_T = 1 \\ [(m_T-1)^{m_T-1} / m_T] (1/C_0) & \text{if } m_T > 1, \end{cases}$$

where  $C_0$  satisfies simultaneously (3.7.12) and (3.7.20), i.e.,

$$\begin{cases} c_1 \leq c_0 \\ c_2 < c_0 \end{cases}$$

and  $c_1$  and  $c_2$  denote the constants in the estimates (3.7.10) and (3.7.19). This concludes the proof of the theorem. —

**Remark 3.7.1.** Sufficient (not necessary) conditions for (3.7.6) to hold are the following:

$$\Omega \in C^{1,1} \text{ and} \quad (3.7.21)$$

$$g \in W_n = \{\xi \in H^{\frac{1}{2}}(\Gamma) \mid \xi=0 \text{ a.e. on } \Gamma_D\} \quad (3.7.22)$$

Under condition (3.7.21), the normal trace of any function  $\underline{v} \in V$  belongs to  $W_n$ ,

$$\gamma_n(\underline{v}) \stackrel{\text{def}}{=} \gamma(\underline{v}) \cdot \underline{n} \in W_n,$$

and  $\gamma_n$  maps  $V$  onto  $W_n$  (see Hünlich and Nauman [1978, Lemma 1.5, page 213]). Consequently, for any  $g$  satisfying (3.7.22) there exists a  $\underline{w}^* \in V$  satisfying (3.7.6).  $\square$

**Remark 3.7.2.** No assumption on the sign of the initial gap  $g$  was made in the above. The conclusions are thus valid both in the case of positive gaps (initially separated bodies) or negative gaps (prescribed indentations of the elastic body by the "foundation"). However, in order to be guaranteed of the existence of steady-sliding solutions, the size of the admissible gaps is restricted by the assumption (3.7.7) that involves the norm of  $\underline{w}^* \in V$  such that  $\underline{w}^* \cdot \underline{n} = g$  a.e. on  $\Gamma_C$  (3.7.6).

Here, we remark that if  $g \geq 0$  a.e. on  $\Gamma_C$ , no restriction on the size of  $g$  is needed to obtain an existence and uniqueness result similar to Theorem 3.7.1. In fact, we only have to observe that for given  $y \geq 0$  and  $m \geq 1$ , and every  $x \in \mathbb{R}$  :

$$[(x-y)_+]^m x \geq 0$$

$$[(x-y)_+]^m \leq |x|^m.$$

Consequently, by taking  $y$  in (3.7.1) equal to  $\underline{u}$  (instead of  $\underline{u}-w^*$ ) we obtain (instead of (3.7.10))

$$\|\underline{u}\| \leq C_1 A \|\underline{u}^*\|^{m_T} + B',$$

with

$$B' = \frac{\|\underline{f}\|_*}{\alpha_a}.$$

Also, the estimate (3.7.19) can be simplified to

$$\begin{aligned} \|\underline{u}_1 - \underline{u}_2\|^2 &\leq C_2 \frac{\|c_T\|_{\infty, \Gamma_C}}{2\alpha_a} \\ &\cdot (\|\underline{u}_1\|^{m_T-1} + \|\underline{u}_2\|^{m_T-1}) \cdot \|\underline{u}_1 - \underline{u}_2\|^2. \end{aligned}$$

With steps similar to those in the proof of Theorem 3.7.1, with assumption (3.7.7) being simplified to

$$\frac{\|c_T\|_{\infty, \Gamma_C}}{\alpha_a} \left( \frac{\|\underline{f}\|_*}{\alpha_a} \right)^{m_T-1} < C,$$

and with no need to assume (3.7.6), it follows that a unique solution to Problem 3 exists in the set

$$K = \{v \in V: \|v\| \leq R\} . \quad \square$$

**Remark 3.7.3.** Similar existence and local uniqueness results are proved in Rabier, Martins, Oden, and Campos [1986] using the Implicit Function Theorem. Since compactness is not required in the proofs, those results apply also to the limit case  $\max\{m_n, m_T\}=3$  with  $N=3$ . Since it is assumed that  $g \geq 0$  on  $\Gamma_C$ , no restrictions on the size of the initial gap are required, which is consistent with Remark 3.7.2 above. Since differentiability is required in the proofs, those results do not apply to the limit case  $\min\{m_n, m_T\}=1$ . Otherwise, the assumptions in that work are similar to those here, particularly: small applied forces ( $f$ ) and arbitrary friction ( $c_T$ ), or small friction and arbitrary forces. In the first of these cases it is shown that the assumption of smallness of the forces can be partially relaxed: only the smallness of the action of  $f$  on elements of  $V$  with non-vanishing normal traces on  $\Gamma_C$  is required.

---

### 3.8. An eigenvalue problem.

We are interested here in the analysis of the dynamic stability of the steady sliding equilibrium positions  $u_0$ . We restrict ourselves to two dimensional problems ( $N=2$ ) and we assume  $m_n, m_T > 1$ . A natural idea is to study the behavior of a linearized version of (3.3.13) for the displacement-velocity pairs in a small neighborhood of  $(u_0, 0) \in V \times V$ . As in Section 3.5, we assume that  $b, t$ , and  $\dot{u}_T^C$  are independent of time and that  $\dot{u}_T^C$  is different from zero everywhere on  $\Gamma_C$ . Considering only velocities that are sufficiently

regular and small that the relative sliding velocity on  $\Gamma_c$  is nowhere equal to zero, denoting  $\underline{w}(\underline{x}, t) = \underline{u}(\underline{x}, t) - \underline{u}_0(\underline{x})$ , and observing that  $P$  and  $J_n$  are continuously differentiable in  $V$ , we are led to the formally linearized version of (3.3.13):

$$\begin{aligned} & (\ddot{\underline{w}}(t), \underline{v}) + c(\dot{\underline{w}}(t), \underline{v}) + a(\underline{w}(t), \underline{v}) \\ & + \langle DP(\underline{u}_0) \cdot \underline{w}(t), \underline{v} \rangle + \langle DJ_n(\underline{u}_0) \cdot \underline{w}(t), \underline{v} \rangle = 0 \quad \forall \underline{v} \in V \end{aligned}$$

where  $DP(\underline{u}_0) \in L(V, V')$  and  $DJ_n(\underline{u}_0) \in L(V, V')$  denote the derivatives of  $P$  and  $J_n$ , respectively, at  $\underline{u}_0 \in V$ .

Working now with the complex numbers field, we define the sesquilinear forms:

$$\begin{aligned} a_0(\underline{z}, \underline{v}) &= \int_{\Omega} A_{ijkl} z_{k,l} \bar{v}_{i,j} dx \\ &+ \int_{\Gamma_c} K_n z_n \bar{v}_n ds + \int_{\Gamma_c} K_{Tn} z_n \bar{v}_n ds \\ c_0(\underline{z}, \underline{v}) &= \int_{\Omega} C_{ijkl} z_{k,l} \bar{v}_{i,j} dx \end{aligned}$$

for every  $\underline{z}$  and  $\underline{v}$  in the space  $V$  (now a space of complex functions). Here, superimposed bars denote complex conjugation,  $v_n = \underline{v}_T \cdot \underline{n}$  on  $\Gamma_c$ ,  $K_n$  denotes the linearized normal stiffness of the foundation at the equilibrium position  $\underline{u}_0$  and  $K_{Tn}$  denotes the coupling stiffness coefficient between normal displacements and tangential stresses, also at the equilibrium position  $\underline{u}_0$ , i.e.,

$$K_n = m_n c_n [(u_{0n} - g)_+]^{m_n - 1}$$

$$K_{Tn} = -m_T c_T [(u_{0n} - g)_+]^{m_T - 1}.$$

Assuming solutions of the form  $\underline{w}(\underline{x}, t) = \underline{w}(\underline{x}) e^{\lambda t}$  we are led to the nonsymmetric eigenvalue problem:

**Problem 4.** Find  $\lambda \in \mathbb{C}$  for which there exists  $\underline{w} \in V$ ,  $\underline{w} \neq 0$  such that

$$a_0(\underline{w}, \underline{v}) + \lambda c_0(\underline{w}, \underline{v}) + \lambda^2(\underline{w}, \underline{v}) = 0 \quad \forall \underline{v} \in V. \quad (3.8.1)$$

Here the  $H$ -inner product is now  $(\underline{z}, \underline{v}) = \int_{\Omega} z_i \bar{v}_i dx$ ,  $\underline{u}, \underline{v} \in H$ .

**Remark 3.8.1.** Sufficient conditions for the above *formal* procedure to be rigorous require additional study. In the (finite dimensional) rigid body case to be presented in the next chapter a similar linearization procedure is rigorous. Occurrence of some eigenvalues of (3.8.1) with positive real parts suggests instability of the steady-sliding equilibrium, and occurrence of negative real parts for all the eigenvalues of (3.8.1) suggests a stable steady-sliding equilibrium.  $\square$

**Remark 3.8.2.** The continuous differentiability of the operators  $P$  and  $J_n$  can be proved directly using estimations of the type used in earlier sections of this chapter or using general results on the differentiability of functions in  $L^p$ -spaces (see Rabier, Martins, Oden and Campos [1986]).  $\square$

## CHAPTER 4

### A RIGID BODY MODEL

#### 4.1. Governing Equations.

We consider here a rigid block (see Figure 4.1.1) with dimensions  $L \times H \times B$ , weight  $W$ , mass  $M$ , moment of inertia with respect to the axis through the mass center  $I = M(L^2 + H^2)/12$ , restrained by a horizontal arm with elastic stiffness  $K_x (> 0)$  and damping coefficient  $C_x (\geq 0)$ , and sliding with friction on a surface which moves with a prescribed tangential velocity  $\dot{U}_x^C$ . The block is supposed to have plane motion, the corresponding degrees-of-freedom being: the tangential and normal (penetrating) displacements of the center of mass  $G(u_x$  and  $u_y$ , respectively) and the rotation ( $u_\theta$ ), as depicted in Fig. 4.1.1. The rotation  $u_\theta$  is assumed to be small so that  $\sin u_\theta \approx \tan u_\theta \approx u_\theta$  and  $\cos u_\theta \approx 1$ . Along the flat candidate contact surface  $\Gamma_C$  the contact laws (2.5.2,3) are assumed to hold. In view of the geometry of the present problem, and assuming zero initial gap, it follows from the normal contact equation (2.5.2) that the vector of generalized forces  $\underline{\Sigma}_n$  associated with the normal stresses on  $\Gamma_C$  satisfies, at each time  $t$ ,

$$-\underline{\Sigma}_n(t) = \underline{P}(\underline{u}(t)) + \underline{Q}(\underline{u}(t), \dot{\underline{u}}(t))$$

where  $\underline{u}(t) = [u_x(t), u_y(t), u_\theta(t)]^t \in \mathbb{R}^3$  is the vector of generalized displacements at time  $t$ , and



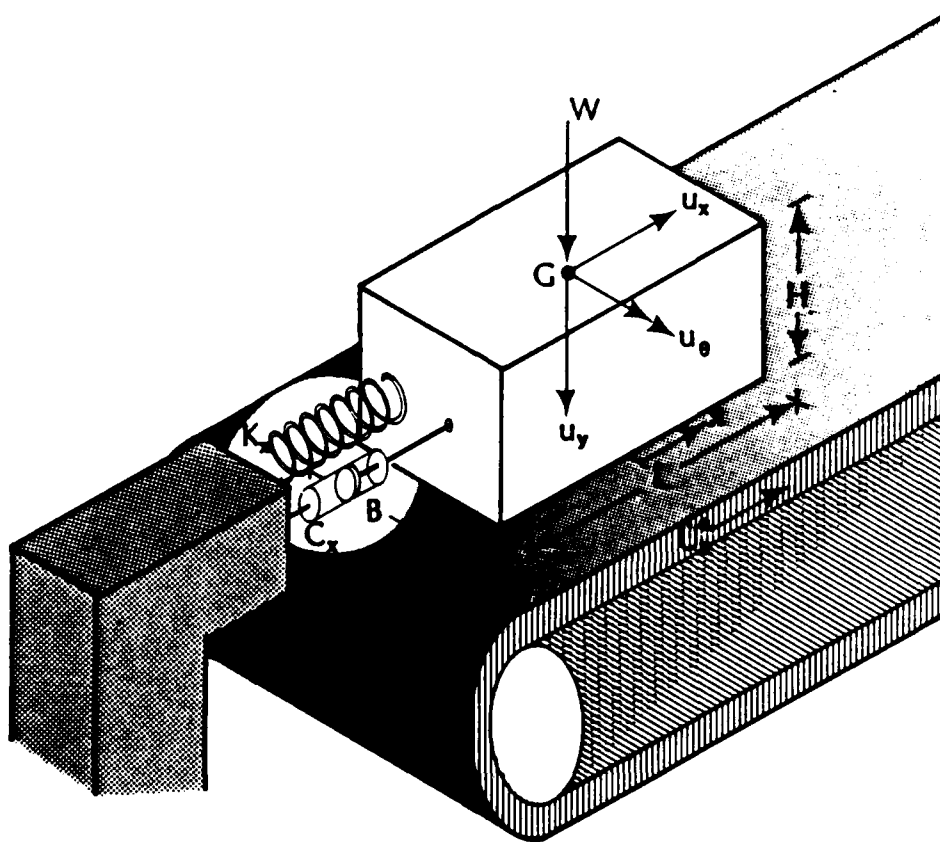


Figure 4.1.1. Geometry and degrees-of-freedom of a rigid block sliding with friction on a moving foundation.

$$\underline{w} \in \mathbb{R}^3 \rightarrow \underline{p}(\underline{w}) = Bc_n \int_{-L/2}^{L/2} [(w_y - xw_\theta)_+]^m_n \begin{Bmatrix} 0 \\ 1 \\ -x \end{Bmatrix} dx \quad (4.1.1)$$

$$(\underline{w}, \underline{v}) \in \mathbb{R}^3 \times \mathbb{R}^3 \rightarrow \underline{q}(\underline{w}, \underline{v}) = Bb_n \int_{-L/2}^{L/2} [(w_y - xw_\theta)_+]^1_n (v_y - xv_\theta) \begin{Bmatrix} 0 \\ 1 \\ -x \end{Bmatrix} dx \quad (4.1.2)$$

On the other hand, from the friction law (2.5.3) it follows that the vector of generalized forces  $\underline{\Sigma}_T$  associated with the friction astresses on  $\Gamma_C$  satisfies at each time  $t$

$$-\underline{\Sigma}_T(t) \in \underline{J}(\underline{u}(t), \dot{\underline{u}}(t) - \dot{\underline{\Phi}}(t))$$

where

$$(\underline{w}, \underline{v}) \in \mathbb{R}^3 \times \mathbb{R}^3 \rightarrow \underline{J}(\underline{w}, \underline{v}) = Bc_T \operatorname{sgn}(v_x + \frac{H}{2} v_\theta) \begin{Bmatrix} 1 \\ 0 \\ H/2 \end{Bmatrix} \int_{-L/2}^{L/2} [(w_y - xw_\theta)_+]^m_T dx \quad (4.1.3)$$

$$t \in [0, T] \rightarrow \dot{\underline{\Phi}}(t) = \begin{Bmatrix} \dot{u}_x^c(t) \\ 0 \\ 0 \end{Bmatrix}$$

$$\xi \in \mathbb{R} \rightarrow \operatorname{sgn}(\xi) = \begin{cases} 1 & \text{if } \xi > 0 \\ [-1, 1] & \text{if } \xi = 0 \\ -1 & \text{if } \xi < 0 \end{cases}.$$

For this system the motion  $t \in [0, T] \rightarrow \underline{u}(t) \in \mathbb{R}^3$  has thus to satisfy, for a.e.  $t$ , the following differential inclusion:

$$\begin{aligned} & \underline{M} \ddot{\underline{u}}(t) + \underline{C} \dot{\underline{u}}(t) + \underline{K} \underline{u}(t) \\ & + \underline{p}(\underline{u}(t)) + \underline{q}(\underline{u}(t), \dot{\underline{u}}(t)) \\ & + \underline{J}(\underline{u}(t), \dot{\underline{u}}(t) - \dot{\underline{\Phi}}(t)) \ni \underline{F} \end{aligned} \quad (4.1.4)$$

and, at  $t=0$ , the initial conditions

$$\underline{u}(0) = \underline{\bar{u}}_0, \quad \dot{\underline{u}}(0) = \underline{\bar{u}}_1. \quad (4.1.5)$$

Here  $\underline{\underline{M}}, \underline{\underline{C}}, \underline{\underline{K}} \in \mathbb{R}^3 \times \mathbb{R}^3$  denote the symmetric mass, linear damping and linear stiffness matrices and  $\underline{\underline{F}}(t) \in \mathbb{R}^3$  denotes the vector of applied forces at time  $t$ . The matrix  $\underline{\underline{M}}$  is positive definite and the matrices  $\underline{\underline{C}}$  and  $\underline{\underline{K}}$  are positive semi-definite. The form of these matrices and vector in the present problem is

$$\underline{\underline{M}} = \begin{bmatrix} \underline{\underline{M}} & 0 & 0 \\ 0 & \underline{\underline{M}} & 0 \\ 0 & 0 & \underline{\underline{I}} \end{bmatrix}; \quad \underline{\underline{C}} = \begin{bmatrix} \underline{\underline{C}} & 0 & 0 \\ 0^x & 0 & 0 \\ 0 & 0 & 0 \end{bmatrix}; \quad \underline{\underline{K}} = \begin{bmatrix} \underline{\underline{K}} & 0 & 0 \\ 0^x & 0 & 0 \\ 0 & 0 & 0 \end{bmatrix}; \quad \underline{\underline{F}}(t) = \begin{Bmatrix} 0 \\ \underline{\underline{W}} \\ 0 \end{Bmatrix}. \quad (4.1.6)$$

The problem defined by (4.1.4,5) is the rigid body analog of Problem 2 in the previous chapter.

For given  $\underline{\underline{F}} \in \mathbb{R}^3$  and  $\dot{\underline{\underline{U}}}_x^C \in \mathbb{R} - \{0\}$ , both independent of time, the rigid body analog of Problem 3 consists of finding  $\underline{\underline{u}}_0 \in \mathbb{R}^3$  satisfying (set  $\dot{\underline{\underline{u}}} = \ddot{\underline{\underline{u}}} = 0$  in (4.1.4)):

$$\underline{\underline{K}} \underline{\underline{u}}_0 + \underline{\underline{P}}(\underline{\underline{u}}_0) + \underline{\underline{J}}_{\eta}(\underline{\underline{u}}_0) = \underline{\underline{F}} \quad (4.1.7)$$

where

$$\underline{\underline{w}} \in \mathbb{R}^3 \rightarrow \underline{\underline{J}}_{\eta}(\underline{\underline{w}}) \stackrel{\text{def}}{=} -\underline{\underline{B}} \underline{\underline{C}}_T \eta \begin{Bmatrix} 1 \\ 0 \\ H/2 \end{Bmatrix} \int_{-L/2}^{L/2} [(\underline{\underline{w}}_y - x \underline{\underline{w}}_{\theta})_+]^m dx (= \underline{\underline{J}}(\underline{\underline{w}}, 0 - \frac{1}{2})) \quad (4.1.8)$$

and

$$\eta \stackrel{\text{def}}{=} \text{sgn}(\dot{\underline{\underline{U}}}_x^C) = \dot{\underline{\underline{U}}}_x^C / |\dot{\underline{\underline{U}}}_x^C|, \quad \dot{\underline{\underline{U}}}_x^C \neq 0.$$

**Remark 4.1.1.** For every  $\underline{\underline{v}} \in N_{\delta}(0) = \{\underline{\underline{v}} \in \mathbb{R}^3 : |\underline{\underline{v}}_x| + |\underline{\underline{v}}_y| + |\underline{\underline{v}}_{\theta}| < \delta = |\dot{\underline{\underline{U}}}_x^C| / \max(1, H/2)\}$  we have  $|\underline{\underline{v}}_x + (H/2)\underline{\underline{v}}_{\theta}| < |\dot{\underline{\underline{U}}}_x^C|$  so that  $\text{sgn}(\underline{\underline{v}}_x + (H/2)\underline{\underline{v}}_{\theta} - \dot{\underline{\underline{U}}}_x^C) = \text{sgn}(-\dot{\underline{\underline{U}}}_x^C) = -\eta$ , and  $\forall (\underline{\underline{w}}, \underline{\underline{v}}) \in \mathbb{R}^3 \times N_{\delta}(0)$   $\underline{\underline{J}}(\underline{\underline{w}}, \underline{\underline{v}} - \frac{1}{2}) = \underline{\underline{J}}_{\eta}(\underline{\underline{w}})$ , i.e., for  $(\underline{\underline{w}}, \underline{\underline{v}})$  in a sufficiently small neighborhood in the phase space  $\mathbb{R}^3 \times$

$R^3$  of the equilibrium position  $(\underline{u}_0, \underline{0})$ ,  $J(\underline{w}, \underline{v} - \frac{\dot{\underline{w}}}{\gamma})$  is single valued and independent of  $\underline{v}$  (velocity). For  $m_n, m_T, l_n > 1$  it results that  $P(\cdot)$ ,  $Q(\cdot, \cdot)$ ,  $J_n(\cdot)$  are continuously differentiable in a sufficiently small neighborhood of the equilibrium position.  $\equiv$

In a sufficiently small neighborhood of the equilibrium position  $(\underline{u}_0, \underline{0})$  the differential inclusion reduces to the equation

$$M \ddot{\underline{u}} + C \dot{\underline{u}} + K \underline{u} + P(\underline{u}) + Q(\underline{u}, \dot{\underline{u}}) + J_n(\underline{u}) = F. \quad (4.1.8)$$

With  $m_n, m_T, l_n > 1$  and taking  $\underline{w}(t) = \underline{u}(t) - \underline{u}_0$  we obtain the linearized equation

$$M \ddot{\underline{w}} + C_0 \dot{\underline{w}} + K_0 \underline{w} = 0 \quad (4.1.9)$$

where

$$\left. \begin{aligned} C_0 &\stackrel{\text{def}}{=} C + C^Q(\underline{u}_0) \\ K_0 &\stackrel{\text{def}}{=} K + K^P(\underline{u}_0) + K^Q(\underline{u}_0, \underline{0}) + K_n^J(\underline{u}_0) \end{aligned} \right\} \quad (4.1.10)$$

and, for  $(\underline{w}, \underline{v})$  in a small neighborhood of  $(\underline{u}_0, \underline{0}) \in R^3 \times R^3$ ,

$$\left. \begin{aligned} K^P(\underline{w}) &\stackrel{\text{def}}{=} \frac{\partial}{\partial \underline{w}} P(\underline{w}) \\ K^Q(\underline{w}, \underline{v}) &\stackrel{\text{def}}{=} \frac{\partial}{\partial \underline{w}} Q(\underline{w}, \underline{v}) & C^Q(\underline{w}) &= \frac{\partial}{\partial \underline{v}} Q(\underline{w}, \underline{v}) \\ &= 0, \text{ if } \underline{v} = \underline{0} \\ K_n^J(\underline{w}) &\stackrel{\text{def}}{=} \frac{\partial}{\partial \underline{w}} J_n(\underline{w}) \\ &= \frac{\partial}{\partial \underline{w}} J(\underline{w}, \underline{v}) \Big|_{\underline{v} = -\frac{\dot{\underline{w}}}{\gamma}} \end{aligned} \right\} \quad (4.1.11)$$

The rigid body analog of Problem 4 consists thus of seeking  $\lambda \in \mathbb{C}$ ,  $\underline{W} \in \mathbb{C}^3$ ,  $\underline{W} \neq \underline{0}$  such that

$$[K_0 + \lambda C_0 + \lambda^2 M] \underline{W} = \underline{0}. \quad (4.1.12)$$

#### 4.2. Steady-sliding equilibrium and linear stability analysis.

##### 4.2.1. Nondimensional form of the equations.

Assuming, for definiteness,  $\dot{U}_x^C > 0$  ( $n=+1$ ) and introducing the nondimensional variables

$$u_x = u_x/X, u_y = u_y/Y, u_\theta = u_\theta L/Y, \quad (4.2.1)$$

with

$$X = W/K_x, \quad (4.2.2)$$

$$Y = (W/c_n BL)^{1/m_n}, \quad (4.2.3)$$

the equilibrium equations (4.1.7) become

$$\begin{cases} u_{x0} = f \cdot I_x^J(u_{y0}, u_{\theta 0}) \end{cases} \quad (4.2.4)$$

$$\begin{cases} I_y^P(u_{y0}, u_{\theta 0}) = 1 \end{cases} \quad (4.2.5)$$

$$\begin{cases} I_\theta^P(u_{y0}, u_{\theta 0}) - \frac{f \cdot h}{2} I_x^J(u_{y0}, u_{\theta 0}) = 0 \end{cases} \quad (4.2.6)$$

where we introduced the nondimensional parameters:

$$f = \frac{c_T}{c_n} \left( \frac{W}{BL} \right)^{\frac{m_T}{m_n} - 1} \quad (4.2.7)$$

$$h = \frac{H}{L} \quad (4.2.8)$$

and the functions

$$(w_y, w_\theta) \in R^2 \rightarrow I_x^J(w_y, w_\theta) = \int_{-\frac{1}{2}}^{+\frac{1}{2}} [(w_y - \xi w_\theta)_+]^{m_T} d\xi$$

$$(w_y, w_\theta) \in R^2 \rightarrow I_y^P(w_y, w_\theta) = \int_{-\frac{1}{2}}^{+\frac{1}{2}} [(w_y - \xi w_\theta)_+]^{m_n} d\xi$$

$$(w_y, w_\theta) \in R^2 \rightarrow I_\theta^P(w_y, w_\theta) = \int_{-\frac{1}{2}}^{+\frac{1}{2}} [(w_y - \xi w_\theta)_+]^{m_n} (-\xi) d\xi.$$

The parameters governing the steady-sliding equilibrium problem are thus the powers  $m_n$  and  $m_T$ , the friction parameter  $f$  and the geometric parameter  $h$ .

With respect to the eigenvalue problem (4.1.12), we observe that in the present case  $K_{yx0} = K_{\theta x0} = C_{yx0} = C_{\theta x0} = M_{yx} = M_{\theta x} = 0$ , so that the characteristic equation for (4.1.12) decouples into

$$K_x + \lambda_x C_x + \lambda_x^2 M = 0 \quad (4.2.9)$$

$$\det(K_0^* + \lambda^* C_0^* + \lambda^{*2} M^*) = 0. \quad (4.2.10)$$

Here, the superscript  $*$  on a matrix denotes the submatrix associated with the normal and rotational degrees-of-freedom.

From (4.2.9) it is clear that the eigenvalues associated with the tangential motion are always imaginary ( $C_x = 0$ ) or have negative real parts ( $C_x > 0$ ).

In order to study the stability of normal and rotational motions, it is convenient to use the nondimensional variables  $u_{y0}$  and  $u_{\theta 0}$  (see (4.2.1) above) and the nondimensional eigenvalues

$$\Lambda = \lambda^* / \omega_{y0} \quad (4.2.11)$$

where  $\omega_{y0}$  denotes the frequency of the free normal oscillation of the block for the linearized normal stiffness at the (frictionless) equilibrium position  $u_{y0} = u_{y0}/Y=1$ , i.e.,

$$\omega_{y0} = (m_n c_n B L Y^{m_n-1} / M)^{\frac{1}{2}}. \quad (4.2.12)$$

The characteristic equation (4.2.10) becomes then

$$\det \left( \int_{-\frac{1}{2}}^{+\frac{1}{2}} [a_0(\xi)]^{m_n-1} \begin{bmatrix} 1-\xi & -\xi \\ -\xi & \xi^2 \end{bmatrix} d\xi - \frac{f m_T h}{2 m_n} \int_{-\frac{1}{2}}^{+\frac{1}{2}} [a_0(\xi)]^{m_T-1} \begin{bmatrix} 0 & 0 \\ 1 & -\xi \end{bmatrix} d\xi \right. \\ \left. + 2 \Lambda \hat{z} \int_{-\frac{1}{2}}^{+\frac{1}{2}} [a_0(\xi)]^{l_n} \begin{bmatrix} 1 & -\xi \\ -\xi & \xi^2 \end{bmatrix} d\xi + \Lambda^2 \begin{bmatrix} 1 & 0 \\ 0 & (1+h^2)/12 \end{bmatrix} \right) = 0 \quad (4.2.13)$$

where we have used the notation  $a_0(\xi) = (u_{y0} - \xi u_{\theta 0})_+$  and we have introduced the interface normal damping parameter

$$\hat{z} = \frac{\sqrt{W/M}}{2V m_n} \frac{b_n}{c_n^{(l_n+1/2)/m_n}} \left( \frac{W}{BL} \right)^{(l_n+1/2)/m_n - 1}$$

It is clear from (4.2.13) that the parameters that govern the linear stability of the steady-sliding are the powers  $m_n$ ,  $m_T$  and  $l_n$ , the friction parameter  $f$ , the normal damping parameter  $\hat{z}$  and the geometric parameter  $h$ . It is also clear that the contribution of the frictional resistance to the eigenvalue problem (4.2.13) is a nonsymmetric matrix.

#### 4.2.2. Numerical results

In order to study numerically the steady-sliding equilibrium and its linear stability we first select values for  $m_n, m_T$  and  $h$  and solve the problem (4.2.4-6) for increasing values of  $f$  in the

range  $[0, \bar{f})$ , where  $\bar{f} = \bar{f}(m_n, m_T, h)$  denotes the value of  $f$  for which steady sliding equilibrium ceases to be possible due to the tumbling of the block (for  $m_n = m_T$  it is easy to see that  $\bar{f} = 1/h = L/H$ ). For each of the values of  $f$  considered and for some  $l_n$  and  $\hat{z}$  the eigenvalue problem (4.1.12) is then solved numerically. For details on the numerical computations see Chapter 5. For simplicity, we shall restrict ourselves in the examples presented here to the particular situation  $m_n = m_T = 1$ , hence  $f \leq 1$ ; for the study of some cases involving  $m_n \neq m_T$  see Martins and Oden [1986].

Typical results for the normal ( $u_{y0}$ ) and rotational ( $u_{\theta 0}$ ) equilibrium displacements as the friction parameter is increased are shown in Figs. 4.2.1 and 4.2.2. It is clear that, as should be expected, both  $u_{y0}$  and  $u_{\theta 0}$  grow unboundedly as  $f$  approaches  $\bar{f}$ .

In Figs. 4.2.3 and 4.2.4 we plot typical evolutions of the eigenvalues  $\Lambda$  as the friction parameter  $f$  is increased, when the normal interface damping is zero (Fig. 4.2.3) or different from zero (Fig. 4.2.4).

It is clear that, in both cases, for some range of  $f$ , the nonsymmetry of the friction contributions in (4.2.13) originates eigenvalues  $\Lambda$  with positive real part, and this implies the dynamic instability of the corresponding steady sliding equilibrium positions.

These regions of instability are identified in the  $(h, f)$ -parameter plane (Figs. 4.2.5, 6) for some values of  $m_n = m_T = 1$  and  $\hat{z}$ .

**Remark 4.2.1.** For each  $h > 0$ , the regions of instability in Figs. 4.2.5, 6 are delimited from below by the values  $(f_1)$  at which



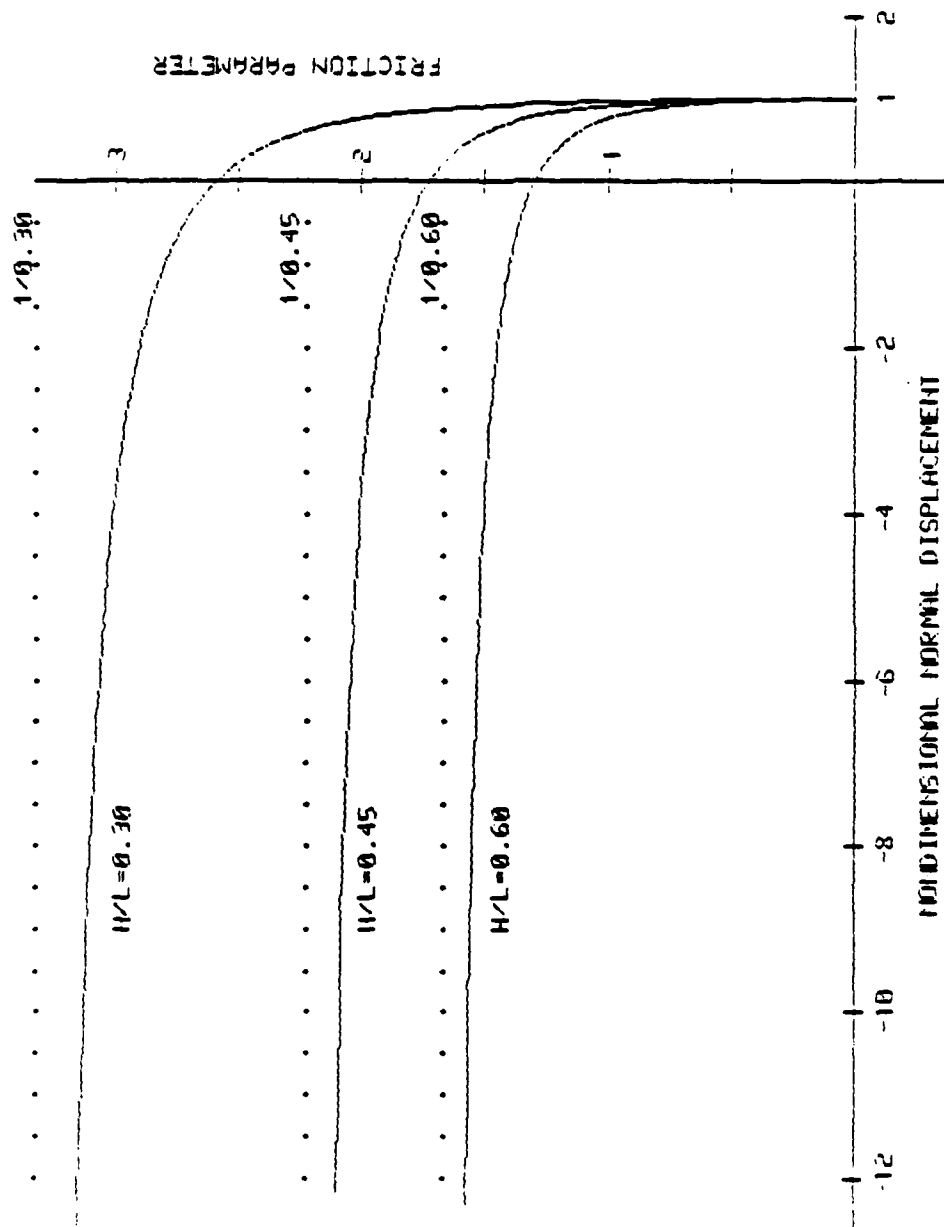


Figure 4.2.1. Steady-sliding normal displacement ( $u_0$ ) of a rigid block as a function of the friction parameter ( $f=\mu$ ) for  $m_T=m_n=2.5$  and three values of the geometric parameter ( $h=H/L$ ).

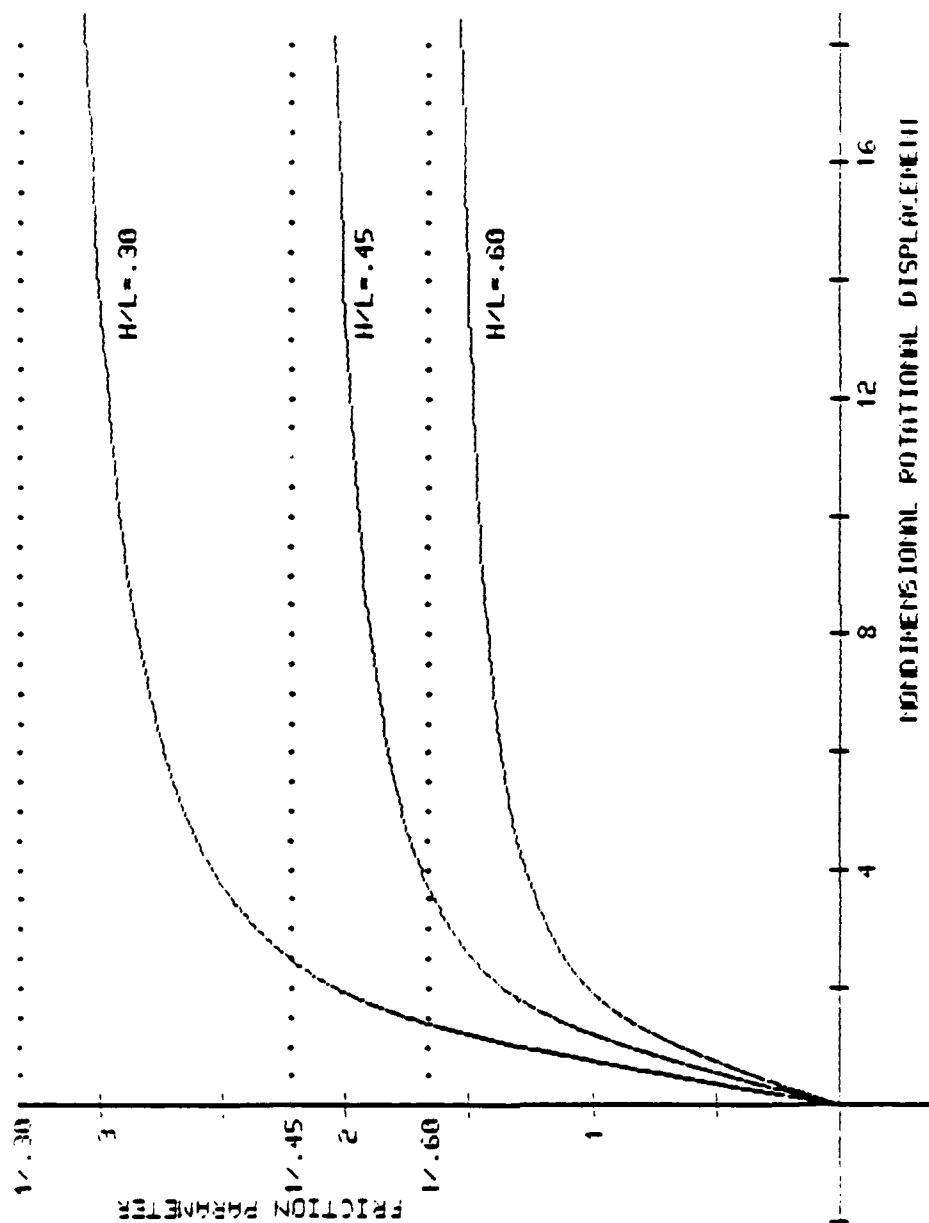


Figure 4.2.2. Steady-sliding rotational displacement ( $u_{\theta}$ ) of a rigid block as a function of the friction parameter ( $f = \mu$ ) for  $m_T = m_n = 2.5$  and three values of the geometric parameter ( $h = H/L$ ).

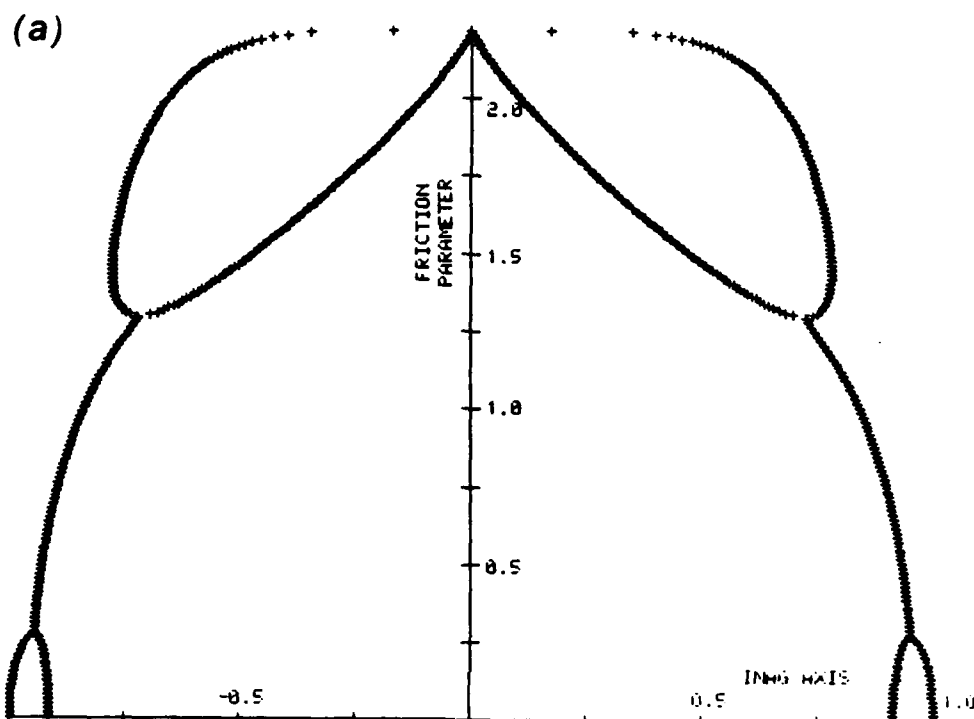


Figure 4.2.3. Orthographic projections (a,b,c) and perspective (d) of the root curves of the characteristic equation (4.2.13) for the admissible range of the friction parameter  $f \in [0, 1/0.45)$  with  $m_n = m_T = 2.5$ ,  $h = 0.45$  and  $\hat{z} = 0.00$  fixed.

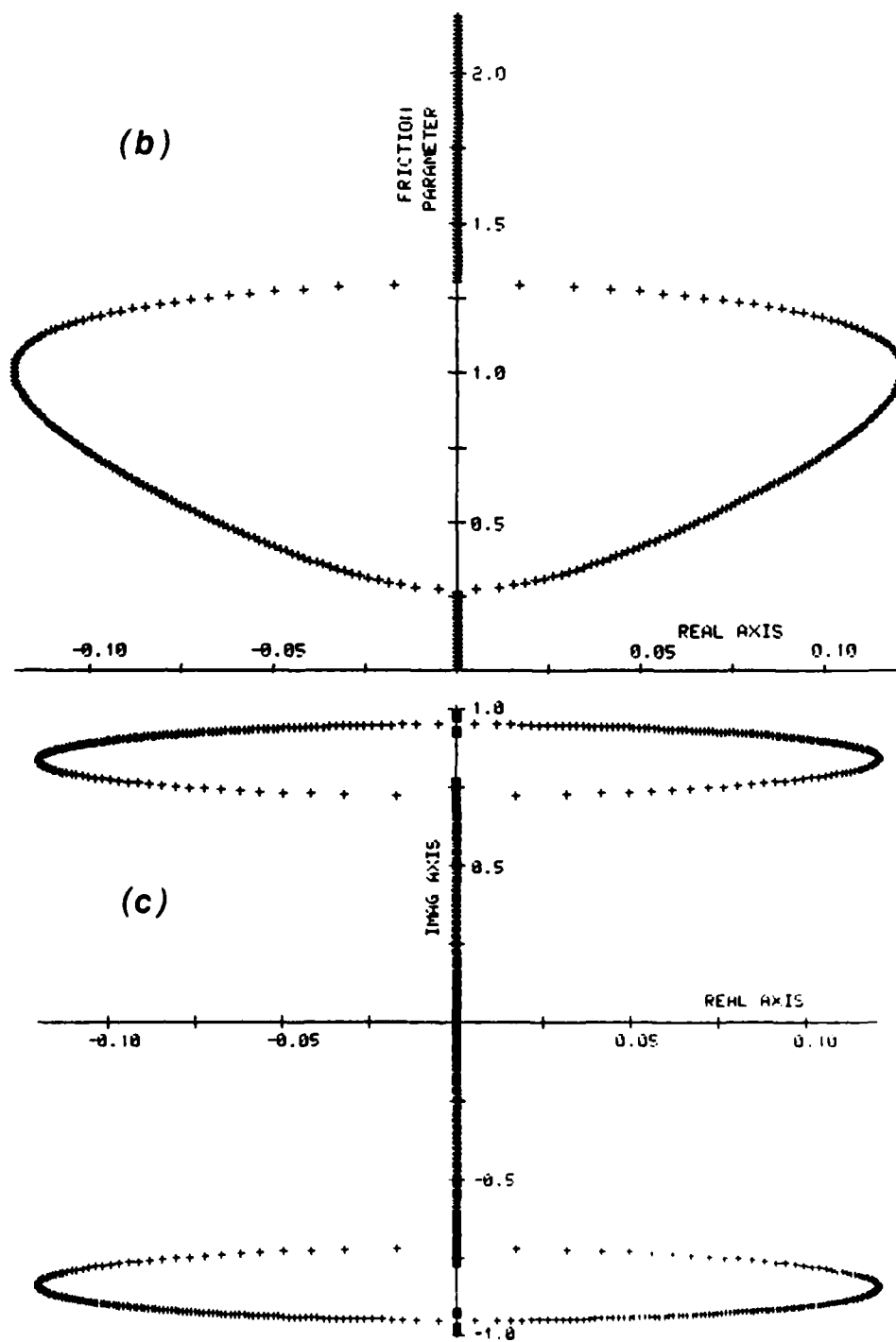


Figure 4.2.3.(b) and (c)

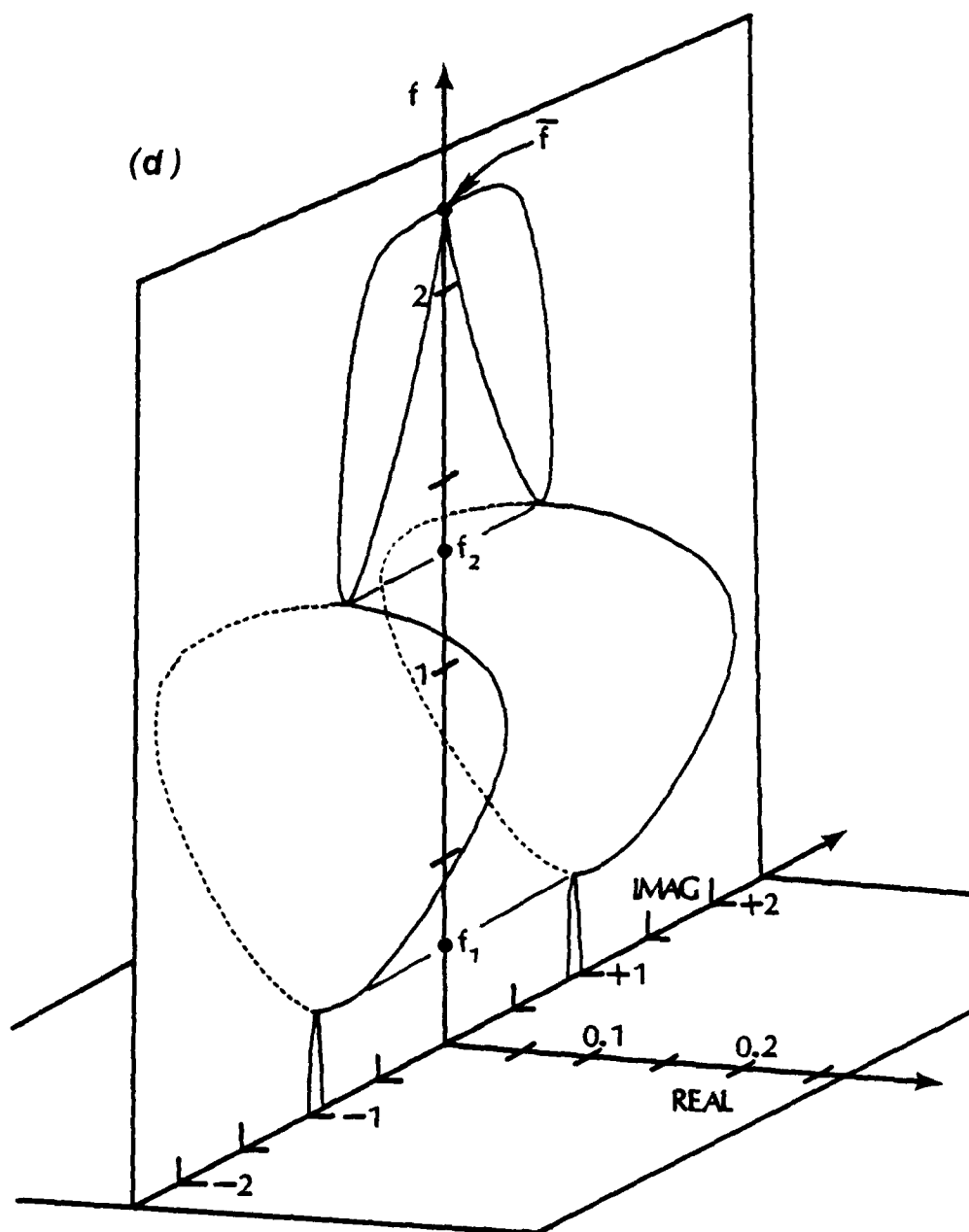


Figure 4.2.3.(d)

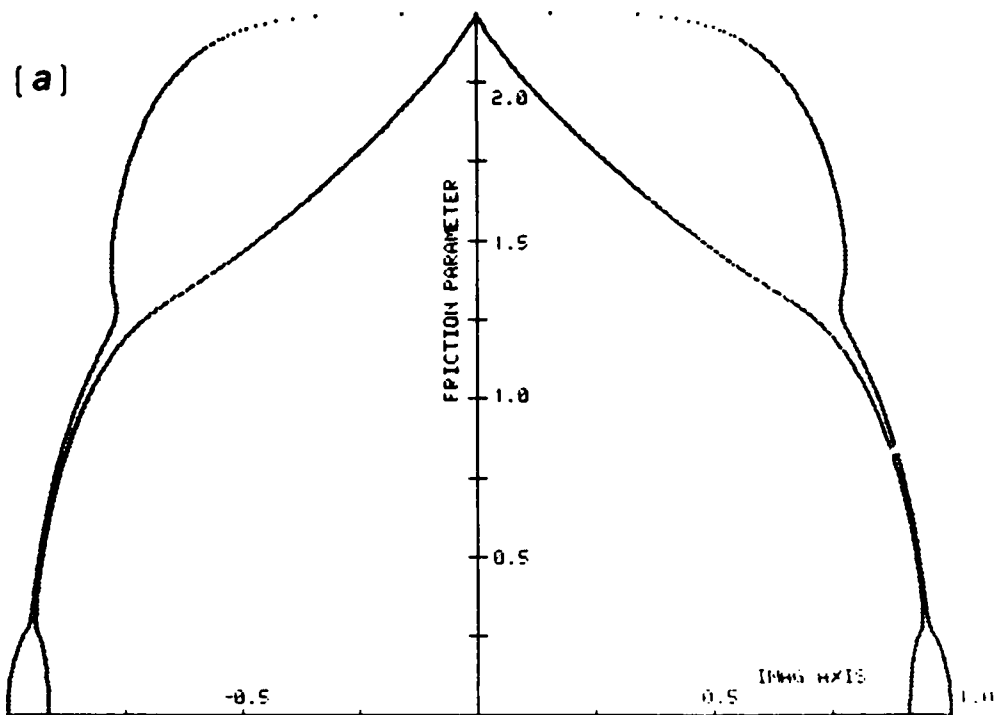


Figure 4.2.4. Orthographic projections of the root curves of the characteristic equation (4.2.13) for the admissible range of the friction parameter  $f \in [0, 1/0.45)$  with  $m_n = m_T = \frac{\lambda}{n} = 2.5$ ,  $h = 0.45$  and  $\hat{z} = 0.02$  fixed.

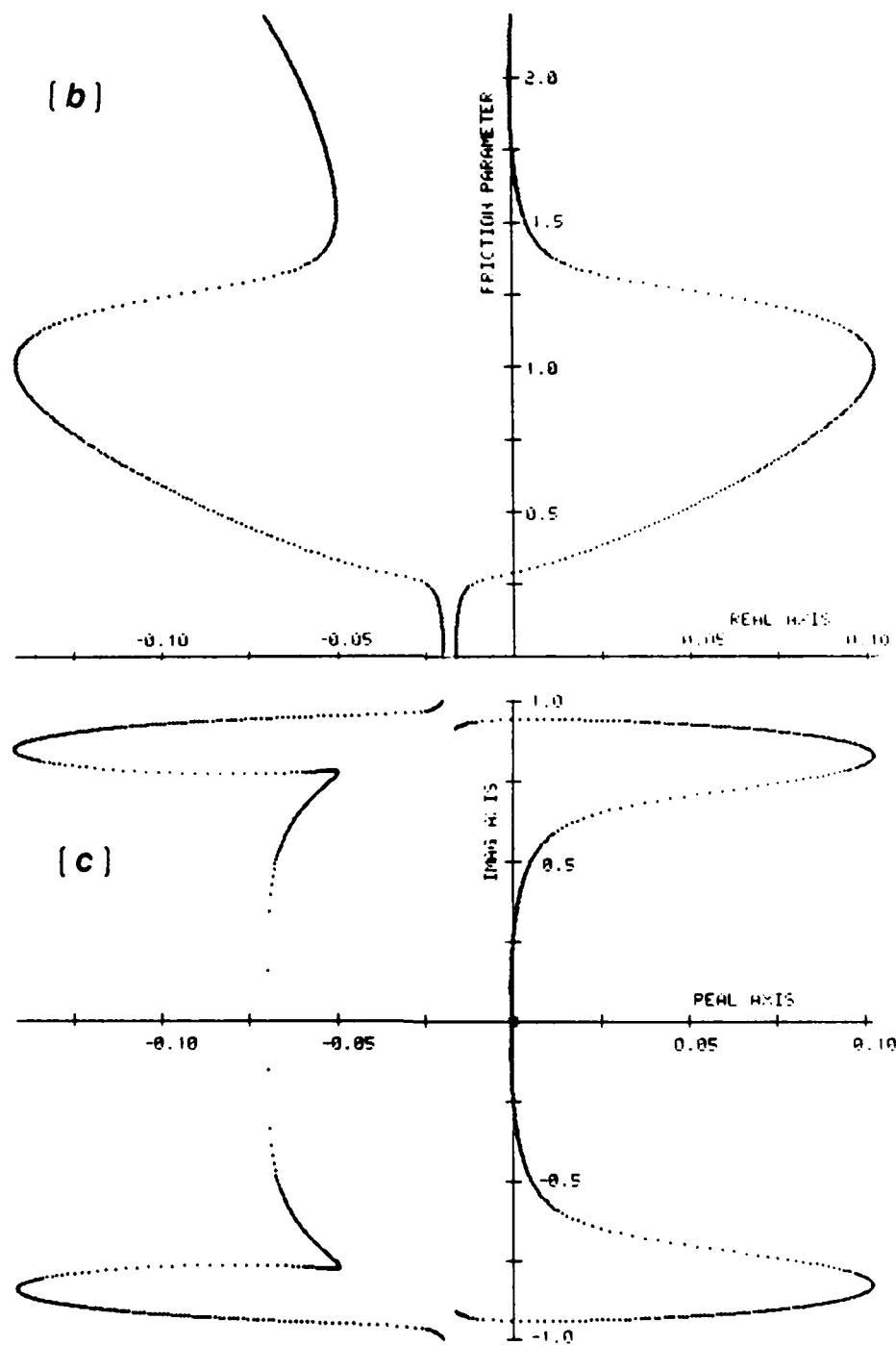


Figure 4.2.4.(b) and (c).

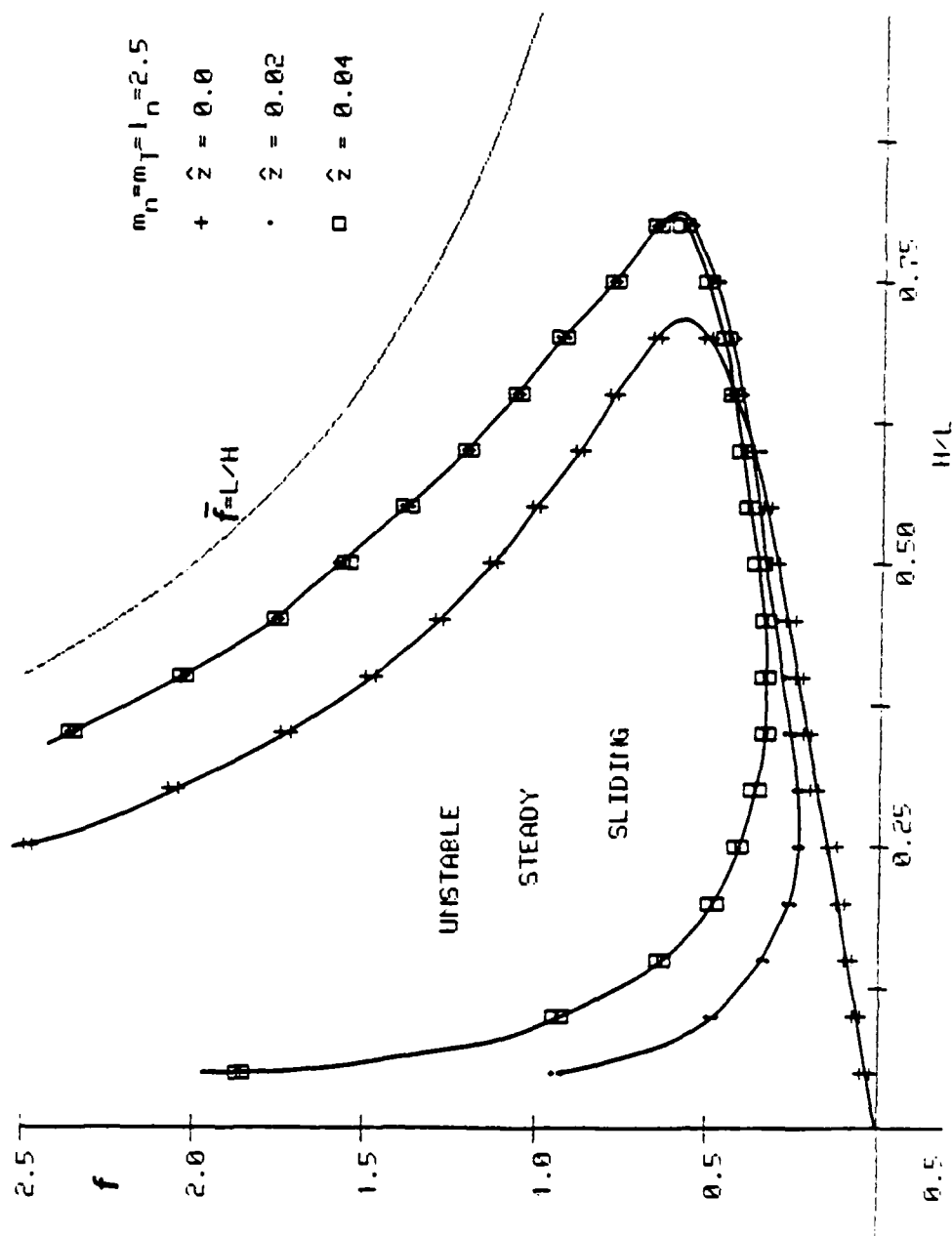


Figure 4.2.5 Effect of the normal interface damping on the stability of the steady-sliding equilibrium of a rigid block.



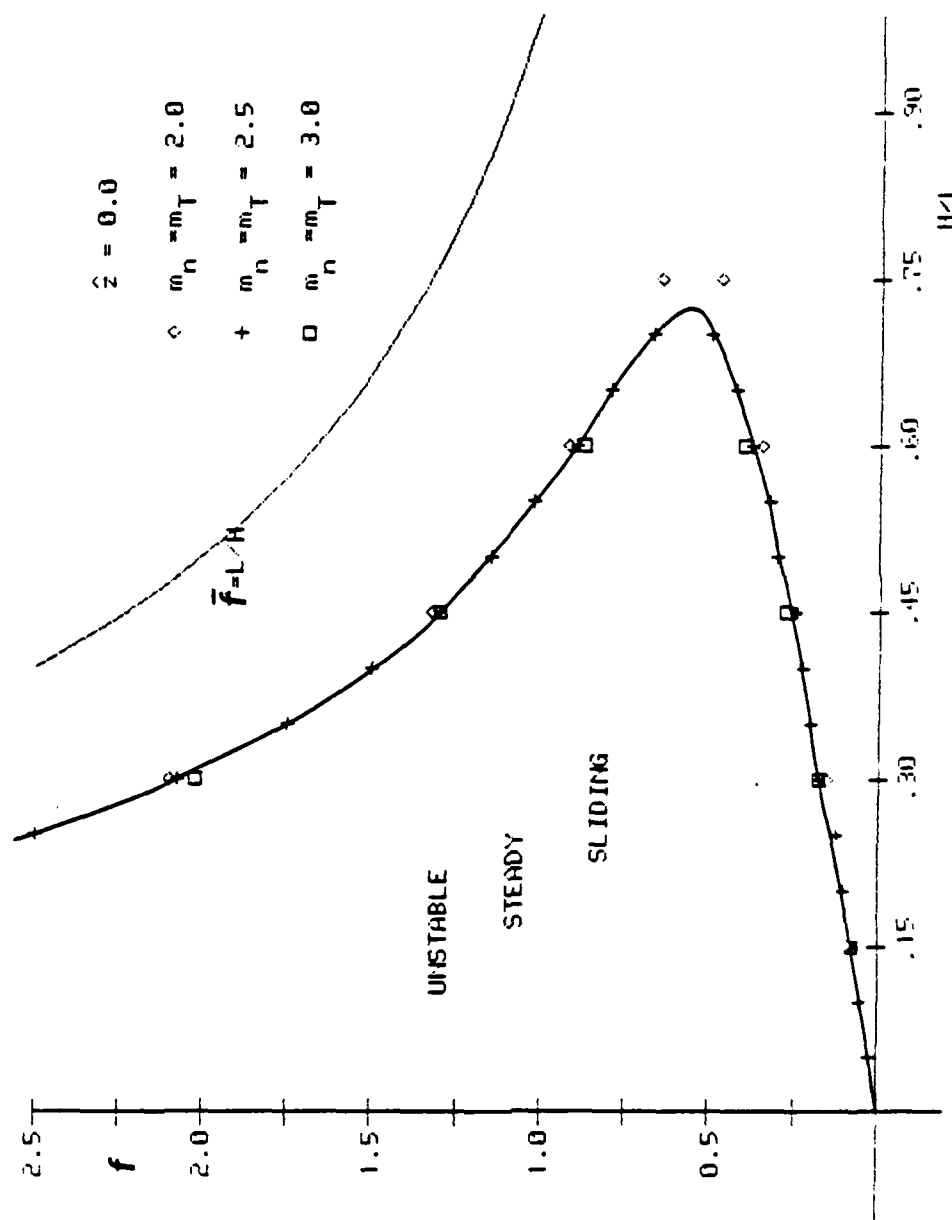


Figure 4.2.6 Effect of the value of the powers  $m_n = m_T$  on the stability of the steady-sliding equilibrium of a rigid block.

a pair of conjugate eigenvalues  $\Lambda$  starts to have positive real parts and from above by the values  $(f_2)$  at which such positive real parts cease to exist. Since our numerical results were obtained by incrementing the value of  $f$  without searching for the exact values of  $f_1$  and  $f_2$ , these values are represented in Fig. 4.2.5 by the pairs of endpoints of the increments of  $f$  at which the above mentioned transitions occur. For clarity, in Fig. 4.2.6, the transitional increments' endpoints lying inside the instability region are omitted.

We also remark that, if some eigenvalue of (4.1.12) has a zero real part no definitive conclusion on the stability of the equilibrium solution can be obtained from the eigenvalue problem (4.1.12). Since we are mostly interested in showing that, for some range of the parameters involved, steady-sliding is unstable, we shall not pursue here the study of what happens outside the region of instability in Figs. 4.2.5,6 when  $\hat{z}=0$  (recall from Fig. 4.2.3 that in those regions the eigenvalues  $\Lambda$  have zero real parts). However if  $C_x > 0$  and  $b_n > 0$  ( $\hat{z} > 0$ ), the points outside the region of instability in Fig. 4.2.5 correspond to asymptotically stable steady-sliding positions (all the eigenvalues of (4.1.12) have negative real parts).  $\square$

#### 4.2.3. Discussion

We observe that the small rotations assumption adopted in this work (recall Section 4.1) implies that, for  $f$  close to

$\bar{f}$ , the results obtained here do not represent the true behavior of the system, since, for such values of  $f$ , large rotations do occur. We remark that these limitations on the validity of our results do not affect the fundamental observation of the previous section, i.e., that for some range of  $f$  and appropriate values of the other parameters, steady-sliding is not stable: as seen in Fig. 4.2.2 and Figs. 4.2.5,6 the transitions on the nature of the eigenvalues of (4.2.13) occur when the rotations  $u_{\theta 0}$  are still very small (note that for  $L$  in the range 1 to 100 cm and  $Y$  in the range 0.3 to 10  $\mu\text{m}$  the rotation  $u_{\theta 0}$  would be in the range  $3 \times 10^{-7} u_{\theta 0}$  to  $10^{-3} u_{\theta 0}$  rad). Only somewhere above the upper boundary of instability in Figs. 4.2.5,6 the small rotations assumption ceases to be valid. Furthermore, we believe that, in practice, the geometric nonlinearity does not play any significant role in block-on-slideway sliding systems of the type studied in this chapter: it is reasonable to expect that no one would operate or run an experiment with such a system allowing for the occurrence of large rotations. Of course, the same may not be true in other circumstances, namely with some pin-on-disk friction apparatus having very flexible arms and very small contact regions.

From Fig. 4.2.6 it can be concluded that, when the coefficient of friction is independent of the normal pressure, the specific value of  $m_n (=m_T)$  in the typical range [2,3] does not affect considerably the boundaries of the region of instability.

In Fig. 4.2.5 it can be observed that, for small values of the geometric parameter  $h(=H/L)$ , the interface normal damping increases the value of the friction parameter at which the instability initiates, i.e., it reduces the region of instability. However, it is also clear from the same figure that the normal damping moves up the upper boundary of the instability region, i.e., it increases the region of instability. Hence, addition of normal interface damping in the form adopted here may indeed have a destabilizing effect on the steady-sliding equilibrium for some ranges of values of the parameters involved. Situations of this type, in which positive viscous "damping" contributions may have a destabilizing effect, are common in nonconservative systems. Such effects were first discovered by Ziegler [1952] and have since been analyzed by various authors in connection with the study of critical loads for beams subjected to follower forces, stability of fluid conveying pipes, panel flutter, etc. (see, e.g., the books of Ziegler [1968], Leipholz [1970], Huseyin [1978] or Guckenheimer and Holmes [1983]). A detailed discussion of these effects in the present problem falls outside the scope of this work. Here we only remark that, with a *deformable* block and even with *no normal interface damping*, the steady-sliding equilibrium is unstable in the region of the  $(h-f)$ -parameter plane where the destabilizing effects of the normal damping are *more significant* (the region above the upper boundary of the *rigid body* instability); see Example 3 in Section 5.5.

### 4.3. Low-frequency stick-slip motion and apparent reductions of kinetic friction.

#### 4.3.1. Nondimensional form of the equations of motion.

We denote by  $\tau$  the nondimensional time

$$\tau = \omega t \quad (4.3.1)$$

and we choose  $\omega$  to be the frequency of the free tangential oscillation of the block, i.e.,

$$\omega = (K_x/M)^{1/2}. \quad (4.3.2)$$

Using again the nondimensional displacements  $u_x$ ,  $u_y$  and  $u_\Theta$  defined in (4.2.1-3), the governing system (4.1.4) becomes

$$\left. \begin{aligned} \underline{M} \underline{u}''(\tau) + \underline{C} \underline{u}'(\tau) + \underline{K} \underline{u}(\tau) \\ + \underline{P}(\underline{u}(\tau)) + \underline{Q}(\underline{u}(\tau), \underline{u}'(\tau)) \\ + \underline{J}(\underline{u}(\tau), \underline{u}'(\tau) - \underline{\Phi}') \ni \underline{F} \end{aligned} \right\} \quad (4.3.3)$$

where

$$\underline{M} = \begin{bmatrix} 1 & 0 & 0 \\ 0 & s^2 & 0 \\ 0 & 0 & s^2(1+h^2)/12 \end{bmatrix}; \quad \underline{K} = \begin{bmatrix} 1 & 0 & 0 \\ 0 & 0 & 0 \\ 0 & 0 & 0 \end{bmatrix}; \quad \underline{C} = 2 \begin{bmatrix} z_x & 0 & 0 \\ 0 & 0 & 0 \\ 0 & 0 & 0 \end{bmatrix} \quad (4.3.4)$$

$$\underline{P}(\underline{u}) = s \int_{-\frac{1}{2}}^{+\frac{1}{2}} [a(\xi)]^{m_n} \begin{Bmatrix} 0 \\ 1 \\ -\xi \end{Bmatrix} d\xi \quad (4.3.5)$$

$$(4.3.6)$$

$$\underline{Q}(\underline{u}, \underline{u}') = 2 \hat{z} (m_n)^{1/2} s^{3/2} \int_{-\frac{1}{2}}^{+\frac{1}{2}} [a(\xi)]^{l_n} (v_y - \xi v_\Theta) \begin{Bmatrix} 0 \\ 1 \\ -\xi \end{Bmatrix} d\xi \quad (4.3.6)$$

$$\tilde{J}(\omega, \nu) = f \operatorname{sgn}(\nu_x + \frac{sh}{2} \nu_\theta) \left\{ \begin{array}{c} 1 \\ 0 \\ \frac{sh}{2} \end{array} \right\} \int_{-\frac{1}{2}}^{+\frac{1}{2}} [a(\xi)]^{m_T} d\xi \quad (4.3.7)$$

$$\tilde{\phi}' = \left\{ \begin{array}{c} u'_x \\ 0 \\ 0 \end{array} \right\} \quad u'_x = \dot{u}_x^C / \omega X \quad (4.3.8)$$

$$\tilde{F} = \left\{ \begin{array}{c} 0 \\ s \\ 0 \end{array} \right\} \quad (4.3.9)$$

Here  $a(\xi) = (\omega_y - \xi \omega_\theta)_+$ ,  $( )'$  denotes differentiation with respect to the nondimensional time  $\tau$ , and, in addition to the parameters  $f$ ,  $h$  and  $\hat{z}$  defined earlier, we have introduced the parameters

$$s = Y/X = \frac{K_x}{W} \left( \frac{W}{c_n B L} \right)^{1/m_n} \quad (4.3.10)$$

$$z_x = \frac{c_x}{2 \sqrt{MK_x}} \quad (4.3.11)$$

The parameter  $s$ , hereafter called the *stiffness parameter*, measures the stiffness of the tangential spring relatively to the normal stiffness of the contact. In fact,  $s$  can be rewritten as  $s = m_n (K_x / m_n c_n B L Y^{m_n - 1})$  where  $K_x$  is the stiffness of the tangential spring and  $m_n c_n B L Y^{m_n - 1}$  is the (linearized) normal stiffness of the contact at the frictionless equilibrium position  $u_{y0} = u_{y0}/Y = 1$ . Note that these two stiffnesses are equal when  $s = m_n$ . The parameter  $z_x$  is the (usual) *tangential damping parameter*.

The initial conditions (4.1.5) become now

$$\underline{u}(0) = \underline{u}_0, \quad \underline{u}'(0) = \underline{u}_1 \quad (4.3.12)$$

Finally we observe that, for computational purposes, problem (4.3.3,12) is regularized using the procedure employed in Section 3.4. In the present chapter,  $\epsilon$  denotes the *nondimensional regularization parameter* [ $\epsilon = (\text{dimensional } \epsilon) / \omega X$ ].  $\Delta t_{\max} (\Delta \tau_{\max})$  denotes the dimensional (nondimensional) maximum time step for the numerical integration of the equations of motion (see Chapter 5).

#### 4.3.2. Numerical results and discussion.

A complete qualitative study of the system (4.1.4,5) is not available yet<sup>3</sup>. Here we present several numerical studies designed to reveal the effect that some of the governing parameters have on the behavior of the system and, whenever possible, we qualitatively compare our numerical results with experimental observations.

First we consider briefly what happens when the coefficient of friction is sufficiently small that the eigenvalues  $\lambda^*$  (equation 4.2.10) are pure imaginary (in the absence of any normal or rotational damping). In the remainder of the section various situations are considered which involve coefficients of friction sufficiently large that some of the eigenvalues  $\lambda^*$  have positive real parts. The resulting low-frequency stick-slip motions or apparently smooth sliding motions are then described and the effect of the normal interface damping on these behaviors is pointed out. The dependence of the stick-slip amplitude and frequency on the driving velocity and the stiffness parameter is also studied. Finally various cases

---

<sup>3</sup>Existence and uniqueness of solution to that problem can, of course, be proved using techniques similar to those used in Section 3.4. For an outline of the proof see Martins and Oden [1986].

are studied for which apparently smooth sliding motions at apparent coefficients of kinetic friction lower than the coefficient of static friction are obtained. The corresponding plots of the variation of the apparent coefficient of kinetic friction with the average sliding velocity are presented and interpreted.

**The small friction case.** We first consider a case for which the steady-sliding position corresponds to a point outside the instability region depicted in Fig. 4.2.5 for  $\hat{z} = 0$ . The data used is the following:

$$M = 450 \text{ Kg} \quad I = \frac{M}{12} (L^2 + H^2) = 1.242 \times 10^5 \text{ Kg cm}^2$$

$$C_x = 0.0$$

$$K_x = 1.11 \times 10^7 \text{ Kg s}^{-2}$$

$$c_n = 10^{13} \text{ Kg cm}^{-3.5} \text{ s}^{-2}; m_n = m_T = 2.5; c_T = \mu c_n; \mu = 0.15$$

$$b_n = 0$$

$$L = 48.8 \text{ cm}; H = 30.5 \text{ cm}; B = 30.5 \text{ cm}$$

$$W = 4.5 \times 10^5 \text{ Kg cm s}^{-2}$$

$$\dot{U}_x^C = 0.08 \text{ cm s}^{-1}$$

$$\bar{u}_0 = u_0; \bar{u}_1 = \{0.0, -0.01 \text{ cm s}^{-1}, 0.0\}^t.$$

$$\Delta t_{\max} = 1 \times 10^{-5} \text{ s}.$$

Note that this data corresponds to a point  $(h, f) = (0.625, 0.15)$  in Fig. 4.2.5. The initial conditions indicated above correspond to a small perturbation of the steady-sliding equilibrium position:



a small normal (upwards) velocity.

In Figs. 4.3.1 and 4.3.2 we show phase plane plots of the resulting normal and rotational oscillations. Despite the complexity of the resulting oscillation *its amplitude* (for a small initial perturbation) *is small and does not grow with time*. At all instants the body remains sliding so that the instantaneous ratio friction force/normal contact force is equal to the coefficient of friction  $\mu=0.15$  and, in average, the ratio friction force/normal load (weight) is also equal to that coefficient. Since the amplitude of the oscillation is small its effect on the tangential displacement trace is small ( $<0.2\%$ ) so that the perturbation of the steady-sliding does not have a significant effect in the present case. Furthermore, if some damping were taken into account ( $C_x > 0$ ,  $b_n > 0$ ) this oscillation would be damped out and the steady-sliding would be essentially attained after a period of time.

**Low frequency stick-slip motion and apparently smooth sliding.** More interesting situations arise when the data is chosen such that the steady-sliding equilibrium is unstable. In the examples studied in the remainder of this section the following common data has been used

$$\left. \begin{aligned} m_n = m_T = I_n &= 2.5 \\ h &= 0.45 \\ f &= 0.6 \end{aligned} \right\} \quad (4.3.13)$$

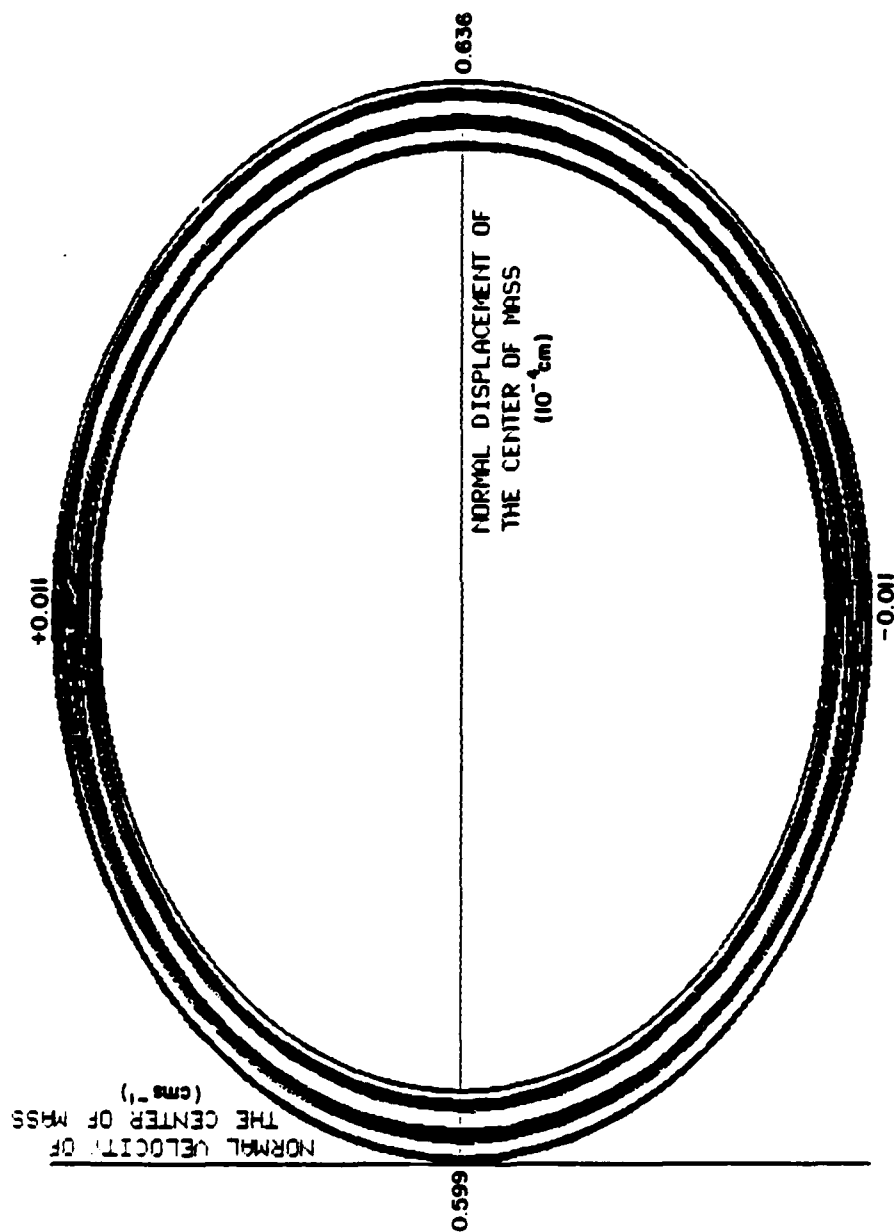


Figure 4.3.1. Phase plane plot for the normal motion of the center of mass. Small friction case:  $(h, f) = (0.625, 0.15)$ .

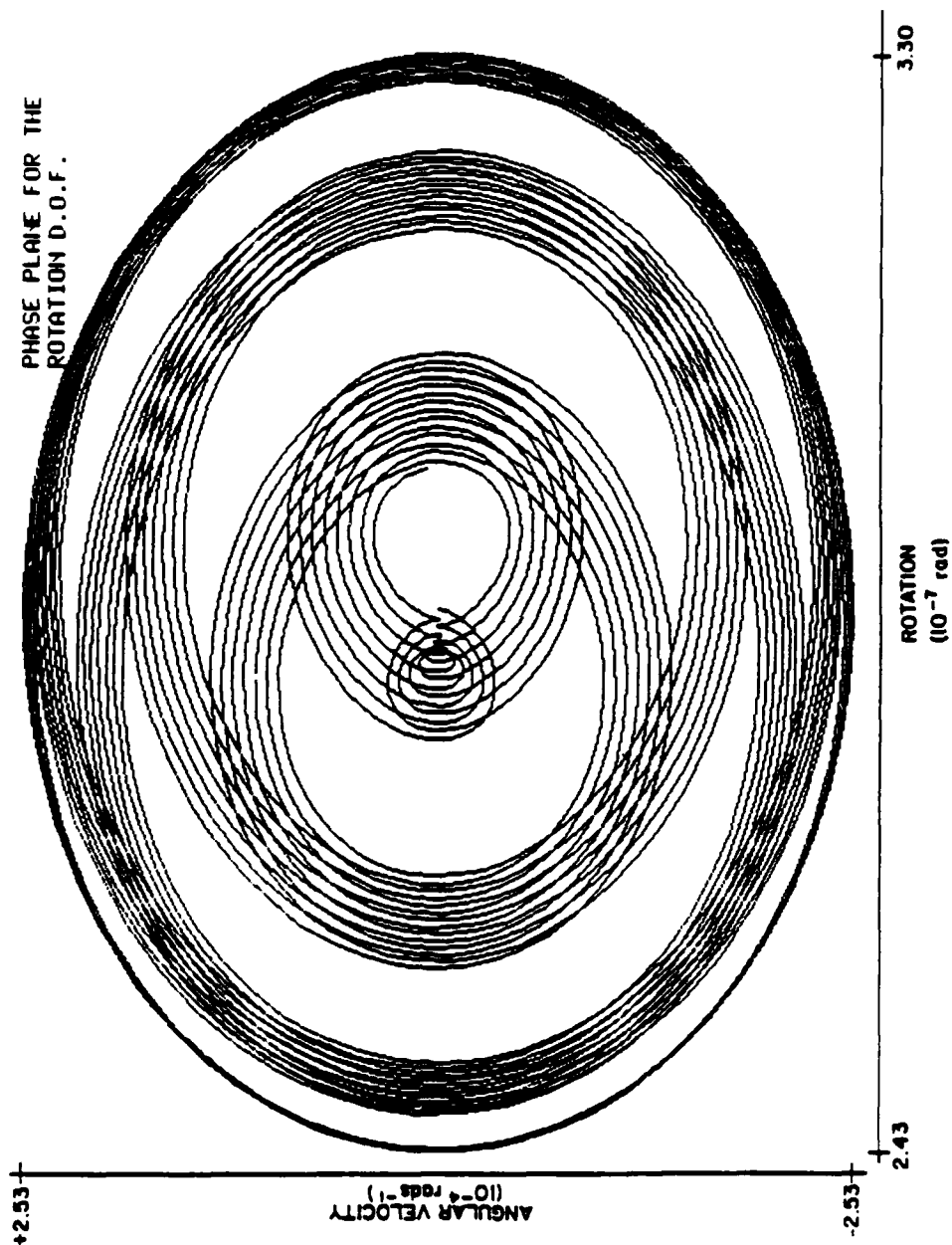


Figure 4.3.2. Phase plane plot for the rotation of the block. Small friction case:  $(h, f) = (0.625, 0.15)$ .

In the computations described next we used, in addition, the following data

$$s = 0.01 \quad (4.3.14)$$

$$z_x = 0.001 \quad (4.3.15)$$

$$\hat{z} = 0.01 \quad (4.3.16)$$

$$\epsilon/u'_x{}^C \leq 0.1 \quad (4.3.17)$$

$$\Delta\tau_{\max} \leq \frac{2\pi}{100} \frac{\omega}{\omega_{y0}} \quad (4.3.18)$$

and various values of the driving velocity  $u'_x{}^C$  as indicated on the figures. The initial conditions were the following

$$\left. \begin{aligned} \bar{u}_{x0} &= u_{x0}, \quad \bar{u}_{y0} = u_{y0} + p_{u_y}, \quad \bar{u}_{\theta 0} = u_{\theta 0}, \\ \bar{u}_1 &= 0, \end{aligned} \right\} \quad (4.3.19)$$

where  $p_{u_y}$  is a small normal displacement perturbation:

$$p_{u_y} = -0.01 \text{ or } -0.001. \quad (4.3.20)$$

The values of  $s$  and  $z_x$  considered above are "in the small range" and the initial conditions (4.3.19) correspond to a small normal perturbation of the steady-sliding equilibrium state.

The following remarks give a summary description and interpretation of the numerical results obtained for the conditions indicated above:

(i) Due to the instability of the normal and rotational modes, the normal and rotational oscillations grow (see Fig. 4.3.3)

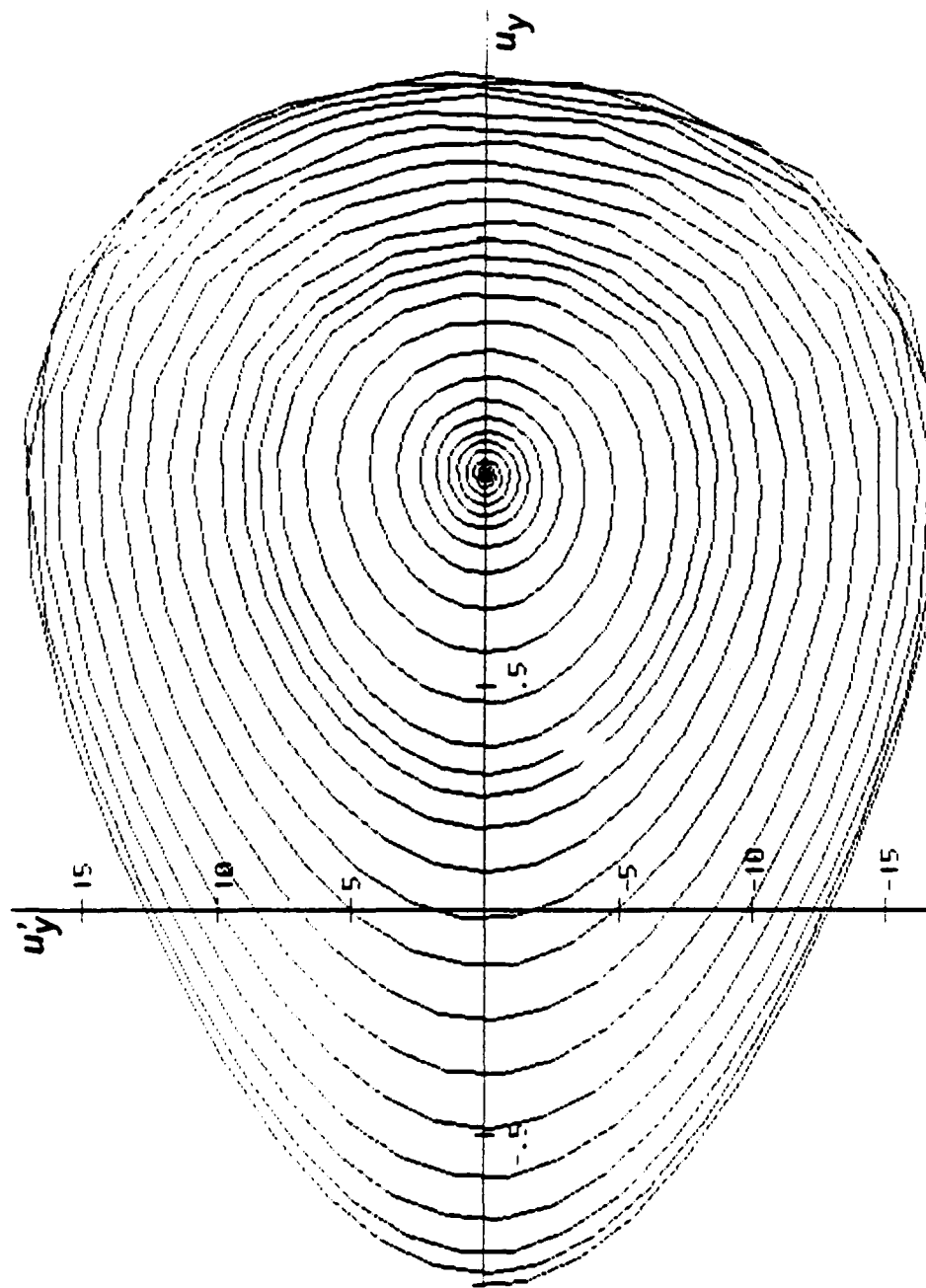


Figure 4.3.3. Phase plane plot of the growing portion of the normal oscillation of the center of mass in the course of low-frequency stick-slip motion.  $u'_x \dot{C} = 0.01$ . (Note: not all the computed points are plotted).

(ii) The variation of the normal force on the contact produces changes in the sliding friction force which in turn produce a tangential oscillation.

(iii) The tangential oscillation may then become sufficiently large that, for small values of the driving velocity  $u_x^C$  the points of the body on the contact surface attain the velocity  $u_x^C$  and the body sticks for short intervals of time (see Fig. 4.3.4).

(iv) With the growing of the normal oscillation actual normal jumps of the body may occur (see Fig. 4.3.3).

(v) The repeated periods of adhesion have the result of decreasing the average value of the friction force on the contact and, due to the absence of equilibrium with the restoring force on the tangential spring, the tangential displacement of the center of mass decreases (see Figs. 4.3.5 and 4.3.6).

(vi) Then, one of the two following situations may occur:

(a) *for values of  $u_x^C$  larger than some critical value, the normal, rotational and tangential oscillations evolve to what appears to be a steady oscillation with successive periods of adhesion and sliding, the average values of the friction force and of the spring elongation being smaller than those corresponding to the steady-sliding equilibrium position (see Figs. 4.3.5 and 4.3.7 to 4.3.10).*

(b) *for values of  $u_x^C$  lower than the critical value, and at a sufficiently small value of the spring elongation, the normal interface damping is able to damp out the normal (and rotational)*

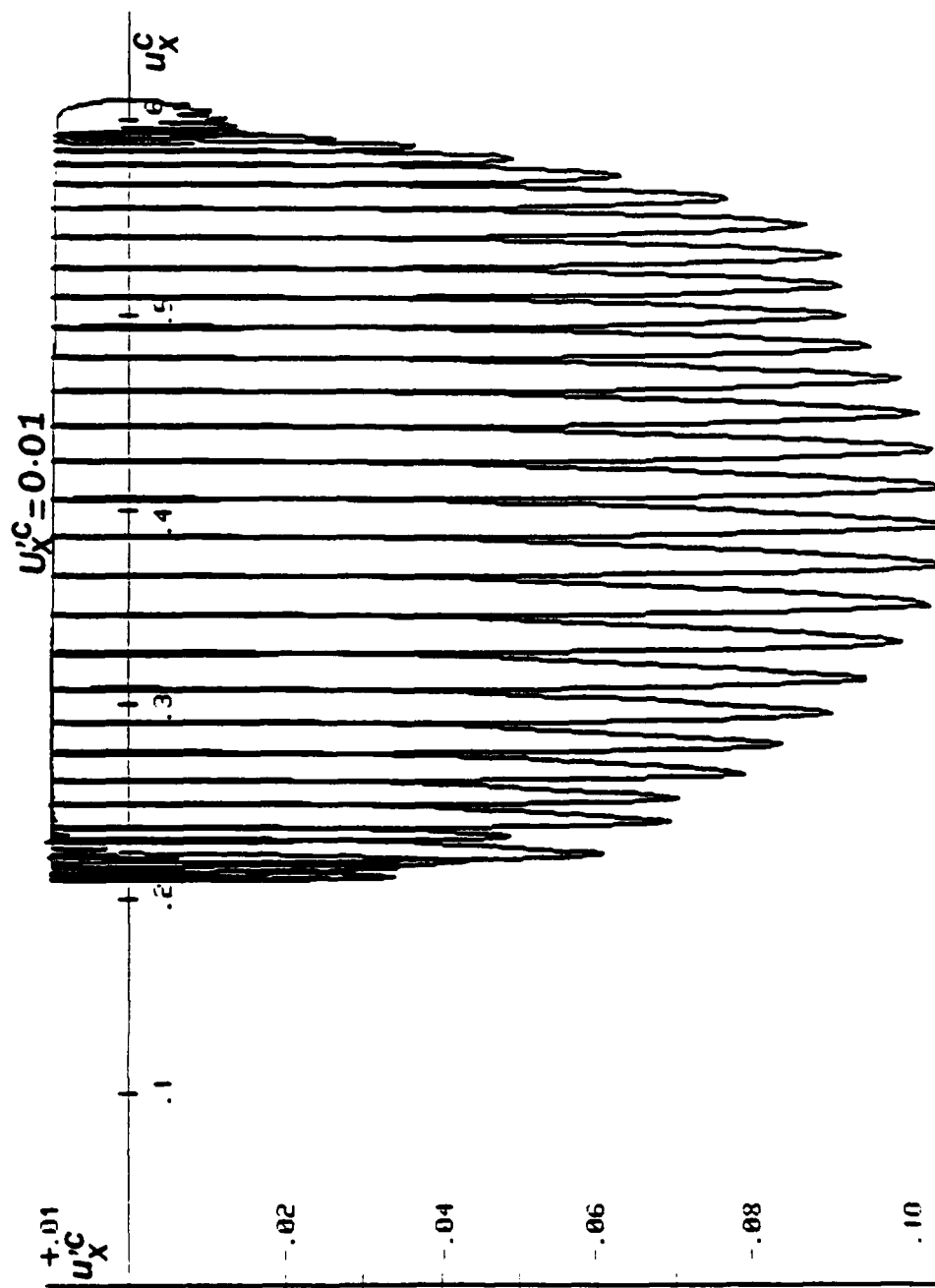


Figure 4.3.4. Phase plane plot of the tangential motion of the points of the block on the contact surface during one period of the low-frequency stick-slip motion.

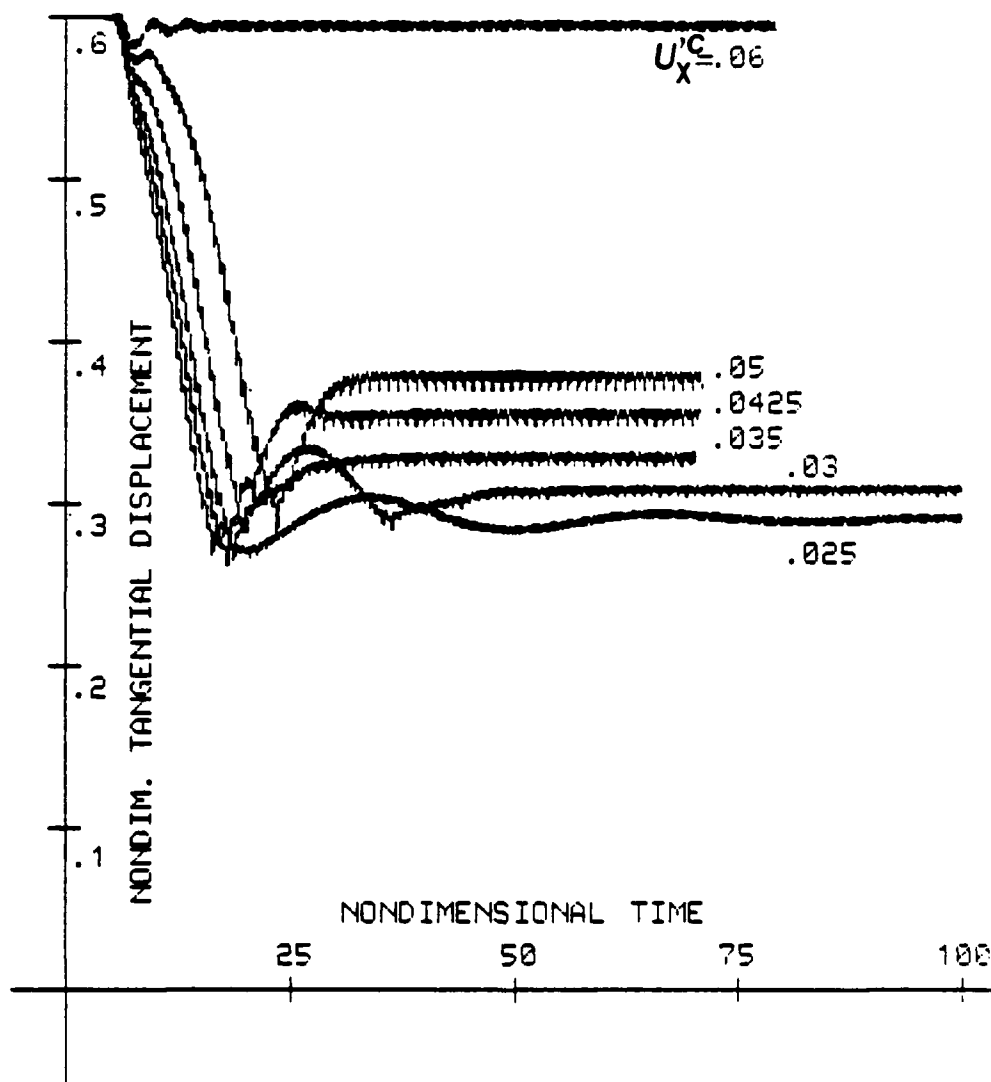


Figure 4.3.5. Apparently smooth sliding for small  $s$ , small  $z_x$ , large  $U'_x$  ( $s=0.01$ ,  $z_x=0.001$  and  $U'_x$  successively equal to 0.025, 0.030, 0.035, 0.0425, 0.05, 0.06).



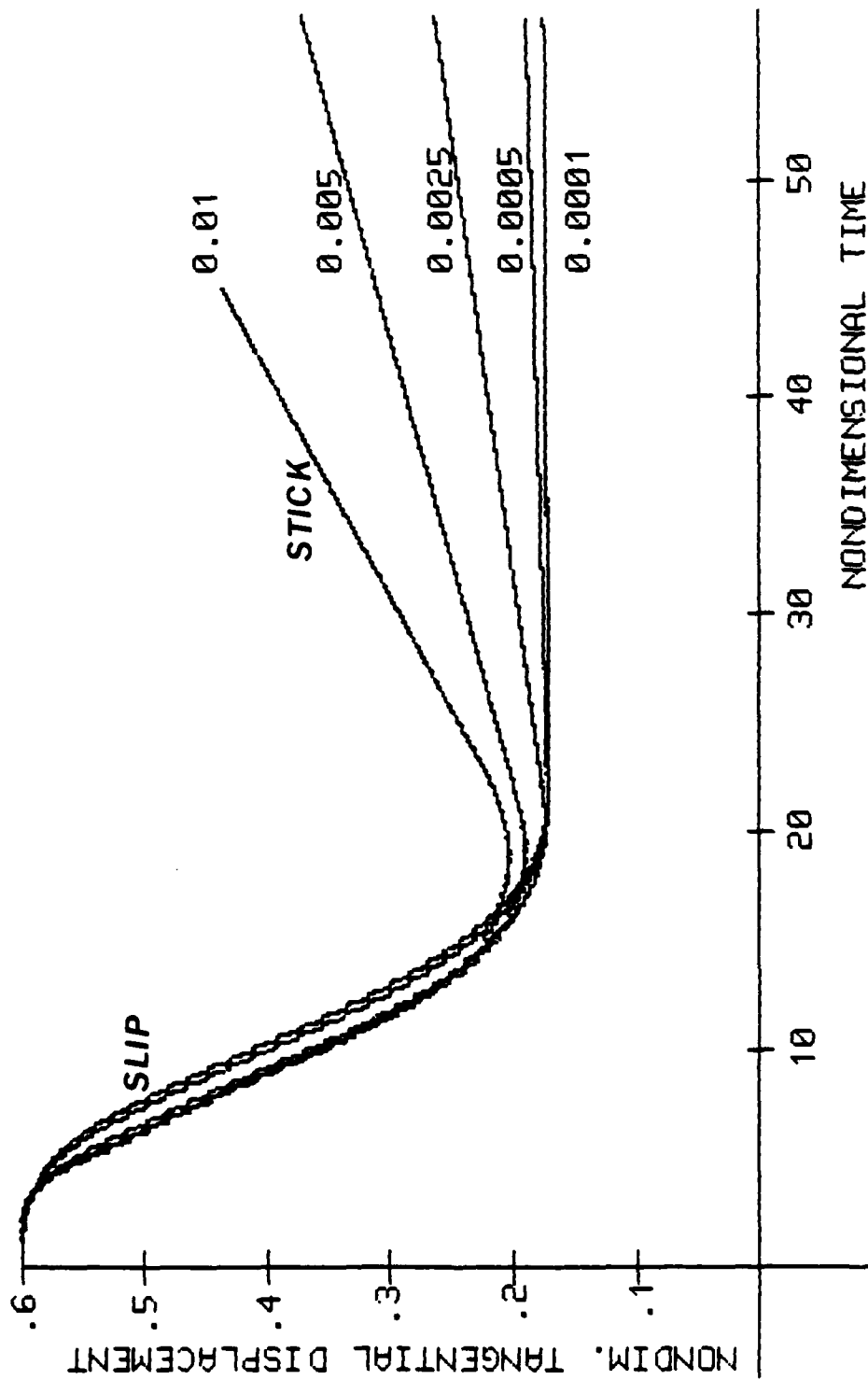


Figure 4.3.6. Low-frequency stick-slip motions for various small driving velocities ( $s=0.01$ ,  $z_x = 0.001$  and  $U_x^0$  successively equal to 0.01, 0.005, 0.0025, 0.0005, 0.0001).

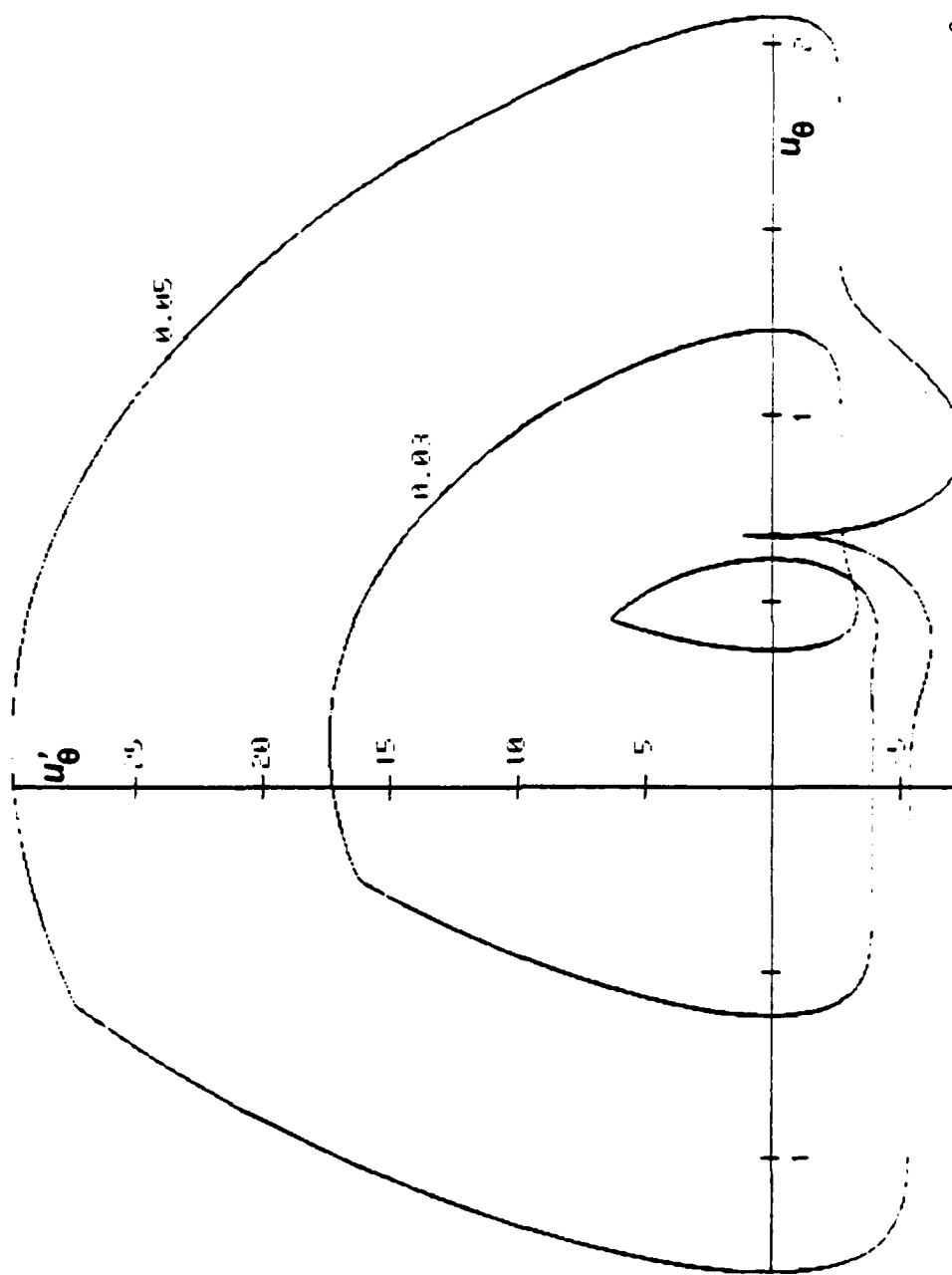


Figure 4.3.7. Phase plane plots for the rotation degree-of-freedom ( $s=0.01$ ,  $z = 0.001$  and  $U^1C = 0.03$  and  $0.05$ ). Final self-excited oscillation (the last 2000 time steps computed).

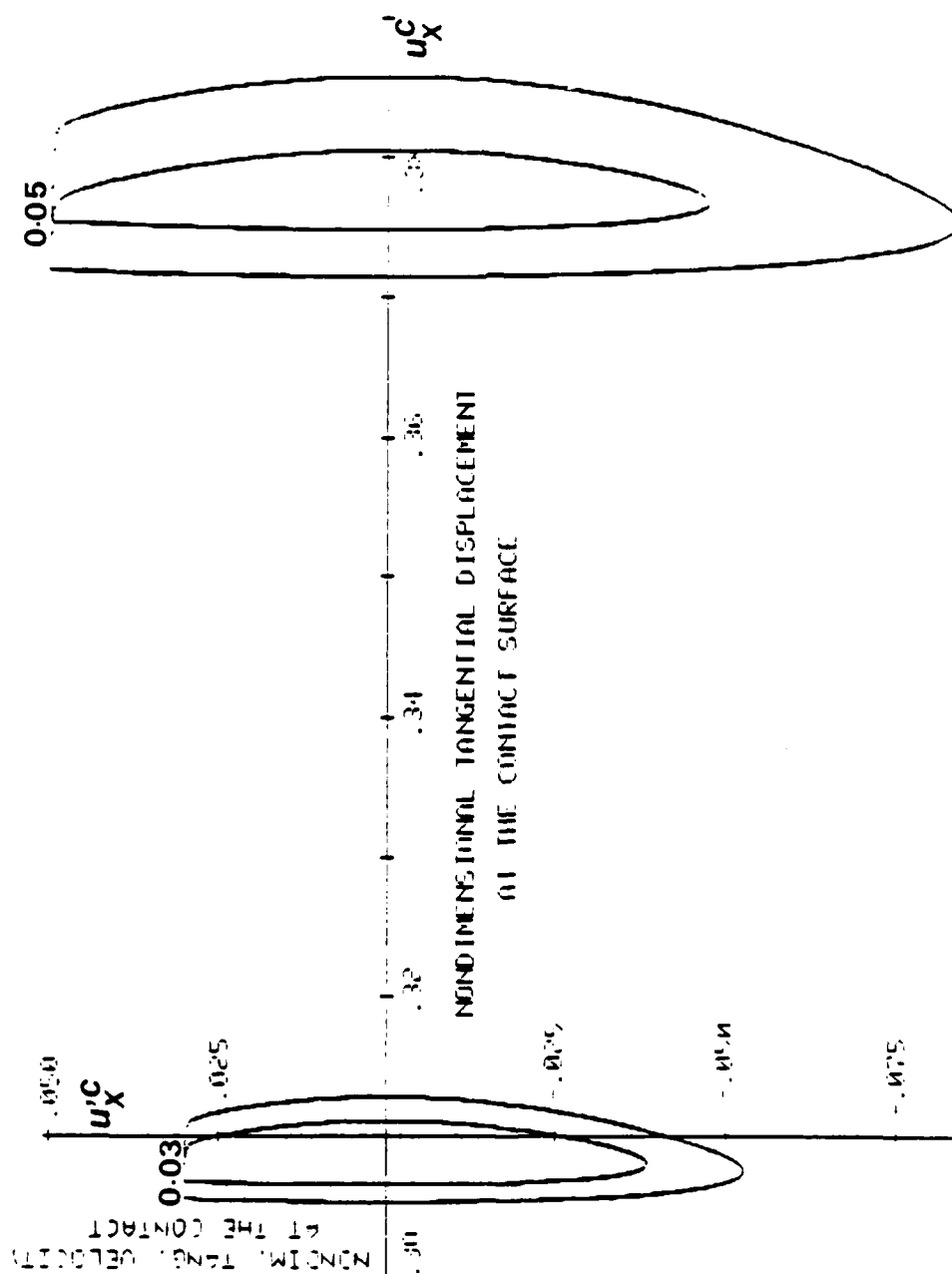


Figure 4.3.8. Phase plane plots for the tangential motion of the points of the block on the contact surface ( $s=0.01$ ,  $z_x^C=0.001$  and  $u_x^C=0.03$  and  $0.05$ ).

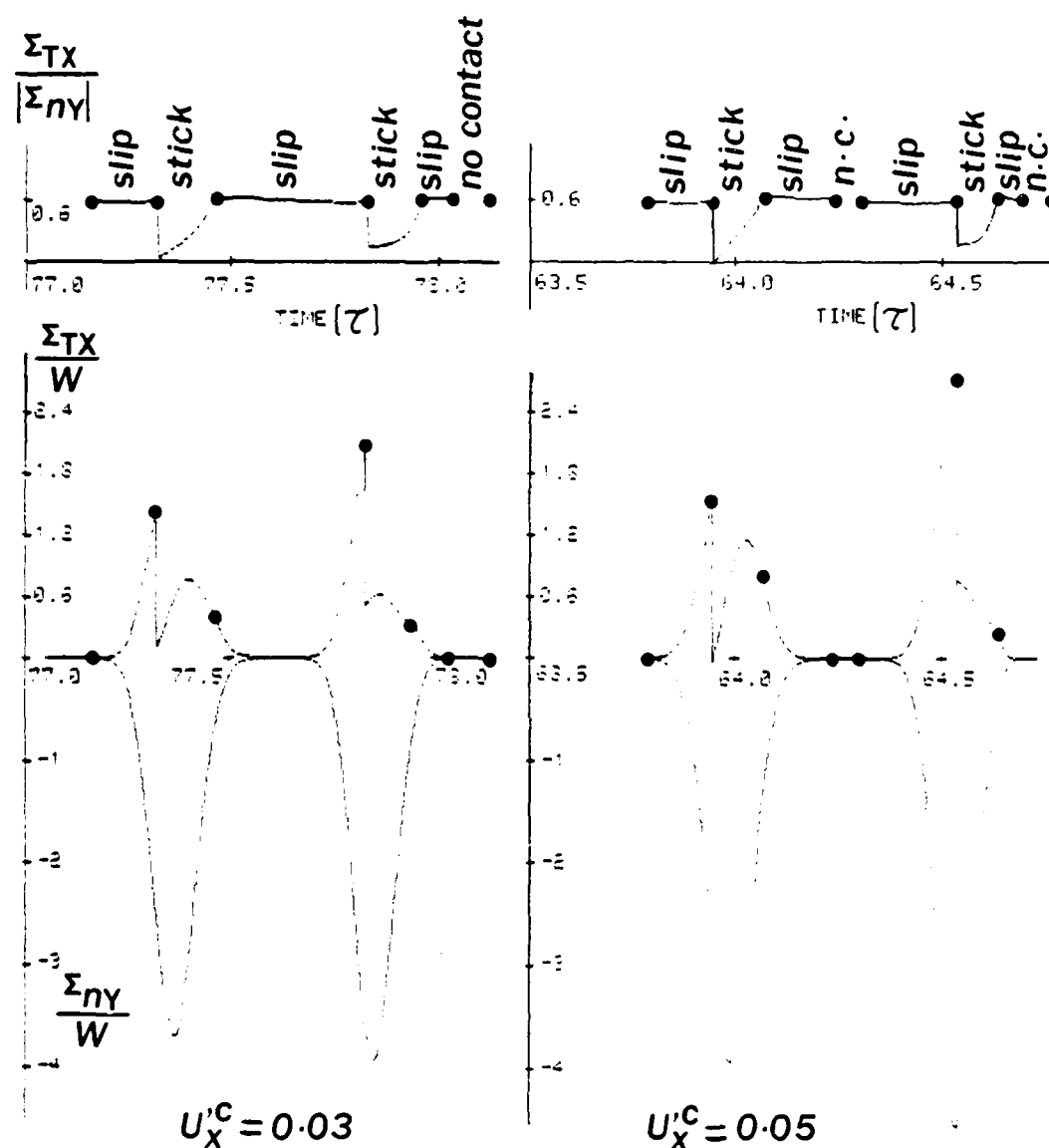


Figure 4.3.9. Evolution of the normal contact force ( $\Sigma_{nY}$ ), the friction force ( $\Sigma_{TX}$ ) and the ratio friction force/absolute value of the normal force, for one cycle of oscillation ( $s=0.01$ ,  $z_1=0.001$  and  $U'_X=0.03$  or  $0.05$ ).

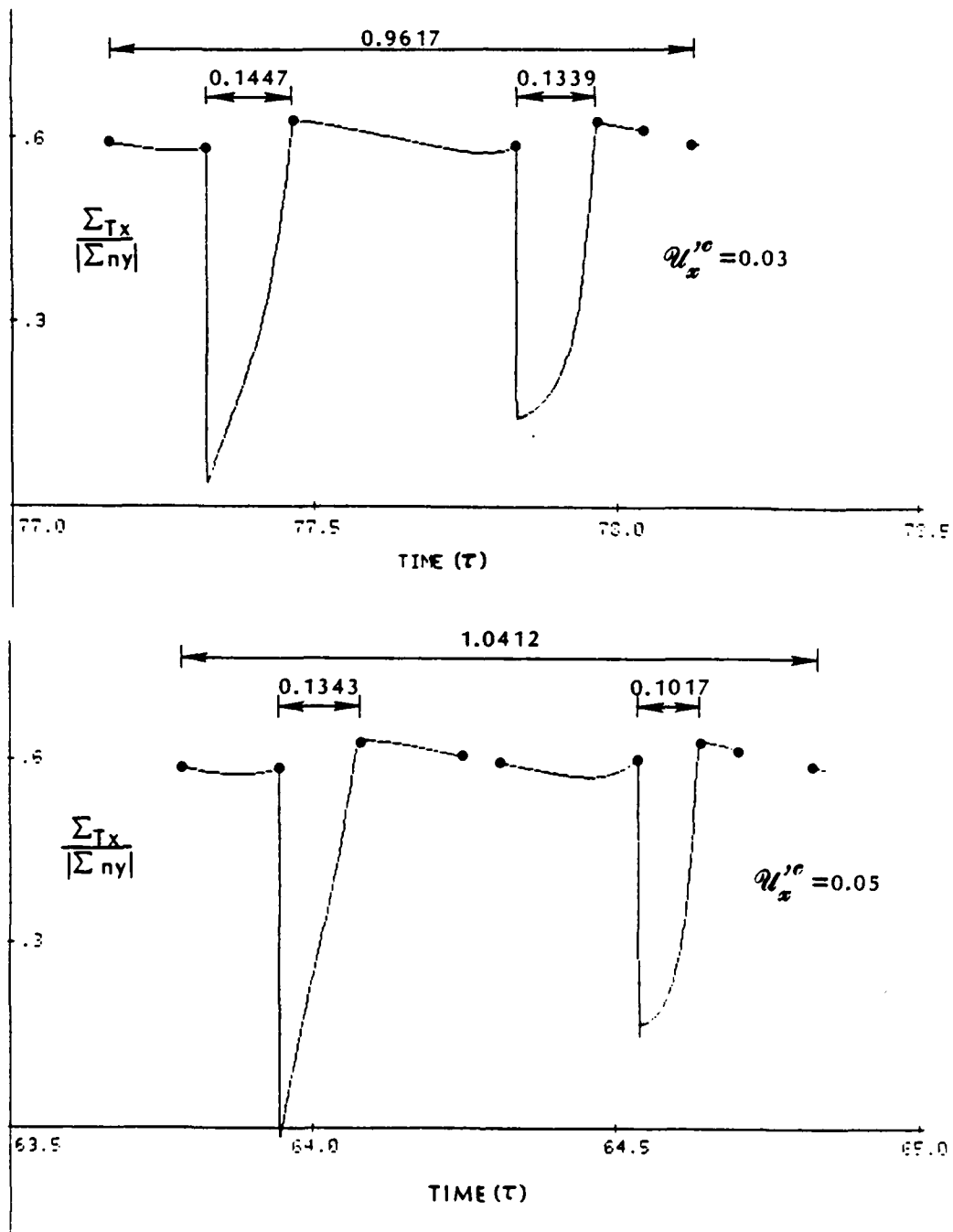


Figure 4.3.10 The decrease of the time of stick with the increase of the driving velocity ( $s=0.01$ ,  $z_x=0.001$  and  $U'_x=0.03$  or  $0.05$ ).

oscillation (see Fig. 4.3.11) and the body sticks (see Fig. 4.3.6) since the restoring force of the spring is then smaller than the maximum available friction force.

*Thus, monitoring the spring elongations, as is often done in friction experiments, case (a) would be perceived as an apparently smooth sliding with a coefficient of kinetic friction smaller than the coefficient of static friction and case (b) would be perceived as a (low-frequency) stick-slip motion.*

**The role of the normal interface damping.** It is clear from the results presented above that for "small" tangential stiffness and damping, the size of the driving velocity plays an important role on the occurrence of low-frequency stick-slip motion or apparently smooth sliding motions. It is also clear that when a low frequency stick-slip motion occurs the normal oscillation that accompanies the sliding phase of the stick-slip cycles is damped out when the spring elongation is close to its minimum. The role played by the normal interface damping on the qualitative behavior of the rigid block is made clear in Figs. 4.3.12 and 4.3.13. The values used in the computations are those indicated in (4.3.13-15) and (4.3.17-20) but now we fix  $u_x^C = 0.01$  and we vary  $\hat{\gamma}$  as indicated on the figures. In Fig. 4.3.13 it can be observed that, for very small or null interface normal damping ( $\hat{\gamma}=0.002$  or  $\hat{\gamma}=0.000$ ) an apparently smooth sliding motion is obtained. As the interface normal damping is increased ( $\hat{\gamma}=0.005, 0.01, 0.02, 0.05$ ) a low fre-

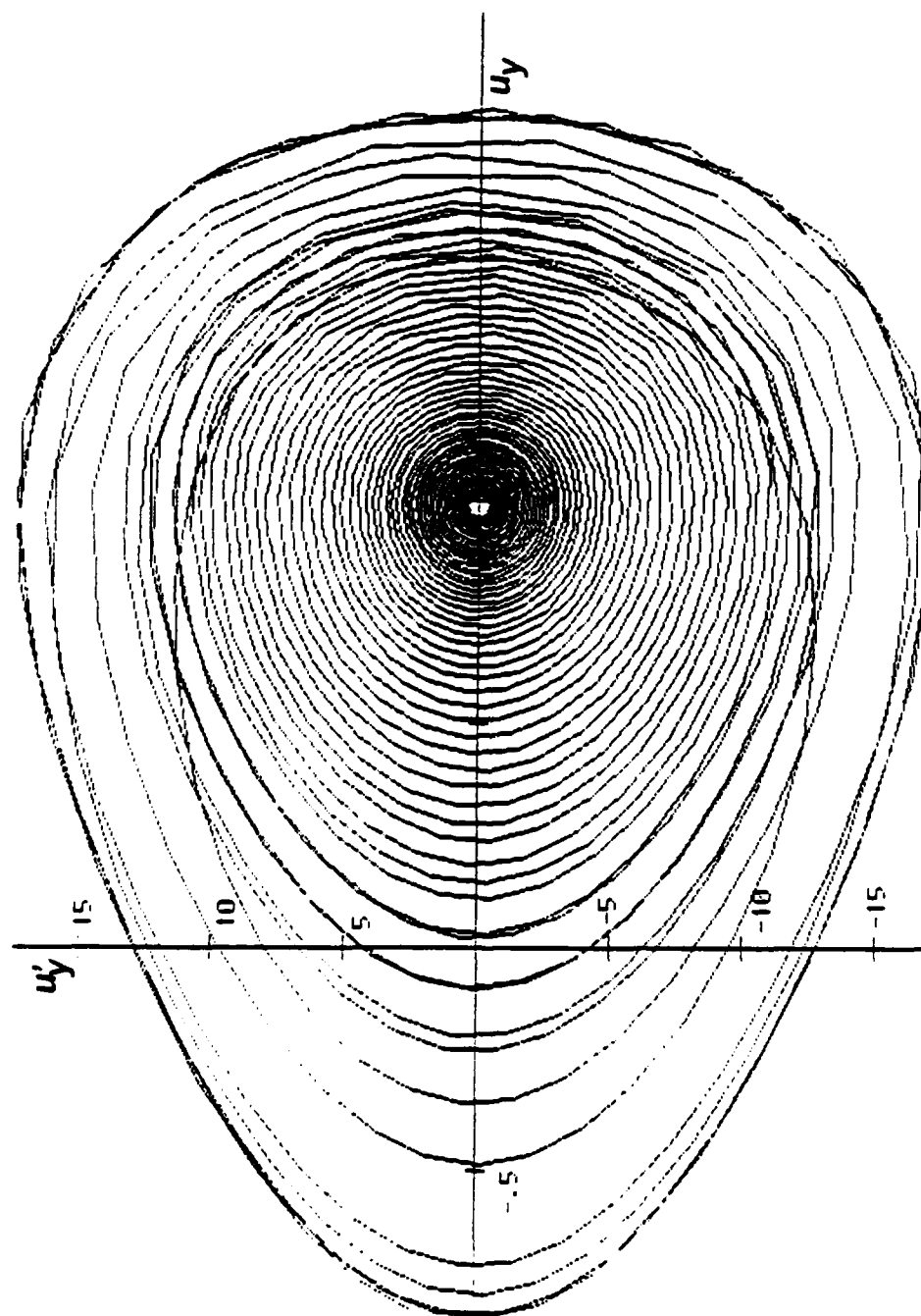


Figure 4.3.11 Phase plane plot of the decaying portion of the normal oscillation of the center of mass in the course of low-frequency stick-slip motion.  $U^*C=0.01$ . (Note: not all the computed points are plotted.)

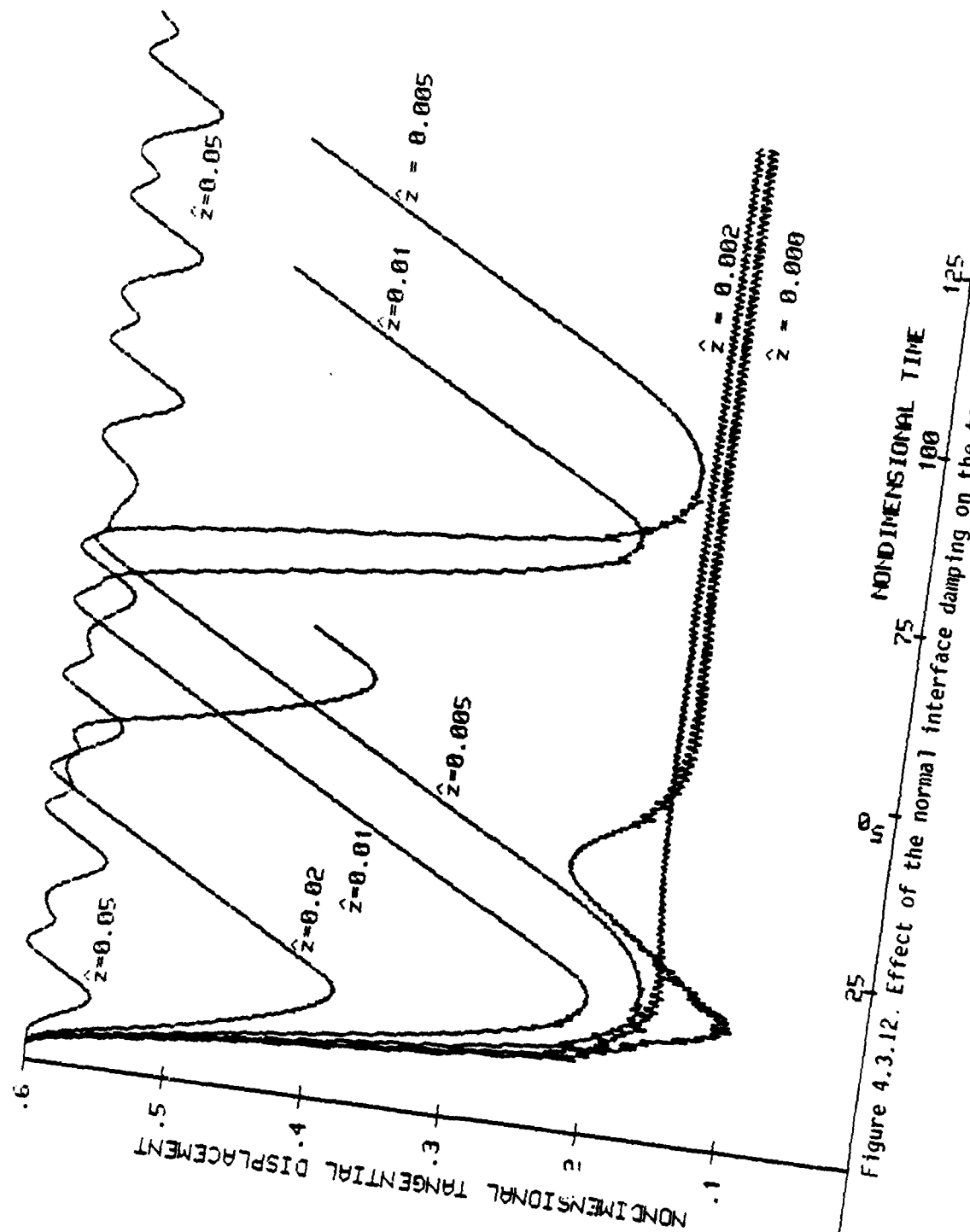


Figure 4.3.12. Effect of the normal interface damping on the tangential trace.



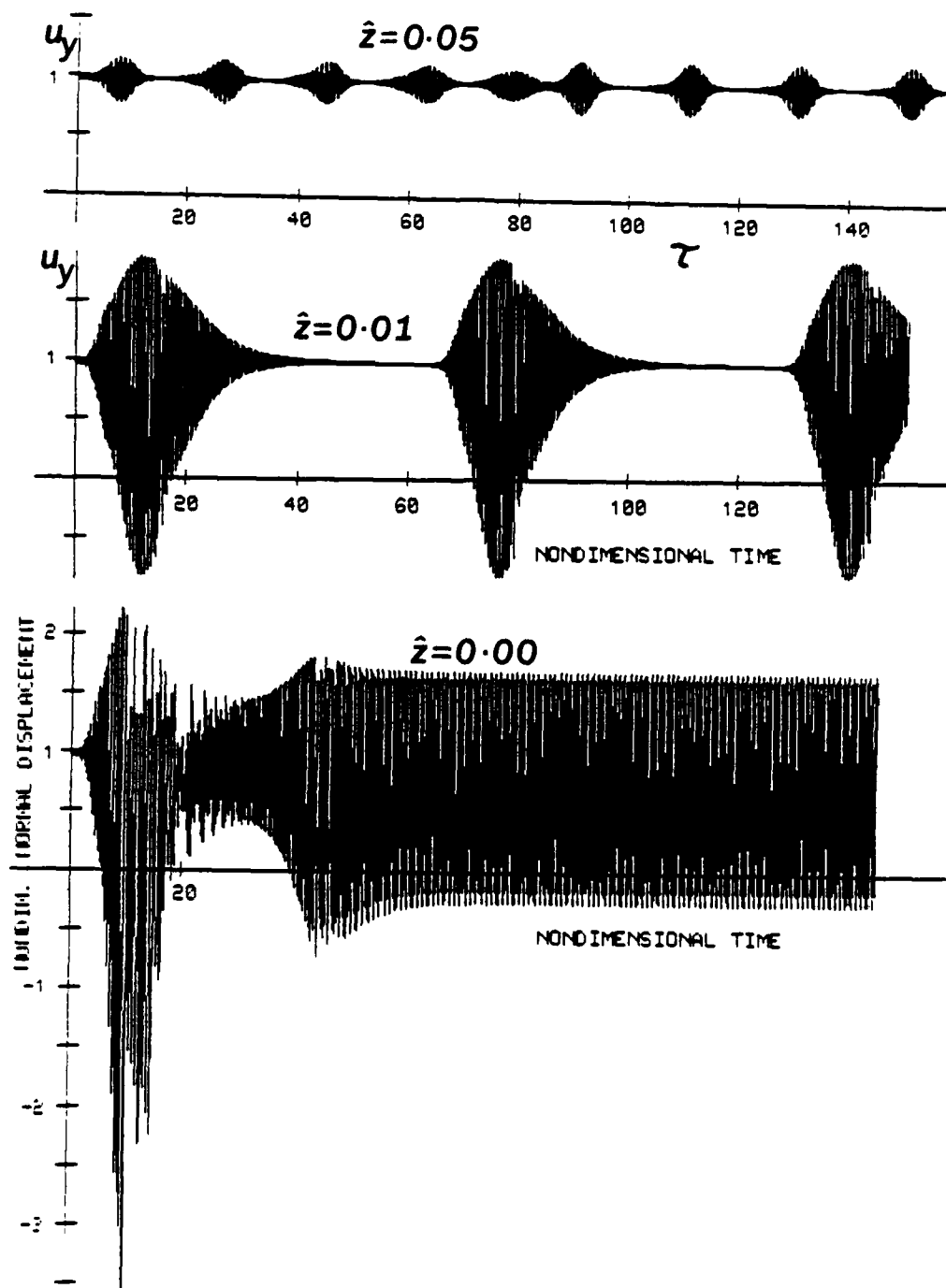


Figure 4.3.13. Effect of the normal interface damping on the normal oscillations.

quency stick-slip oscillation is observed. The amplitude of that oscillation decreases with the increase of  $\hat{z}$  as shown in Fig. 4.3.12. The steadiness of the normal oscillation when  $\hat{z}=0.0$  and the intermittency of the normal oscillation when low-frequency stick-slip motions occur ( $\hat{z}=0.01$  and  $\hat{z}=0.05$ ) is made clear in Fig. 4.3.13. The decrease of the amplitude of the normal oscillation when  $\hat{z}$  is increased can also be observed on the same figure. The phase plane plots of the normal oscillation and of the tangential oscillation of the points of the block on  $\Gamma_C$  when  $\hat{z}=0$  are shown in Figs. 4.3.14,15.

From the observations above we conclude that some normal interface damping is needed for the occurrence of low-frequency stick-slip motion. In physical terms, this means that *some plastic deformation (penetration) of the interface must occur at the end of the sliding portion/beginning of the stick portion of the stick-slip cycles and it is that plastic deformation that is responsible for the damping of the normal oscillation.*

Figure 4.3.13 suggests another comment: the form of the decay of the normal oscillation at the end of the sliding portion of the stick-slip cycles reveals in a clear manner the *viscous* nature of the nonlinear term in equation 4.1.4 that is responsible for that dissipation. Experimental observations of the same phenomenon with actual metallic surfaces may suggest more appropriate forms for that normal dissipative term.

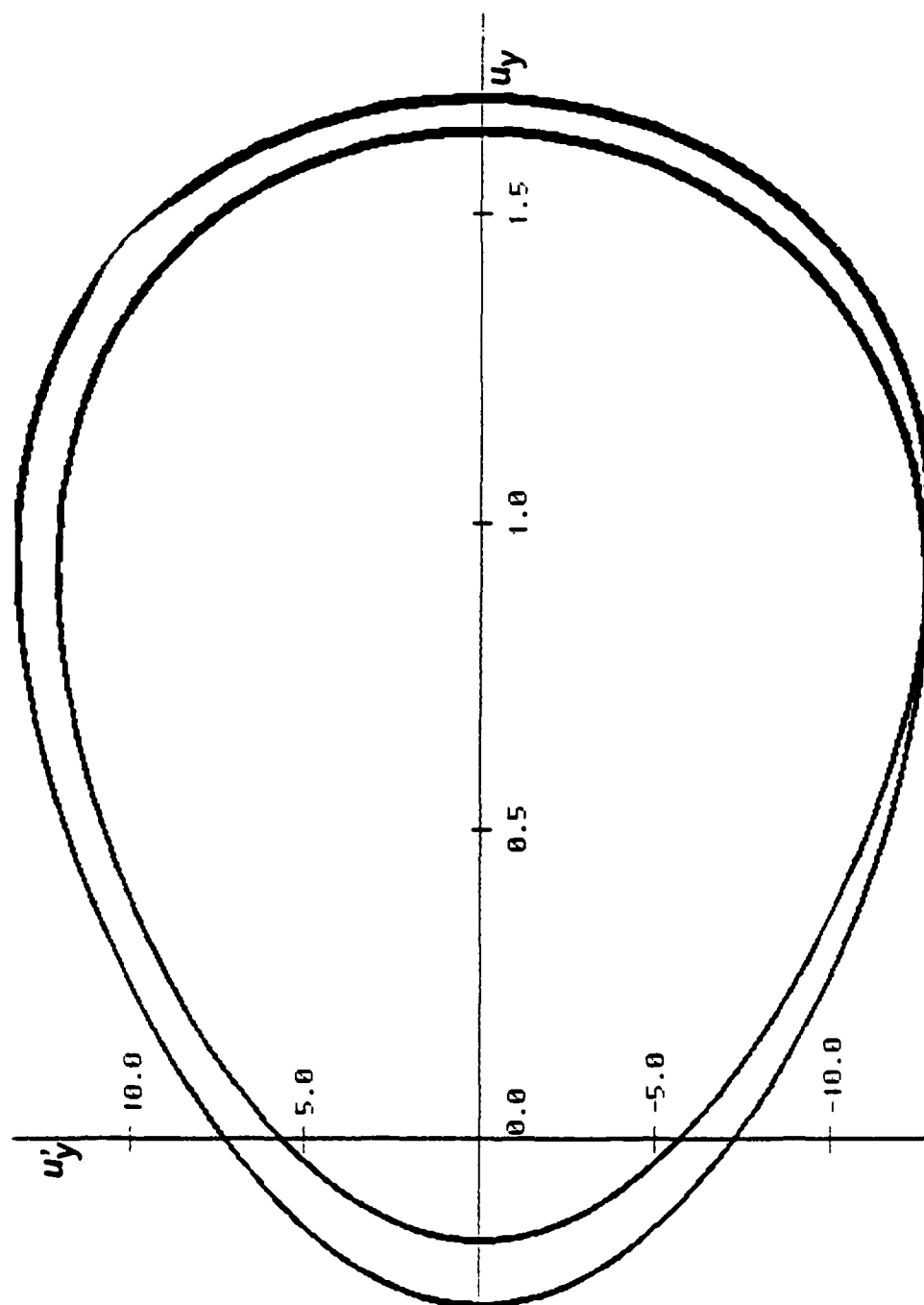


Figure 4.3.14. Phase plane plot of the steady normal oscillation of the center of mass for  $\hat{z}=0.0$   
 (Note: not all the computed points are plotted.)

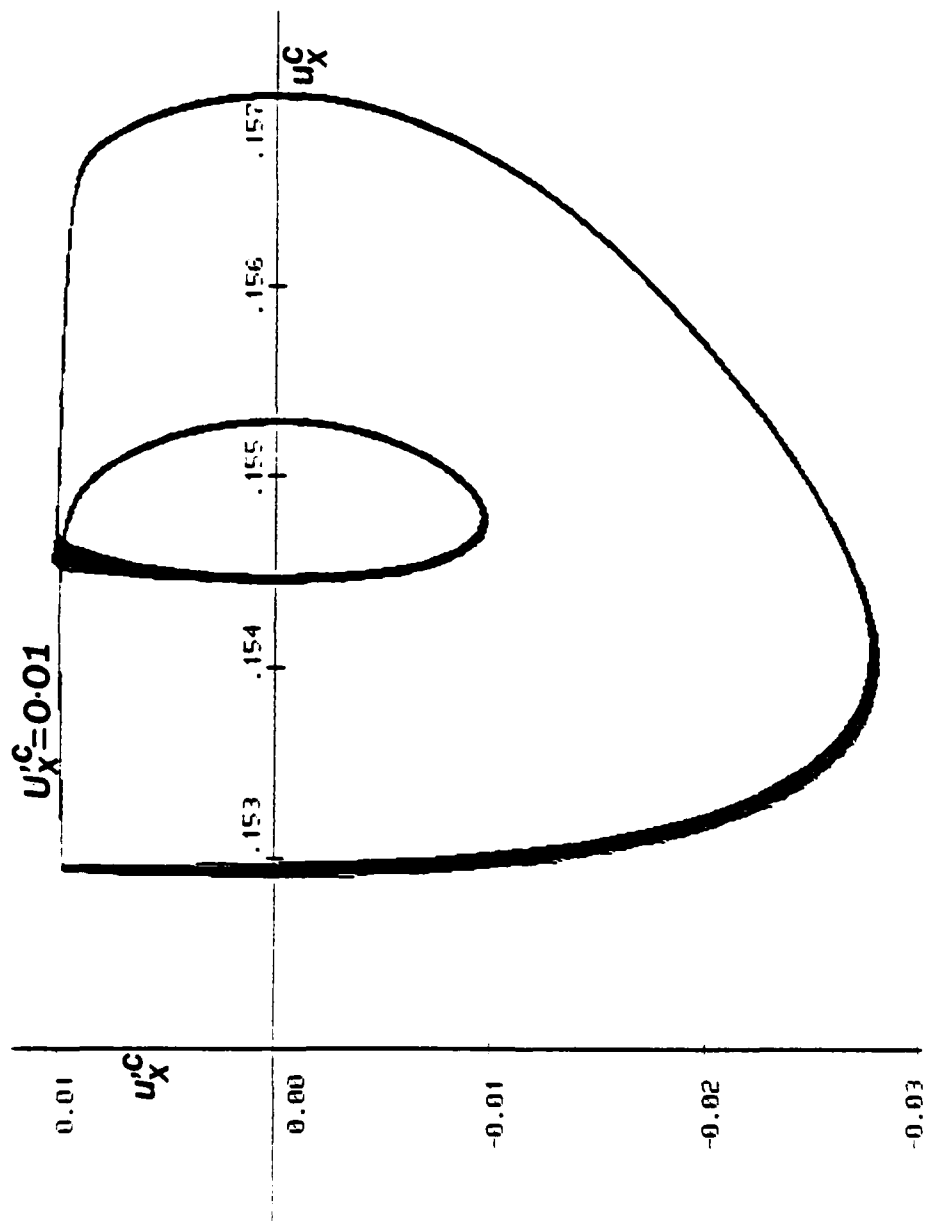


Figure 4.3.15. Phase plane plot of the steady tangential oscillation of the points of the block on the contact surface for  $\hat{z}=0.0$  (Note: not all the computed points are plotted.)

The effect of the stiffness parameter and the driving velocity on the amplitude and frequency of the low-frequency stick-slip motion. In order to study the influence of these parameters, we fixed the data (4.3.13)(4.3.15,16) and (4.3.19) and we assigned to  $s$  and  $u'_x{}^C$  various values in the small ranges for which low-frequency stick-slip motion is observed. In Figs. 4.3.16 and 4.3.17 we plot the amplitudes of the low frequency stick-slip oscillations against the driving velocities for each of the values considered for the stiffness parameter. The nondimensional amplitude  $\Delta u_x$  and the nondimensional driving velocity  $u'_x{}^C$  are used in the plot of Fig. 4.3.16. In Fig. 4.3.17 different nondimensional variables are used: the amplitude  $\Delta u_x / s (= \Delta u_x / Y)$  and the driving velocity  $u'_x{}^C / \sqrt{s} (= \dot{u}_x^C / \sqrt{gY})$  where  $Y$  is the quantity defined in (4.2.3) and  $g (= W/M)$  denotes here the gravity acceleration. The plots of Fig. 4.3.17 represent thus the behavior of the dimensional amplitude  $\Delta u_x$  when the changes in  $s$  and  $u'_x{}^C$  result from changes in  $K_x$  and  $\dot{u}_x^C$ , respectively, while using the same body and the same contact surface (the same  $W$ , the same  $M$  and the same  $Y$ ). The decrease of the dimensional stick-slip amplitude with the increase of the tangential stiffness can be observed in Fig. 4.3.17.

For the range  $0.0004 \leq s \leq 0.01$  of the stiffness parameter, the amplitude of the low-frequency stick-slip motion decreases only slightly with the increase of the driving velocity, which appears consistent with the small slopes of the amplitude-driving velocity plots

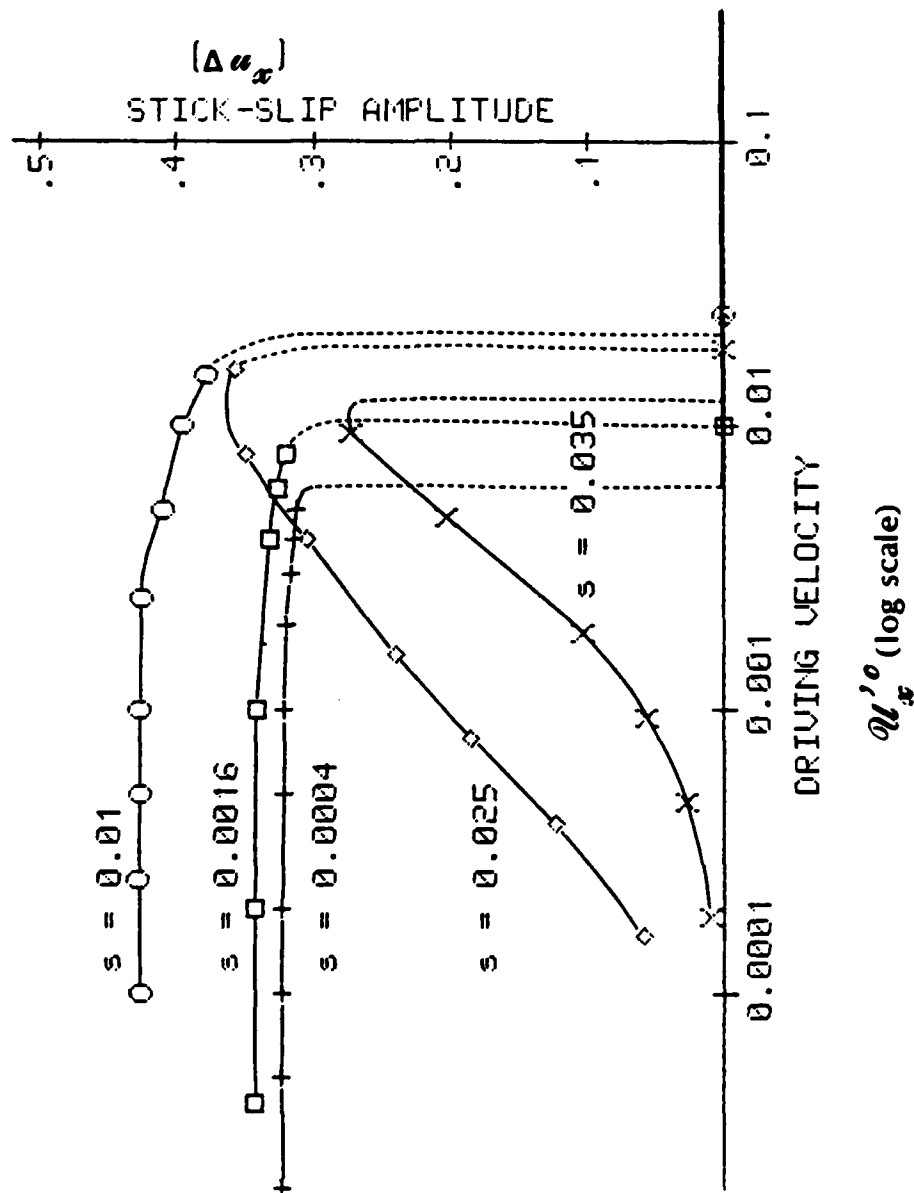


Figure 4.3.16. Amplitude of the low-frequency stick-slip motion  $(\Delta u_x)$  vs. driving velocity  $(u_x^{*0})$ .

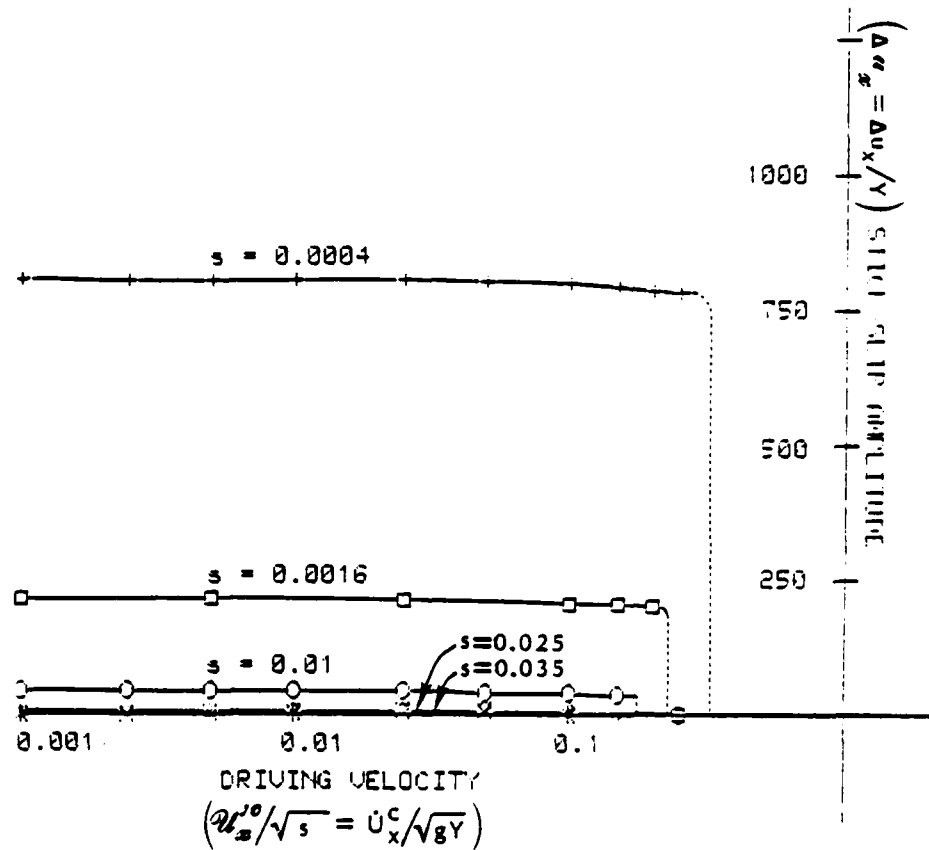


Figure 4.3.17. Amplitude of the low-frequency stick-slip motion  $(\Delta u_x/s = \Delta u_x/Y)$  vs. driving velocity  $(u'_x/\sqrt{s} = u_x^c/\sqrt{gY})$ .

at small driving velocities, obtained experimentally by several authors (Rabinowicz [1965], Brockley, Cameron and Potter [1967], Kato and Matsubiashi [1970]). Also in agreement with some experimental observations (recall e.g. Fig. 2.2.1) *the transition from low-frequency stick-slip motion to apparently smooth sliding is abrupt.* For small tangential stiffnesses, the critical driving velocity at which that transition occurs is not very dependent on the stiffness: a small decrease of the dimensional critical speed  $\dot{U}_x^C$  with the increase of the tangential stiffness is observed in Fig. 4.3.17.

Finally, we observe that the larger stiffness parameters considered ( $s=0.025$  and  $s=0.035$ ) correspond to a transition between the range of values of  $s$  for which low frequency stick-slip oscillations occur at low driving velocities and the range of values of  $s$  for which no low frequency stick-slip motions can occur at any driving velocity. For these values of  $s$  an increase of the amplitude of the stick-slip motion with the increase of the sliding velocity can be observed in Fig. 4.3.16, and this is followed also by an abrupt transition to apparently smooth sliding motion at some critical driving velocity. Although increases of amplitude of the stick-slip motion with the driving velocity are not frequently reported in the literature, we observe that in some cases such phenomenon has indeed been observed: as an example we mention the work of Brockley and Ko [1970], (in particular see Fig. 13, page 555 of their work for the small velocity range at which the friction induced oscillation has a saw-tooth wave form).



In Fig. 4.3.18 a plot of the variation of the nondimensional stick-slip frequency with the nondimensional driving velocity  $u_x^C$  is presented. The nondimensional stick-slip frequency is equal to the ratio  $\omega^{ss}/\omega$  where  $\omega^{ss}$  denotes the dimensional ( $\text{rad s}^{-1}$ ) stick-slip frequency and  $\omega$  denotes the frequency of the tangential free oscillation (4.3.2). For the small stiffness parameters ( $s=0.0004$ ;  $s=0.0016$  and  $s=0.01$ ) an essentially linear relationship between the stick-slip frequency and the driving velocity is obtained which results from the small dependence of the stick-slip amplitude on the driving speed (Figs. 4.3.16 and 4.3.17) and which also bears some similarity with the results of Dokos [1946] (recall Fig. 2.2.2 in Chapter 2). In Fig. 4.3.18 it can be observed that the low-frequency stick-slip motion ceases when its frequency is still well below the natural frequency of the tangential motion. Situations of this type have been reported by Kato and Matsubiashi [1970] but, as observed in Chapter 2, it is frequently observed that the low frequency stick-slip motion persists up to the natural frequency of the free tangential motion. At this point it is unclear, if for some values of the governing parameters, our interface model and the rigid block considered here may simulate such a behavior. See Section 4.4 for further related discussions.

The apparent coefficient of kinetic friction-sliding velocity plots for the apparently smooth sliding motions. For "small" stiffness and tangential damping parameters and with a small driving

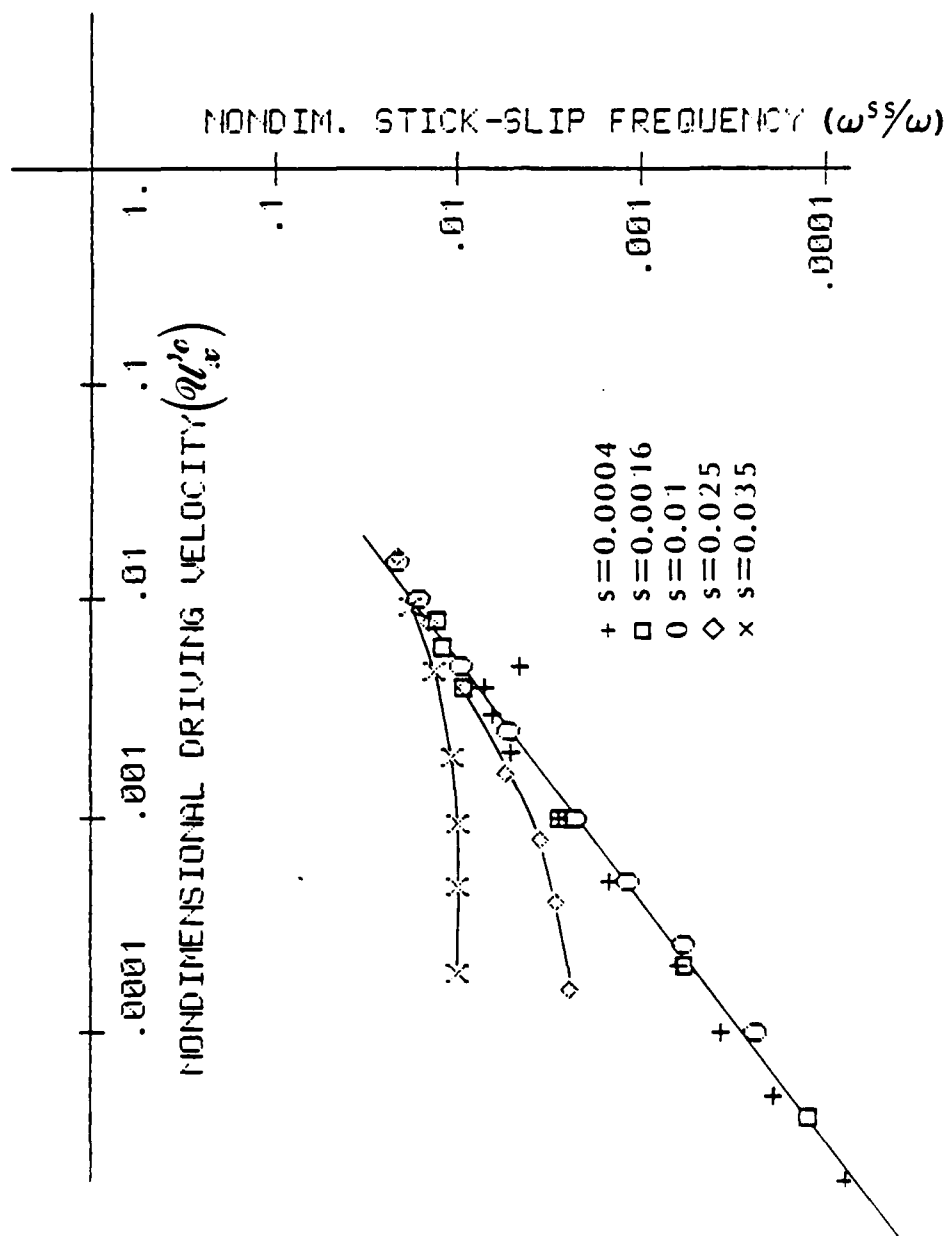


Figure 4.3.18. Frequency of the low frequency stick-slip motion vs. driving velocity.

velocity a low frequency stick-slip motion is obtained while, with a large driving velocity, an apparently smooth sliding results. It is also known that two means for obtaining experimentally a smooth sliding at low sliding speeds are: the use of a very stiff tangential spring or a very strong tangential damping. Here we show that our model predicts these behaviors.

In Fig. 4.3.19 the tangential displacements obtained with the data (4.3.13), (4.3.15,16), a "large" stiffness parameter ( $s=0.1$ ) and various driving velocities are presented. It can be seen that these traces consist of a self-excited oscillation (*without the typical saw-tooth wave form*) about a constant average displacement which corresponds to an apparent coefficient of kinetic friction lower than the coefficient of static friction.

In Fig. 4.3.20 similar results are shown but now the stiffness parameter has the "small" value  $s=0.01$  while the damping parameter has the "large" value  $z_x=10$ .

In Figs. 4.3.21 and 4.3.22 we plot the apparent coefficients of kinetic friction as a function of the driving velocity (=average sliding speed) for the three cases of apparently smooth sliding that have been considered: small  $s$ , small  $z_x$  and large  $u'_x{}^C$ ; large  $s$ , small  $z_x$  and arbitrary  $u'_x{}^C$ ; small  $s$ , large  $z_x$  and arbitrary  $u'_x{}^C$ . In the second case (large  $s$ ), since the nondimensional amplitude of the self-excited oscillations is significant for some speeds, we also indicate those amplitudes on the plot.

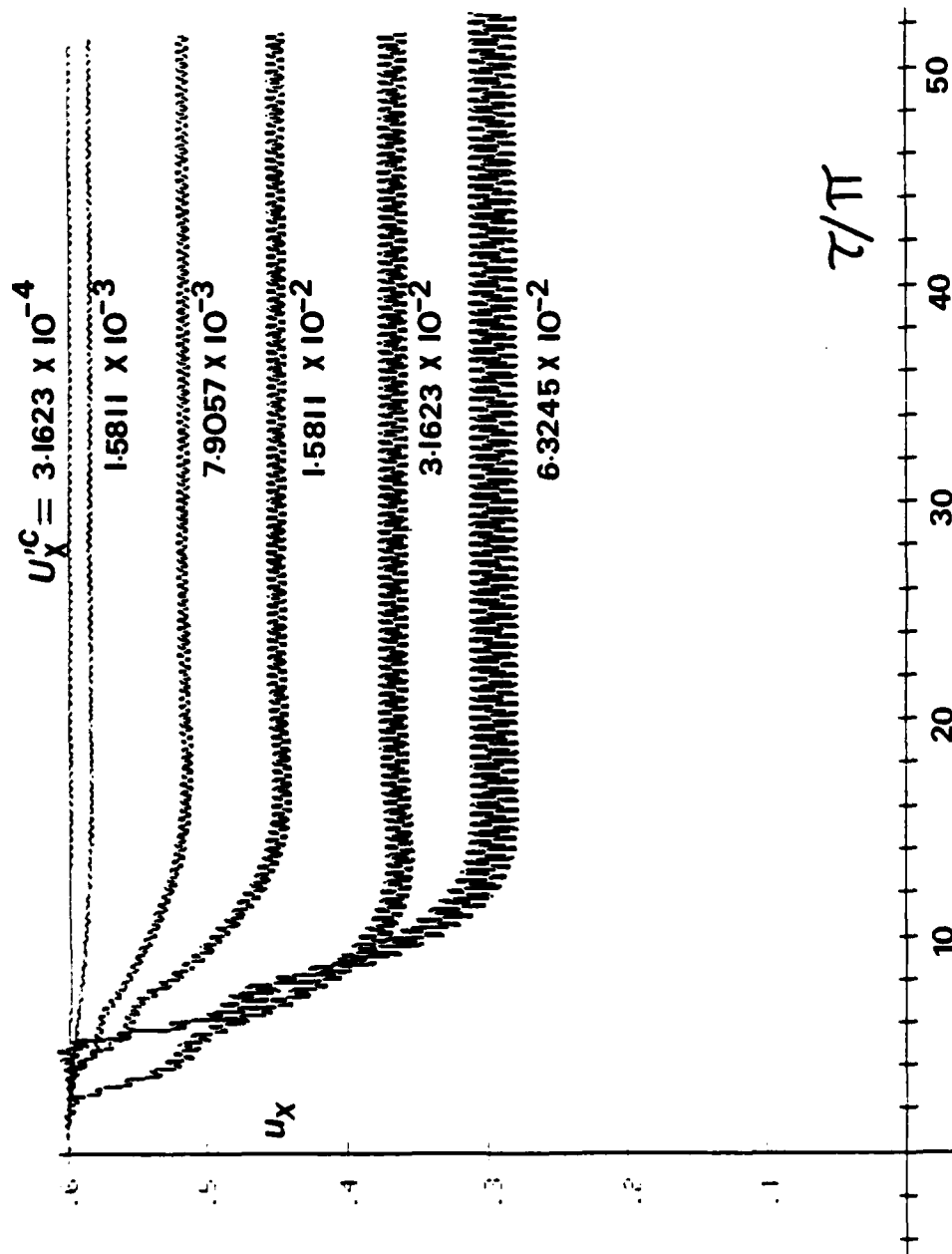


Figure 4.3.19. Tangential displacement traces for large  $s$ , small  $z_x$  and various  $U_X^C(s=0.1, z_x=0.001)$ .

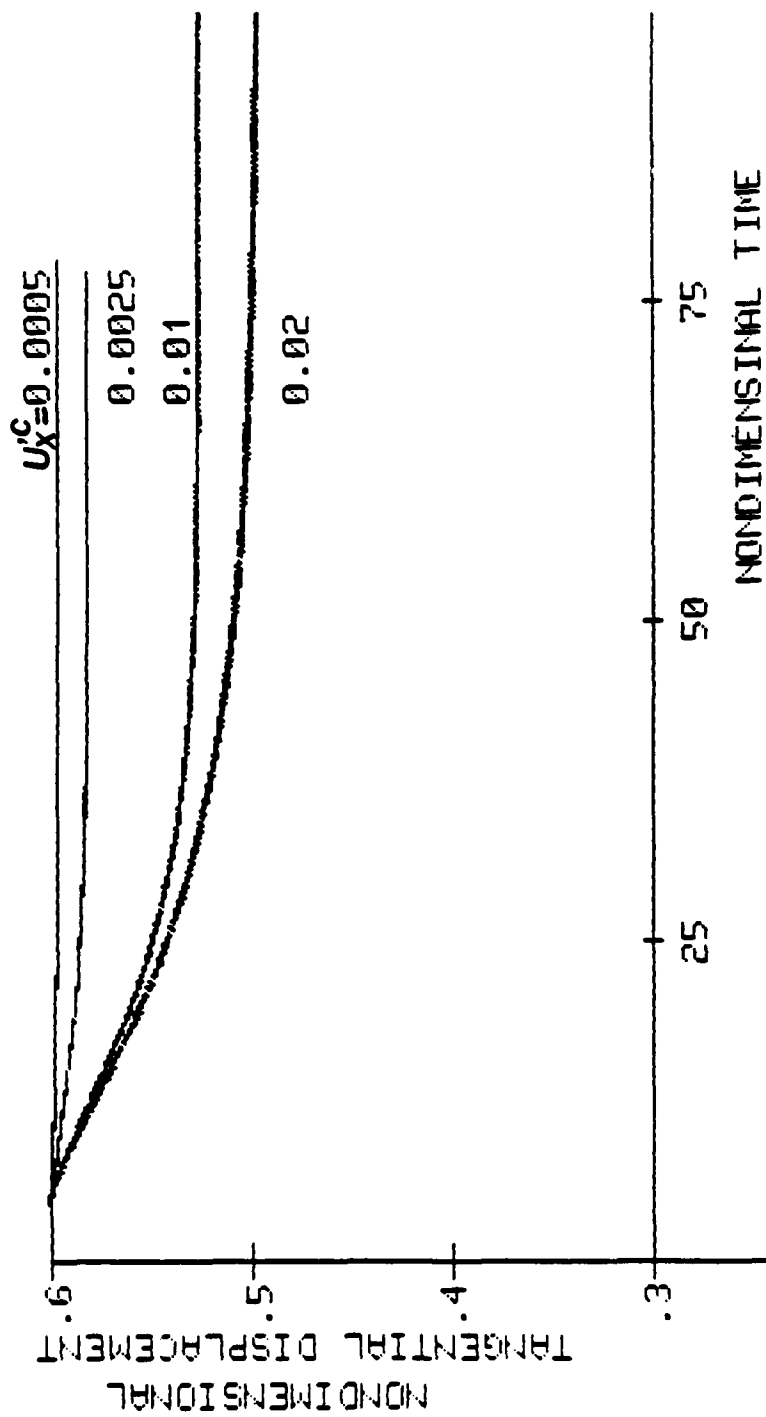


Figure 4.3.20. Tangential displacement traces for small  $s$ , large  $z_x$  and various  $u_x^C$  ( $s=0.01$ ,  $z_x=10$ ).

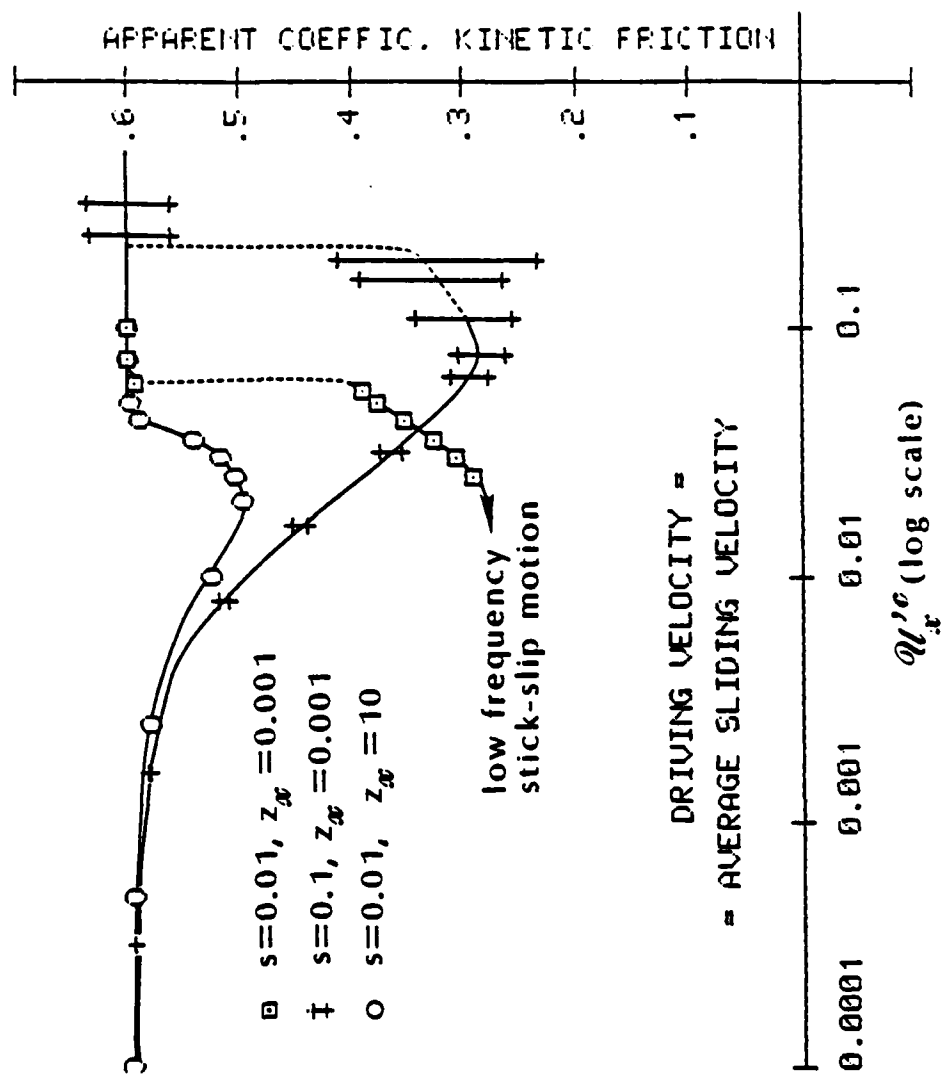


Figure 4.3.21. Apparent coefficient of kinetic friction vs. average sliding velocity (log scale).

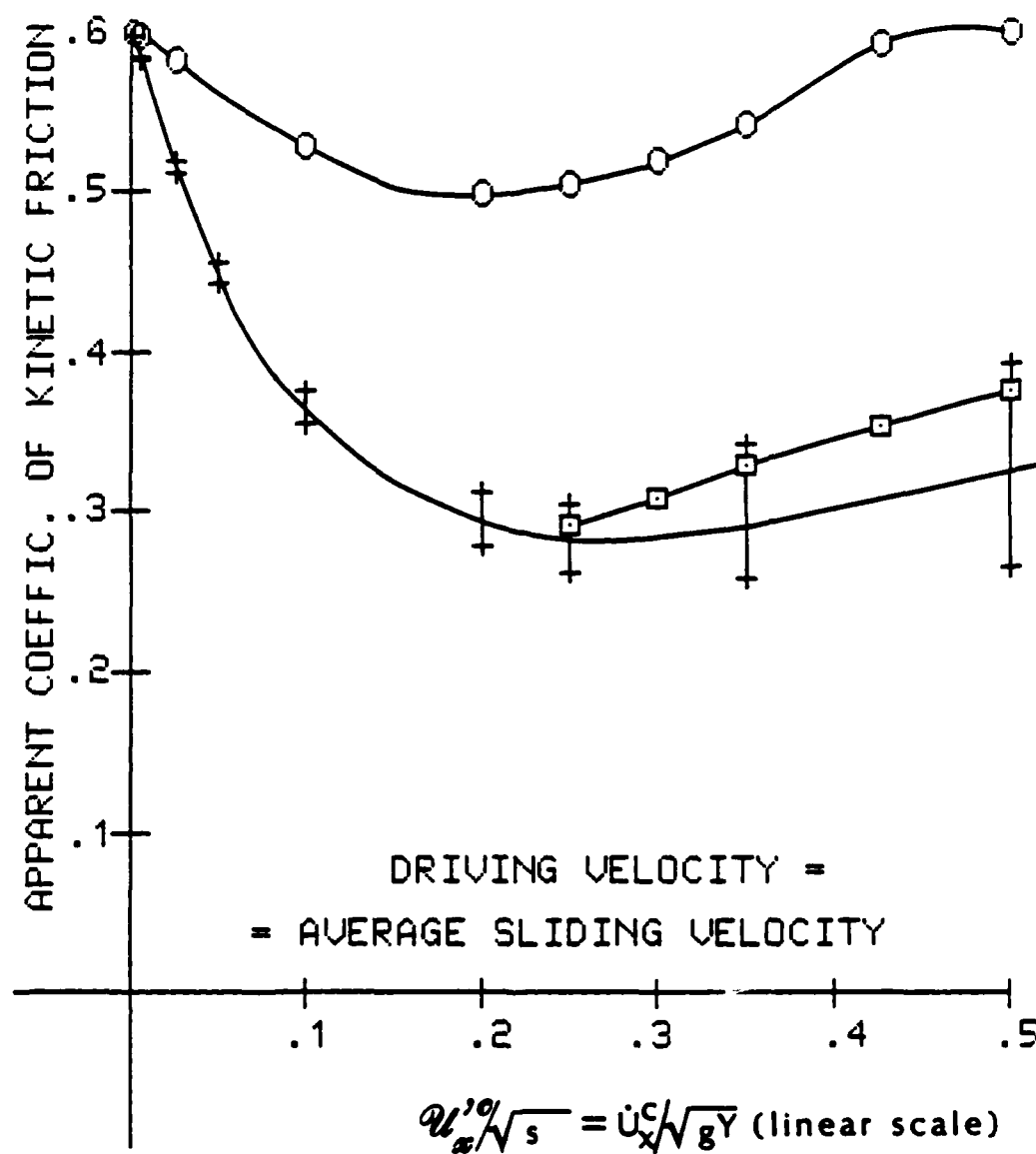


Figure 4.3.22. Apparent coefficient of kinetic friction vs. average sliding velocity (linear scale).  $\square$   $s=0.01$ ,  $z_x=0.001$ ;  $\pm$   $s=0.1$ ,  $z_x=0.001$ ;  $\circ$   $s=0.01$ ,  $z_x=10$ .

The following remarks provide an explanation for apparent coefficients of kinetic friction that are lower than the coefficient of (static) friction and some additional comments:

(i) All the low apparent coefficients of kinetic friction in our computations result from the occurrence of a period of stick during each period of oscillation of the body (see Figs. 4.3.8-10 and 4.3.24,25). The ratio (friction force/normal contact force), when the body sticks, is smaller than the coefficient of friction, so that the time average of the friction force is smaller than the product of the coefficient of (static) friction and the time average of the normal contact force (the weight of the body). *This is precisely the high-frequency stick-slip mechanism proposed by Budanov, Kudinov and Tolstoi [1980] (recall Section 2.3).*

(ii) If the driving velocity is sufficiently small that periods of stick are possible during each cycle of oscillation the following effects can be observed:

(a) The periods of stick occur in the portion of each cycle for which the normal contact force has larger absolute values (see Figs. 4.3.9 and 4.3.25)

(b) As should be expected, a discontinuity of the friction force occurs at the instant of each transition slip to stick (see Figs. 4.3.9,10 and 4.3.25)

(c) For otherwise similar conditions, larger driving velocities imply larger self-excited oscillations (compare in each of Figs. 4.3.7,8 and 4.3.23,24 the results obtained with



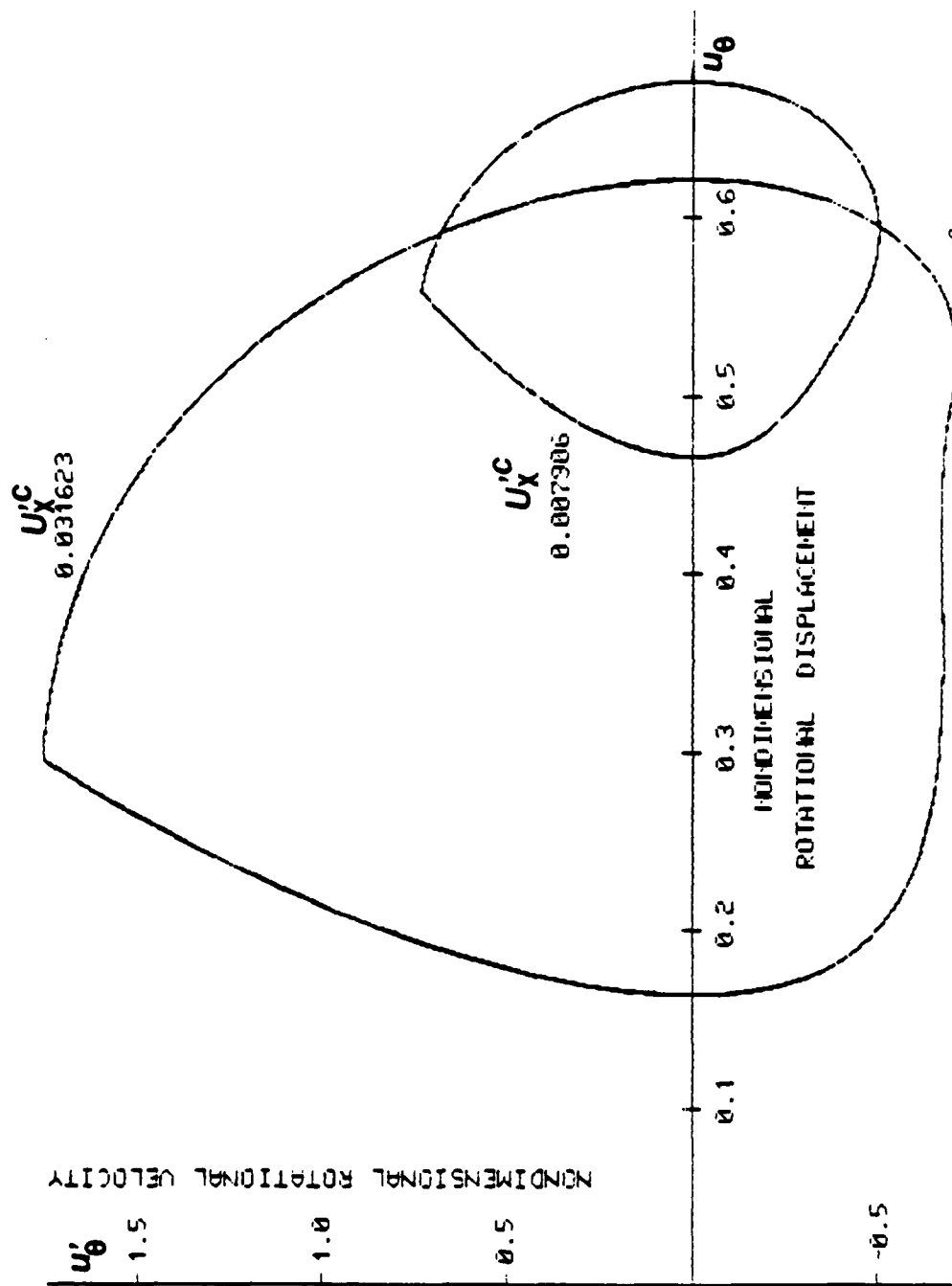


Figure 4.3.23. Phase plane plots for the rotational motion ( $s=0.1$ ,  $z=0.001$  and  $u_X^C=0.007906$  or  $0.031623$ ). Final self-excited oscillation (the last 2000 steps computed).

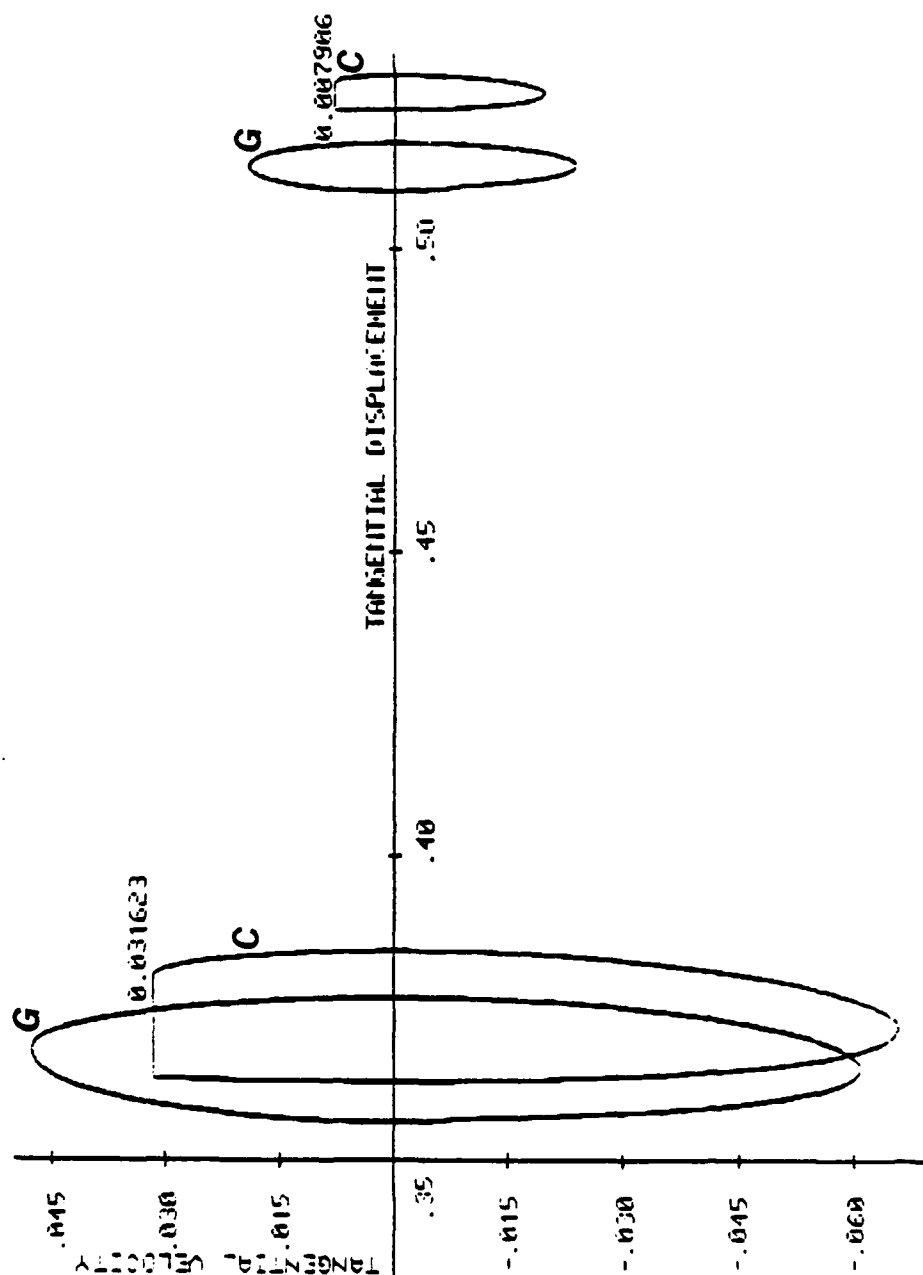


Figure 4.3.24. Phase plane plots for the tangential motion of the center of mass (G) and the points of the block on the contact surface (C) ( $s=0.1$ ,  $z_x=0.001$  and  $u'_x=0.007906$  or  $u'_x=0.031623$ ). Final self-excited oscillation.

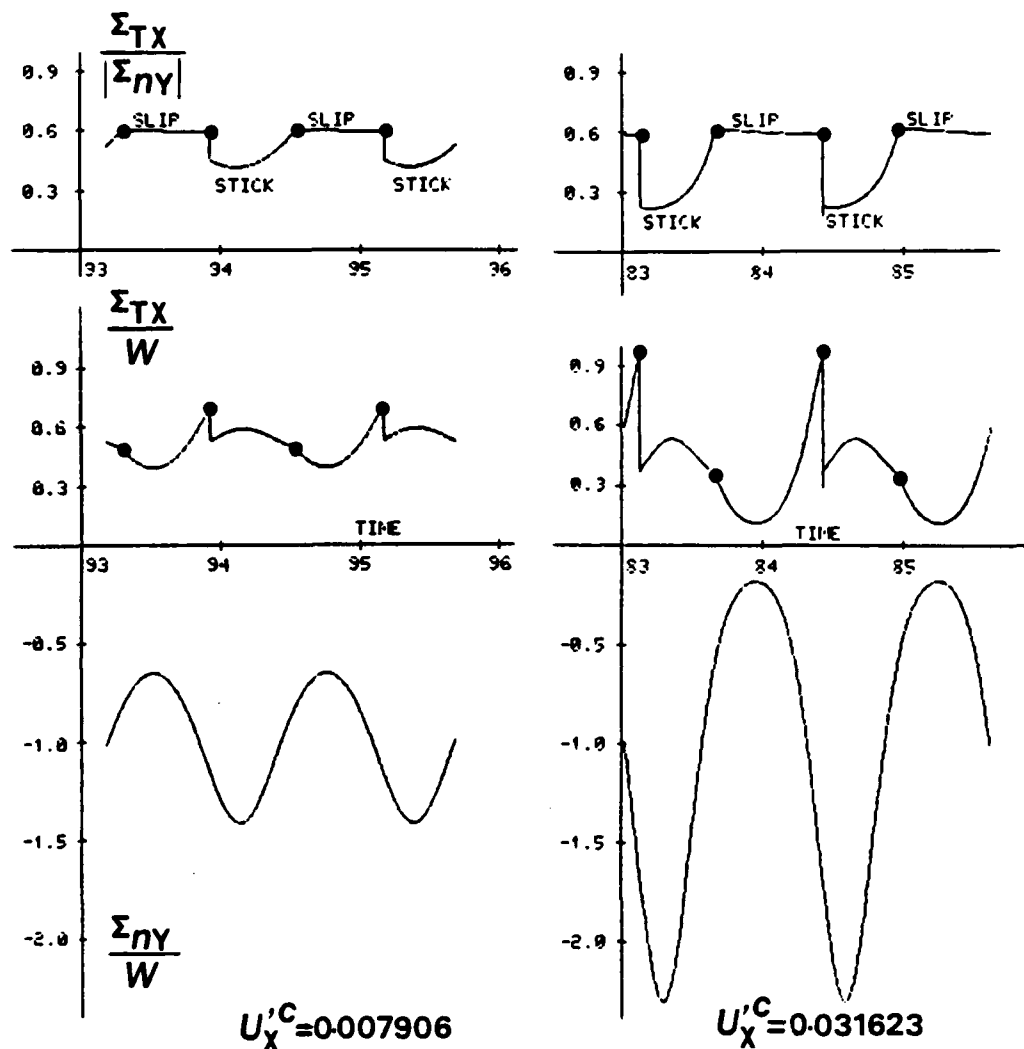


Figure 4.3.25. Evolution of the normal contact force ( $\Sigma_{NY}$ ), the friction force ( $\Sigma_{TX}$ ) and the ratio friction force/absolute value of the normal force, for two cycles of oscillation ( $s=0.1$ ,  $z_x=0.001$  and  $U'_C=0.007906$  or  $0.031623$ ).

different driving velocities)

(d) Also for otherwise similar conditions, larger driving velocities imply smaller periods of stick, relatively to the total period of one oscillation (see Figs. 4.3.9,10 and 4.3.25).

(iii) Increases of apparent coefficient of kinetic friction with the increase of driving velocity result essentially from the effect (d) above (see Fig. 4.3.10). This is (with the extra complexity inherent to having a three degrees-of-freedom system instead of a two degrees-of-freedom system) what Budanov, Kudinov and Tolstoi [1980] suggested to explain apparent coefficients of kinetic friction *increasing* with the average sliding speed (recall mechanism (II) in Section 2.3).

(iv) Decreases of apparent coefficient of kinetic friction with the increase of driving velocity are associated with the effects (a), (b) and (c) above. Compare in Fig. 4.3.25, for the two driving velocities considered, the minimum values of the friction force (sliding phase), the size of the discontinuities in friction force, and the values of the friction force at the points of maximum normal force (stick phase).

(v) For a sufficiently large driving velocity, no stick state occurs during the oscillation so that, since we do not take into account any thermal softening effects, the average coefficient of kinetic friction is equal to the coefficient of static friction.

(vi) In the case of the large tangential damping ( $s=0.01$ ,  $z_x=10$ ) we can describe our results using precisely the words of

Tolstoi [1967]: "sufficiently heavy damping of tangential vibrations alone could suppress these vibrations [the low frequency stick-slip motions] but failed to affect the negative slope of the friction-velocity curve." On this respect we note that the decoupling (4.2.9,10) of the characteristic equation for the eigenvalue problem (4.1.12) implies that, for the present geometry, the introduction of heavy external tangential damping does not affect at all the instability of the steady-sliding. For viscous stabilization of an unstable steady-sliding sufficiently strong normal and rotational damping are required (see Oden and Martins [1985]). This, of course, agrees with the observations of Tolstoi summarized in Section 2.3.

(vii) Fig. 4.3.24 contains an important warning to experimental researchers of sliding friction: a small, apparently negligible oscillation on the tangential displacement trace at the point where it is being recorded (in our case the center of mass of the block or the tangential spring) may be the subtle manifestation of a stick-slip motion on the contact surface. Another misleading point is the fact that the wave form of the recorded oscillation may be very different from the typical saw-tooth wave form.

(viii)  $\mu$ - $v_T$  plots for apparently smooth sliding motions obtained with different "experimental apparati" (different  $s$  and  $z_x$ ) may be clearly distinct (see Figs. 4.3.21,22)

(ix) The initially decreasing portions of the  $\mu$ - $v_T$  curves in Figs. 4.3.21 and 4.3.22 are qualitatively similar to those

experimentally obtained by Rabinowicz [1965, Fig.4.45, page 101] and by Bell and Burdekin [1969-70b, Fig. 4, page 1078], respectively.

#### 4.4. Apparent reductions of static friction due to normal perturbations.

##### 4.4.1. Introduction.

In Section 4.2 we studied the linear stability of the steady-sliding equilibrium and showed that for some range of the parameters involved steady-sliding could not be stable: consequences of this on the dynamic behavior of the slider were shown in Section 4.3. Here we are interested in analyzing the effect of normal perturbations on the loading path of the slider - the stick portion of the stick-slip cycles. In a sense, we should like to determine some sort of stability statement concerning that loading path: if a perturbation is introduced while the body sticks, will the body "recuperate" from such a perturbation and keep stuck until the tangential displacement attains the value at which the unperturbed system initiates sliding or, on the contrary, will the body initiate sliding "prematurely" with an apparent coefficient of static friction lower than the true one? We also want to know what effect the driving velocity (or, equivalently, the rate of application of the tangential force) has on the apparent value of the coefficient of static friction at which the perturbed system initiates sliding.

#### 4.4.2. Numerical results.

The results reported in this section were obtained with the common data (4.3.13-16).

First we ran our program with the driving velocity successively assuming the values  $u'_{xk}{}^c = 2.5 \times 10^{-3}$ ,  $5 \times 10^{-3}$ ,  $1 \times 10^{-2}$ ,  $2.5 \times 10^{-2}$ ,  $5 \times 10^{-2}$ ,  $1 \times 10^{-1}$ ,  $2.5 \times 10^{-1}$ , and with the initial conditions  $\bar{u}_{x0} = \bar{u}_{\theta 0} = \bar{u}_{y1} = \bar{u}_{\theta 1} = 0$ ,  $\bar{u}_{x1} = u'_{xk}{}^c$ ,  $\bar{u}_{y0} = 1$ , i.e., the body initiates its motion stuck with the moving surface and no normal perturbation is introduced either at start-up or during the subsequent motion. In the subsequent motion, the body remains stuck until the nondimensional tangential displacement attains a value of the order of  $f$  at which sliding initiates. More precisely, sliding always initiates at a value of  $u_x$  somewhat in excess of  $f$ , due to the inertia acquired by the slider during the stick phase: this excess is almost imperceptible ( $\sim 10^{-4}$ ) for the smallest driving velocities and clearly noticeable ( $\sim 10^{-2}$ ) for the largest velocities considered. For each of the driving velocities considered the maximum tangential displacement of the slider  $u_{xk}^{max} = u_x^{max}(u'_{xk}{}^c)$  is recorded. Then, for each of the driving velocities  $u'_{xk}{}^c$  considered, the program is successively run starting at the time  $\tau_{ki}$  at which the unperturbed tangential displacement was equal to successively decreasing values  $u_{xi} = 0.575$ ;  $0.550$ ;  $0.525$ ; ... The initial conditions for these successive runs are the following: the tangential displacement and velocity, the normal velocity, and the rotational displacement and velocity ( $u_{xi}$ ,  $u'_{xki}$ ,  $u'_{yki}$ ,  $u_{ki}$ ,  $u'_{ki}$ , respectively) are precisely the same

as those of the unperturbed system at the time  $\tau_{ki}$ ; the normal displacement is made equal to the unperturbed normal displacement at  $\tau_{ki}$  ( $u_{yki}$ ) plus a perturbation  $p_{u_{yj}}$  successively equal to -0.05, -0.10, -0.15, -0.20. In other words, for each driving velocity  $u'_{xk}$  we introduce, at the time  $\tau_{ki}$  at which the unperturbed tangential displacement was equal to  $u_{xi}$ , a normal displacement perturbation  $p_{u_{yj}}$ .

The numerical results obtained show that *normal perturbations can produce apparent reductions of the coefficient of static friction and that a fixed level of perturbation has a "destabilizing" effect that increases with the increase of the driving velocity, i.e., a certain amount  $p_{u_{yj}}$  of normal perturbation at a fixed  $u_{xi}$  is more likely to produce a "premature" sliding if the driving velocity is large than if it is small. We illustrate this in Figs. 4.4.1 and 4.4.2.*

In Fig. 4.4.1 we can observe that a normal perturbation  $p_{u_{yj}} = -0.05$  at  $u_{xi} = 0.575$  is capable of producing a premature sliding for the larger driving velocities  $u'_{xk} = 5 \times 10^{-3}$ ,  $2.5 \times 10^{-3}$  and  $1 \times 10^{-3}$ , but, for  $u'_{xk} = 5 \times 10^{-4}$  the system, after short periods of sliding immediately after the perturbation, sticks again and the maximum tangential displacement is essentially equal to the unperturbed  $u_{xk}^{max}$ . In Fig. 4.4.2 a normal perturbation  $p_{u_{yj}} = -0.1$  at  $u_{xi} = 0.55$  produces a "premature" sliding for  $u'_{xk} = 1 \times 10^{-2}$ ,  $5 \times 10^{-3}$  and  $2.5 \times 10^{-3}$  but, for  $u'_{xk} = 1 \times 10^{-3}$  the body "recuperates" from the perturbation.

Additional qualitative information can be obtained from the numerical results by searching, for each fixed pair  $(u'_{xk}, p_{u_{yj}})$ ,



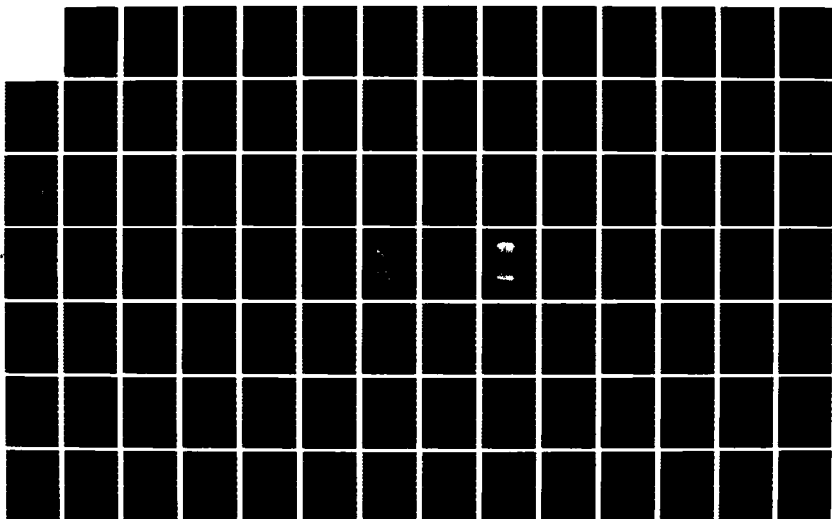
AD-A174 585

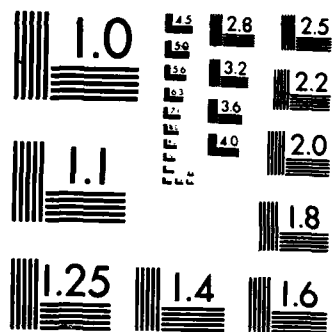
COMPUTATIONAL METHODS FOR NONLINEAR DYNAMICS PROBLEMS  
IN SOLID AND STRUCT (U) COMPUTATIONAL MECHANICS CO INC  
AUSTIN TX J T ODEN 31 MAR 86 TR-86-02 AFOSR-TR-86-2015  
F49620-84-C-0024 F/G 20/11

3/4

UNCLASSIFIED

NL





MICROCOPY RESOLUTION TEST CHART  
NATIONAL BUREAU OF STANDARDS-1963-A

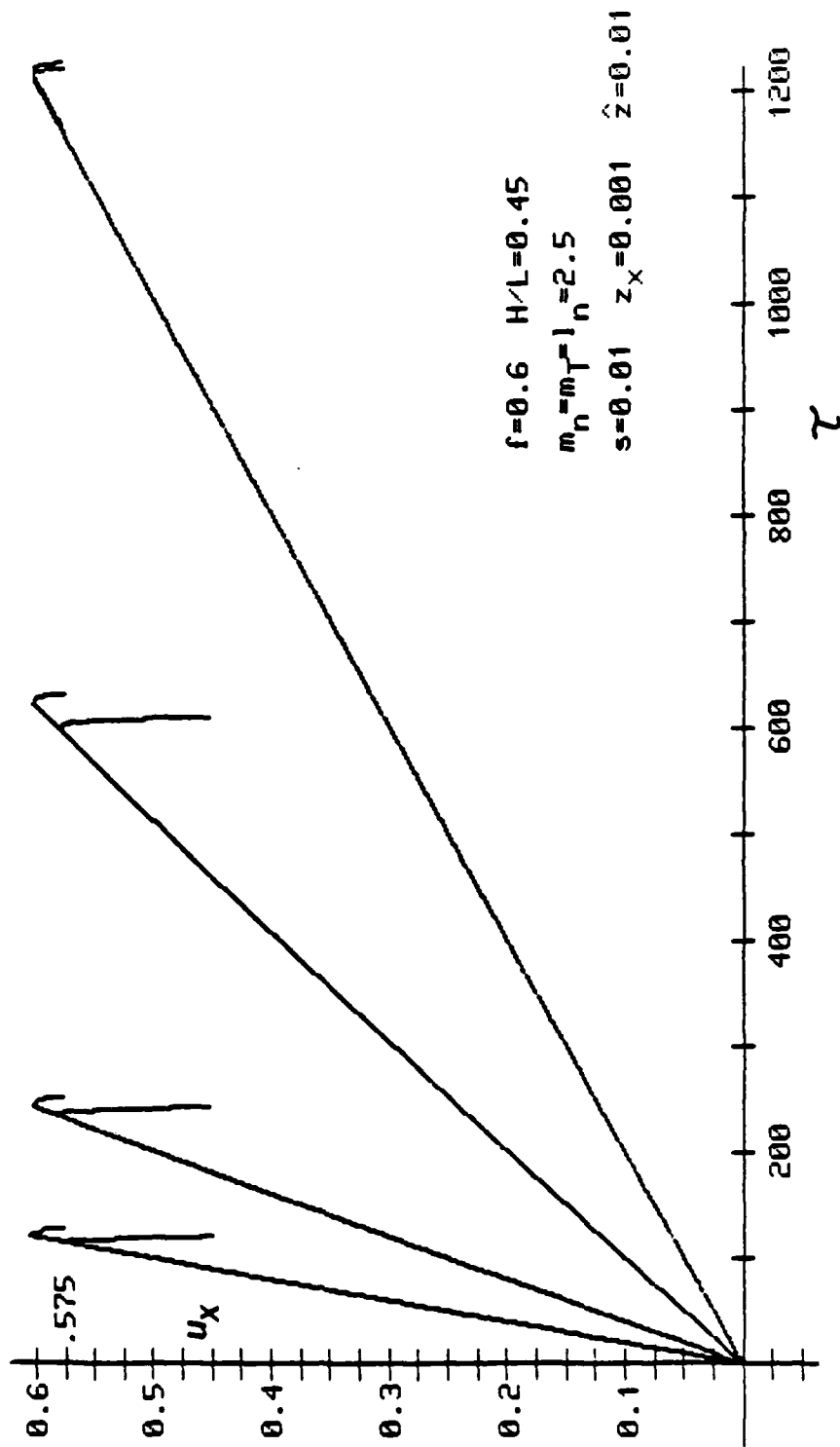


Figure 4.4.1. Unperturbed and perturbed tangential displacements for a normal perturbation  $p_{u_j} = -0.05$  at  $u_{xj} = 0.575$ . Driving velocities  $u'_{xj} = 5 \times 10^{-3}$ ,  $2.5 \times 10^{-3}$ ,  $1 \times 10^{-3}$  and  $5 \times 10^{-4}$ .

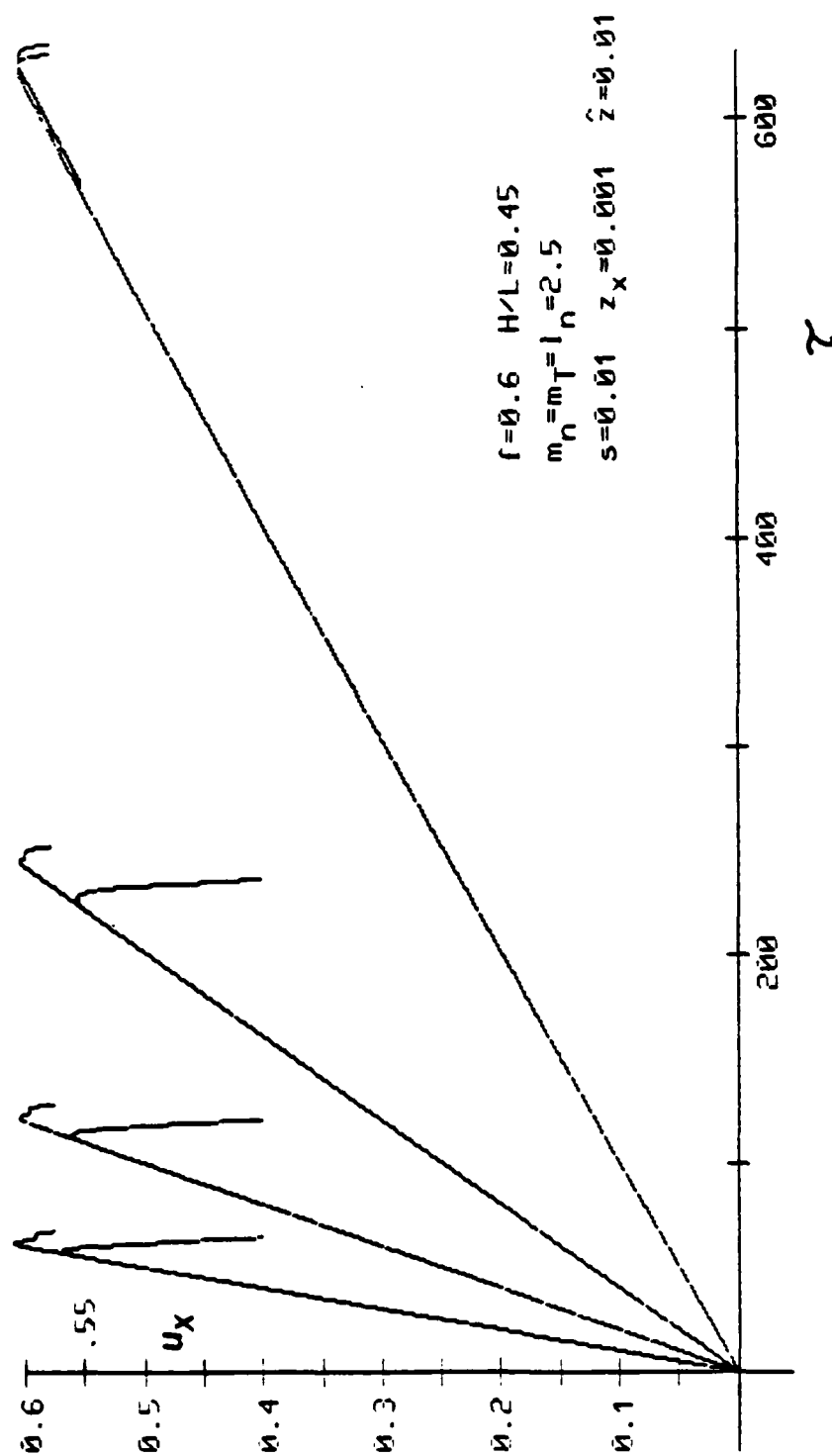


Figure 4.4.2. Unperturbed and perturbed tangential displacements for a normal perturbation  $p_{u_{-3}} u_{-3} = -0.10$  at  $u_{x0} = 0.55$ . Driving velocities:  $u'_{xk} = 1 \times 10^{-2}$ ,  $5 \times 10^{-3}$  and  $1 \times 10^{-3}$ .

the minimum value of  $u_{xi}$  at which the normal perturbation considered originates a "premature" sliding. Since actual perturbations are somehow distributed throughout time, it is reasonable to expect that the accumulation of the destabilizing effects of the perturbations will produce a "premature" sliding shortly after the above mentioned minimum of  $u_{xi}$  is achieved along the (stick) loading path. A difficulty however arises: since the unperturbed system has its maximum tangential displacement at a value  $u_{xk}^{max}$  that is not equal to  $f$  and that increases with  $u_x^c$  we cannot decide whether "premature" sliding of the perturbed system occurs or not by simply comparing the maximum value of the perturbed tangential displacement with  $f$ . In the results reported below we use the following arbitrary criterion: "premature" sliding occurs if the maximum tangential displacement of the perturbed system ( $p_{u_{xk}}^{max}$ ) is at least 1% smaller than the corresponding maximum tangential displacement of the unperturbed system ( $u_{xk}^{max}$ ) for the same driving velocity  $u_x^c$ , i.e., if  $(u_{xk}^{max} - p_{u_{xk}}^{max}) / u_{xk}^{max} \leq 0.01$ . We also note that, since we only considered perturbations at discrete locations  $u_{xi} = 0.575, 0.550, 0.525, \dots$ , to say, for instance, that  $u_{xi} = 0.550$  is the minimum value of  $u_x$  at which some perturbation produces "premature" sliding only means that such perturbation at  $u_{xi} = 0.575$  and  $0.550$  produces "premature" sliding while the same perturbation at  $u_{xi} = 0.525, 0.500, \dots$  does not produce "premature" sliding.

With these conventions in mind we summarize the results obtained in Fig. 4.4.3. In addition to observations made earlier we

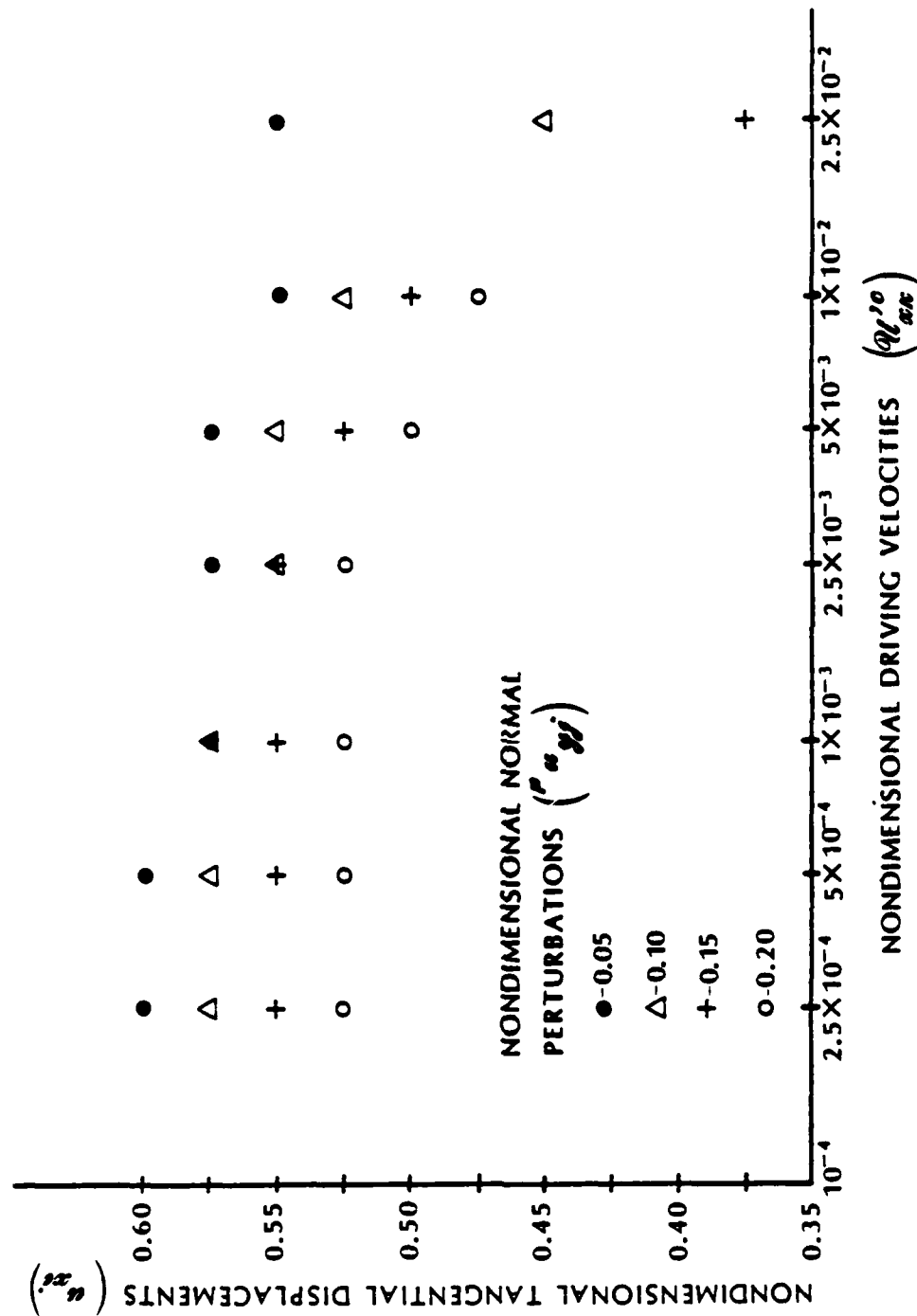


Figure 4.4.3. Minimum tangential displacement  $u_{x'}$  along the "stick" loading path at which a normal perturbation  $p''^u y_j$  produces "premature" sliding, when the driving velocity is  $u_{x'}$ .

observe, as might be expected, that *large perturbations produce a "pre-mature" sliding more easily than small ones*. We observe also that *sufficiently large normal perturbations can produce apparent reductions of the coefficient of static friction even for the smallest driving velocities considered*.

#### 4.4.3. Discussion.

The previous results, however suggestive they are, should be analyzed having in mind the admitted limitations of the model used: preliminary tangential displacements occurring before gross sliding and the details of the plastic deformation of the interface cannot be modelled with the constitutive laws (2.5.2,3) adopted in this work. Since these effects may have some importance along the quasistatic loading process studied here, the results above should be viewed only as indicators of what to expect when using more complex models of the interface behavior.

A question that is important to discuss is the size of the normal perturbations considered. As we decrease the size of the perturbation its destabilizing effect of course is reduced (recall Fig. 4.4.2). It is easy to anticipate, and we confirmed it numerically, that sufficiently small normal perturbations have negligible effect on the initiation of sliding. However we observe that the size of the perturbations considered here, although "mathematically not small", are indeed "physically quite small" and of the order of magnitude of the microseisms mentioned in Section 2.3.

For static penetrations  $Y = (W/c_n BL)^{1/m_n}$  in the range 0.3 to 10  $\mu\text{m}$ , the perturbations considered here would be in the range 0.015 to 2  $\mu\text{m}$ .

Apparent decreases of the coefficient of static friction with the increase of driving velocity, as suggested by the numerical results above would affect the stick-slip results of Section 4.3.2 (recall that in the computations leading to Figs. 4.3.16 to 4.3.18 no reductions of static friction were taken into account). Smaller stick-slip amplitudes and more pronounced slopes of the amplitude-velocity curves in Figs. 4.3.16 and 4.3.17 should be expected as a result of the reductions of static friction. On the other hand, these reductions would lead to smaller periods of stick and consequently to larger frequencies in Fig. 4.3.18, more close to the natural frequency of the tangential motion of the system. These effects would certainly improve on what appears to be an "excessive" sharpness of the transition stick-slip to apparently smooth sliding in Figs. 4.3.16, 17 and also on the smallness of the maximum stick-slip frequencies in Fig. 4.3.13.

It is thus clear that the "rate dependence" of the coefficient of static friction plays an important role on the stick-slip oscillations, precisely as it has been assumed in previous analyses. The question that we raise here and that needs further study is solely related with its origin - is it an intrinsic property of the contacting surfaces or is it the result of a (still not well defined) "instability" along the stick portion of the stick-slip cycles? Much theoretical, numerical and experimental work is



still needed before a definitive answer to this question can be given.

#### 4.5. Some remarks on the numerical results.

The nature of the problems studied in this chapter leads to the two following difficulties when numerical solutions for them are sought : firstly, the friction law introduces a multi-valued operator and discontinuous accelerations and friction forces result at the transitions slip to stick; secondly, in the physically interesting situations, the periods of response in the tangential direction that are of interest to span are much larger than the periods of the normal and rotational oscillations of the body: although we may not be too interested in knowing very accurately how many microns or fractions of the micron the interface penetration is at each time, we cannot afford to lose too much accuracy in that computation since that may affect the rapidly varying values of the friction force to an extent that the whole average behavior in the tangential direction may become meaningless.

To handle the first difficulty, a regularization technique has been used which, for the continuous in time problem (4.1.4,5) can be shown to lead to approximate solutions that converge, as the regularization parameter  $\epsilon \rightarrow 0$ , to the solution of (4.1.4,5). The proof of this is essentially the same as the one presented earlier in Section 3.4. When used in conjunction with the time discretization, it is reasonable to expect (although not proved) that the time step will

have to decrease to zero at a rate somehow related to the rate of decrease of  $\epsilon$ , if convergence is to be assured. In the absence of such convergence studies the choice of  $\epsilon$  has been dictated only by how physically reasonable the numerical results look, in particular, how well stick states are modelled. For the small driving velocities  $U_x^c$  considered in most of the examples of this chapter, values of  $\epsilon/U_x^c \leq 0.1$  lead to results with well-defined stick states (see, for example, Figs. 4.3.8, 4.3.15 and 4.3.24).

With respect to the second difficulty mentioned above, there seems to be no other alternative than to use time steps of a size sufficiently small that the normal oscillation is integrated with sufficient accuracy. Values of the maximum time step  $\Delta t_{\max}$  (see Chapter 5) have been used that are at most 1/50 and, usually, 1/100 of the period of the linearized normal free oscillation ( $2\pi/\omega_{y0}$ ).

The numerical results shown in Figs. 4.5.1 and 4.5.2 illustrate our contention that, for "regular" cases (see below), the qualitative behavior and the essential quantitative features of the motions (amplitudes, frequencies, average sliding velocities) are not sensitive to reasonable (and sometimes not so reasonable) variations in  $\epsilon$  and  $\Delta t_{\max}$  or changes in the method of integration (see also Martins and Oden [1986]). By "regular" cases we mean all the motions that, despite their complexity, occupy after a sufficiently large time, a well defined region of the phase space and reveal a pattern that "essentially" repeats itself in time, namely:

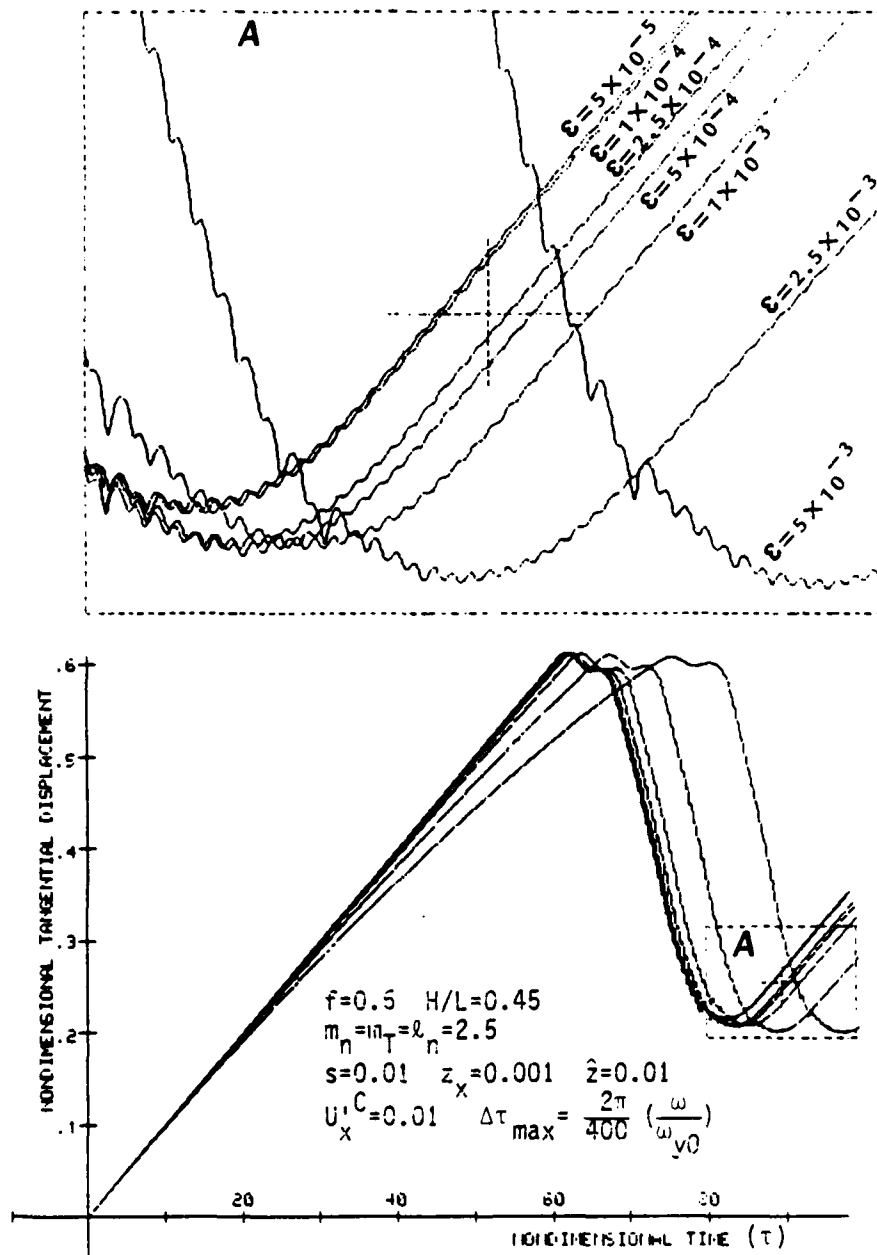


Figure 4.5.1. Effect of the regularization parameter on the computed stick-slip motion. Note that the major error in the solution for unreasonably large values of  $\epsilon$  is the creeping along the large stick phase of the low-frequency stick slip motion. The amplitudes of the stick-slip motion obtained with different values of  $\epsilon$  differ by less than 4%.

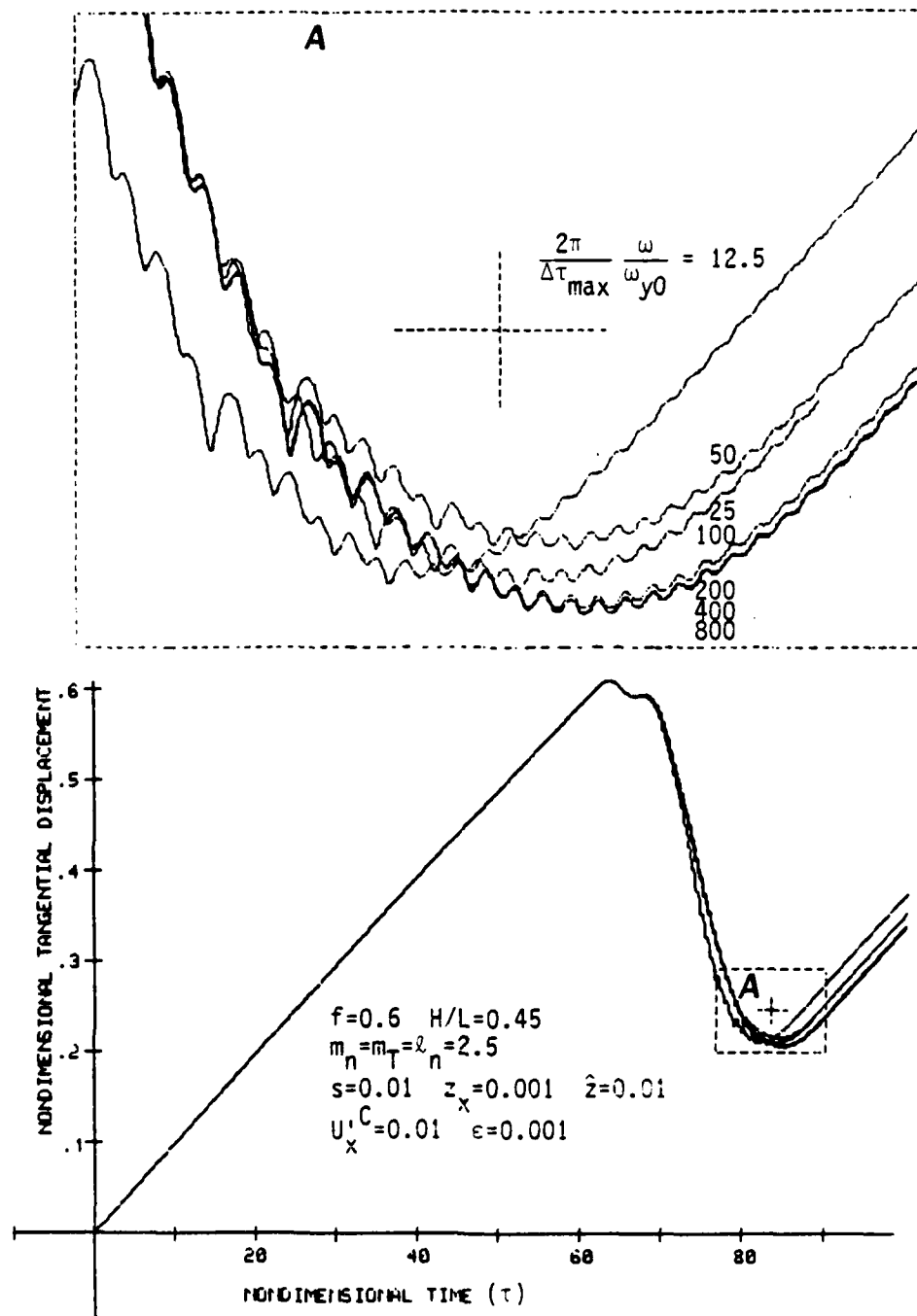


Figure 4.5.2. Effect of the maximum time step size ( $\Delta\tau_{\max}$ ) on the computed stick-slip motion.

the low-frequency stick-slip motions and the apparently smooth sliding motions of Section 4.3. For these cases, we may say that our code behaves in a robust manner. If high accuracy is desired (very accurate stick states, very accurate values for the instantaneous penetrating approaches and rotations) the analysis may become too expensive for the small number of degrees of freedom involved. In order to improve on this it seems advisable to use, at least in the rigid body case, other standard techniques of integration of systems of ordinary differential equations that allow for the estimation of the errors introduced at each stage and the automatic time step control. This may permit increasing the time step in a controlled manner during periods of no contact and extended periods of stick and reduce it during short periods of contact and transitions stick to slip. Radical improvements in computational time should not be expected however, due to the steep slopes of the regularized friction law that are needed for very accurate stick state modelling.

We report now on some situations for which we found a "severe sensitivity" of the numerical solutions to the numerical parameters  $\epsilon$  and  $\Delta t_{\max}$ , and to every small change in computational algorithm or data. Such situations may occur in applications of the type presented in Section 4.3 when the normal damping parameter  $\lambda$  is equal to zero or is very small and some values are chosen for the other governing parameters.

"Regular" results with zero normal interface damping ( $\hat{\gamma}=0$ ) were earlier presented in Figs. 4.3.14 and 4.3.15. However, when other values are assumed for the other governing parameters, the trace of the tangential motion may be extremely "irregular", with regions of sliding and sticking alternating in a irregular and unpredictable manner. For the times spanned by our computations those "irregular" motions do not appear to be converging to any more predictable oscillation. Small changes in data, computational algorithm or numerical parameters lead to solutions that only have in common with each other their extreme irregularity and unpredictability. We illustrate these difficulties in Fig. 4.5.3, where we reproduce the tangential displacements obtained with three different maximum time steps and keeping constant all the other parameters.

Situations of this type should not be surprising. It is now well known that other nonlinear nonconservative systems with three or more phase space variables may reveal equally unpredictable irregular behavior. An example that has in common with the present problem the fact that it also leads to a nonsymmetric  $2 \times 2$  stiffness matrix (recall equation 4.2.13) is the problem of a double pendulum subjected to a follower force (see e.g. Takens [1974a,b] and for related problems Holmes [1977] and Holmes and Marsden [1978]).

On physical grounds, we conjecture that the irregular motions that we have obtained numerically are of the same type as some

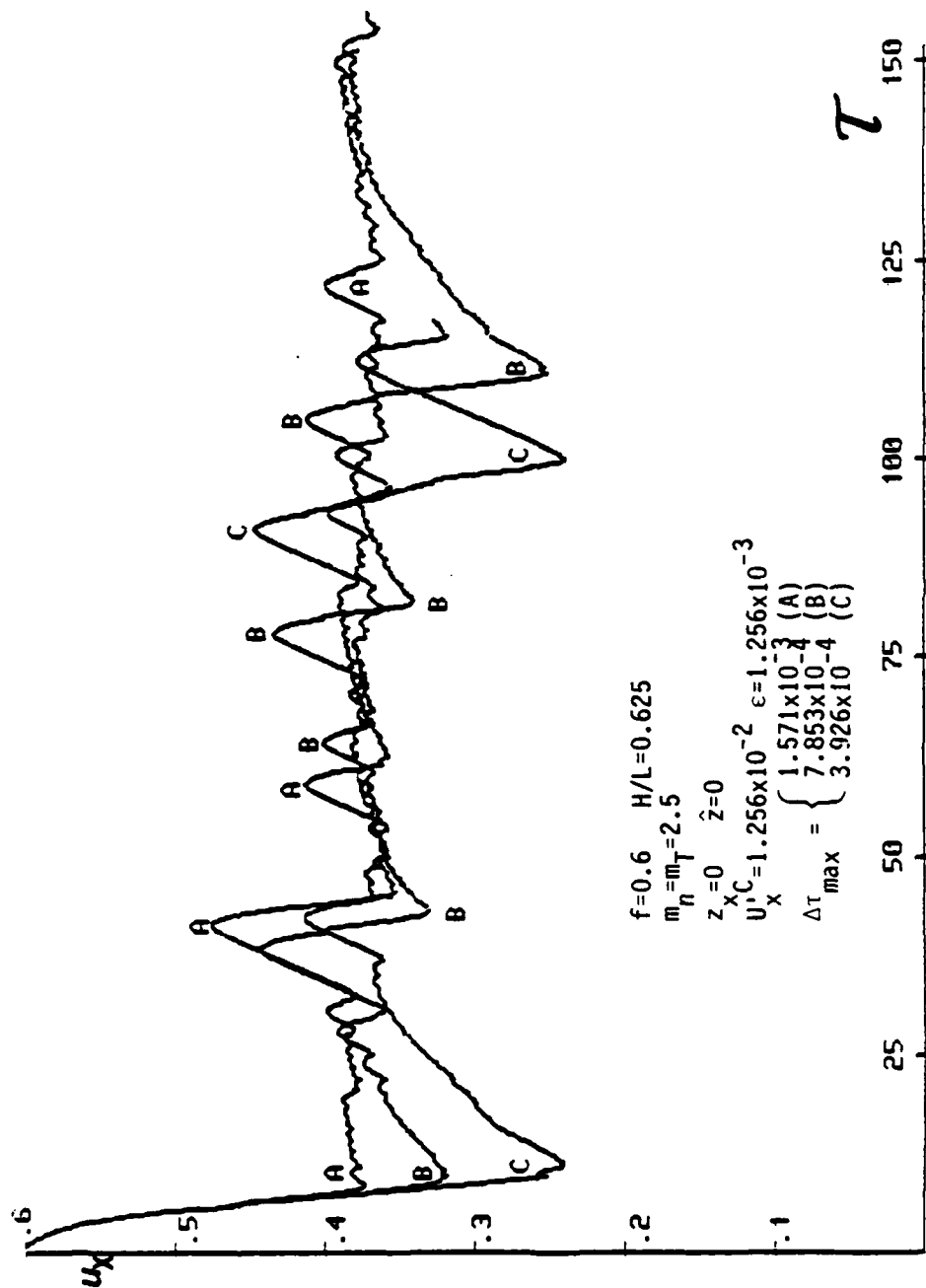


Figure 4.5.3. "Irregular" tangential displacement traces obtained numerically with three different time step sizes.

if not all of the irregular experimental friction traces obtained by Bowden and Leben [1939], Bowden and Tabor [1939], and Rabinowicz [1965]. For each of the irregular plots obtained numerically it is always easy to find some experimental trace in the literature that is qualitatively very similar (just as an example, compare Fig. 4.5.3 with Fig. 8e, Plate 22 in Bowden and Leben [1939] or with Fig. 8b, Plate 26, in Bowden and Tabor [1939]).

We suspect thus that those "irregular" motions and the associated numerical difficulties are inherent to the governing equations (4.1.4,5) for some ranges of the governing parameters. Only a detailed qualitative study of that system may confirm (or not) the truth of this conjecture.



## CHAPTER 5

### FINITE ELEMENT MODELS

#### 5.1. Finite element approximations

Using standard finite element procedures, approximate versions of the Problems 2, 3 and 4 (Chapter 3) can be constructed in finite dimensional subspaces  $V_h (\subset V \subset V')$ . For a certain mesh ( $h$ ) the approximate displacements, velocities and accelerations at each time  $t \in [0, T]$  are elements of  $V_h$ ,

$$\underline{v}^h(t), \underline{\dot{v}}^h(t), \underline{\ddot{v}}^h(t) \in V_h.$$

Within each element  $(e)_{\Omega}$  ( $e=1,2,\dots,E_h$ ;  $E_h$ =total number of elements in the mesh) the displacement components are expressed in the form

$$v_j^h(\underline{x}, t) = \sum_{I=1}^{N_e} v_{Ij}^h(t) N_I(\underline{x}), \quad j=1,2,\dots,N, \quad (5.1.1)$$

and similar expressions hold for their time derivatives. In (5.1.1),  $N_e$  is the number of nodes of the element  $e$ ;  $v_{Ij}^h(t)$  denotes the  $j$ -th displacement component of node  $I$  at time  $t$ , and  $N_I$  is the element shape function associated with the node  $I$ . The particularization of the above when no time dependence exists (Problem 3 and 4) is obvious.

Hereafter, we confine our attention to plane problems ( $N=2$ ) and we consider two types of finite element approximations: four-node,

bilinear ( $Q_1$ ) elements and nine-node, biquadratic ( $Q_2$ ) elements.

The finite dimensional versions of the variational statements (3.3.13), (3.6.1) and (3.8.1) are immediate. On the other hand, the systems of ordinary differential inclusions or algebraic equations to be solved are precisely of the form found in the previous chapter with the rigid body model: (4.1.4,5), (4.1.7) and (4.1.12).

Clearly, the vectors and matrices appearing now in those equations have the dimensions  $2 \times N_h$  and  $(2 \times N_h) \times (2 \times N_h)$ , respectively ( $N_h$  = total number of nodes in the mesh). It is also clear that all of them depend on the mesh parameter  $h$ , which, for simplicity, will be omitted in the notations.

## 5.2. A regularization of the Coulomb friction law

Computationally, it is desirable to work with a system of ordinary differential equations rather than a system of differential inclusions of the type in (4.1.4). We achieve this by using a regularization technique of the type employed earlier in Section 3.4: recall, in particular, the assumptions (3.4.35-39) on the regularization function  $\psi_\epsilon$ , and the definitions (3.4.40,41) and (3.4.43,44) of the regularized continuum problem and its finite dimensional approximation, respectively. The variational statement governing the finite element regularized dynamic friction problem is precisely of the form (3.4.43). The corresponding system of ordinary differential equations has the form

$$\left. \begin{aligned} M \ddot{u}(t) + C \dot{u}(t) + K u(t) \\ + P(u(t)) + Q(u(t), \dot{u}(t)) + J_\varepsilon(u(t), \dot{u}(t)) = F(t) \end{aligned} \right\} \quad (5.2.1)$$

with initial conditions

$$u(0) = \bar{u}_0, \quad \dot{u}(0) = \bar{u}_1. \quad (5.2.2)$$

Here we take into account normal interface dissipative effects, we omit in the notations the dependence of the solutions upon the regularization parameter  $\varepsilon$ , and, for simplicity, we assume  $\bar{u}_0$  and  $\bar{u}_1$  to be given in  $V_h$ .

The function  $\psi_\varepsilon \in C^1(\mathbb{R}^2, \mathbb{R})$  employed in the computations reported in this work has the form, with  $\varepsilon > 0$ ,

$$\psi_\varepsilon(\xi) = \begin{cases} \varepsilon \left| \frac{\xi}{\varepsilon} \right|^2 \left( 1 - \frac{1}{3} \left| \frac{\xi}{\varepsilon} \right| \right) & \text{if } |\xi| \leq \varepsilon \\ \varepsilon \left( \left| \frac{\xi}{\varepsilon} \right| - \frac{1}{3} \right) & \text{if } |\xi| > \varepsilon. \end{cases}$$

The corresponding directional derivative at  $\xi$  in the direction of  $\alpha$  is

$$\psi'_\varepsilon(\xi)(\alpha) = \begin{cases} \frac{1}{\varepsilon} \left( 2 - \left| \frac{\xi}{\varepsilon} \right| \right) (\xi \cdot \alpha) & \text{if } |\xi| \leq \varepsilon \\ \frac{1}{|\xi|} (\xi \cdot \alpha) & \text{if } |\xi| > \varepsilon. \end{cases}$$

In order to visualize this regularization procedure, we denote by  $\tau$  a unit tangent vector along the (uni-dimensional and sufficiently smooth) contact boundary  $\Gamma_C$ . With  $\xi$  and  $\alpha$  tangent to  $\Gamma_C$  (recall Section 3.4), we denote the components of  $\xi$  and  $\alpha$

along  $\underline{T}$  by  $\underline{\xi}$  and  $\underline{\alpha}$  respectively (i.e.,  $\underline{\xi} = \underline{\xi} \underline{T}$  and  $\underline{\alpha} = \underline{\alpha} \underline{T}$ ), and we can define the real valued function of a real variable  $\hat{\psi}_{\epsilon}$ , such that  $\hat{\psi}_{\epsilon}(\underline{\xi}) = \psi_{\epsilon}(\underline{\xi})$  and  $\hat{\psi}'_{\epsilon}(\underline{\xi})(\underline{\alpha}) = \psi'_{\epsilon}(\underline{\xi})(\underline{\alpha})$ . The functions  $\hat{\psi}_{\epsilon}$  and  $\hat{\psi}'_{\epsilon}$  are depicted in Fig. 5.2.1 together with the function  $|\cdot|$  and the multivalued application  $\text{sgn}(\cdot)$  which, respectively, they approximate.

Many examples of similar regularization procedures in dynamic friction problems can be found in the literature. Among them we refer to Duvaut and Lions [1976] for mathematical aspects; to Threlfall [1978] and Rooney and Deravi [1982] for computational applications to Theory of Mechanisms and to Martins and Oden [1983] for a finite element analysis of a simplified friction problem.

**Remark 5.2.1.** Let us assume that:

- (i) The family  $\{V_h\}$  of finite element subspaces is endowed with standard asymptotic interpolation properties as  $h \rightarrow 0$  (see e.g. Ciarlet [1978] or Oden and Carey [1983]).
- (ii) The assumptions of Theorem 3.4.2 hold with, for simplicity,  $\bar{\phi}$  in (3.4.32) and  $\bar{u}_0$  and  $\bar{u}_1$  in (3.4.33) belonging to all the  $V_h$  in the family  $\{V_h\}$  with  $h$  sufficiently small.

Then the family  $\{V_h\}$  satisfies conditions of the type (3.4.5-7) and, with the same proofs of Lemma 3.4.1 and Theorem 3.4.2 and the observations of Remark 3.4.5, it follows that the finite elements regularized solutions converge to the non-regularized continuum solutions of Problem 2, as  $h \rightarrow 0$  and  $\epsilon \rightarrow 0$ , in the topologies indicated in Remark 3.4.5.  $\square$

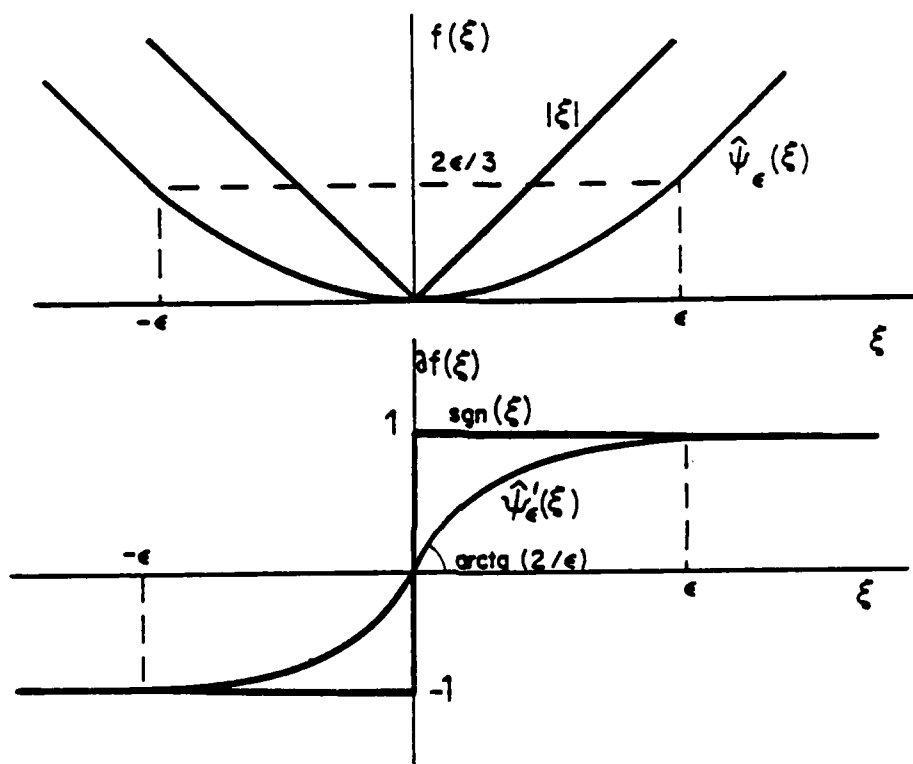


Figure 5.2.1. Graphs of  $|\cdot|$ ,  $\text{sgn}(\cdot)$  and of their regularized approximations  $\hat{\psi}_\epsilon(\cdot)$  and  $\hat{\psi}'_\epsilon(\cdot)$ .

$$\hat{\psi}_\epsilon(\xi) = \begin{cases} \epsilon \left| \frac{\xi}{\epsilon} \right|^2 \left( 1 - \frac{1}{3} \left| \frac{\xi}{\epsilon} \right| \right) & \text{if } |\xi| \leq \epsilon \\ \epsilon \left( \left| \frac{\xi}{\epsilon} \right| - \frac{1}{3} \right) & \text{if } |\xi| > \epsilon \end{cases}$$

$$\hat{\psi}'_\epsilon(\xi) = \begin{cases} \left( 2 - \left| \frac{\xi}{\epsilon} \right| \right) \frac{\xi}{\epsilon} & \text{if } |\xi| \leq \epsilon \\ \text{sgn}(\xi) & \text{if } |\xi| > \epsilon \end{cases}$$

### 5.3. Algorithms for transient analysis

The algorithms that we have used for solving the discrete dynamic system (5.2.1,2) involve variants of standard schemes in use in nonlinear structural mechanics calculations: Newmark's method and central-difference technique, both associated with Newton-Raphson iterations within each time step.

Let us consider a partition of the time domain  $[0, T]$  into  $M$  intervals of length  $\Delta t = t_{K+1} - t_K$  with  $0 = t_0, t_1, \dots, t_K, \dots, t_M = T$ .

Choosing as fundamental unknowns at time  $t_K$ , for example, the velocities  $\dot{\underline{u}}_K \equiv \dot{\underline{u}}(t_K)$ , the displacements and accelerations at time  $t_K$  can be expressed as linear combinations of  $\dot{\underline{u}}_K$  and the (known) variables at  $t_{K-1}$ , according to the Newmark formulae:

$$\left. \begin{aligned} \ddot{\underline{u}}_K &= (1 - 1/\gamma) \ddot{\underline{u}}_{K-1} + (\dot{\underline{u}}_K - \dot{\underline{u}}_{K-1})/\gamma \Delta t \\ \underline{u}_K &= \underline{u}_{K-1} + \Delta t (1 - \frac{\beta}{\gamma}) \dot{\underline{u}}_{K-1} + \frac{\Delta t^2}{2} (1 - \frac{2\beta}{\gamma}) \ddot{\underline{u}}_{K-1} + \frac{\Delta t^2 \beta}{\gamma} \ddot{\underline{u}}_K \end{aligned} \right\} \quad (5.3.1)$$

where  $\beta$  and  $\gamma$  are the so-called Newmark parameters. For  $\beta = 1/4$ ,  $\gamma = 1/2$  the average acceleration method is recovered and for  $\beta = 0$ ,  $\gamma = 1/2$  the central-difference method is recovered.

Substituting the above relations into equation (5.2.1) we obtain the following equation at time  $t_K$ :

$$\underline{R}_K(\dot{\underline{u}}_K) = \underline{0} \quad (5.3.2)$$

where

$$\underline{R}_K(\dot{\underline{u}}_K) \stackrel{\text{def}}{=} \left[ \frac{1}{\gamma \Delta t} \underline{M} + \underline{C} + \frac{\Delta t \beta}{\gamma} \underline{K} \right] \dot{\underline{u}}_K + \underline{N}(\dot{\underline{u}}_K) - \hat{\underline{F}}_K \quad (5.3.3)$$

$$\underline{N}(\dot{\underline{u}}_K) \stackrel{\text{def}}{=} \underline{P}(\underline{u}_K) + \underline{Q}(\underline{u}_K, \dot{\underline{u}}_K) + \underline{J}_\varepsilon(\underline{u}_K, \dot{\underline{u}}_K) \quad (5.3.4)$$

$$\begin{aligned} \hat{\underline{F}}_K &\stackrel{\text{def}}{=} \underline{F}_K - M[(1 - \frac{1}{Y})\ddot{\underline{u}}_{K-1} - \frac{1}{Y\Delta t} \dot{\underline{u}}_{K-1}] \\ &\quad - K[\underline{u}_{K-1} + \Delta t(1 - \frac{\beta}{Y})\dot{\underline{u}}_{K-1} + \frac{\Delta t^2}{2}(1 - \frac{2\beta}{Y})\ddot{\underline{u}}_{K-1}] \end{aligned} \quad (5.3.5)$$

with  $\underline{u}_K$  in (5.3.4) given by (5.3.1)<sub>2</sub>.

In order to solve the nonlinear equation (5.3.2) the Newton-Raphson iteration technique is used: given a starting value  $\dot{\underline{u}}_K^{(0)}$  successive approximations of the solution  $\dot{\underline{u}}_K$  are computed using the recurrence formula

$$\dot{\underline{u}}_K^{(i+1)} = \dot{\underline{u}}_K^{(i)} - [\hat{\underline{C}}_K^{(i)}]^{-1} \underline{R}_K^{(i)} \quad (5.3.6)$$

where  $i=0,1,2,\dots$  denotes the iteration counter,

$$\underline{R}_K^{(i)} \equiv \underline{R}_K(\underline{u}_K^{(i)}) \quad (5.3.7)$$

$$\begin{aligned} \hat{\underline{C}}_K^{(i)} &\stackrel{\text{def}}{=} \frac{\partial}{\partial \dot{\underline{u}}_K} (\underline{R}_K(\dot{\underline{u}}_K)) \Big|_{\dot{\underline{u}}_K = \dot{\underline{u}}_K^{(i)}} \\ &= \frac{1}{Y\Delta t} \underline{M} + [\underline{C} + \underline{C}_K^Q(i) + \underline{C}_{\varepsilon K}^J(i)] \\ &\quad + \frac{\beta\Delta t}{Y} [\underline{K} + \underline{K}_K^P(i) + \underline{K}_K^Q(i) + \underline{K}_{\varepsilon K}^J(i)] . \end{aligned} \quad (5.3.8)$$

The form of the element contributions to the vectors and matrices in the above equations is the following:

$$\begin{aligned} {}^{(e)}p_{I_j}(\underline{w}) &= \int_{{}^{(e)}\Gamma_c} c_n[(\underline{w}_n - \underline{g})_+]^{m_n} n_j N_I \, ds \\ {}^{(e)}q_{I_j}(\underline{w}, \underline{v}) &= \int_{{}^{(e)}\Gamma_c} b_n[(\underline{w}_n - \underline{g})_+]^{l_n} v_n n_j N_I \, ds \end{aligned}$$

$$(e)_{J_{\epsilon I_j}}(\underline{w}, \underline{v}) = \int_{(e)_{\Gamma_C}} c_T [(w_n - g)_+]^{m_T} \hat{\psi}'_{\epsilon} (v_T - \dot{U}_T^C) T_j N_I ds$$

$$(e)_{K_{M_i N_j}^P}(\underline{w}) = \int_{(e)_{\Gamma_C}} c_n m_n [(w_n - g)_+]^{m_n - 1} n_i n_j N_M N_N ds$$

$$(e)_{K_{M_i N_j}^Q}(\underline{w}, \underline{v}) = \int_{(e)_{\Gamma_C}} b_n l_n [(w_n - g)_+]^{l_n - 1} v_n n_i n_j N_M N_N ds$$

$$(e)_{K_{\epsilon M_i N_j}^J}(\underline{w}, \underline{v}) = \int_{(e)_{\Gamma_C}} c_T m_T [(w_n - g)_+]^{m_T - 1} \hat{\psi}'_{\epsilon} (v_T - \dot{U}_T^C) T_i n_j N_M N_N ds$$

$$(e)_{C_{M_i N_j}^Q}(\underline{w}) = \int_{(e)_{\Gamma_C}} b_n [(w_n - g)_+]^{l_n} n_i n_j N_M N_N ds$$

$$(e)_{C_{\epsilon M_i N_j}^J}(\underline{w}, \underline{v}) = \int_{(e)_{\Gamma_C}} c_T [(w_n - g)_+]^{m_T} \hat{\psi}''_{\epsilon} (v_T - \dot{U}_T^C) T_i T_j N_M N_N ds$$

where  $(\underline{w}, \underline{v}) \in V_h \times V_h$ ,  $v_T = v_T(\underline{s})$  and  $\dot{U}_T^C = \dot{U}_T^C(\underline{s})$  denote the components of  $\underline{v}_T = \underline{v}_T(\underline{s})$  and  $\dot{\underline{U}}_T^C = \dot{\underline{U}}_T^C(\underline{s})$  along the unit vector  $\underline{T} = \underline{T}(\underline{s})$  tangent to  $\Gamma_C$ ,  $(e)_{\Gamma_C}$  denotes the portion of  $\Gamma_C$  belonging to the element  $e$ , and

$$\hat{\psi}''_{\epsilon}(\xi) = \begin{cases} \frac{2}{\epsilon} (1 - |\frac{\xi}{\epsilon}|) & \text{if } |\xi| \leq \epsilon \\ 0 & \text{if } |\xi| > \epsilon. \end{cases}$$

The linear damping matrix  $\underline{\underline{C}}$  considered in the finite element code has the general form:

$$\underline{\underline{C}} = c_K \underline{\underline{K}} + c_M \underline{\underline{M}}.$$

It is clear from (5.3.8) that, if the central-difference technique is used ( $B=0$ ) no stiffness contributions to the matrix



$\hat{\underline{C}}_K^{(i)}$  exist. The matrix  $\hat{\underline{C}}_K^{(i)}$  is then a symmetric matrix. If diagonalized mass and damping matrices ( $\underline{M}$  and  $\underline{C}$ ) are used, then the only possible nondiagonal entries of  $\hat{\underline{C}}_K^{(i)}$  result from the element segments on  $\Gamma_C$ . The matrix  $\hat{\underline{C}}_K^{(i)}$  becomes diagonal when, in addition, a transformation (rotation) of the degrees of freedom on  $\Gamma_C$  is performed in such a manner that the final degrees of freedom have the direction of the normal and the tangent to  $\Gamma_C$  at each contact node, and the element contributions to  $\underline{C}_K^{Q(i)}$  and  $\underline{C}_{\in K}^{J(i)}$  are computed with a quadrature rule which uses the nodes as integration points (e.g., trapezoidal rule for linear elements and Simpson's rule for quadratic elements). The resulting explicit form of (5.3.6) is then a clear advantage of the central-difference technique over the implicit members of the Newmark family of methods.

**Remark 5.3.1.** In the actual computer implementation of the implicit members of the Newmark family of methods the displacements  $\underline{u}_K$  at time  $t_K$  were taken to be the fundamental unknowns. The nonlinear equation to be solved iteratively involves thus displacements, rather than velocities. The same happens with the recurrence formula (5.3.6) where, instead of an effective damping matrix ( $\hat{\underline{C}}_K$ ), an effective stiffness matrix is used (see Oden and Martins [1985] for the details of the equivalent formulation).  $\square$

**Remark 5.3.2.** The discontinuity (actually, the multivaluedness) of the Coulomb's friction law at zero sliding velocity is a major source of computational difficulties in friction problems.

Even though, in the algorithms described in this section, a regularized form of that law is used, those difficulties cannot be completely avoided. The situation which may arise when using the methods described here with a constant time step is the following: in unloading situations (passage from sliding to adhesion) the Newton-Raphson iterative techniques may fail to converge if  $\epsilon$  is very small and the time step too large. We observe that similar difficulties may occur even when different regularizations of the friction law and different iterative schemes are used (see Martins and Oden [1983]). The difficulty appears to be the result of the steep changes in  $\hat{\psi}_\epsilon$  (recall Fig. 5.2.1) in the region where its curvature changes sign, i.e., in the interval  $[-\epsilon, \epsilon]$ . We observe also that it is in transitions from sliding to adhesion that the most drastic changes in the solution are expected to occur: with a single degree-of-freedom sliding system a discontinuity of the tangential acceleration (and of the friction force) arises at the transitions from slip to stick.

One simple remedy for these difficulties is the use of smaller time steps whenever such nonconvergences occur. The need to reduce the time step when load-deflection curves present an inflection and Newton iterations are performed within each time step has been reported earlier by other authors (Geradin, Hogge and Idelsohn [1983]).

In the computer codes developed in the course of this work (either with the finite element models or the rigid body models)

reduction of the maximum time step prescribed in the input ( $\Delta t_{\max}$ ) is only performed if the Newton-Raphson iteration fails to converge in a prescribed number MAXITE of iterations. In that situation, successively smaller time steps  $\Delta t$  are tried until a convergent solution is obtained. This smaller time step is then kept for a prescribed number of steps KSTEPR during which the most drastic changes in the solution are expected to occur. After this time interval, the time step is gradually increased again to  $\Delta t_{\max}$ .

It was found that for the smaller time steps, a reduction below  $0.1\Delta t_{\max}$  was rarely needed if a  $\Delta t_{\max}$  was used which provided simultaneously for accurate computation of dynamic response and for the stability of the central difference technique and if the values of  $\epsilon$  used were not too small. The parameter MAXITE has been set usually to 5 and KSTEPR to a number in the range 10-20.

An indication of the extra computational work resulting from the reduced time steps is given by the quotient  $T'/T$ , where  $T$  is the total physical time spanned by our analysis with some total number of time steps, and with time step reductions, and  $T'$  is the total physical time that would be possible to span with the same total number of time steps if no reduction of time steps were needed. In most of the computations, values of this ratio of the order 1.2-1.5 were experienced. If more restrictive values of  $\epsilon$  are used without decreasing the input value of  $\Delta t_{\max}$ , the result may be a significant increase on the ratio  $T'/T$ : for example, for  $\epsilon = 0.02 \text{ cms}^{-1}$  in Example 1 of Section 5.5, a ratio  $T'/T = 4.2$  was

obtained.

#### 5.4. Algorithm for steady-sliding and linear stability analysis

In order to compute the solutions of the finite dimensional versions of Problem 3 for a certain range  $[0, \bar{c}_T]$  of values of  $c_T$  we subdivide the interval  $[0, \bar{c}_T]$  into a prescribed number NINCT of increments  $\Delta c_T = \bar{c}_T / \text{NINCT}$  and, for each increment  $K=0, 1, \dots, \text{NINCT}$  we again use the Newton-Raphson method to solve the nonlinear system of equations at each value of  $c_T$ . For the Newton process at  $c_T=0$  ( $K=0$ ) the input of some (very simple) initial guess is required. For  $K \geq 1$ , the starting value for the equilibrium iterations at the  $K$ -th increment is the (converged) solution for the  $(K-1)$ -th increment.

For the computed equilibrium position at each increment  $K$ , the finite dimensional versions of the nonsymmetric eigenvalue Problem 4 are solved using standard routines.

#### 5.5. Numerical results

Our first example is designed more to test the performance of the algorithms described in Section 5.3 than as a model of complex dynamic friction phenomena.

**Example 1** (*A slab subjected to periodic loading*). We study here the motion of the slab shown in Fig. 5.5.1. The dimensions of the slab are 16cm x 2cm, as indicated, and it is assumed to be in a state of plane strain. The linear elasticity properties of the material of which the slab is constructed are: Young's

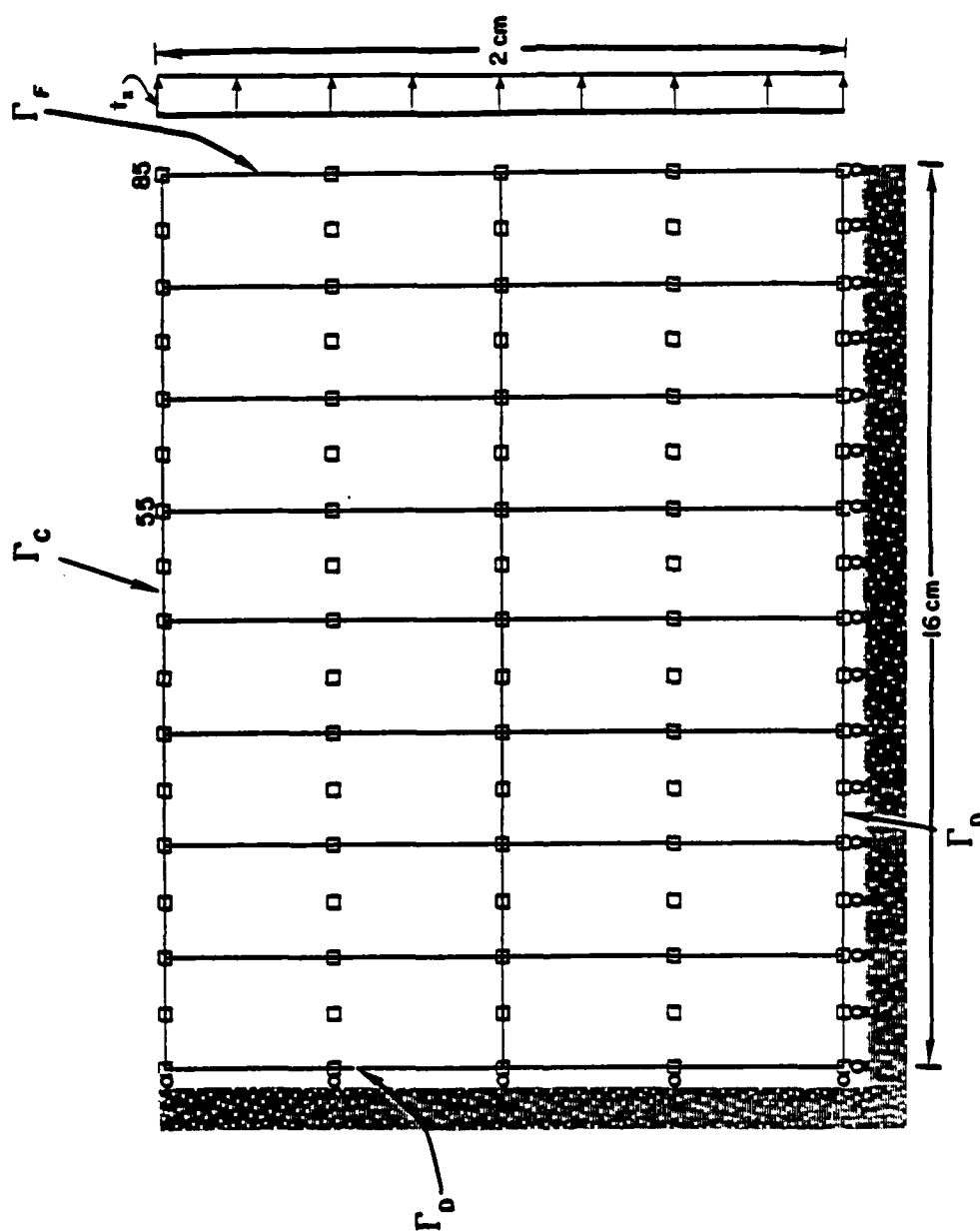


Figure 5.5.1. Dimensions and finite element discretization of a deformable slab.

modulus  $E=1.4 \times 10^6 (10^3 \text{Kg cm}^{-1} \text{s}^{-2})$  and Poisson's ratio  $\nu=0.25$ . The mass density of the material is  $\rho=7 \times 10^{-6} (10^3 \text{Kg cm}^{-3})$ .

The slab is simply supported on the portion  $\Gamma_D$  of its boundary and is compressed along a frictional interface  $\Gamma_C$  by a flat 'rigid' surface, the vertical downward displacement of which is prescribed. This corresponds to prescribing an initial uniformly distributed gap  $g=-5 \times 10^{-4} \text{cm}$ . The prescribed tangential velocity of the 'rigid' surface is zero ( $\dot{U}_T^C=0$ ). The normal contact properties of the interface were taken from Table 1 of Back, Burdekin and Cowley [1973], assuming that the surfaces in contact are of cast iron hand-scraped with a surface finish (peak to valley distance) in the range  $6-8 \mu\text{m}$ . The coefficient  $m_n$  is then equal to 2 and, after a change of units,  $c_n=10^8 (10^3 \text{Kg cm}^{-3} \text{s}^{-2})$ . The friction coefficient along  $\Gamma_C$  was arbitrarily assumed to be  $\mu=0.3$  and independent of the normal load. Consequently,  $m_T=2$  and  $c_T=0.3 \times 10^8 (10^3 \text{Kg cm}^{-3} \text{s}^{-2})$ .

On one of its ends ( $\Gamma_F$ ), the slab is subjected to a time-dependent uniformly distributed force

$$t_x = \bar{t} \sin \bar{\omega} t,$$

where  $\bar{t}=30 (10^3 \text{Kg cm}^{-1} \text{s}^{-2})$  and  $\bar{\omega}=3 \times 10^4 \text{rad s}^{-1}$ .

The prescribed initial conditions are as follows: the initial velocities in all the slab are zero ( $\bar{U}_1=0$ ) and the initial displacements are the static equilibrium displacements of the slab due to the normal compression exerted by the flat surface on  $\Gamma_C$  alone (no friction on  $\Gamma_C$  and no applied tractions on  $\Gamma_F$ ).

We observe that, due to the normal deformation of the interface, the equilibrium normal displacements and normal pressure on  $\Gamma_c$  are not known a priori. The initial equilibrium displacements solution is obtained by solving the following system of nonlinear algebraic equations:

$$K \bar{u}_0 + P(\bar{u}_0) = 0$$

The numerical solution of this frictionless unilateral contact problem is obtained by using a standard Newton-Raphson algorithm analogous to that discussed in Section 5.4.

The finite element mesh used in this analysis consists of 16 nine-node isoparametric quadratic elements, as illustrated in Fig. 5.5.1. The regularization parameter  $\epsilon$  for the Coulomb friction law was taken, successively, to be equal to 1, 0.1 and 0.02 cm s<sup>-1</sup>. The dynamical equations of this discrete model were integrated using Newmark's method, as discussed earlier, with parameters  $\beta=0.25$ ,  $\gamma=0.5$  and a maximum time step of  $\Delta t_{\max}=10^{-6}$  s.

The distributions of normal stresses at several time instants obtained with  $\epsilon=0.1$  cm s<sup>-1</sup>, are shown in Fig. 5.5.2.

The distributions of friction stresses on  $\Gamma_c$  at several time instants are shown in Fig. 5.5.3. The travelling wave type evolution of these stresses can be clearly observed in that figure as can the sharp transition between the sliding and adhesion regions on  $\Gamma_c$ .

The effect of the regularization parameter  $\epsilon$  on the evolution of the displacements, velocities, and friction stresses at the

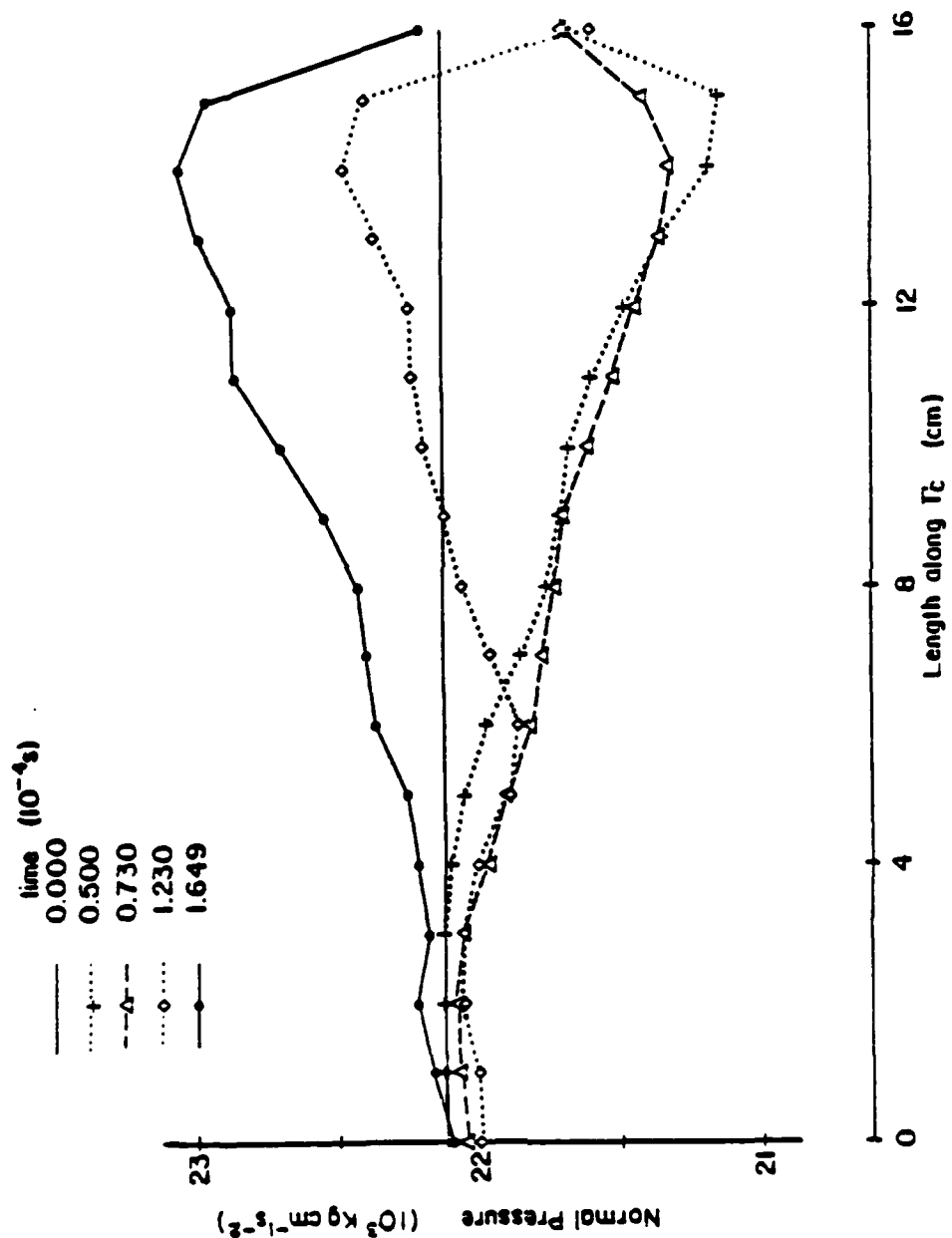


Figure 5.5.2. Distribution of normal stresses on  $l_c$  at several time instants due to periodic loading on  $l_f$ .



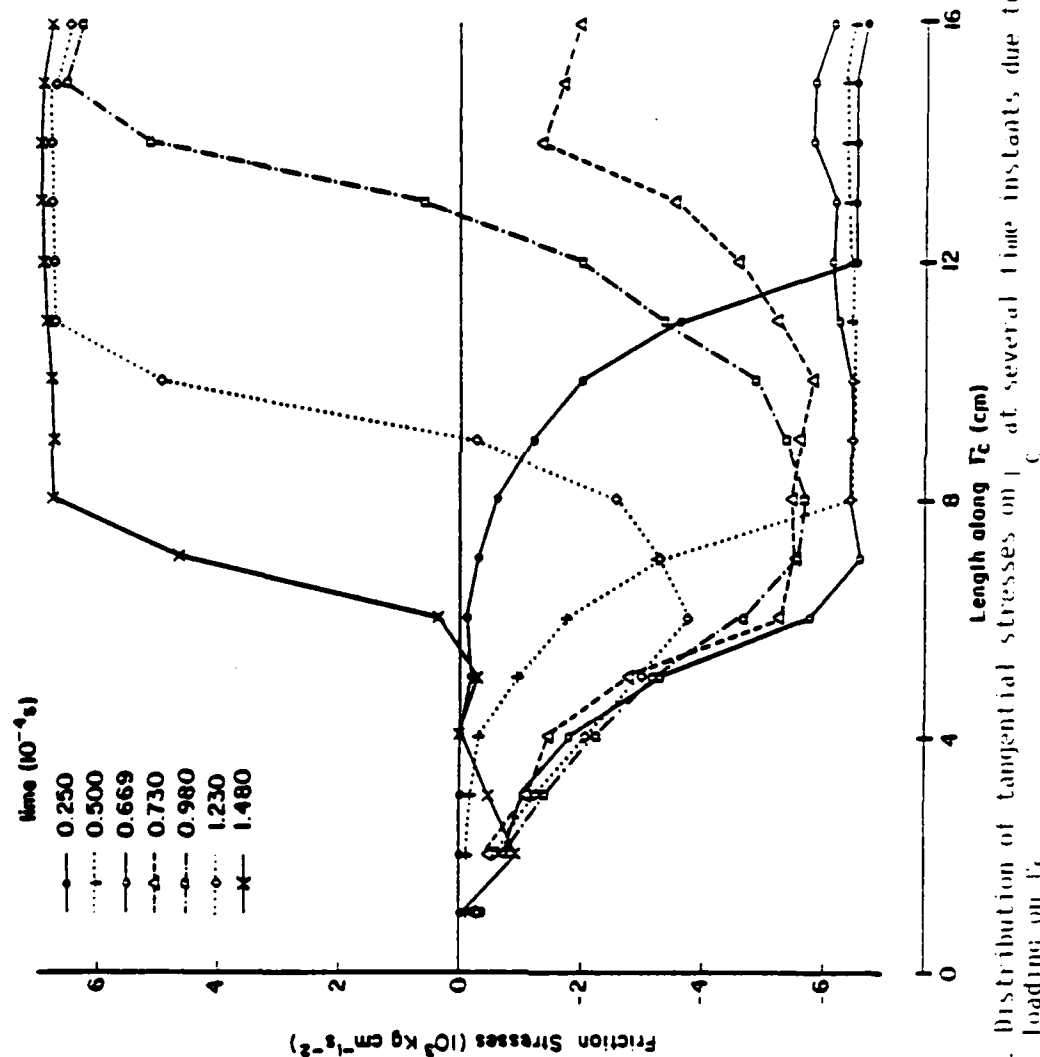


Figure 5.5.3. Distribution of tangential stresses on  $l_c$  at several time instants, due to periodic loading on  $l_q$ .

contact node 55 is shown in Figs. 5.5.4 to 5.5.6. As might be expected, smaller values of  $\epsilon$  lead to sharper transitions between sliding and adhesion states; large values of  $\epsilon$  smooth out those transitions. An examination of the computed variation in the tangential displacements and velocities leads us to the conclusion that the essential effect of the reduction of  $\epsilon$  is to produce more accurate adhesion states. High values of  $\epsilon$  (e.g.  $\epsilon=1$ ) lead to solutions which only vaguely resemble those obtained with smaller values of  $\epsilon$ , no meaningful conclusion relative to stick or slip being possible. From a practical point of view it appears reasonable to choose values of  $\epsilon$ , that are sufficiently small relative to the order of magnitude of the tangential velocities that occur during the sliding states. In this manner, sliding and adhesion will be essentially relative and not absolute concepts. We observe that for tangential velocities on the order of  $1 \text{ cm s}^{-1}$  the value of  $\epsilon=1 \text{ cm s}^{-1}$  is obviously inadequate while results obtained with  $\epsilon=0.1, 0.02 \text{ cm s}^{-1}$  seem to be physically reasonable.

All the computations performed in Section 4.2 with a rigid body can also be done with finite element models of linearly elastic or viscoelastic bodies. The essential effects observed there are also observed with the deformable bodies.

**Example 2** (*Steady-sliding of a compressed slab and its dynamic stability*). We consider here a slab similar to the one presented in Fig. 5.5.1. The material and normal contact properties and

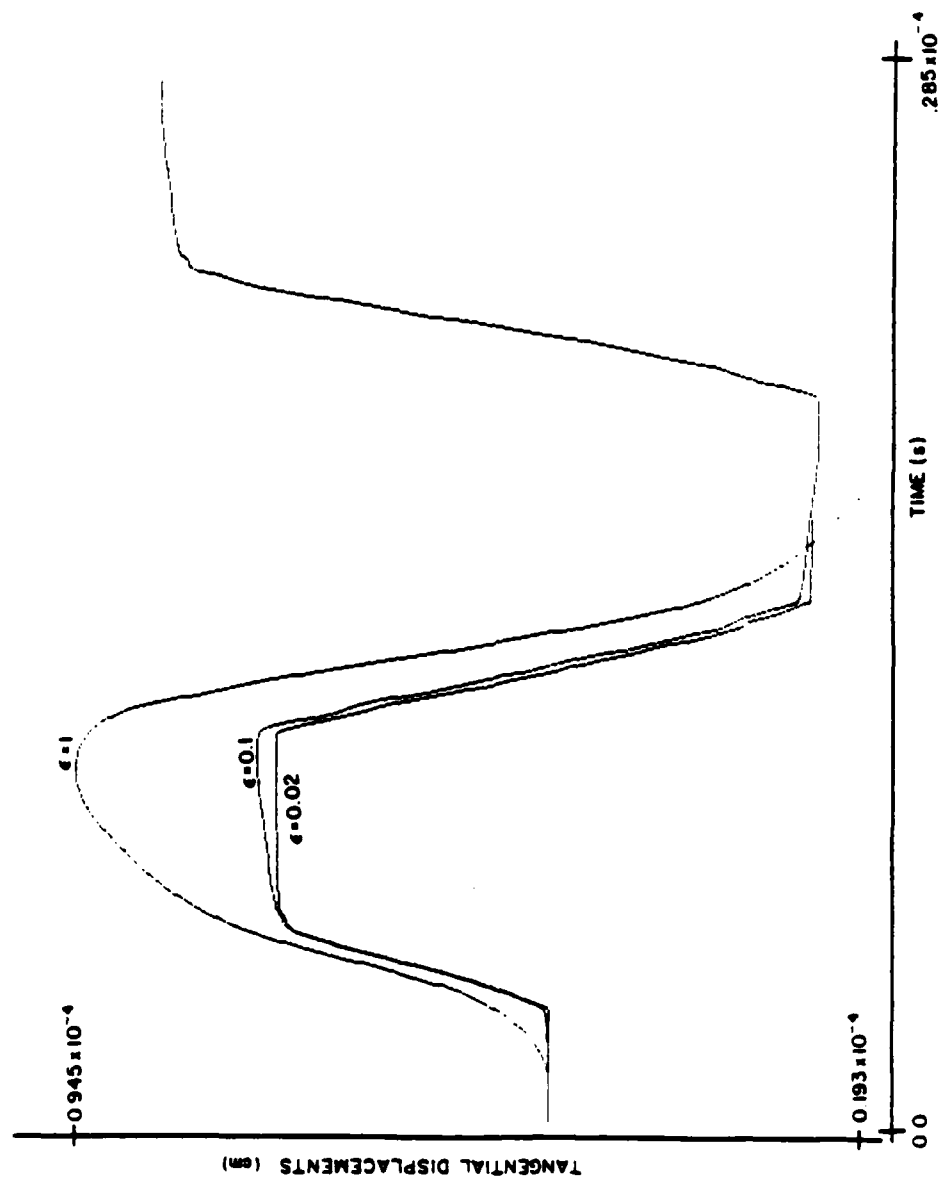


Figure 5.5.4. Tangential displacements at Node 55 using different values of  $\epsilon$ .

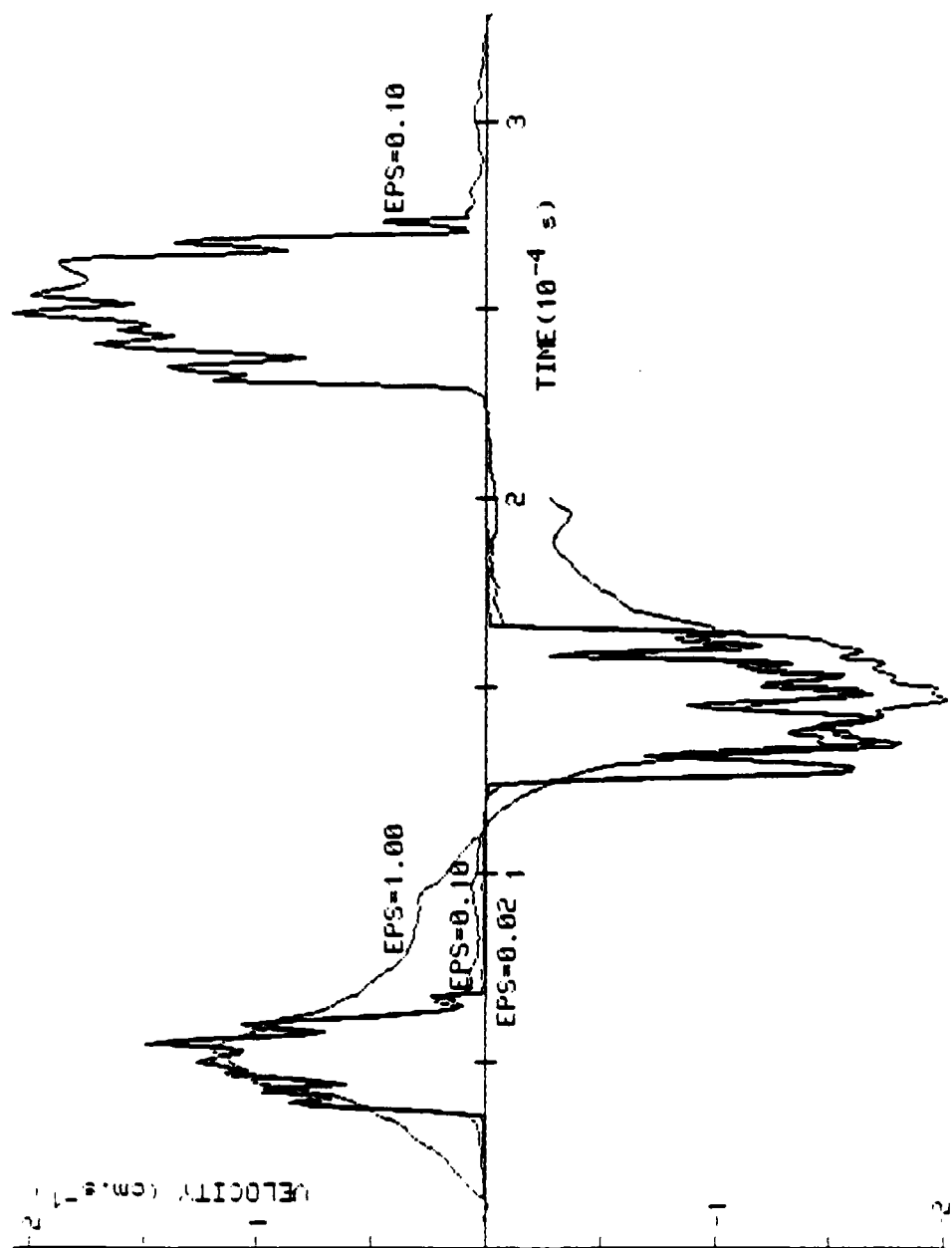


Figure 5.5.5. Tangential velocities at Node 55, using different values of  $\epsilon$ .

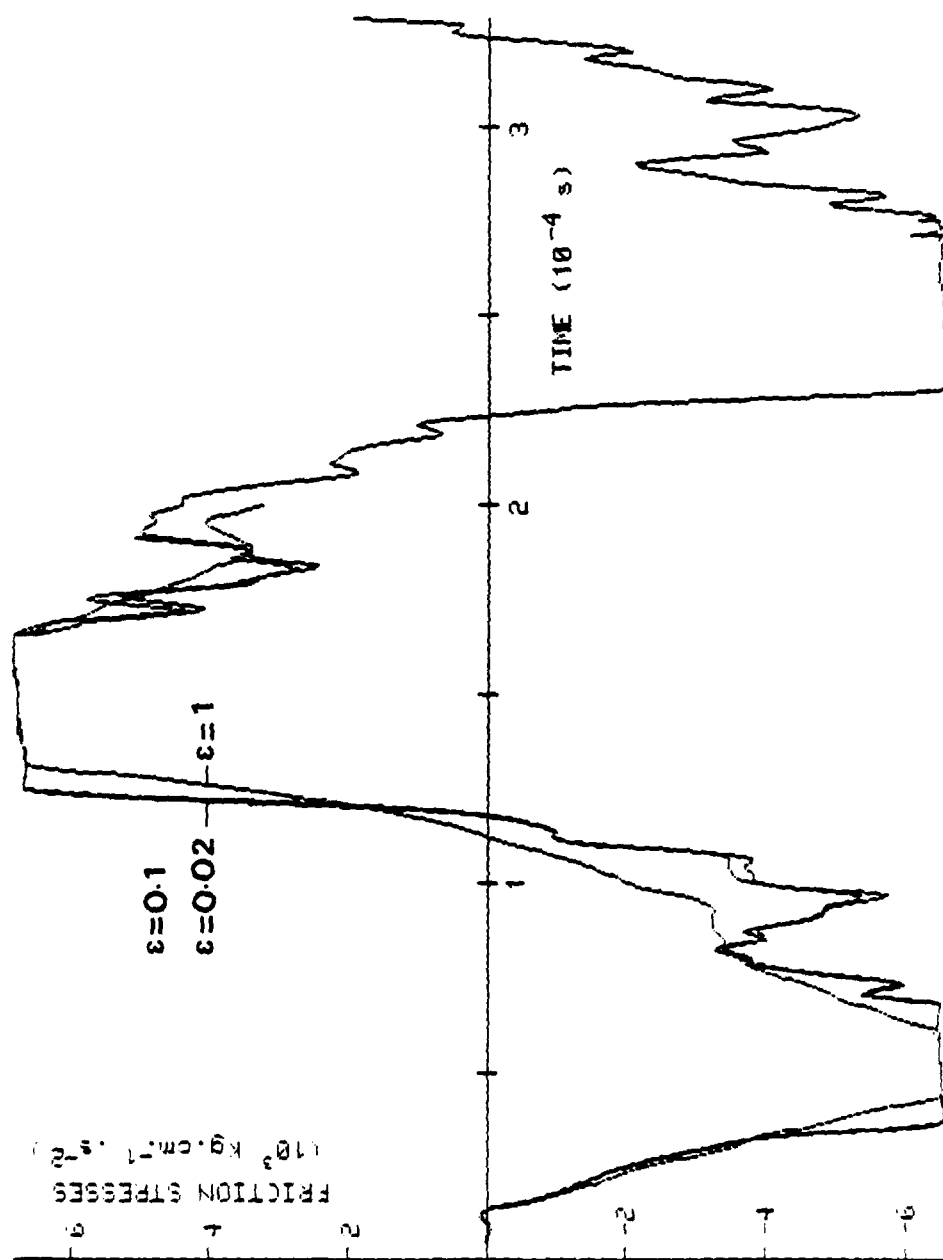


Figure 5.5.6. Friction stress at Node 55 using different values of  $\epsilon$ .

the boundary conditions on  $\Gamma_D$  are the same as those in Example 1. The dimensions are now 16 cm x 1 cm and the finite element mesh consists of  $9 \times 2$  nine-node isoparametric elements. The initial negative normal gap on  $\Gamma_C$  was taken successively to be  $5 \times 10^{-4}$  cm and  $1 \times 10^{-3}$  cm. The 'rigid' flat surface that compresses the body along  $\Gamma_C$  is assumed now to have a velocity towards the right. No forces act now either in  $\Omega$  or on  $\Gamma_F$ .

The steady-sliding equilibrium positions of this slab (the finite-element approximate solution to Problem 3) and the corresponding approximate eigenvalues (Problem 4) were computed for increasing values of  $c_T$  in the range  $[0,1]$  (NINCT=10), for zero viscous damping and zero normal interface damping.

Deformed mesh configurations and distributions of normal stresses on  $\Gamma_C$  are shown in Figs. 5.5.7 and 5.5.8 for  $g = 1 \times 10^{-3}$  cm. The corresponding friction stresses on  $\Gamma_C$  are, of course, equal to  $\mu$  times the normal pressure. For  $\mu \geq 0.3$ , if  $g = -5 \times 10^{-4}$  cm, and for  $\mu \geq 0.2$ , if  $g = -1 \times 10^{-3}$ , eigenvalues with significant positive real parts were obtained. In Fig. 5.5.9 a plot of all the eigenvalues in the first quadrant of the complex plane obtained for all the values of  $\mu$  considered is presented. It can be seen that larger compression produces increased instability.

The essential fact to be gained from this example results from the observation that the body considered has no rigid body freedoms. *All the instabilities arising in this case are associated with "deformation" modes, not rigid body modes.* We finally observe

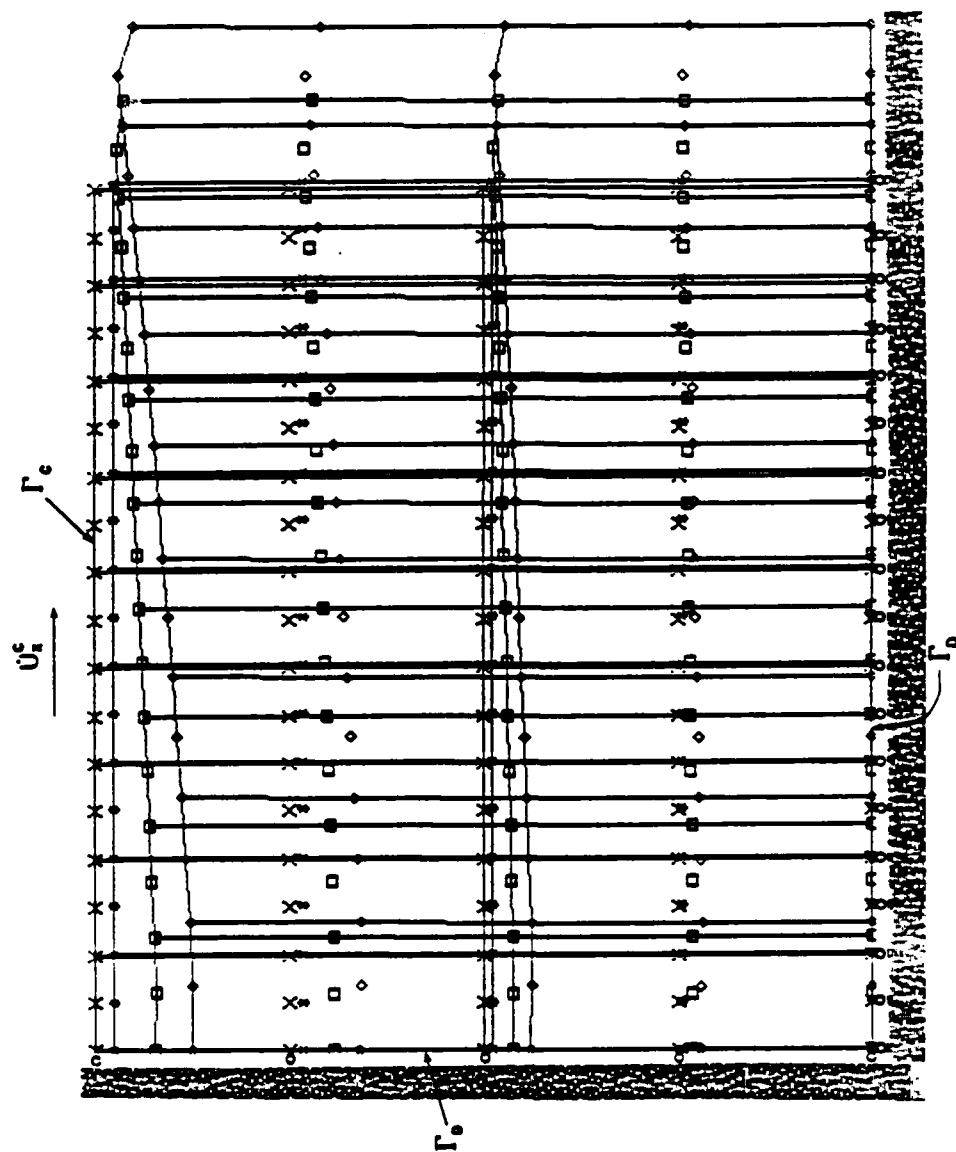


Figure 5.5.7. Undeformed ( $\times$ ), and deformed mesh configurations of a compressed slab in steady sliding equilibrium for  $u = 0(\times)$ ,  $u = 0.5$  ( $\square$ ), and  $u = 1.0$  ( $\diamond$ ).

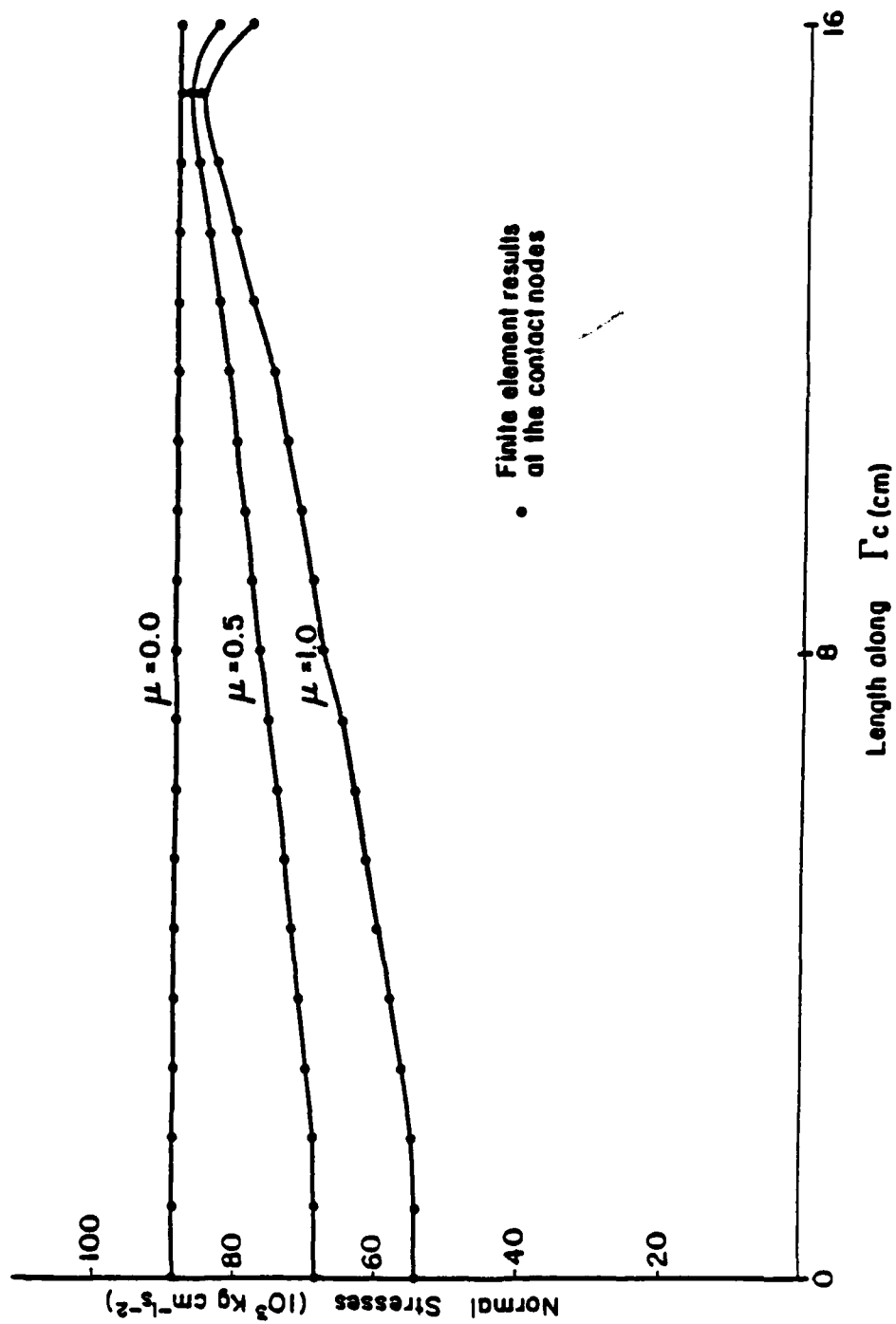


Figure 5.5.8. Distribution of normal stresses on  $\Gamma_c$  for the steady sliding equilibrium of a compressed slab at various values of  $\mu$ .



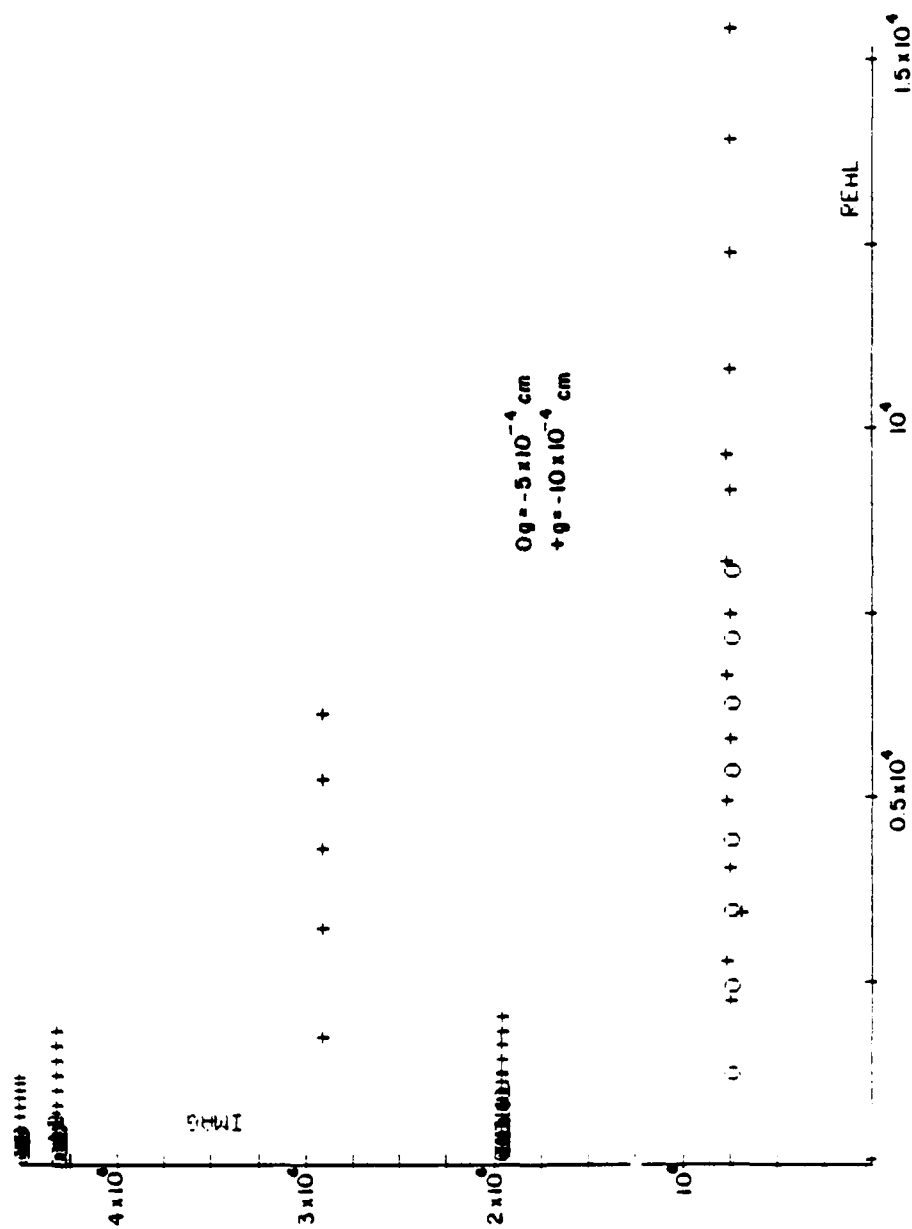


Figure 5.5.9. Effect of increasing the compression on the eigenvalues with positive real part of a compressed slab.

that in the present example no eigenvalue approaches the origin of the complex plane, for the range of  $c_T$  considered: the steady-sliding solution exists and is unique for all the range  $[0,1]$  of values of  $c_T$ .

**Example 3** (Steady-sliding and dynamic stability of a deformable block). We consider here a homogenous block sliding, with friction, on a moving foundation (see Fig. 4.1.1). We assume that the block has a linearly elastic behavior with a Young's modulus  $E = 1.4 \times 10^6 (10^3 \text{Kg cm}^{-1} \text{s}^{-2})$  and a Poisson's ratio  $\nu = 0.25$ . We assume that the body is in a state of plane strain. The geometry, total mass (M), total weight (W), total tangential stiffness ( $K_x$ ) and contact properties are given as follows:

$$\begin{aligned} L &= 48.8 \text{ cm} & M &= 450 \text{ Kg} \\ H &= 30.5 \text{ cm} & W &= 450 \cdot 10^3 \text{Kg cm s}^{-2} \\ B &= 30.5 \text{ cm} & K_x &= 2388 \cdot 10^3 \text{Kg s}^{-2} \\ c_n &= 10^{10} \cdot 10^3 \text{Kg cm}^{-3.5} \text{s}^{-2} & m_n = m_T &= 2.5, c_T = \mu c_n. \end{aligned} \quad (5.5.1)$$

As in Section 4.2 a necessary condition for equilibrium is  $\mu < L/H = 1.6$ .

The finite element model consists of a  $4 \times 3$  mesh of nine-node isoparametric elements as depicted in Fig. 5.5.10.

In this section we compute the steady sliding equilibrium positions of the block for several values of  $\mu$  in the admissible range  $[0, 1.6)$  and, for each of those configurations we solve the finite element version of the eigenvalue Problem 4, in the absence of any damping.

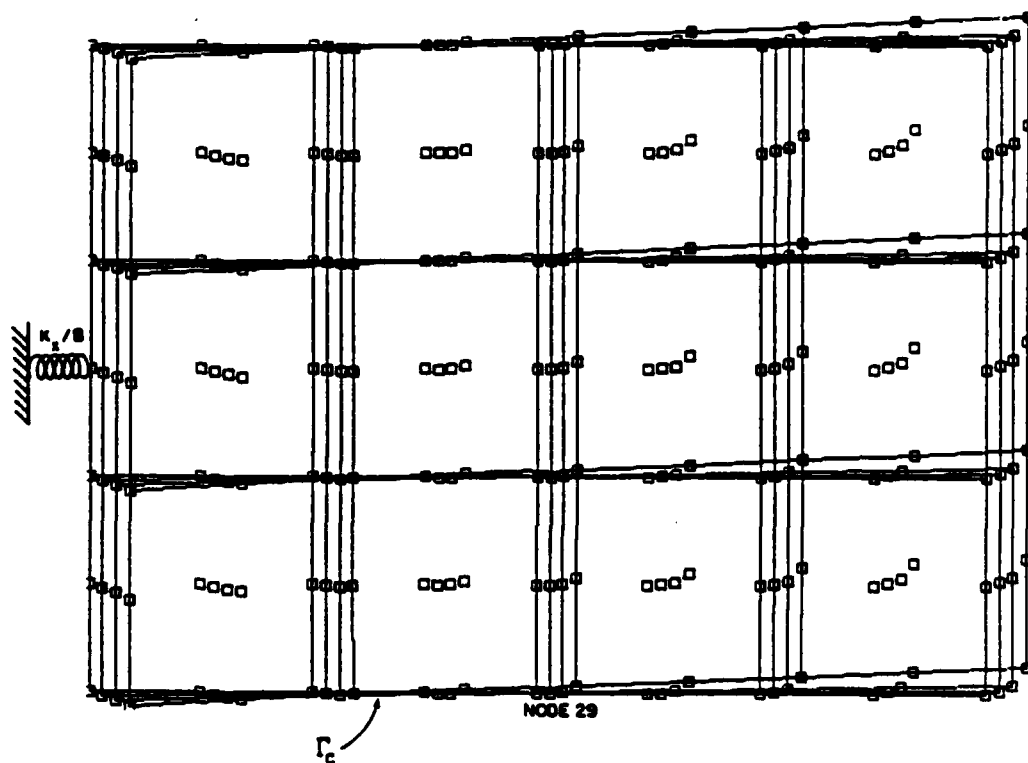


Figure 5.5.10. Deformed configurations of a linearly elastic block for the steady sliding equilibrium configurations at several values of  $u$ . (Note: Nodal coordinates and nodal displacements are not to scale - the apparent distortion of the body results from an amplification of the vertical displacements  $10^3$  larger than the one used for the horizontal displacements; this was needed in order to make visible the rotation of the body).

In Fig. 5.5.10, we show the deformed mesh configurations for the steady sliding equilibrium positions at several values of the coefficient of friction  $\mu$ . The expected increase of the rotation with the increase of  $\mu$  can be observed in that figure: for the level of forces in presence the block behaves much like a rigid body.

As in the rigid body case, all the eigenvalues are pure imaginary for small values of  $\mu$  (in the absence of damping). For values of  $\mu \geq 0.32$  (see Fig. 5.5.11) the occurrence of eigenvalues with positive real parts is again observed. All the eigenvalues in the first quadrant of the complex plane, together with the corresponding ranges of  $\mu$  for which they were observed, are plotted in Fig. 5.5.11. Similar computations were done with the same block but assuming it as a rigid body. In Fig. 5.5.12 we compare the rigid body model eigenvalues associated with the normal and rotation displacements with those from the finite element model which are associated with similar modes. The results are close: the deformability of the body does not affect much the evolution of the eigenvalues. Finally we observe that *the essential difference between the results obtained with the rigid body and the deformable body models is that, in the latter case, there are eigenvalues which correspond to unstable modes that are not "rigid body" modes.* The eigenvalues corresponding to those "deformation modes" have larger imaginary components and one of them does appear for values of  $\mu$  below the value at which the rigid body instability initiates.

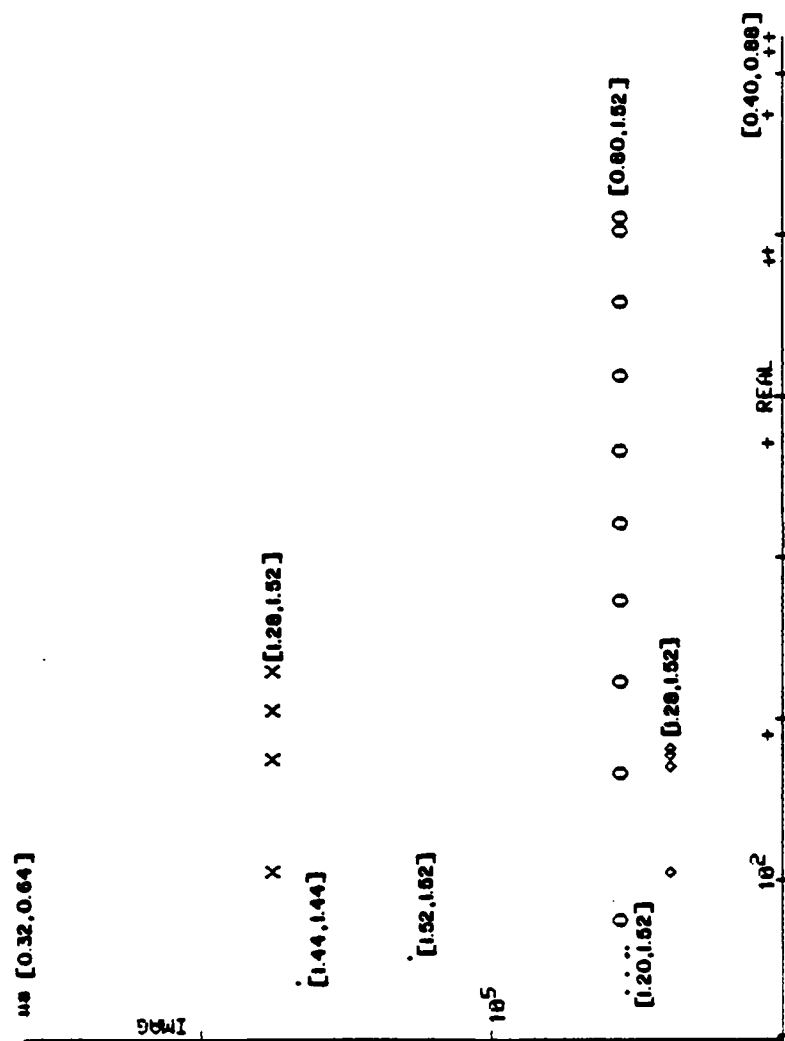


Figure 5.5.11. Eigenvalues with positive real parts for a finite element discretization of a block in steady sliding on a moving belt. The ranges of  $\mu$  for which these eigenvalues were obtained are indicated on the figure between brackets. NINCT = 20.  $\mu \in [0, 1.6]$ . Maximum value of  $\mu$  for which the equilibrium solution was successfully computed = 1.52. Eigenvalues corresponding to the "rigid body" normal and rotational modes [+].

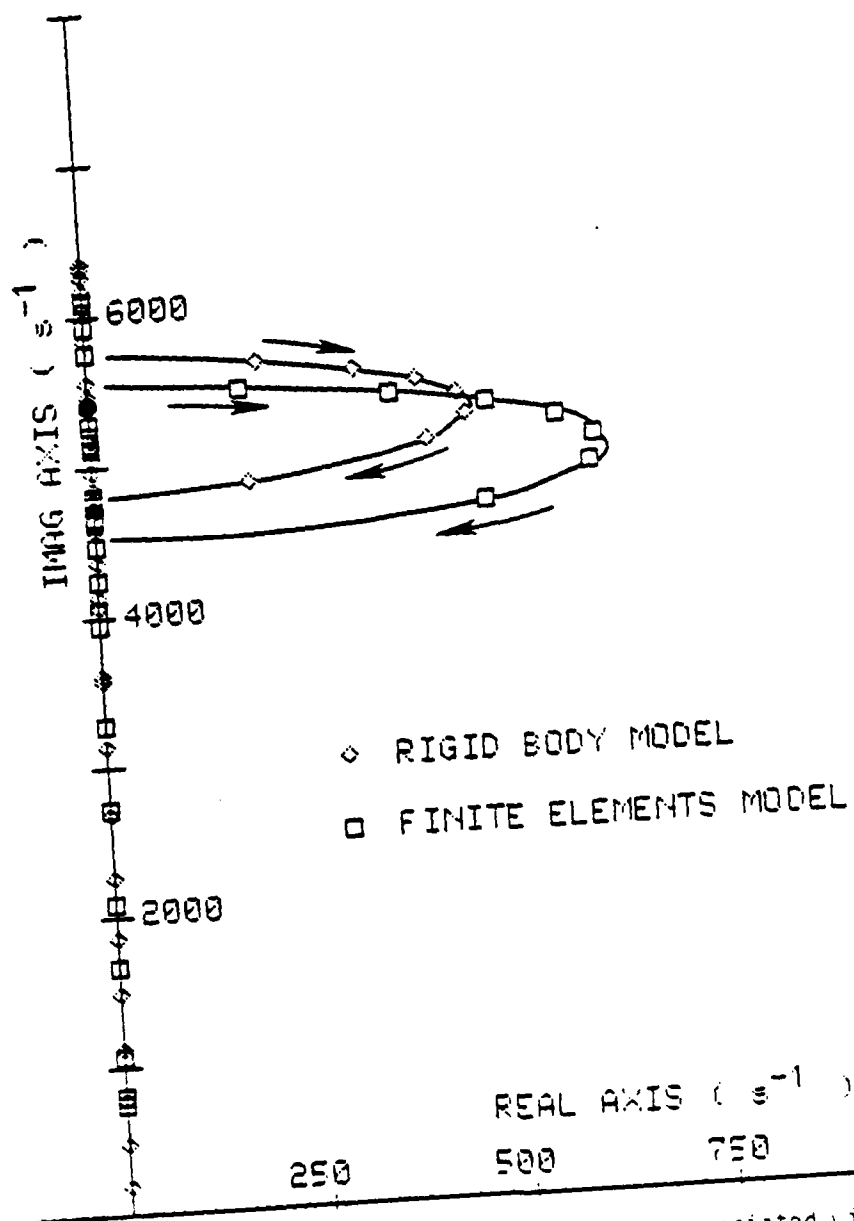


Figure 5.5.12. Comparison of the eigenvalues associated with 'normal and rotational modes' obtained with the rigid body and the finite element models (first quadrant of the complex plane).

Consequences of the dynamic instability of the steady-sliding on the motion of a deformable body are shown in the next example.

**Example 4** (*Friction-induced oscillations of a deformable block sliding on a moving foundation*). Our final numerical applications consist of obtaining the dynamic response of the linearly elastic block of the previous example with the following initial conditions: the initial displacements are those of the steady sliding equilibrium configuration appropriate for the value of  $\mu$  considered; the initial velocities represent a small (upwards) perturbation of that equilibrium, i.e.,  $\bar{u}_0 = u_0$ ,  $\bar{u}_{x1} = 0.0$ ,  $\bar{u}_{y1} = 0.01 \text{ cm s}^{-1}$  in all the block.

In this example, the geometry, normal contact properties and total mass are the same as in (5.5.1). We will now assume the total tangential stiffness  $K_x$  equal to 11100 ( $10^3 \text{ Kg s}^{-2}$ ), the coefficient of friction  $\mu$  equal to 0.60 and the velocity  $\dot{u}_x^C$  successively equal to 0.01, 0.08, 0.80  $\text{cm s}^{-1}$ . No damping effects will be considered when modelling the interior of the linearly elastic body, but normal dissipation on the contact boundary is considered with  $b_n = 0.381 \cdot 10^{10}$  ( $10^3 \text{ Kg cm}^{-4.5} \text{ s}^{-1}$ ) and  $l_n = 2.5$ .

The evolution of the elongation of the spring is shown in Fig. 5.5.13 for the three velocities  $\dot{u}_x^C$  considered. The resulting low-frequency stick-slip motion for the two smaller velocities can be observed in that figure. In Fig. 5.5.14 we show a phase

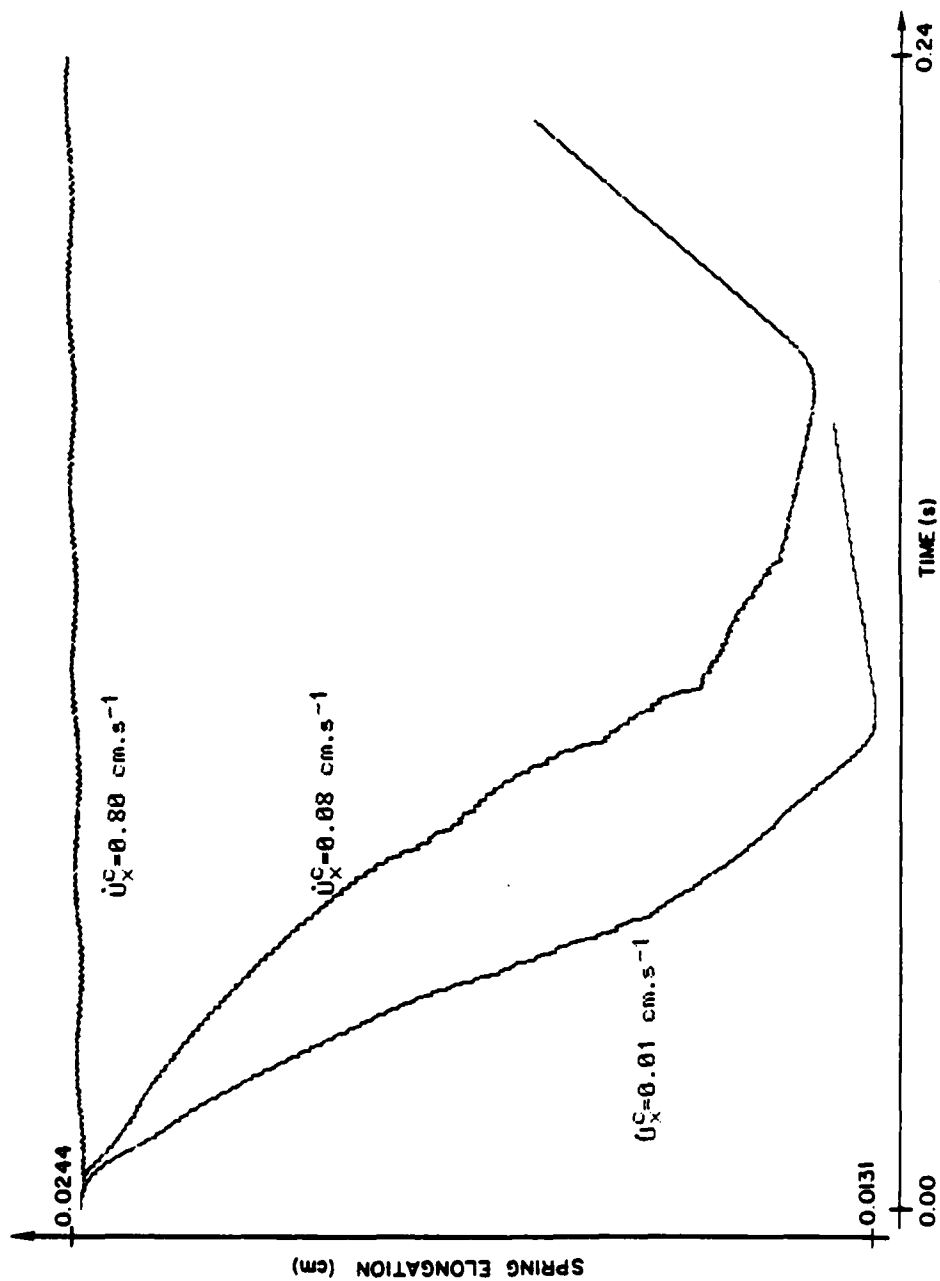


Figure 5.5.13. Evolution of the spring elongation for different velocities  $\dot{u}_x^C$ .



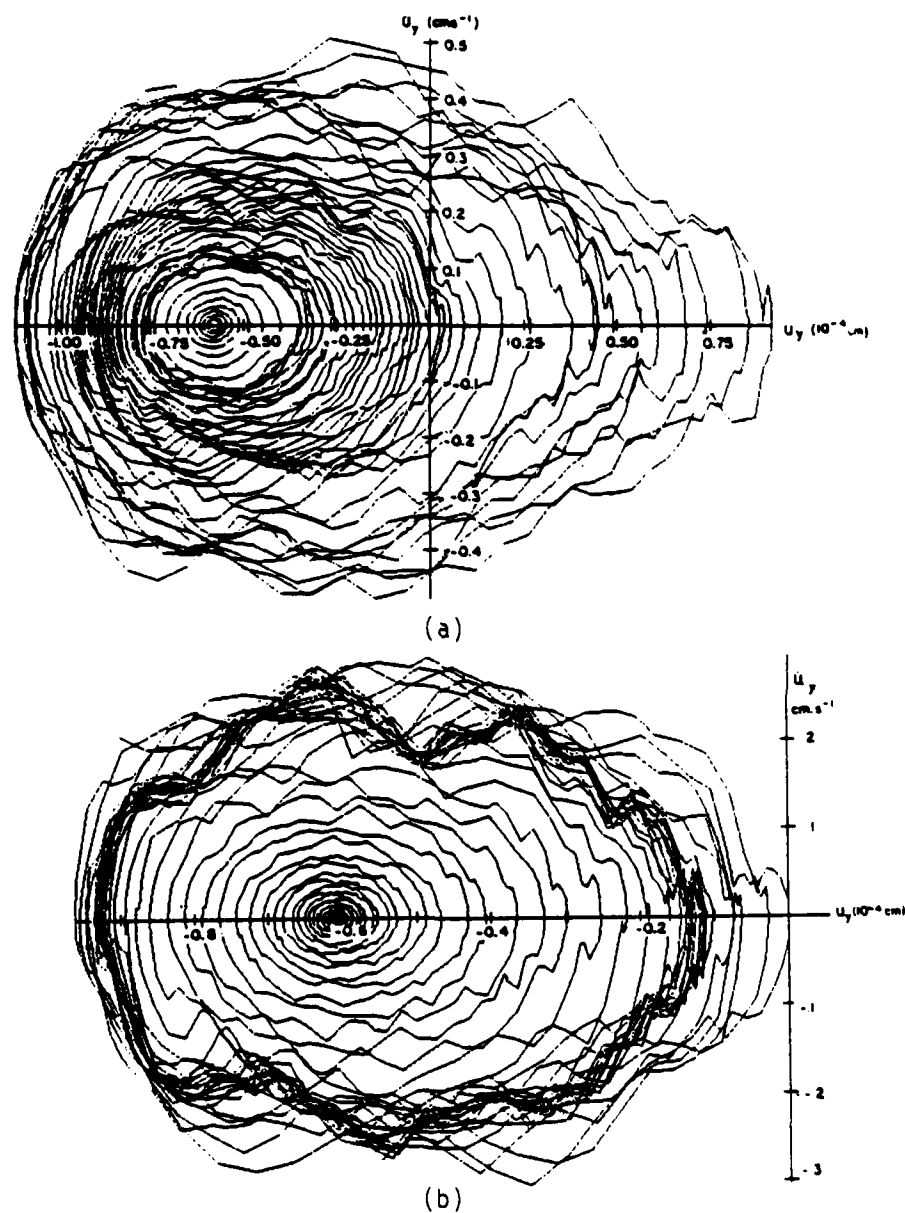


Figure 5.5.14. Phase plane plots of the normal oscillation of the contact node 29 during the "sliding" portion of the low-frequency stick-slip motion. (a) Initial part (growing oscillation). (b) Final part (decreasing oscillation). (Note: only 1 for each 5 computed points is plotted.)

plane plot of the normal oscillations of the node 29 and in Figs. 5.5.15 and 5.5.16 we show the evolution of the normal and friction stresses on the same node. In Figs. 5.5.17 and 5.5.18 we show what one of the numerous spikes in Figs. 5.5.15 and 5.5.16 looks like with a different time scale. The corresponding evolution of the ratio  $\sigma_T/|\sigma_n|$  during the same cycle of contact is shown in Fig. 5.5.19. In that figure, and also in Fig. 5.5.18, the occurrence at each cycle of contact of periods of adhesion and sliding is indicated. Also in Fig. 5.5.18, it can be seen that during sliding the ratio  $\sigma_T/|\sigma_n|$  is not exactly equal to the prescribed coefficient of friction 0.6; this is due to the small normal interface damping considered. As noted in Chapter 2, the Coulomb friction law is recovered exactly by our model when  $m_n=m_T$  and no normal interface damping is considered. However, if the normal interface damping is small, as we always assume, the opposite contributions of the dissipative term in (2.5.2) during the "impact" and "rebound" phases of a cycle of contact essentially compensate so that in average the Coulomb's law of friction is satisfied. The important reductions of average friction force are *not* the result of those effects but, as is made clear from Fig. 5.5.19, they are the result of the periods of stick during each cycle of contact, i.e., the high-frequency stick-slip mechanism proposed by Budanov, Kudinov and Tolstoi [1980] (recall Section 2.3).

It is also important to observe that, having used values for the normal contact properties  $(c_n, m_n)$  taken from Table 1

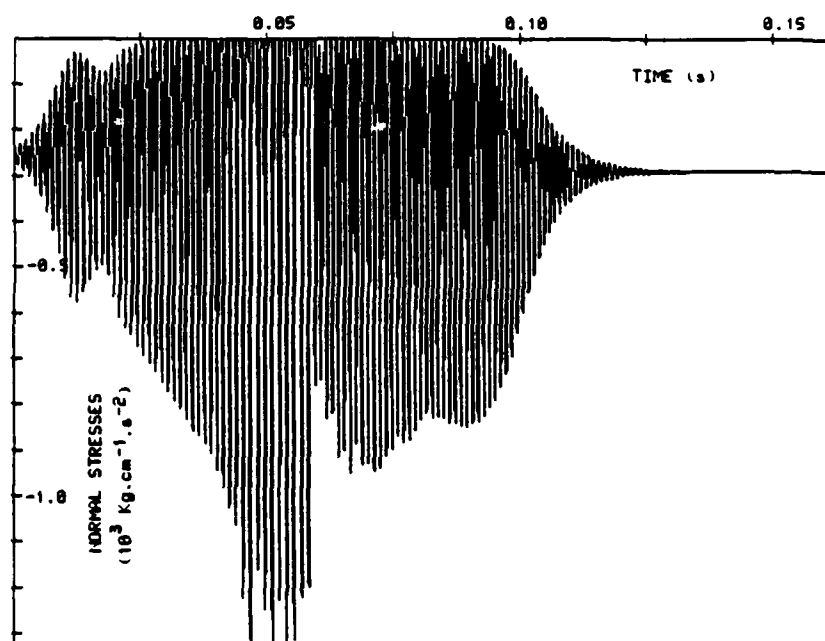


Figure 5.5.15. Evolution of the normal stresses on the contact Node 29 ( $U_x^C = 0.01 \text{ cm s}^{-1}$ ).

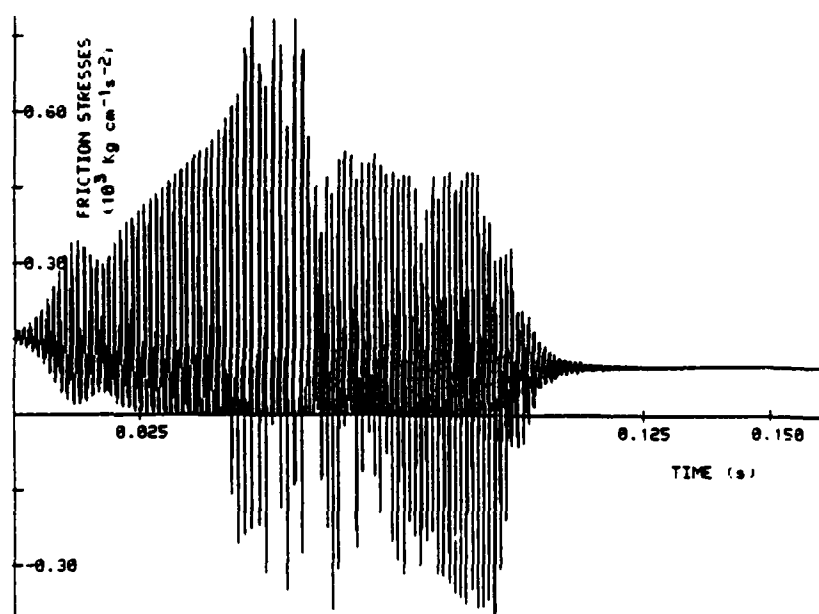


Figure 5.5.16. Evolution of the friction stresses on the contact Node 29 ( $U_x^C = 0.01 \text{ cm s}^{-1}$ ).

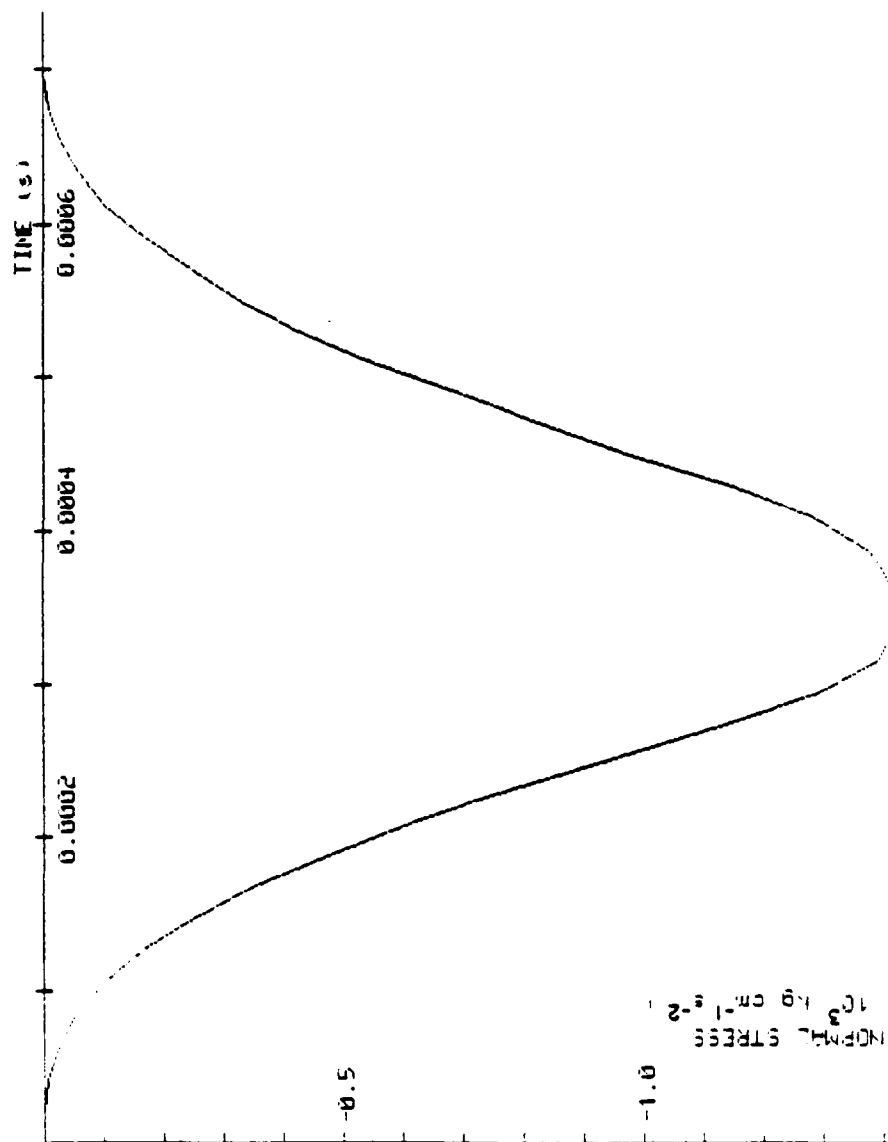


Figure 5.5.17. Evolution of the normal contact stress at Node 29 during the contact portion of a cycle of normal oscillation ( $U_C=0.08 \text{ cm s}^{-1}$ ). Time zero in this figure is time  $9.29985 \times 10^{-2} \text{ s}$  in Fig. 5.5.13.

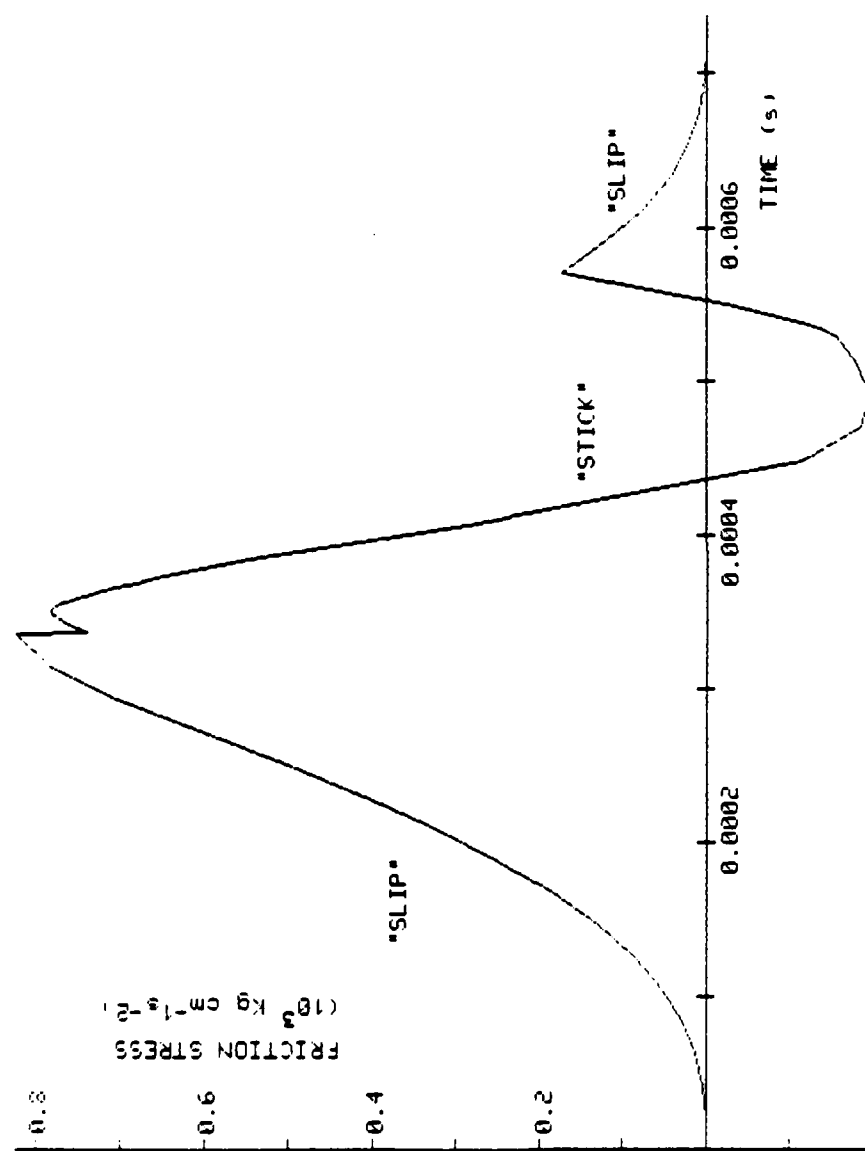


Figure 5.5.18. Evolution of the friction stress at Node 29 during the contact portion of a cycle of normal oscillation ( $\dot{U}_x^C = 0.08 \text{ cm s}^{-1}$ ).

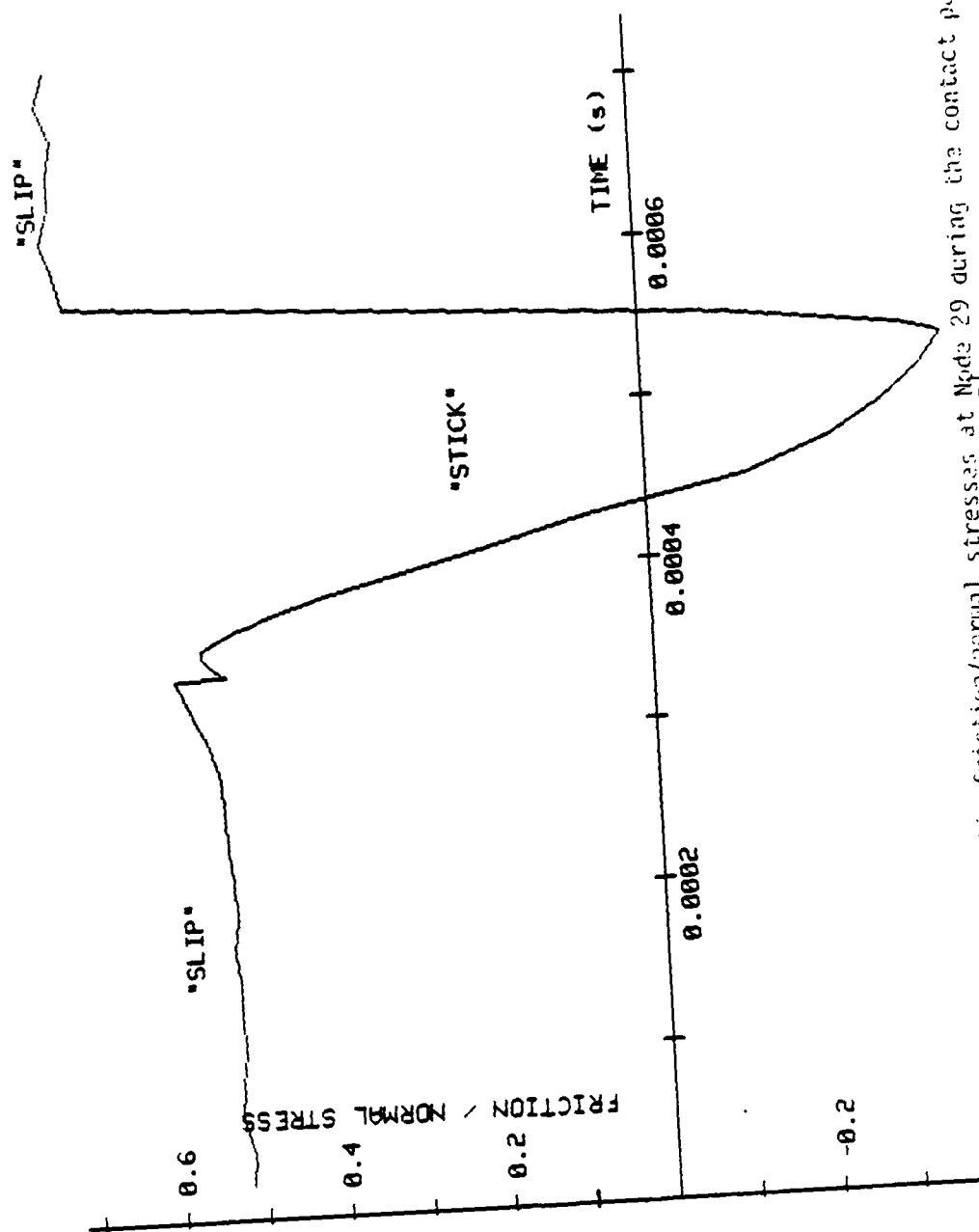


Figure 5.5.19. Evolution of the ratio friction/normal stresses at Node 29 during the contact perturbation of a cycle of normal oscillation ( $\dot{U}_x = 0.08$  cm/s).

of Back, Burdekin and Cowley [1973], and having considered a block with dimensions and weight close to those used by Bell and Burdekin [1969-70], it turns out that the frequency of the normal contact oscillations observed in Figs. 5.5.16-20 is of the order of magnitude indicated by Tolstoi [1967] as typical:  $10^3$  Hz (recall Remark 7 in Section 2.5).

For the case of the larger velocity ( $\dot{U}_x^C = 0.8 \text{ cm s}^{-1}$ ), that velocity is sufficiently large that the tangential oscillation of the body is not sufficient to produce any stick state. Consequently, the average coefficient of friction during sliding is equal to the static coefficient of friction. We note also that the instability of the equilibrium position makes it impossible for the contact damping to damp out the normal oscillation. A steady self-excited oscillation is then attained. That can be observed in Fig. 5.5.13 (horizontal oscillation of the node connected to the spring) and in Fig. 5.5.20 (normal oscillation of the contact node 29).

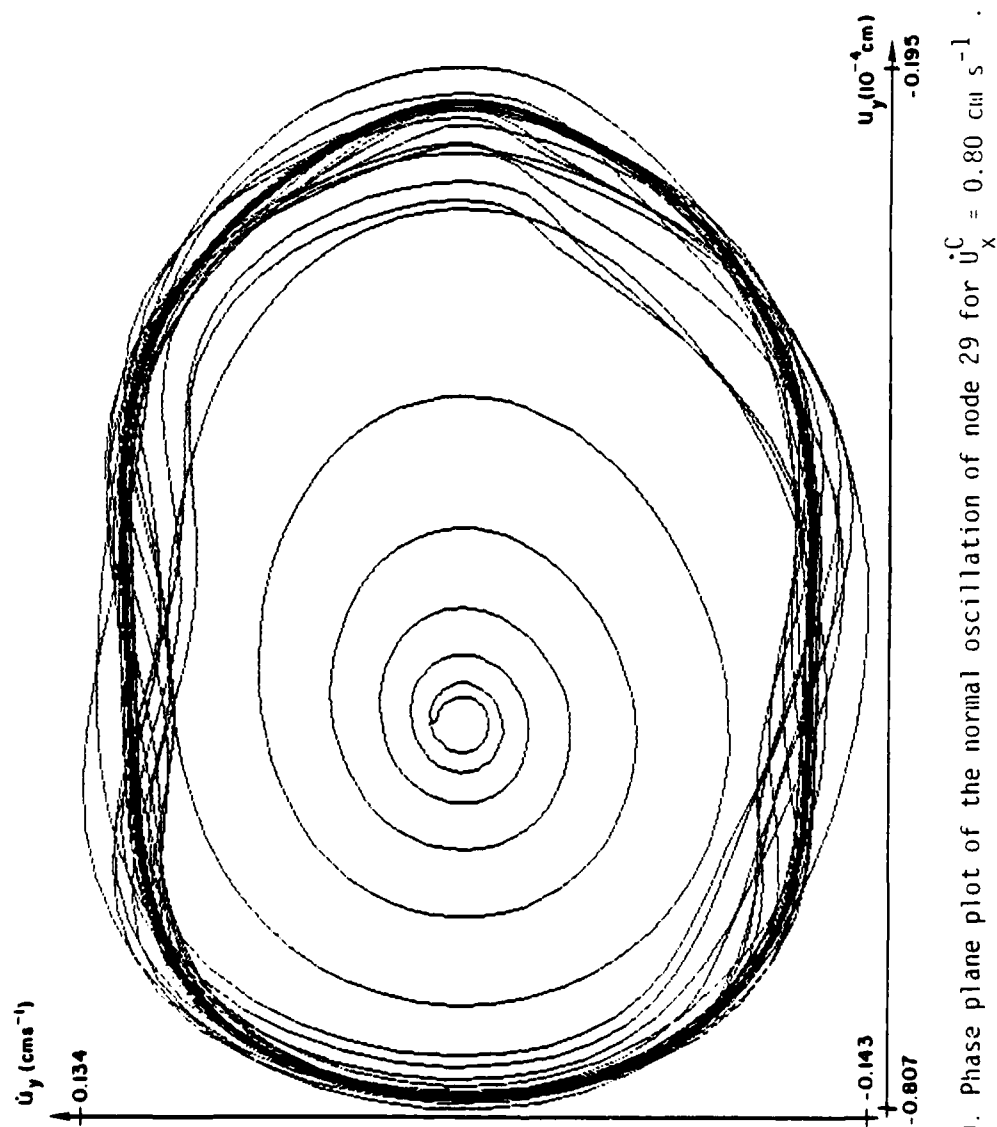


Figure 5.5.20. Phase plane plot of the normal oscillation of node 29 for  $\dot{u}_x^C = 0.80 \text{ cm s}^{-1}$ .



CHAPTER 6  
CONCLUSIONS AND  
SUGGESTIONS FOR FURTHER RESEARCH

In this study a simple model of interface response is developed for the study of dynamic frictional contact problems involving metallic bodies. This model is consistent with a large body of experimental evidence on the behavior of metallic interfaces and it incorporates a constitutive law for the normal deformability of the interface and Coulomb's law of friction.

Taking into account the normal deformability of the interface leads to mathematically tractable problems in continuum mechanics: variational formulations and existence and uniqueness results for steady-sliding and dynamic frictionless or frictional contact problems are established in the present work. Semi-discrete finite element approximations to dynamic contact problems are also shown to converge, in appropriately weak topologies, to the solutions of the corresponding continuum problems.

From the physical point of view, the incorporation of the normal deformability of the interface allows for the modeling of normal oscillations that are commonly observed in the course of sliding motions. It is a fundamental result of this work that, for sufficiently large friction, the nonsymmetry of the coupling between normal and tangential deformations of the interface may lead to unstable steady-sliding equilibria. Such instabilities

may occur either with rigid or with deformable bodies and they may occur even when the coefficient of static friction is equal to the coefficient of kinetic friction and the latter does not decrease with the sliding speed. It is also a fundamental result of this work that instability of steady-sliding equilibria and consequent high-frequency normal oscillations may lead to low frequency stick-slip motions or to apparently smooth sliding motions at apparent values of the coefficient of kinetic friction that are lower than the coefficient of static friction.

The numerical results presented in this dissertation confirm and give further insight to essential aspects of the experimentally-based ideas of Tolstoi [1967] and Budanov, Kudinov, and Tolstoi [1980] on the role played by normal oscillations in sliding friction phenomena. Particularly, the high-frequency stick-slip mechanism (mechanism (II) in Section 2.3) proposed by Budanov, Kudinov and Tolstoi [1980] emerges in the present work as the essential mechanism responsible for the occurrence of average friction forces (during apparently smooth sliding or during the slip phase of low frequency stick-slip motions) that are smaller than the static friction force. A new mechanical explanation for the occurrence of such high-frequency normal motions, which does not rely on the excitation by shocks between opposing asperities, emerges from the present work: those motions are the necessary consequence of the dynamic instability of the steady sliding equilibrium.

Numerical studies on the effect of the variation of several

governing parameters on the behavior of sliding bodies at small speeds lead to very promising *qualitative* comparisons between numerical results and experimental observations.

The results reported in this final report should be the starting point for many studies in dynamic frictional phenomena. Full understanding of these complex phenomena can only be achieved with a close interaction between mathematical analysis, numerical computations and experimental work.

The following mathematical studies are suggested:

(i) A detailed qualitative study of finite dimensional dynamical systems of the type (4.1.4,5) (the choice of model problem(s) involving some simplifications to the rigid body model considered here is recommended);

(ii) A study of the regularity of the solutions to the steady-sliding and dynamic contact problems formulated in Chapter 3, and a mathematically rigorous study of the stability of steady-sliding equilibria in the deformable body case;

(iii) The construction and study of simple examples of non-existence and/or non-uniqueness of solution to steady-sliding problems;

(iv) A study of the mathematical difficulties arising when the normal interface stiffness is made to increase to infinity (the analysis of known examples of non-existence and/or non-uniqueness of solution to finite dimensional dynamic contact problems may prove very useful in this context).

The numerical techniques used to solve dynamic contact

problems deserve the following additional studies:

(v) An analysis of the convergence of fully discrete approximations when the time step, the regularization parameter, and the mesh parameter (in the finite element case) converge simultaneously to zero;

(vi) A study on the application to friction problems of time integration techniques that allow for the automatic control of time-step.

Among the numerous numerical studies that are needed, those indicated in the following are expected to provide information that is complementary to the results presented in this report:

(vii) A study of the effect of the parameters that govern the rigid body problem on apparent reductions of static friction;

(viii) A study of apparent reductions of static friction employing finite element models of deformable bodies;

(ix) A study of the stability of steady-sliding equilibrium and the occurrence of friction-induced oscillations with other geometries, particularly "pin-on-flat" experimental apparatus.

Full assessment of the models proposed in this dissertation requires *quantitative* comparisons between theoretical results and experimental observations. The apparatus to be selected for the required experimental work should satisfy the following conditions:

(a) closeness to other apparatus used earlier in the literature (the possibility of *reproducing* earlier experimental results is essential);

(b) possibility of incorporating devices to measure and, when desired, to restrict the normal (and rotational) motions;

(c) simplicity of the theoretical modeling of the dynamic behavior of the apparatus.

In view of the numerical results obtained here the experimental work suggested should, of course, be directed toward the study of the role played by normal (and rotational) degrees-of-freedom on:

(x) the "rate dependence" of the coefficient of static friction;

(xi) the occurrence of stick-slip and other friction-induced oscillations;

(xii) the dependence of the kinetic friction on the sliding speed.

## REFERENCES

- Amerio, L., and Prouse, G., [1975], "Study of the Motion of a String Vibrating Against an Obstacle," Rend. Mat., (2)8, Ser. VI, pp. 563-585.
- Amerio, L., [1976], "Su un Problema di Vincoli Unilaterali per l'Equazione non Omogenea della Corda Vibrante, IAC (Inst. per le Applicazioni del Calcolo "Mauro Picone") Publicazioni, Ser. D 109, pp. 3-11.
- Amerio, L., [1977], "On the Motion of a String Vibrating Through a Moving Ring with a Continuously Varying Diameter," Atti Accad. Naz. Lincei Rend., Sc. Fis. Mat. e Nat., 62, pp. 134-142.
- Andrew, C., Cockburn, J. A. and Waring, A.E. [1967-68], "Metal Surfaces in Contact Under Normal Forces: Some Dynamic Stiffness and Damping Characteristics," Proc. Instn. Mech. Engrs., 182(3K), pp. 92-100.
- Antoniou, S. S., Cameron, A. and Gentle, C. R. [1976], "Friction-Speed Relation from Stick-Slip Data," Wear, 36, pp. 235-254.
- Archard, J. F. [1957], "Elastic Deformation and the Laws of Friction," Proc. Roy. Soc. Lond., A243, pp. 190-205.
- Archard, J. F. [1974], "Surface Topography and Tribology," Tribology International, 7, pp. 213-220.
- Aronov, V., D'Souza, A. F., Kalpakjian, S. and Shareef, I. [1983], "Experimental Investigation on the Effect of System Rigidity on Wear and Friction-Induced Vibrations," J. Lubr. Technol., 105, pp. 206-211.
- Aronov, V., D'Souza, A. F., Kalpakjian, S. and Shareef, I. [1984], "Interactions Among Friction, Wear and System Stiffness - Part 1: Effect of Normal Load and System Stiffness; Part 2: Vibrations Induced by Dry Friction; Part 3: Wear Model," J. Lubr. Technol., 106, pp. 54-69.
- Back, N., Burdekin, M. and Cowley, A. [1973], "Review of the Research on Fixed and Sliding Joints," Proc. 13th International Machine Tool Design and Research Conference, pp. 87-97, ed. by S. A. Tobias and F. Koenigsberger, MacMillan, London.
- Back, N., Burdekin, M. and Cowley, A. [1974], "Analysis of Machine Tool

- Joints by the Finite Element Method, "Proc. 14th International Machine Tool Design and Research Conference, pp. 529-537, ed. by S. A. Tobias and F. Koenigsberger, MacMillan, London.
- Bamberger, A., and Schatzman, M. [1983], "New Results on the Vibrating String with a Continuous Obstacle," SIAM J. Math. Anal., 14, pp. 560-595.
- Banerjee, A. K. [1968], "Influence of Kinetic Friction on the Critical Velocity of Stick-Slip Motion," Wear, 12, pp. 107-116.
- Barwell, F. T. [1959], "Friction and Its Measurement," Metallurgical Reviews, 4(14), pp. 141-177.
- Bay, N. and Wanheim, T. [1976], "Real Area of Contact and Friction Stresses at High Pressure Sliding Contact," Wear, 38, pp. 201-209.
- Bell, R. and Burdekin, M. [1969-70], "A Study of the Stick-Slip Motion of Machine Tool Feed Drives," Proc. Inst. Mech. Engrs., 184(1), pp. 543-557.
- Bell, R. and Burdekin, M. [1969-70a], "An Investigation into the Steady-State Characteristics of Plain Slideways," Proc. Instn. Mech. Engrs., 184-Pt 1(59), pp. 1075-1087.
- Bhushan, B. [1980], "Effect of Strain Rate and Interface Temperature on the Static and Kinetic Frictions," Seventh Leeds-Lyon Symposium, Leeds, England.
- Bikerman, J. J. [1976], "Adhesion in Friction," Wear, 39, pp. 1-13.
- Blok, H. [1940], "Fundamental Mechanical Aspects of Boundary Lubrication," S.A.E. J., 46(2), pp. 54-68.
- Bo, L. C. and Pavelescu, D. [1982], "The Friction-Speed Relation and its Influence on the Critical Velocity of Stick-Slip Motion," Wear, 82, pp. 277-289.
- Bochet, M. [1861], "Nouvelles Recherches Expérimentales sur le Frottement de Glissement," Ann. Mines, xix, pp. 27-120.
- Bowden, F. P. and Leben, L. [1939], "The Nature of Sliding and the Analysis of Friction," Proc. Roy. Soc. London, A169, pp. 371-391.
- Bowden, F. P. and Tabor, D. [1939], "The Area of Contact Between Stationary and Between Moving Surfaces," Proc. Roy. Soc. London, A169, pp. 391-413.
- Bowden, F. P. and Tabor, D. [1950], The Friction and Lubrication of

Solids, Clarendon Press, Oxford, England.

- Bowden, F. P. and Tabor, D. [1964], The Friction and Lubrication of Solids, Part II, Clarendon Press, Oxford, England.
- Brockley, C. A., Cameron, R. and Potter, A. F. [1967], "Friction-induced Vibration," J. Lubr. Technol., 89, pp. 101-108.
- Brockley, C. A. and Davis, H. R. [1968], "The Time Dependence of Static Friction," J. Lubr. Technol., 90, pp. 35-41.
- Brockley, C. A. and Ko, P. L. [1970], "Quasi-Harmonic Friction-induced Vibration," J. Lubr. Technol., Trans. ASME, Oct., pp. 550-556.
- Budanov, B. V., Kudinov, V. A. and Tolstoi, D. M. [1980], "Interaction of Friction and Vibration," Trenie i Iznos, 1(1), pp. 79-89.
- Burwell, J. T. and Rabinowicz, E. [1953], "The Nature of the Coefficient of Friction," J. Appl. Phys., 24(2), pp. 136-139.
- Burridge, R., Kappraff, J. and Morrshedi, C. [1982], "The Sitar String, a Vibrating String with a One-sided Inelastic Constraint," SIAM J. Appl. Math., 42, pp. 1231-1251.
- Buttazzo, G. and Percivale, D. [1981], "Sull' Approssimazione del Problema del Rimbalzo Unidimensionale," Ricerche Mat., 30, pp. 217-231.
- Buttazzo, G., and Percivale, D. [1983], "On the Approximation of the Elastic Bounce Problem on Riemannian Manifolds," J. Diff. Equations, 47, pp. 227-245.
- Carriero, M. and Pascali, E. [1980], "Il Problema del Rimbalzo Unidimensionale e sue Approssimazioni con Penalizzazioni non Convesse," Rend. Mat., (6) 13, 4, pp. 541-553.
- Carriero, M. and Pascali, E. [1982], "Uniqueness of the One-Dimensional Bounce Problem as a Generic Property in  $L^1([0,T];R)$ ," Bolletino U. M.I., (6) 1-A, pp. 87-91.
- Ciarlet, P. G. [1978], The Finite Element Method for Elliptic Problems, North-Holland, Amsterdam.
- Citrini, C. [1975], "Sull'Urto Parzialmente Elastico o Anelastico di una Corda Vibrante Contro un Ostacolo I," Atti Accad. Naz. Lincei, Rend. Sc. Fis. Mat. e Nat., 59, pp. 368-376.
- Citrini, C. [1975], "Sull'Urto Parzialmente Elastico o Anelastico di una Corda Vibrante Contro un Ostacolo II," Atti Accad. Naz. Lincei, Rend. Sc. Fis. Mat. e Nat., 59, pp. 667-676.



- Citrini, C. [1977], "The Energy Theorem in the Impact of a String Vibrating Against a Point Shaped Obstacle," Atti Accad. Naz. Lincei, Rend. Sc. Fis. Mat. e Nat., 62, pp. 143-149.
- Conti, P. [1875], "Sulla Resistenza di Attrito," Atti R. Accad. Lincei, 11, p. 16.
- Coulomb, C. A. [1785], "Théorie des Machines Simples," Mémoire de Mathématique et de Physique de l'Académie Royale, pp. 161-342.
- Coulomb, J. [1956], "L'Agitation Microsismique," Encyclopedia of Physics, XLVII, Ed. S. Flügge, Geophysics I, Group Ed. J. Bartels, Springer-Verlag, Berlin, Göttingen, Heidelberg.
- Courtney-Pratt, J. S. and Eisner, E. [1957], "The Effect of a Tangential Force on the Contact of Metallic Bodies," Proc. Roy. Soc. Lond., A238, pp. 529-550.
- Degiovani, M. [1984], "Multiplicity of Solutions for the Bounce Problem," J. Diff. Equations, 54, pp. 414-428.
- Demkowicz, L., and Oden, J. T. [1982], "On Some Existence Results in Contact Problems with Nonlocal Friction," Nonlinear Analysis, Theory, Methods and Applications, 6(10), pp. 1075-1093.
- Derjaguin, B. V., Push, V. E. and Tolstoi, D. M. [1957], "A Theory of Stick-Slip Sliding of Solids," Proc. Conf. on Lubrication and Wear, Inst. Mech. Eng., London, pp. 257-268.
- Dokos, S. J. [1946], "Sliding Friction Under Extreme Pressures - 1," J. Appl. Mechanics, 68, pp. A148-156.
- Dowson, D. [1978], History of Tribology, Longman, London.
- Duvaut, G. [1982], "Loi de Frottement Non Locale," J. de Mécanique Théorique et Appliquée, Numéro spécial.
- Duvaut, G. and Lions, J. L. [1976], Inequalities in Mechanics and Physics, Springer-Verlag, Berlin, Heidelberg, New York.
- Earles, S. W. E. and Badi, M. N. M. [1984], "Oscillatory Instabilities Generated in a Double-pin and Disc Undamped System: a Mechanism of Disc-Brake Squeal," Proc. Instn. Mech. Engrs., 198C(4), pp. 43-50.
- Earles, S. W. E. and Lee, C. K. [1976], "Instabilities Arising from the Frictional Interaction of a Pin-Disk System Resulting in Noise Generation," J. of Engineering for Industry, Transactions of the ASME, Feb., pp. 81-86.

- Elder, J. A., Jr. and Eiss, N. S., Jr. [1969], "A Study of the Effect of Normal Stiffness on Kinetic Friction Forces Between Two Bodies in Sliding Contact," ASLE Transactions, 12, pp. 234-241.
- Euler, L. [1750], Histoire de l'Académie Royale à Berlin, iv(1748), pp. 313.
- Felder, E. [1985], "Formulation Thermodynamique des Interactions Superficielles Entre Deux Corps," Journal de Mécanique Théorique et Appliquée, 4(2), pp. 283-303.
- Galton, D. [1878], Engineering, 23, pp. 153, 154; 25, pp. 469-472.
- Geradin, M., Hogge, M. and Idelsohn, S. [1983], "Implicit Finite Element Methods" in Computational Methods for Transient Analysis, Vol. 1, Chap. 9, Ed. T. Belytschko and T. J. R. Hughes, North-Holland, Amsterdam, New York, Oxford.
- Godfrey, D. [1967], "Vibration Reduces Metal to Metal Contact and Causes an Apparent Reduction in Friction," ASLE Transactions, 10, pp. 183-192.
- Greenwood, J. A. [1984], "A Unified Theory of Surface Roughness," Proc. R. Soc. Lond., A393, pp. 133-157.
- Greenwood, J. A., Johnson, K. L. and Matsubara, E. [1984], "A Surface Roughness Parameter in Hertz Contact," Wear, 100, pp. 47-57.
- Greenwood, J. A., and Williamson, J. B. P. [1966], "Contact of Nominally Flat Surfaces," Proc. Roy. Soc. Lond., A295, pp. 300-319.
- Gu, J.-C., Rice, J. R., Ruina, A. L. and Tse, S. T. [1983], "Slip Motion and Stability of a Single Degree of Freedom Elastic System with Rate and State Dependent Friction," submitted to J. Mech. Phys. Solids.
- Guckenheimer, J. and Holmes, P. [1983], Nonlinear Oscillations, Dynamical Systems, and Bifurcation Theory, Springer, Berlin.
- Halling, J. and Nuri, K. A. [1974], Proc. Symp. IUTAM, pp. 330-341, ed. by A. D. de Pater and J. J. Kaiker, Delft Univ. Press, Delft.
- Heilmann, P. and Rigney, D. A. [1981], "An Energy-Based Model of Friction and its Application to Coated Systems," Wear, 72, pp. 195-217.
- Heyman, F., Rabinowicz, E., and Rightmire, B. G. [1955], Rev. Sci. Instrum., 26, p. 56.

- Hirn, G. [1854], "Sur les Principaux Phénomènes qui Présentent les Frottements Médiats," Bull. Soc. Ind. Mulhouse, 26, pp. 188-277.
- Holmes, P. J. [1977], "Bifurcations to Divergence and Flutter in Flow-induced Oscillations: A Finite Dimensional Analysis," J. Sound Vibration, 53(4), pp. 471-503.
- Holmes, P. and Marsden, J. [1978], "Bifurcation to Divergence and Flutter in Flow-induced Oscillations: An Infinite Dimensional Analysis," Automatica, 14, pp. 367-384.
- Hünlich, R., and Nauman, J. [1978], "On General Boundary Value Problems and Duality in Linear Elasticity, I.," Applicace Matematiky, 23(3), pp. 208-229.
- Hunt, J. B., Torbe, I. and Spencer, G. C. [1965], "The Phase-Plane Analysis of Sliding Motion," Wear, 8, pp. 455-465.
- Hunt, K. H. and Crossley, F. R. E., [1975], "Coefficient of Restitution Interpreted as Damping in Vibroimpact," Journal of Applied Mechanics, June, pp. 440-445.
- Huseyn, K. [1978], Vibrations and Stability of Multiple Parameter Systems, Noordhoff International Publishing, Alphen Aan Den Rijn, The Netherlands.
- Ishlinski, A. Y. and Kraghelsky, I. V. [1944], J. Techn. Phys. (Russian), 14, p. 276.
- Jarušek, J. [1983], "Contact Problems with Bounded Friction, Coercive Case," Czechoslovak Math. J., 33(108), pp. 337-361.
- Jarvis, R. P. and Mills, B. [1963-64], "Vibrations Induced by Dry Friction," Proc. Instn. Mech. Engrs., 178-Pt 1(32), pp. 847-866.
- Jean, M., and Pratt, E. [1985], "A System of Rigid Bodies with Dry Friction," Int. J. Engng. Sci., 23(5), pp. 497-513.
- Jenkin, F. and Ewing, J. A. [1877], "On Friction Between Surfaces Moving at Low Speeds," Phil. Trans. R. Soc. Lond., 167, pp. 509-528.
- Johannes, V. I., Green, M. A. and Brockley, C. A. [1973], "The Role of the Rate of Application of the Tangential Force in Determining the Static Friction Coefficient," Wear, 24, pp. 384-385.
- Kaidanovski, N. L. and Haikin, S. E. [1933], J. Techn. Phys. (Russian), 3, p. 1.

- Kato, S. and Matsubayashi, T. [1970], "On the Dynamic Behavior of Machine-Tool Slideway - 1st Report," Bull. J. S. M. E., 13(55), pp. 170-179.
- Kato, K., Iwabuchi, A. and Kayaba, T. [1982], "The Effects of Friction-induced Vibration on Friction and Wear," Wear, 80, pp. 307-320.
- Kikuchi, N. and Oden, J. T. [1986], Contact Problems in Elasticity, SIAM, Philadelphia.
- Kimball, A. L. [1877], "Sliding Friction on an Inclined Plane," Am. J. Sci. Arts, xiii (Silliman's Journal), p. 151; "A New Investigation on the Laws of Friction," Am. J. Sci. Arts, xiii (Silliman's Journal), p. 353.
- Kragelskii, I. V. [1965], Friction and Wear, Butterworths, Washington.
- Kragelskii, I. V., Dobychin, M. N. and Kombalov, V. S. [1982], Friction and Wear: Calculation Methods, Pergamon Press.
- Kudinov, V. A. [1958], "An Investigation of the Vibrations of Machine Tools," Mashgiz (State Mech. Eng. Press), p. 251.
- Kufner, A., John, O. and Fučík, S. [1977], Function Spaces, Noordhoff International Publ., Leyden.
- Kuhlman-Wilsdorf, D. [1981], "Dislocation Concepts in Friction and Wear," Fundamentals of Friction and Wear of Materials, American Society for Metals, Ohio.
- Lebeau, G., and Schatzman, M. [1984], "A Wave Problem in a Half-Space, with a Unilateral Constraint at the Boundary," J. Diff. Equations, 53, pp. 309-361.
- Leipholz, H. H. E. [1970], Stability Theory, Academic Press, Inc., New York and London.
- Lenkiewicz, W. [1969], "The Sliding Friction Process - Effect of External Vibrations," Wear, 13, pp. 99-108.
- Lions, J. L. [1969], Quelques Méthodes de Résolution des Problèmes aux Limites Non Linéaires, Dunod, Paris.
- Lötstedt, P. [1982], "Mechanical Systems of Rigid Bodies Subject to Unilateral Constraints," SIAM J. Appl. Math., 42(2), pp. 281-296.
- Lötstedt, P. [1984], "Coulomb Friction in Two-Dimensional Rigid Body Systems," ZAMM, 61, pp. 605-615.

- Madakson, P. B. [1983], "The Frictional Behavior of Materials," Wear, 87, pp. 191-206.
- Martins, J. A. C. and Oden, J. T. [1983], "A Numerical Analysis of a Class of Problems in Elastodynamics with Friction," Comput. Meths. Appl. Mech. Engrg., 40, pp. 327-360.
- Martins, J. A. C. and Oden, J. T. [1986], "Static and Kinetic Friction - A Numerical Study," (in preparation).
- Moore, D. F. [1975], Principles and Applications of Tribology, Pergamon Press, Oxford.
- Morin, A. J. [1833-36], Mém. Savans Etrang., (Paris), iv, pp. 1-128; iv, pp. 591-696; vi, pp. 641-785; Ann. Min., iv, pp. 271-321; vi, pp. 73-96; x, pp. 27-56.
- Nečas, J., Jarušek, J., and Haslinger, J. [1980], "On the Solution of the Variational Inequality to the Signorini Problem with Small Friction," Bolletino U.M.I., 5, 17-B, pp. 796-811.
- Oden, J. T. [1986], Qualitative Methods in Nonlinear Mechanics, Prentice Hall, Englewood Cliffs.
- Oden, J. T. and Carey, G. F. [1983], Finite Elements: Mathematical Aspects, Prentice-Hall, Englewood Cliffs, N. J.
- Oden, J. T. and Martins, J. A. C. [1985], "Models and Computational Methods for Dynamic Friction Phenomena," Computer Methods in Appl. Mech. and Engrg., 52, pp. 527-634.
- Oden, J. T. and Pires, E. B. [1983], "Nonlocal and Nonlinear Friction Laws and Variational Principles for Contact Problems in Elasticity," J. Appl. Mech., 50(1), pp. 67-76.
- Percivale, D. [1985], "Uniqueness in the Elastic Bounce Problem," J. Diff. Equations, 56, pp. 206-215.
- Pires, E. B. [1982], "Analysis of Nonclassical Friction Laws for Contact Problems in Elastostatics," Ph.D. Dissertation, University of Texas at Austin.
- Pires, E. B. and Oden, J. T. [1983], "Analysis of Contact Problems with Friction Under Oscillating Loads," Comput. Meths. Appl. Mech. Engrg., 39, pp. 337-362.
- Poirée [1852], Mém. Soc. Ing. Civ. Fr.
- Rabier, P., Martins, J. A. C., Oden, J. T. and Campos, L. T. [1986],

"Existence and Local Uniqueness of Solutions to Contact Problems in Elasticity with Nonlinear Friction Laws," to appear in International Journal of Engineering Science.

- Rabinowicz, E. [1951], "The Nature of the Static and Kinetic Coefficients of Friction," J. Appl. Physics, 22(11), pp. 1373-1379.
- Rabinowicz, E. [1958], "The Intrinsic Variables Affecting the Stick-Slip Process," Proc. Phys. Soc., 71, pp. 668-675.
- Rabinowicz, E. [1965], Friction and Wear of Materials, John Wiley and Sons, New York.
- Reed, M. [1976], Abstract Non-Linear Wave Equations, Lecture Notes in Mathematics, No. 507, Springer-Verlag, Berlin, Heidelberg, New York.
- Rennie, G. [1829], "Experiments on the Friction and Abrasion of the Surfaces of Solids," Phil. Trans. R. Soc. Lond., 34, Pt I, pp. 143-170.
- Rice, S. L., Hans, N. and Steven, F. W. [1982], "The Role of Specimen Stiffness in Sliding and Impact Wear," Wear, 77, pp. 13-28.
- Rice, J. R. and Ruina, A. L. [1983], "Stability of Steady Frictional Slipping," Paper No. 83-APM-16, ASME Applied Mechanics, Bioengineering, and Fluids Engineering Conference, Houston, TX.
- Richardson, R. S. H. and Nolle, H. [1976], "Surface Friction Under Time-dependent Loads," Wear, 37, pp. 87-101.
- Rigney, D. A. and Hirth, J. P. [1979], "Plastic Deformation and Sliding Friction of Metals," Wear, 53, pp. 345-370.
- Rooney, G. T. and Deravi, P. [1982], "Coulomb Friction in Mechanism Sliding Joints," Mech. Machine Theory, 17, pp. 207-211.
- Ruina, A. L. [1980], "Friction Laws and Instabilities: A Quasistatic Analysis of Some Dry Frictional Behavior," Ph.D. Thesis, Brown University, Providence, RI.
- Ruina, A. L. [1983], "Slip Instability and State Variable Friction Laws," J. Geophys. Res..
- Sampson, J. B., Morgan, F., Reed, D. W., and Muskat, M. [1943], "Friction Behavior During the Slip Portion of the Stick-Slip Process," J. Appl. Phys., 14, pp. 689-700.
- Schatzman, M. [1978], "A Class of Nonlinear Differential Equations of Second Order in Time," Nonlinear Analysis, Theory, Methods, and Applications, 2, pp. 355-373.

- Schatzman, M. [1980], "A Hyperbolic Problem of Second Order with Unilateral Constraints: The Vibrating String with a Concave Obstacle," J. Math. Anal. Appl., pp. 138-191.
- Schatzman, M. [1980], "Un Problème Hyperbolique du 2ème Ordre avec Contrainte Unilatérale: la Corde Vibrante avec Obstacle Ponctuel," J. Diff. Equations, 36, pp. 295-334.
- Schatzman, M. and Bercovier, M. [1985], On the Numerical Approximation of a Vibration Problem with Unilateral Constraints, Centre de Mathématiques Appliquées, Unité de Recherche Associé au CNRS-756, Ecole Polytechnique, Palaiseau, France, Rapport Interne No. 124.
- Shobert, E. I. [1957], "Carbon Brush Friction and Chatter," Trans. Amer. Inst. Elect. Engrs., 76, Part III, p. 268.
- Showalter, R. E. [1979], Hilbert Space Methods for Partial Differential Equations, Pitman, San Francisco.
- Simkins, T. E. [1967], "The Mutuality of Static and Kinetic Friction," Lubr. Engrg, 23, pp. 26-31.
- Soda, N., Kimura, Y. and Tanaka, A. [1975], "Wear of Some f.c.c. Metals During Unlubricated Sliding. Part I: Effects of Load, Velocity and Atmosphere Pressure on Wear," Wear, 33, pp. 1-16.
- Soom, A. and Kim, C. [1983], "Interactions Between Dynamic Normal and Friction Forces During Unlubricated Sliding," J. Lubr. Technol., 105, pp. 221-229.
- Soom, A. and Kim, C. [1983], "Roughness-induced Dynamic Loading at Dry and Boundary-lubricated Sliding Contacts," J. Lubr. Technol., 105, pp. 514-517.
- Spurr, R. T. [1961-62], "A Theory of Brake Squeal," Proc. Instn. Mech. Engrs. (A.D.), 1, pp. 33-52.
- Suh, N. P. and Sin, H.-C. [1981], "The Genesis of Friction," Wear, 69, pp. 91-114.
- Tabor, D. [1972], "Friction, Lubrication and Wear," in Surface and Colloid Science, 5, ed. E. Matijevic, Wiley, New York, pp. 245-312.
- Tabor, D. [1975], "Interaction Between Surfaces: Adhesion and Friction," Chap. 10 in Surface Physics of Materials, Vol. 2, ed. J. M. Blakely, Academic Press, New York.
- Tabor, D. [1981], "The Present State of our Understanding," J. Lubr. Technol., 103, pp. 169-179.

Review of Experimental Work," Wear, 58, pp. 331-340.

Ziegler, H. [1952], "Die Stabilitätskriterien der Elastomechanik,"  
Ingenieur-Archiv., 20, pp. 49-56.

Ziegler, H. [1968], Principles of Structural Stability, Blaisdell  
Publ. Co.



**APPENDIX:**  
**SOLUTION TO THE SIGNORINI-LIKE CONTACT PROBLEMS**  
**THROUGH INTERFACE MODELS**

In this Appendix, we present a study of contact problems usually modeled by Signorini's problem. Our approach differs in that we make use of the constitutive relations for the normal response along the candidate contact surface developed earlier in this report. The form of these models is dictated by experimental evidence and they lead to a variational equality instead of an inequality. We focus on the most delicate case of contact-traction boundary conditions for which we obtain existence and optimal uniqueness results under physically realistic assumptions. The other usual boundary conditions can be dealt with similarly with simplifications in the proofs. Signorini's problem is shown to be recovered as the limiting case of an infinite normal stiffness, while our model allows for perturbations describing friction phenomena, according to Coulomb's law or generalizations of it.

Serious mathematical difficulties arise from the fact that the most general type of interface models rules out the use of Sobolev's embedding theorem, without which the problem is no longer in the province of standard convex analysis but rather lies in the realm of the theory of hypermaximal monotone operators having a domain with empty interior. Several auxiliary results, including an apparently new property in Sobolev spaces, are proven which, together with the general method of proof, should be of interest in other problems.

The contact-traction boundary conditions require compatibility conditions to be introduced. They have a somewhat more sophisticated form than the standard ones involved in Signorini's problem and further examination shows that their physical content agrees strikingly with common sense physical observations.

### 1. Introduction.

Let  $\Omega$  be an open, bounded subset of  $\mathbb{R}^N$  with a Lipschitz continuous boundary  $\Gamma$ , the disjoint union  $\Gamma_C \cup \Gamma_F$  with  $\Gamma_C$  and  $\Gamma_F$  measurable and  $\text{meas}(\Gamma_C) > 0$ . For  $N = 2$  or  $N = 3$ ,  $\Omega$  represents the reference configuration of a body in geometrical contact with another body along  $\Gamma_C$ . In other words, no external forces are present and the boundaries of the two bodies coincide along  $\Gamma_C$ . Suppose now that the body occupying the domain  $\Omega$  is submitted to external forces  $\underline{f}$ , consisting of body forces  $\underline{b}$  defined in  $\Omega$  and tractions  $\underline{t}$  prescribed on  $\Gamma_F$ . Assuming that no point of  $\Gamma_F$  may come in contact with the second body under the action of the forces  $\underline{f}$ , i.e., that  $\Gamma_C$  is the candidate contact surface for the deformed configuration, and that the material has a linear elastic behavior, the problem of contact with no friction is usually understood as the Signorini problem: Minimize

$$\frac{1}{2} a(\underline{v}, \underline{v}) - \langle \underline{f}, \underline{v} \rangle_{\Omega} \quad , \quad (1.1)$$

over the closed convex subset of the Sobolev space  $(H^1(\Omega))^N$ ,

$$K = \{ \underline{v} \in (H^1(\Omega))^N, \quad v_n \leq 0 \text{ on } \Gamma_C \} . \quad (1.2)$$

In (1.1) and (1.2) above,  $a(\cdot, \cdot)$  denotes the symmetric bilinear form associated with the virtual work of stresses  $\underline{\sigma}(\underline{u})$  on strains  $\underline{\varepsilon}(\underline{v})$  ( $a(\underline{u}, \underline{v}) = \int_{\Omega} \underline{\sigma}(\underline{u}) : \underline{\varepsilon}(\underline{v}) \, dx$ ),  $\langle \cdot, \cdot \rangle_{\Omega}$  the duality pairing between the space  $(H^1(\Omega))^N$  and its dual, and  $v_n$  the component of the displacement  $\underline{v}$  along the outward normal vector  $\underline{n}$ :  $v_n = \underline{v} \cdot \underline{n}$  (euclidian inner product). Problem (1.1)-(1.2) is a formal variational formulation of the equilibrium equations between the stresses  $\underline{\sigma}(\underline{u})$  and the external forces  $\underline{b}$  and  $\underline{t}$ :

$$\operatorname{div} \underline{\sigma}(\underline{u}) + \underline{b} = \underline{0} \quad \text{in } \Omega , \quad (1.3)$$

$$\underline{\sigma}(\underline{u}) \cdot \underline{n} = \underline{t} \quad \text{on } \Gamma_F , \quad (1.4)$$

and, on  $\Gamma_C$ ,

$$u_n \leq 0 , \quad (1.5)$$

$$\underline{\sigma}(\underline{u}) \cdot \underline{n} = \underline{0} \quad \text{if } u_n < 0 , \quad (1.6)$$

$$\underline{\sigma}(\underline{u}) \cdot \underline{n} = -\alpha \underline{n} , \quad \alpha \geq 0 , \quad \text{if } u_n \neq 0 . \quad (1.7)$$

A "qualification" of the formality of this interpretation can be found among the by-products of our approach (cf. Remark 5.2)

Existence of solutions to problem (1.1)-(1.2) is known under a simple necessary and sufficient compatibility condition on the applied forces (Fichera [4]; see also Lions and Stampacchia [9]). The idea of using variational inequalities for solving contact problems goes back to Fichera [4] and Stampacchia [9], but the theory has not been very successful in the more complicated problem with friction despite recent contributions by Necas, Jarusek and Haslinger [5, 12].

With the aim of analyzing problems of friction, Oden and Martins [13] have developed a different approach to contact problems. The key ingredient of their theory is the introduction of a model for the normal response at points of  $\Gamma_C$  at which contact may occur. To do this, it is essential to remove the non-penetration condition  $u_n \leq 0$  on  $\Gamma_C$ : The normal response at a point  $\tilde{x} \in \Gamma_C$  is then a function of  $(u_n)_+(\tilde{x})$ . Contrary to a first natural reaction, removing the nonpenetration condition  $u_n \leq 0$  is not physical nonsense. Indeed, in any mathematical model, the boundary  $\Gamma_C$  is an idealized average candidate contact surface, the real candidate contact surface differing from  $\Gamma_C$  by a layer of asperities. How different the real surface is from  $\Gamma_C$  "measures" its roughness, a factor increasingly believed to originate friction phenomena (see, e.g., [13,17,19]). When contact occurs, the deformation of these asperities (incidentally of a nature totally different from the "visible" deformation of the body) allows small displacements of the boundary  $\Gamma_C$  towards the obstacle, violating the

condition  $u_n \leq 0$ . Accordingly, when positive, the displacement  $u_n$  should nevertheless remain small. This point will be examined later on. In this view, removing the condition  $u_n \leq 0$  does not amount to accepting actual penetration of the two bodies in contact but merely allows the average surface  $\Gamma_C$  to get closer to the obstacle. On the experimental side, these features of actual surfaces have been observed by many investigators, and the memoir [13] contains extensive arguments in support of such models. On the mathematical side, they present numerous advantages: As we shall see, discrepancies between variational and boundary value problem formulations vanish, new compatibility conditions with precise physical interpretations are involved, perturbations allowing for friction phenomena become manageable, etc.

In such models, the normal response caused by the normal displacement  $u_n(x)$  at  $x \in \Gamma_C$  is then of the form  $\phi(x, u_n(x))$  where  $\phi: \Gamma_C \times \mathbb{R} \rightarrow \mathbb{R}$  verifies  $\phi \geq 0$  and  $\phi(x, t) = 0$  for  $t \leq 0$  [so that  $\phi(x, u_n(x))$  actually depends only on  $(u_n)_+(x)$ ]. The function  $\phi$  depends on the interface condition and a few of its properties are dictated by common sense observations: It is intuitively clear that any positive normal displacement should produce a positive normal response, so that  $\phi(x, t) > 0$  for  $t > 0$ . Next, an increase of

the normal displacement must produce an increase of the normal response so that  $\phi(\underline{x}, t)$  is increasing w.r.t.  $t \geq 0$ . Further, the resistance to penetration of the bodies suggests for a positive normal displacement  $u_n(\underline{x})$  that the ratio  $\phi(\underline{x}, u_n(\underline{x}))/u_n(\underline{x})$  (normal response versus normal displacement) be an increasing function of  $u_n(\underline{x})$ , namely that  $\phi(\underline{x}, t)/t$  is increasing w.r.t.  $t > 0$ .

Denoting by  $\tilde{\phi}(u_n)$  the function  $\tilde{\phi}(u_n)(\underline{x}) = \phi(\underline{x}, u_n(\underline{x}))$  for  $\underline{x} \in \Gamma_C$ , the contact problem (1.3)-(1.7) becomes, in this approach: Find  $\underline{u} \in (H^1(\Omega))^N$  such that

$$\operatorname{div} \underline{\sigma}(\underline{u}) + \underline{b} = \underline{0} \quad \text{in } \Omega, \quad (1.8)$$

$$\underline{\sigma}(\underline{u}) \cdot \underline{n} = \underline{t} \quad \text{on } \Gamma_F, \quad (1.9)$$

$$\underline{\sigma}(\underline{u}) \cdot \underline{n} = -\tilde{\phi}(u_n)\underline{n} \quad \text{on } \Gamma_C. \quad (1.10)$$

In §3, we shall see that problem (1.8)-(1.10) has the equivalent formulation: Find  $\underline{u} \in (H^1(\Omega))^N$  such that

$$a(\underline{u}, \underline{v}) + \int_{\Gamma_C} \tilde{\phi}(u_n) v_n \, ds = \langle \underline{f}, \underline{v} \rangle_{\Omega} \quad \text{for every } \underline{v} \in (H^1(\Omega))^N. \quad (1.11)$$

Experimental evidence shows that the normal response  $\phi(\underline{x}, t)$  has a power-like behavior for small values of  $t > 0$ , growing up to exponential as  $t$  is increased. Roughly speaking, the power zone

("light" normal loads) authorizes sliding, prohibited in the exponential zone ("heavy" normal loads); see [13, Fig. 48]. For this reason, in a study of similar static contact problems with friction (cf. [10]), we have limited ourselves to considering the choice

$\phi(\underline{x}, t) = c_n(\underline{x})(t_+)^{m_n}$  with (experimentally justified) values of the exponent  $m_n$  allowing the use of Sobolev's embedding theorems and under convenient boundary conditions avoiding the need for compatibility conditions.

This paper is devoted to the study of problem (1.8)-(1.10) with a general  $\phi$ . On comparison with the situation in [10], we face several new difficulties. First and foremost, the variational formulation (1.11) is a priori not well posed since Sobolev embedding theorems are not available without serious restrictions on the growth of the function  $t \rightarrow \phi(\underline{x}, t)$  as  $t$  tends to  $+\infty$ . In particular, exponential growth is prohibited when  $N \geq 3$ . This difficulty has been overcome by requiring  $\tilde{\phi}(u_n)$  to belong to the space  $L^1(\Gamma_C)$  as an additional condition to (1.8)-(1.10) and proving in this assumption that  $\tilde{\phi}(u_n)v_n$  belongs to  $L^1(\Gamma_C)$  for every  $\underline{v} \in (H^1(\Omega))^N$  as soon as  $\underline{u}$  is a solution to (1.8)-(1.10) (Theorem 3.1). Once the variational formulation (1.11) has been justified, we show that it is equivalent to the minimization of a weakly sequentially lower semicontinuous convex functional over  $(H^1(\Omega))^N$  with values in  $\mathbb{R}^* = \mathbb{R} \cup \{+\infty\}$ . In this process, other difficulties arise because the functional in question is nowhere continuous in the general case (i.e., its domain is empty), and the desired properties must be established by using convexity of the function  $t \rightarrow \int_0^t \phi(\underline{x}, \tau) d\tau$  rather than that of the functional. Another

technicality is to prove that the minimizers do verify equations (1.8)-(1.10) in the sense of distributions, and the condition  $\phi(u_n) \in L^1(\Gamma_C)$ .

From these introductory comments, one might have guessed that the problem is, in some respects, pertaining to the theory of hypermaximal monotone operators (cf. Deimling [1] for an excellent account) rather than standard convex analysis. However, we have found no significant advantage in using the specialized vocabulary and the general results of this theory, while doing so might have caused some discomfort to the non-initiated reader. Nonetheless, it can be reasonably speculated on the basis of this relationship that our method of proof can be duplicated in other problems, thus ranging farther than the specific example for which it has been developed here.

Several general properties need to be established. Some of them, specifically related to integration theory, are collected in §2. In this respect, we note an interesting coincidence: Most of the results of §2 hold under the apparently necessary condition that the mapping  $t \rightarrow \phi(\underline{x}, t)$  has (at most) exponential growth at infinity. Other statements of general mathematical interest, related to a seemingly new property in Sobolev spaces, are proved in §3 (Lemmas 3.3 to 3.6).

Coerciveness of the energy functional, hence existence of minimizers, is proved in §4 over an appropriate quotient space (although the functional is not quadratic!) and under a compatibility condition on the applied external forces slightly stronger than that needed for solving problem (1.3)-(1.7). This compatibility condition is independent of the normal response  $\phi$  and, again, the necessary



mathematical assumptions have significant physical counterparts. For instance, coerciveness for every external force  $\underline{f}$  is obtained under a purely geometrical assumption bearing a striking interpretation, namely, that the body is "stuck" due to its contact along  $\Gamma_C$  in the reference configuration (in other words, contact along  $\Gamma_C$  in the reference configuration prevents the body to be moved without exerting external forces).

Uniqueness of the solution to within elements of the space  $N = \{\underline{v} \in (H^1(\Omega))^N, v_n = 0 \text{ on } \Gamma_C\}$ , hence uniqueness if  $N = \{0\}$ , is obtained under another mild compatibility condition as soon as physical contact occurs. In any case, uniqueness of the area of physical contact  $\{\underline{x} \in \Gamma_C; u_n(\underline{x}) > 0\}$  is proved and it is shown that the same result is false in general if the area of physical contact is replaced by the area of geometrical contact  $\{\underline{x} \in \Gamma_C; u_n(\underline{x}) \geq 0\}$ .

Considering problem (1.8)-(1.10) as a model for contact with no friction instead of Signorini's problem thus allows elimination of several ambiguities in the latter. An important question is then to know how they relate to each other. In §5, we present a very simple answer providing one more justification for the use of normal response models: The Signorini problem coincides with the case of an infinite normal response along  $\Gamma_C$ . This takes us back to the natural requirement that, when positive, the displacement  $u_n$  should be "small" along  $\Gamma_C$ . When  $\underline{u}$  is a solution to problem (1.8)-(1.10) and  $\phi$  is a physically admissible normal response, a heuristic but strong argument in this direction is as follows: As a result of resistance to penetration, it is observed in physical experiments that  $\phi(\underline{x}, t)$  is very

large for relatively small values of  $t > 0$  (with  $\phi(\underline{x}, t) = c_n(\underline{x})(t_+)^{m_n}$ ), experiments have provided  $c_n(\underline{x}) = c_n$  in the range of  $10^6$  or  $10^8$ ). On the other hand, by changing any normal response  $\phi$  to  $\lambda\phi$  and letting  $\lambda$  tend to  $+\infty$ , we show in §5 that every solution  $u(\lambda)$  is arbitrarily close to some solution to Signorini's problem in the strong topology of  $(H^1(\Omega))^N$ . Hence,  $u_n(\lambda)$  is close to zero in, say, every space  $L^p(\Gamma_C)$  such that  $H^{\frac{1}{2}}(\Gamma) \hookrightarrow L^p(\Gamma)$ . The interpretation of this result is that  $u_n$  is close to zero on  $\Gamma_C$  if the normal response  $\phi(\underline{x}, t)$  is large for relatively small values of  $t > 0$ , which is precisely the actual physical situation.

Another advantage of the formulation (1.8)-(1.10) is that it admits perturbations allowing consideration of friction phenomena according to Coulomb's law or generalizations of it. In this case, it suffices to consider a power-like normal response (since the exponential zone is characteristic of no sliding). The method of [10] is then available with appropriate modifications (see §5). The other aspects we discuss in §5 are the interpretations of our compatibility conditions for coerciveness and uniqueness in the simple case  $N = 2$ , the admissibility of an initial gap and the possibility of considering other boundary conditions. The use of interface models, such as those described here, together with nonquadratic energies of deformation, is the subject of current studies.

The work is naturally divided into two parts. Part I is composed of paragraphs 2 and 3, and is devoted to the establishment of special mathematical preliminaries and to the formulation of the variational equality which correctly characterizes the traction contact problem

with a nonlinear interface constitutive law. The major issues of existence and uniqueness of solutions are taken up in Part II.

## PART I. PRELIMINARIES AND FORMULATION OF A VARIATIONAL INEQUALITY

### 2. Technical Preliminaries.

We shall begin with a review of some general results. Hypotheses will later be complemented according to the applications we have in mind and further properties will be established.

Let  $\omega$  be an open subset of  $\mathbb{R}^m$ ,  $m \geq 1$ , and  $\phi: \omega \times \mathbb{R} \rightarrow \mathbb{R}$ , a Carathéodory function, i.e.,

$$\begin{aligned} \phi(\underline{x}, \cdot) : \mathbb{R} \rightarrow \mathbb{R} \text{ is continuous for almost all } \underline{x} \in \omega, \\ \phi(\cdot, t) : \Omega \rightarrow \mathbb{R} \text{ is measurable for every } t \in \mathbb{R}. \end{aligned} \quad (2.1)$$

The Nemytskii operator  $\tilde{\phi}$  associated with the function  $\phi$  is defined for every measurable function  $\xi : \omega \rightarrow \mathbb{R}$  by

$$\tilde{\phi}(\xi)(\underline{x}) = \phi(\underline{x}, \xi(\underline{x})) \text{ for almost all } \underline{x} \in \omega. \quad (2.2)$$

It can be shown that  $\tilde{\phi}(\xi)$  is a measurable function. Krasnoselskii [8] has given necessary and sufficient conditions for the operator  $\tilde{\phi}$  to act continuously from  $L^q(\omega)$  into  $L^r(\omega)$  when  $q$  and  $r$  verify the condition  $1 \leq q, r < +\infty$ . Besides, setting

$$\Phi(\underline{x}, t) = \int_0^t \phi(\underline{x}, \tau) d\tau \quad (2.3)$$

and assuming  $q > 1$  and  $r = q^* = q/(q-1)$  (Hölder conjugate of  $q$ ), he has shown under the same assumptions that the functional

$$j(\xi) = \int_{\omega} \tilde{\phi}(\xi) dx, \quad (2.4)$$

is continuously differentiable on  $L^q(\omega)$  with derivative  $\tilde{\phi}$ , in the sense that

$$j'(\xi) \cdot h = \int_{\omega} \tilde{\phi}(\xi) h dx, \quad (2.5)$$

for every pair  $(\xi, h) \in [L^q(\omega)]^2$ . For  $q > 2$ , these results are complemented in [15] by showing, under the additional assumptions that (1) the mapping  $\phi$  is continuously differentiable with respect to  $t$  for almost all  $x \in \omega$  and (2) its derivative  $\phi_t$  verifies an appropriate growth condition (ensuring that  $\tilde{\phi}_t \in C^0(L^q(\omega), L^{(q/2)^*}(\omega))$ ), that the functional  $j$  (2.5) is twice continuously differentiable on  $L^q(\omega)$  with

$$j''(\xi) \cdot (h, k) = \int_{\omega} \tilde{\phi}_t(\xi) h k dx,$$

for every triple  $(\xi, h, k) \in [L^q(\omega)]^3$ . The same conclusion is false for  $q = 2$ , except in the trivial case when  $\phi(x, t) = a(x)t$  and  $a \in L^\infty(\omega)$ , but it can be extended to the case  $q = +\infty$ , of special interest to us in this paper. Proposition 2.1 below summarizes the various statements for  $q = +\infty$  in a form which will be suitable for our later purposes. Details and extensions can be found in [16].

Proposition 2.1: Assume that the Carathéodory function  $\phi$  is of class  $C^1$  with respect to  $t$  for almost all  $x \in \omega$  <sup>(1)</sup> and that  $\phi_t$

---

<sup>(1)</sup> No additional assumption is needed to show that  $\phi_t$  is a Carathéodory function.

verifies the following growth condition: For every  $t_0 > 0$ , there is a function  $a_{t_0} \in L^1(\omega)$  such that

$$|\phi_t(\cdot, t)| \leq a_{t_0} \quad \text{for } |t| \leq t_0. \quad (2.6)$$

Then

$$(i) \quad \tilde{\phi}_t \in C^0(L^\infty(\omega), L^1(\omega))$$

$$(ii) \quad \tilde{\phi} \in C^1(L^\infty(\omega), L^1(\omega)) \quad \text{as soon as } \phi(\cdot, 0) \in L^1(\omega), \quad \text{with}$$

$$D\tilde{\phi}(\xi) \cdot h = \tilde{\phi}_t(\xi) h, \quad (2.7)$$

for every pair  $(\xi, h) \in (L^\infty(\omega))^2$ .

(iii) Setting

$$\phi(\underline{x}, t) = \int_0^t \phi(\underline{x}, \tau) d\tau, \quad (2.8)$$

the functional

$$j(\xi) = \int_\omega \tilde{\phi}(\xi) dx \quad (2.9)$$

is twice continuously differentiable on  $L^\infty(\omega)$  and

$$j'(\xi) \cdot h = \int_\omega \tilde{\phi}(\xi) h dx, \quad (2.10)$$

for every pair  $(\xi, h) \in (L^\infty(\omega))^2$  (note that the combination of (i) and (ii) yields

$$j''(\xi) \cdot (h, k) = \int_\omega \tilde{\phi}_t(\xi) h k dx \quad (2.11)$$

for every triple  $(\xi, h, k) \in (L^\infty(\omega))^3$ .

Suppose now that

$$\phi(\cdot, t) \geq 0 \quad \text{for every } t \in \mathbb{R}. \quad (2.12)$$

Then, for every measurable function  $\xi : \omega \rightarrow \mathbb{R}$ ,  $\tilde{\phi}(\xi)$  is a non-negative measurable function. The functional  $j$  of (2.9) can thus be extended to all measurable real-valued functions as a mapping (still denoted by  $j$ ) with values in  $\mathbb{R}^+ = \mathbb{R} \cup \{+\infty\}$  by setting

$$j(\xi) = \begin{cases} \int_{\omega} \tilde{\phi}(\xi) dx & \text{if } \tilde{\phi}(\xi) \in L^1(\omega), \\ +\infty & \text{otherwise.} \end{cases} \quad (2.13)$$

Proposition 2.2: The extended functional  $j$  is lower semicontinuous on  $L^1(\omega)$ .

Proof: The result follows by combining [3, Prop. 1.1 p. 218 and Cor. 1.2, p. 222].  $\square$

Remark 2.1: The same argument shows that the extended functional  $j$  is lower semicontinuous on  $L^p(\omega)$  for every  $1 \leq p \leq +\infty$ .  $\square$

We shall consider a particular case when assumption (2.12) is satisfied, namely

$$\begin{aligned} \phi_t(\cdot, t) &\geq 0 & \text{for } t > 0, \\ \phi_t(\cdot, t) &= 0 & \text{for } t \leq 0 \end{aligned} \quad (2.15)$$

and

$$\phi(\tilde{x}, t) = \int_0^t \phi_t(\tilde{x}, \tau) d\tau \quad (\Leftrightarrow \phi(\cdot, 0) = 0). \quad (2.16)$$

In this case, the three functions  $\phi_t(\cdot, t)$ ,  $\phi(\cdot, t)$  and  $\phi(\cdot, t)$  are non-negative for every  $t \in \mathbb{R}$  and vanish for  $t \leq 0$ . Together with an appropriate condition limiting the growth of the function  $\phi(\underline{x}, t)$  as  $t$  tends to  $+\infty$ , the above assumptions will now allow us to complement Proposition 2.1 as follows:

Proposition 2.3: Assume that (2.15) and (2.16) hold and suppose further that the function  $\phi_t(\underline{x}, \cdot)$  is nondecreasing for almost all  $\underline{x} \in \omega$  and that there are constants  $T > 0$  and  $\mu > 0$  such that

$$\phi_t(\cdot, t) \leq \mu \phi(\cdot, t) \quad \text{for } t \geq T, \quad (2.17)$$

with  $\phi(\cdot, T) (= \tilde{\phi}(T)) \in L^1(\omega)$ . Then, for every measurable function  $\xi$  such that  $\tilde{\phi}(\xi) \in L^1(\omega)$  and every function  $\eta \in L^\infty(\omega)$  one has

$$\tilde{\phi}(\xi + \eta) \in L^1(\omega), \quad \tilde{\phi}_t(\xi + \eta) \in L^1(\omega)$$

and the functional

$$\eta \in L^\infty(\omega) \rightarrow j_\xi(\eta) = j(\xi + \eta) \quad (2.18)$$

is real-valued and twice continuously differentiable with

$$j'_\xi(\eta) \cdot h = \int_\omega \tilde{\phi}(\xi + \eta) h dx, \quad (2.19)$$

$$j''_\xi(\eta) \cdot (h, k) = \int_\omega \tilde{\phi}_t(\xi + \eta) h k dx, \quad (2.20)$$

for every triple  $(\eta, h, k) \in [L^\infty(\omega)]^3$ .

Proof: As a first step, we show that  $\tilde{\phi}(\xi)$  belongs to  $L^1(\omega)$ :

Integrating both sides of inequality (2.17) we obtain

$$\begin{aligned}\phi(\cdot, t) &\leq \phi(\cdot, T) + \mu \phi(\cdot, t) - \mu \phi(\cdot, T) \\ &\leq \phi(\cdot, T) + \mu \phi(\cdot, t) \quad \text{for } t \geq T .\end{aligned}\quad (2.21)$$

Let then  $\xi : \omega \rightarrow \mathbb{R}$  be a measurable function. From (2.21),

$$\xi(\underline{x}) \geq T \Rightarrow \phi(\underline{x}, \xi(\underline{x})) \leq \phi(\underline{x}, T) + \mu \phi(\underline{x}, \xi(\underline{x})) .$$

On the other hand, it follows from (2.15) that the function  $\phi(\underline{x}, \cdot)$  is non-decreasing for almost all  $\underline{x} \in \omega$ . Hence,

$$\xi(\underline{x}) \leq T \Rightarrow \phi(\underline{x}, \xi(\underline{x})) \leq \phi(\underline{x}, T) \leq \phi(\underline{x}, T) + \mu \phi(\underline{x}, \xi(\underline{x})) .$$

This shows that

$$0 \leq \tilde{\phi}(\xi) \leq \tilde{\phi}(T) + \mu \tilde{\phi}(\xi) \in L^1(\omega) ,$$

proving the relation  $\tilde{\phi}(\xi) \in L^1(\omega)$ .

Setting

$$\phi_{\xi}(\underline{x}, t) = \phi(\underline{x}, \xi(\underline{x}) + t) , \quad (2.22)$$

we now note that  $\phi_{\xi}$  is a Carathéodory function, and the mapping  $t \rightarrow \phi_{\xi}(\underline{x}, t)$  is continuously differentiable for almost all  $\underline{x} \in \omega$  with

$$(\phi_{\xi})_t(\underline{x}, t) = \phi_t(\underline{x}, \xi(\underline{x}) + t) . \quad (2.23)$$

The sole nontrivial part of this assertion is the measurability of the function  $\phi_{\xi}(\cdot, t)$  for every  $t \in \mathbb{R}$ . However, it suffices to notice that the function  $(\underline{x}, \tau) \in \omega \times \mathbb{R} \rightarrow \phi(\underline{x}, \tau + t)$  is (obviously) a Carathéodory function and to apply the measurability result used at the beginning of this section after replacing  $\tau$  by  $\xi(\underline{x})$ .



At this stage, we see that the properties to be established follow from Proposition 2.1, provided we can prove that the function  $\phi_{\xi}$  fulfills the required hypotheses. As  $\phi_{\xi}(\cdot, 0) = \phi(\cdot, \xi(\cdot)) = \tilde{\phi}(\xi)$  is in  $L^1(\omega)$ , as we have just seen, we need only prove for every  $t_0 > 0$  that there is a function  $b_{t_0} \in L^1(\omega)$  such that

$$0 \leq (\phi_{\xi})_t(x, t) \leq b_{t_0}(x) \quad \text{for almost all } x \in \omega \quad \text{and} \quad |t| \leq t_0. \quad (2.24)$$

We begin by observing that an equivalent formulation of assumption (2.17) is

$$\phi(\cdot, \tau+t) \leq e^{\mu t} \phi(\cdot, \tau) \quad \text{for } t \geq 0 \quad \text{and} \quad \tau \geq T, \quad (2.25)$$

the proof of which reduces to a simple verification. In particular,

$$\phi(\cdot, t) \leq e^{\mu(t-T)} \phi(\cdot, T) \quad \text{for } t \geq T.$$

Substituting into (2.17), we arrive at

$$\phi_t(\cdot, t) \leq \mu e^{\mu(t-T)} \phi(\cdot, T) = \mu e^{\mu(t-T)} \tilde{\phi}(T) \quad \text{for } t \geq T.$$

Meanwhile, from the monotonicity of almost all functions  $\phi_t(x, \cdot)$ , one has

$$\phi_t(\cdot, t) \leq \phi_t(\cdot, T) \leq \mu \phi(\cdot, T) = \mu \tilde{\phi}(T) \quad \text{for } t \leq T. \quad (2.26)$$

Hence, given  $t_0 > 0$  and setting

$$a_{t_0} = \alpha \sup \{1, e^{\mu(t_0-T)}\} \tilde{\phi}(T) \in L^1(\omega),$$

we obtain the estimate

$$0 \leq \phi_t(\cdot, t) \leq a_{t_0} \quad \text{for } |t| \leq t_0. \quad (2.27)$$

To prove (2.24), we may assume  $t_0 \geq T$ , since the same function  $b_T$  can be taken as  $b_{t_0}$  when  $t_0 \leq T$ . We shall find an appropriate choice for  $b_{t_0}$  by considering the three cases:  $\xi(\underline{x}) \leq T - t_0$ ,  $T - t_0 < \xi(\underline{x}) < T$  and  $\xi(\underline{x}) \geq T$ . Assume first  $\xi(\underline{x}) \leq T - t_0$ . Then, for  $|t| \leq t_0$ , one has  $\xi(\underline{x}) + t \leq T$ . From (2.23) and (2.26), we deduce

$$0 \leq (\phi_{\xi})_{\underline{t}}(\underline{x}, t) \leq \mu \tilde{\phi}(T)(\underline{x}). \quad (2.28)$$

Next, suppose  $T - t_0 < \xi(\underline{x}) < T$ . Since  $t_0 \geq T > 0$  by hypothesis and for  $|t| \leq t_0$ , we see that  $-2t_0 < \xi(\underline{x}) + t < 2t_0$ . Applying (2.27), we get

$$0 \leq (\phi_{\xi})_{\underline{t}}(\underline{x}, t) \leq a_{2t_0}(\underline{x}). \quad (2.29)$$

Finally, assume that  $\xi(\underline{x}) \geq T$ . For  $0 \leq t \leq t_0$ , relation (2.25) is available with  $\tau = \xi(\underline{x})$  and we obtain

$$\phi(\underline{x}, \xi(\underline{x}) + t) \leq e^{\mu t} \phi(\underline{x}, \xi(\underline{x})) = e^{\mu t} \tilde{\phi}(\xi)(\underline{x}) \leq e^{\mu t_0} \tilde{\phi}(\xi)(\underline{x}).$$

More generally, as soon as  $\xi(\underline{x}) + t \geq T$ , relations (2.17) and (2.23) yield

$$0 \leq (\phi_{\xi})_{\underline{t}}(\underline{x}, t) \leq \mu \phi(\underline{x}, \xi(\underline{x}) + t)$$

Together with the previous inequality, we find

$$0 \leq (\phi_{\xi})_{\underline{t}}(\underline{x}, t) \leq a e^{\mu t_0} \tilde{\phi}(\xi)(\underline{x}), \quad (2.30)$$

for  $0 \leq t \leq t_0$ . Next, due to the monotonicity of almost all functions  $\phi(\underline{x}, \cdot)$  and from (2.17):

$$0 \leq (\phi_{\xi})_t(x, t) \leq \mu \phi(x, \xi(x)) = \mu \tilde{\phi}(\xi)(x)$$

when  $t < 0$  and  $\xi(x) + t \geq T$ . This shows that inequality (2.30) is valid whenever  $\xi(x) \geq T$ ,  $|t| \leq t_0$  and  $\xi(x) + t \geq T$ . It remains to examine the case when  $\xi(x) \geq T$  and  $\xi(x) + t < T$ . If so,  $t$  is negative and

$$-t_0 < T - t_0 \leq \xi(x) + t < T \leq t_0,$$

whence, from (2.23) and (2.27),

$$0 \leq (\phi_{\xi})_t(x, t) \leq a_{t_0}(x). \quad (2.31)$$

According to the estimates (2.28)–(2.31) and since  $\tilde{\phi}(T)$ ,  $\tilde{\phi}(\xi)$ ,  $a_{t_0}$  and  $a_{2t_0}$  belong to the space  $L^1(\omega)$ , we can take

$$b_{t_0} = \sup\{\mu \tilde{\phi}(T), \mu e^{\mu t_0} \tilde{\phi}(\xi), a_{t_0}, a_{2t_0}\} \in L^1(\omega)$$

in (2.24) and the proof is complete.  $\square$

By localization and partition of unity, the results of this section easily carry over to the case in which the open set  $\omega$  is replaced by the Lipschitz continuous boundary  $\Gamma$  of a (bounded) open subset  $\Omega$  of  $\mathbb{R}^N$ . Indeed, this merely introduces positive measurable bounded weights, which does not affect the form of the required hypotheses. Further,  $\Gamma$  can also be replaced by any measurable subset  $\Gamma_C$  for it is immediately seen that the assumptions are not affected by extending all the data by zero for values of the variable  $x$  in  $\Gamma \setminus \Gamma_C$ . Theorem 2.1 below summarizes the conclusions in this new context.

Theorem 2.1: Let  $\Omega$  be an open bounded subset of  $\mathbb{R}^N$  with Lipschitz continuous boundary  $\Gamma$  and surface measure  $ds$  and let  $\Gamma_C \subset \Gamma$  be a measurable subset. Let  $\phi : \Gamma_C \times \mathbb{R} \rightarrow \mathbb{R}$  be a Carathéodory function and assume for almost all  $x \in \Gamma_C$  that the function  $\phi(x, \cdot)$  is continuously differentiable with  $\phi_t(x, \cdot)$  nondecreasing. Assume further

$$\phi_t(\cdot, t) \geq 0 \quad \text{for} \quad t > 0, \quad (2.32)$$

$$\phi_t(\cdot, t) = 0 \quad \text{for} \quad t \leq 0, \quad (2.33)$$

$$\phi(x, t) = \int_0^t \phi_t(x, \tau) d\tau \quad (<=> \phi(\cdot, 0) = 0), \quad (2.34)$$

and that there are constants  $T > 0$  and  $\mu > 0$  such that

$$\phi_t(\cdot, t) \leq \mu \phi_t(\cdot, t) \quad \text{for} \quad t \geq T, \quad (2.35)$$

with  $\phi(\cdot, t) \in L^1(\Gamma_C)$ . Setting

$$\Phi(x, t) = \int_0^t \phi(x, \tau) d\tau \quad (2.36)$$

and denoting by  $\tilde{\phi}_t$ ,  $\tilde{\phi}$  and  $\tilde{\Phi}$  the Nemytskii operators associated with  $\phi_t$ ,  $\phi$  and  $\Phi$  respectively, the following conclusions hold:

(i) The functional

$$j(\xi) = \begin{cases} \int_{\Gamma_C} \tilde{\Phi}(\xi) ds & \text{if } \tilde{\Phi}(\xi) \in L^1(\Gamma_C) \\ +\infty & \text{otherwise,} \end{cases} \quad (2.37)$$

defined for every measurable function  $\xi : \Gamma_C \rightarrow \mathbb{R}$  is lower semicontinuous on the space  $L^1(\Gamma_C)$ .

(ii) For every measurable function  $\xi$  such that  $\tilde{\Phi}(\xi) \in L^1(\Gamma_C)$  and every function  $\eta \in L^\infty(\Gamma_C)$  one has

$$\tilde{\phi}(\xi + \eta) \in L^1(\Gamma_C) , \quad \tilde{\phi}_t(\xi + \eta) \in L^1(\Gamma_C)$$

and the functional

$$\eta \in L^\infty(\Gamma_C) \rightarrow j_\xi(\eta) = j(\xi + \eta) \quad (2.38)$$

is real-valued and twice continuously differentiable with

$$j'_\xi(\eta) \cdot h = \int_{\Gamma_C} \tilde{\phi}(\xi + \eta) h \, ds , \quad (2.39)$$

$$j''_\xi(\eta) \cdot (h, k) = \int_{\Gamma_C} \tilde{\phi}_t(\xi + \eta) h k \, ds , \quad (2.40)$$

for every triple  $(\eta, h, k) \in [L^\infty(\Gamma_C)]^3$ .

Remark 2.2: Functions verifying the assumptions of Theorem 2.1

generate a convex cone containing all functions of the form

$$\phi(\underline{x}, t) = c(\underline{x})(t_+)^m ,$$

where  $m > 1$  is an arbitrary real number,  $t_+$  is the function

$$t_+(t) = \begin{cases} t & \text{if } t \geq 0 , \\ 0 & \text{if } t < 0 , \end{cases}$$

and  $c \in L^1(\Gamma_C)$  is an arbitrary nonnegative given function. Moreover, condition (2.35) allows for a modification of the growth of (convex combinations of) such functions as  $t$  tends to  $+\infty$ , up to and including exponential order.  $\square$

The assumptions on the function  $\phi$  made in Theorem 2.1, and in particular limitation of the growth in  $t$  to exponential order, will later allow us to characterize the solutions to the problem considered in §1 as minimizers of a convex functional with values in  $\mathbb{R}^+$ . As

usual, existence of minimizers will be obtained by establishing a coerciveness property, relying on complementary (and, of course, compatible) specification of the growth of the mapping  $\phi(\underline{x}, \cdot)$  for almost all  $\underline{x} \in \Gamma_C$ . The suitable hypothesis and its main consequences regarding the problem under consideration are examined as the next objective of this section.

As an additional assumption, we shall require that

$$0 \leq \frac{\phi(\underline{x}, t)}{t} \leq \phi_t(\underline{x}, t) \quad \text{for } t > 0 \text{ and almost all } \underline{x} \in \Gamma_C. \quad (2.41)$$

Note since the function  $\phi(\underline{x}, \cdot)$  is continuously differentiable that this new assumption implies  $\phi(\cdot, 0) = 0$  and hence makes condition (2.34) superfluous. Besides, it is easily checked that (2.41) amounts to saying that the function  $t \mapsto \phi(\underline{x}, t)/t$  is nondecreasing on  $(0, +\infty)$  for almost all  $\underline{x} \in \Gamma_C$ . This function is strictly increasing on  $(0, +\infty)$  under the mildly stronger condition

$$0 < \frac{\phi(\underline{x}, t)}{t} < \phi_t(\underline{x}, t) \quad \text{for } t > 0. \quad (2.42)$$

Monotonicity and nonnegativity properties allow us to set for almost all  $\underline{x} \in \Gamma_C$

$$\ell(\underline{x}) = \lim_{t \rightarrow +\infty} \frac{\phi(\underline{x}, t)}{t} \geq 0 \quad (\text{possibly } +\infty) \quad (2.43)$$

and  $\ell(\underline{x})$  is equivalently defined through any sequence  $(\phi(\underline{x}, t_k)/t_k)$  with  $\lim t_k = +\infty$  and verifies

$$\ell(\underline{x}) \geq \frac{\phi(\underline{x}, t)}{t} \quad \text{for every } t > 0$$

$$\text{and almost all } \underline{x} \in \Gamma_C. \quad (2.44)$$

As a result of Egorov's theorem,  $\ell$  is a measurable function on  $\Gamma_C$ .

Remark 2.3: It is obvious that functions verifying property (2.41) form a convex cone and that this assumption does not restrict the class described in Remark 2.2. This shows that adding condition (2.41) is compatible with the assumptions of Theorem 2.1, which is due to the fact that  $T > 0$  can be taken arbitrarily large in (2.35). Roughly speaking, the combination of (2.35) and (2.41) means that the growth of  $\phi(\underline{x}, \cdot)$  is superlinear and at most of exponential order, monotonicity being imposed by (2.32).  $\square$

Theorem 2.2: In addition to the hypotheses of Theorem 2.1, <sup>(2)</sup> assume that (2.41) holds and let  $\xi: \Gamma_C \rightarrow \mathbb{R}$  be a measurable function. Then, the mapping

$$t \mapsto \frac{1}{t^2} j(t\xi) \in \mathbb{R}^+, \quad (2.45)$$

where  $j$  denotes the functional (2.37), is nondecreasing on  $(0, +\infty)$  and

---

<sup>(2)</sup> Although assumption (2.35) can be omitted in this statement.

$$\lim_{t \rightarrow +\infty} \frac{1}{t^2} j(t\xi) = \frac{1}{2} \int_{\Gamma_C} \ell \xi_+^2 ds \quad (3) \quad (2.46)$$

where  $\xi_+ = \sup(\xi, 0)$  and with the (usual) convention that  $\ell(\underline{x}) \xi_+^2(\underline{x}) = 0$  when  $\ell(\underline{x}) = +\infty$  and  $\xi_+(\underline{x}) = 0$ .

Proof: A preliminary observation is that for almost all  $\underline{x} \in \Gamma_C$ , the function  $t \rightarrow \phi(\underline{x}, t)/t^2$  is nondecreasing on  $(0, +\infty)$ : To see this, it suffices to compute

$$\frac{\partial}{\partial t} \left( \frac{\phi(\underline{x}, t)}{t^2} \right) = \frac{1}{t^3} (t\phi(\underline{x}, t) - 2\phi(\underline{x}, t))$$

and note that  $t\phi(\underline{x}, t) - 2\phi(\underline{x}, t) \geq 0$  for  $t > 0$  as it follows by multiplying (2.41) by  $t$  and integrating. This yields the monotonicity of the function (2.45) from the relation (for  $t > 0$ )

$$\frac{1}{t^2} \phi(\underline{x}, t\xi(\underline{x})) = \begin{cases} \frac{\phi(\underline{x}, t\xi(\underline{x}))}{t^2 \xi^2(\underline{x})} \xi^2(\underline{x}) & \text{for } \xi(\underline{x}) > 0, \\ 0 & \text{for } \xi(\underline{x}) \leq 0. \end{cases} \quad (2.47)$$

A second conclusion from the above observation is that  $\lim_{t \rightarrow +\infty} \phi(\underline{x}, t)/t^2$  exists (possibly  $+\infty$ ) for almost all  $\underline{x} \in \Gamma_C$ . Actually, a more precise result is true, namely,

$$\lim_{t \rightarrow +\infty} \frac{\phi(\underline{x}, t)}{t^2} = \frac{1}{2} \lim_{t \rightarrow +\infty} \frac{\phi(\underline{x}, t)}{t} = \frac{1}{2} \ell(\underline{x}). \quad (2.48)$$

---

(3) Allowing, of course, the value  $+\infty$  for the right-hand side.



Although it holds in a much more general context, this relation is easy to prove under our assumptions. Indeed, it is a simple exercise to check that (2.48) follows from de l'Hospital's rule.

We are now in position to prove relation (2.46): Suppose first that the left-hand side of (2.46) is a (nonnegative) real number  $I$ . For every sequence  $t_k$  tending to  $+\infty$ , one has

$$I = \lim_{t_k} \frac{1}{2} \int_{\Gamma_C} \tilde{\phi}(t_k \xi) ds$$

and

$$\frac{1}{2} \int_{\Gamma_C} \tilde{\phi}(t_k \xi) ds \geq I \quad \text{for every } k \in \mathbb{N}. \quad (2.49)$$

On the other hand, it follows from (2.47) and (2.48) (and the convention  $\ell(\underline{x})\xi_+^2(\underline{x}) = 0$  when  $\ell(\underline{x}) = +\infty$  and  $\xi_+(\underline{x}) = 0$ ) that the sequence  $\phi(\underline{x}, t_k \xi(\underline{x}))/t_k^2$  tends to  $\ell(\underline{x})\xi_+^2(\underline{x})/2$  almost everywhere on  $\Gamma_C$ . With (2.49) and Fatou's theorem, it follows that

$$\frac{1}{2} \int_{\Gamma_C} \ell \xi_+^2 ds \leq I.$$

To prove that  $\frac{1}{2} \int_{\Gamma_C} \ell \xi_+^2 ds = I$ , we shall use the inequality

$$\frac{\phi(\underline{x}, t)}{t^2} \leq \frac{1}{2} \ell(\underline{x}) \quad \text{for } t > 0,$$

which follows from (2.48) and the monotonicity of  $\phi(\underline{x}, t)/t^2$ . With (2.47), this yields

$$\frac{1}{2} \ell \xi_+^2 \geq \frac{1}{2} \tilde{\phi}(t \xi) \quad \text{for } t > 0. \quad (2.50)$$

Hence,

$$\frac{1}{2} \int_{\Gamma_C} \lambda \xi_+^2 ds \geq \frac{1}{t^2} \int_{\Gamma_C} \tilde{\phi}(t\xi) ds = \frac{1}{t^2} j(t\xi)$$

and, in the limit as  $t$  tends to  $+\infty$ , we get

$$\frac{1}{2} \int_{\Gamma_C} \lambda \xi_+^2 ds \geq I.$$

Assume next that the right-hand side of (2.46) is a (nonnegative) real number, namely  $\lambda \xi_+^2 \in L^1(\Gamma_C)$ . If so, relation (2.46) follows from Lebesgue's dominated convergence theorem by using a sequence  $t_k > 0$  tending to  $+\infty$  in (2.50). As both sides of (2.46) coincide when either one is finite, they coincide when either one is  $+\infty$  as well, and the proof is complete.  $\square$

### 3. Variational formulation.

This section is intended to show the equivalence of the contact problem described in Section 1 with a minimization problem over the space  $(H^1(\Omega))^N$ . We shall begin with a review of some classical results and introduce a few notations to be used throughout the remainder of this paper.

Given a bounded domain  $\Omega$  with a Lipschitz continuous boundary  $\Gamma$ , the outer normal  $\underline{n}$  is defined almost everywhere (see e.g., [10]) and is a measurable function. Componentwise, we then have

$$n_i \in L^\infty(\Gamma), \quad 1 \leq i \leq N,$$

(3.1)

$$\sum_{i=1}^N n_i^2 = 1 \quad \text{on } \Gamma.$$

AD-A174 585

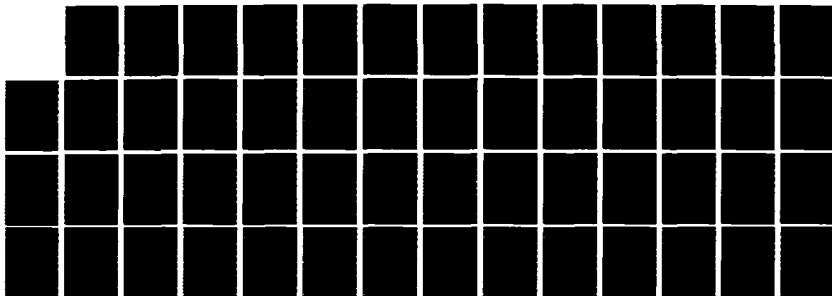
COMPUTATIONAL METHODS FOR NONLINEAR DYNAMICS PROBLEMS  
IN SOLID AND STRUCT (U) COMPUTATIONAL MECHANICS CO INC  
AUSTIN TX J T ODEN 31 MAR 86 TR-86-02 AFOSR-TR-86-2015  
F49620-84-C-0024

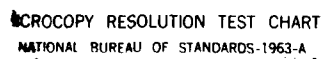
4/4

UNCLASSIFIED

F/G 20/11

NL





XEROCOPY RESOLUTION TEST CHART  
NATIONAL BUREAU OF STANDARDS-1963-A

The space  $H^1(\Omega)$  is the usual Sobolev space of distributions with partial derivatives of order  $\leq 1$  in  $L^2(\Omega)$ . The space  $(H^1(\Omega))^N$  is endowed with the usual inner product inducing the norm

$$\|\underline{v}\|_{1,\Omega} = [\int_{\Omega} (v_i v_i + v_{i,j} v_{i,j}) dx]^{\frac{1}{2}}. \quad (3.2)$$

The trace operator maps the space  $(H^1(\Omega))^N$  linearly and continuously onto the space  $(H^{\frac{1}{2}}(\Gamma))^N$ , with topological dual

$$[(H^{\frac{1}{2}}(\Gamma))^N]' = (H^{-\frac{1}{2}}(\Gamma))^N. \quad (3.3)$$

From (3.1) and for every  $1 \leq p \leq +\infty$ , a given element  $\underline{\xi} \in (L^p(\Gamma))^N$  has a decomposition of the form

$$\underline{\xi} = \underline{\xi}_T + \underline{\xi}_n \underline{n}, \quad (3.4)$$

with

$$\begin{aligned} \underline{\xi}_n &= \underline{\xi} \cdot \underline{n} = \xi_i n_i \in L^p(\Gamma), \\ \underline{\xi}_T &= \underline{\xi} - \underline{\xi}_n \underline{n} \in (L^p(\Gamma))^N. \end{aligned} \quad (3.5)$$

The components  $\underline{\xi}_n$  and  $\underline{\xi}_T$  will be referred to as the normal and tangential components of  $\underline{\xi}$  respectively.

We next make precise the assumptions on the data of the problem: We shall assume that the elasticity coefficients  $E_{ijkl}$  verify

$$E_{ijkl} \in L^\infty(\Omega) \quad (3.6)$$

and that the uniform ellipticity condition

$$E_{ijkl}(x) A_{kl} A_{ij} \geq \alpha A_{ij} A_{ij}$$

holds with some constant  $\alpha$  for almost all  $x \in \Omega$  and every  $N \times N$  symmetric array  $A_{ij}$ .

The body forces are chosen so that

$$\underline{b} \in (L^2(\Omega))^N, \quad (3.7)$$

while the prescribed tractions  $\underline{t}$  on  $\Gamma_F = \Gamma \setminus \Gamma_C$  are submitted to the condition

$$\underline{t} \in (L^2(\Gamma_F))^N. \quad (3.8)$$

The function  $\phi : \Gamma_C \times \mathbb{R} \rightarrow \mathbb{R}$  characterizing the normal response along  $\Gamma_C$  is supposed to fulfill the assumptions of Theorem 2.2, namely  $\phi$  is a Carathéodory function such that the mapping  $\phi(\underline{x}, \cdot)$  is continuously differentiable for almost all  $\underline{x} \in \Gamma_C$  and

$$0 \leq \frac{\phi(\cdot, t)}{t} \leq \phi_t(\cdot, t) \quad \text{for } t > 0 \quad (4) \quad (3.10)$$

$$\begin{aligned} \phi_t(\underline{x}, \cdot) &\text{ is nondecreasing for almost all } \underline{x} \in \Gamma_C, \\ \phi_t(\cdot, t) &= 0 \quad \text{for } t \leq 0, \end{aligned} \quad (3.11)$$

and there are constants  $T > 0$  and  $\mu > 0$  such that

$$\phi_t(\cdot, t) \leq \mu \phi(\cdot, t) \quad \text{for } t \geq T, \quad (3.12)$$

with  $\phi(\cdot, T) \in L^1(\Gamma_C)$ .

Physical justification of these assumptions is provided by Remarks 2.2 and 2.3 and the related comments of §1.

In what follows, we shall denote by  $a(\cdot, \cdot)$  the continuous bilinear form over  $(H^1(\Omega))^N$  defined by

---

(4) Recall that this condition implicitly contains (2.34).

$a(\underline{u}, \underline{v})$  = virtual work produced by the action of the stresses  $\underline{\sigma}(\underline{u})$  on the strains  $\underline{\varepsilon}(\underline{v})$

$$= \int_{\Omega} |\underline{\sigma}(\underline{u}) : \underline{\varepsilon}(\underline{v})| dx = \int_{\Omega} E_{ijkl} \partial_l u_k \partial_j v_i dx \quad (3.13)$$

The external forces (body forces  $\underline{b}$  and prescribed tractions  $\underline{t}$ ) are described by an element  $\underline{f} \in [(H^1(\Omega))^N]^*$  through the relation

$$\langle \underline{f}, \underline{v} \rangle_{\Omega} = \int_{\Omega} \underline{b} \cdot \underline{v} dx + \int_{\Gamma_F} \underline{t} \cdot \underline{v} ds, \quad (3.14)$$

a formula in which  $\langle \cdot, \cdot \rangle_{\Omega}$  stands for the duality pairing between  $(H^1(\Omega))^N$  and its topological dual.

Our aim is to examine how the problem (1.8)-(1.10) relates to the minimization problem: Minimize

$$\frac{1}{2} a(\underline{v}, \underline{v}) + \int_{\Gamma_C} \tilde{\phi}(\underline{v}_n) ds - \langle \underline{f}, \underline{v} \rangle_{\Omega} \quad \text{for } \underline{v} \in (H^1(\Omega))^N,$$

where, as in §2,  $\tilde{\phi}$  is the Nemytskii operator associated with the function  $\phi(\underline{x}, t) = \int_0^t \phi(\underline{x}, \tau) d\tau$ . However, as the integral  $\int_{\Gamma_C} \tilde{\phi}(\underline{v}_n) ds$  is not defined in general, the correct formulation of the above problem is: Minimize

$$\frac{1}{2} a(\underline{v}, \underline{v}) + j(\underline{v}_n) - \langle \underline{f}, \underline{v} \rangle_{\Omega} \quad \text{for } \underline{v} \in (H^1(\Omega))^N,$$

where, for every measurable function  $\xi: \Gamma_C \rightarrow \mathbb{R}$ , we have set

$$j(\xi) = \begin{cases} \int_{\Gamma_C} \tilde{\phi}(\xi) ds & \text{if } \tilde{\phi}(\xi) \in L^1(\Gamma_C), \\ +\infty & \text{otherwise.} \end{cases} \quad (3.16)$$

The first step of our approach is classical and relies upon a generalization of Green's formula, given in Lemma 3.1 below, whose proof can, for instance, be found in [6, Theorems 5.8 and 5.9]. We denote by  $D(\Omega)$  the space of indefinitely differentiable functions with compact support in  $\Omega$ , equipped with the usual inductive limit topology, and by  $D'(\Omega)$  its topological dual, the space of distributions over  $\Omega$ . We shall also make use of the spaces  $D(\bar{\Omega})$  and  $D(\Gamma)$  of restriction to  $\bar{\Omega}$  and  $\Gamma$ , respectively, of indefinitely differentiable functions on  $\mathbb{R}^N$ .

Consider the operator

$$\operatorname{div} \underline{\sigma} : (H^1(\Omega))^N \rightarrow (D'(\Omega))^N \quad (3.17)$$

$$[\operatorname{div} \underline{\sigma}(\underline{v})]_i = \partial_j \sigma_{ij}(\underline{v}) = \partial_j (E_{ijkl} \partial_l v_k)$$

and define the subspace  $H_{\operatorname{div} \underline{\sigma}}(\Omega)$  of  $(H^1(\Omega))^N$  by

$$H_{\operatorname{div} \underline{\sigma}}(\Omega) = \{ \underline{v} \in (H^1(\Omega))^N ; \operatorname{div} \underline{\sigma}(\underline{v}) \in (L^2(\Omega))^N \} . \quad (3.18)$$

Lemma 3.1 (Generalized Green's formula): There is a unique linear continuous operator

$$\pi : H_{\operatorname{div} \underline{\sigma}}(\Omega) \rightarrow (H^{\frac{1}{2}}(\Omega))^N ,$$

satisfying

$$[\pi(\underline{u})]_i = \sigma_{ij}(\underline{u}) n_j \quad \text{on } \Gamma$$

for every  $\underline{u} \in (H^1(\Omega))^N$  such that  $\sigma_{ij}(\underline{u}) = E_{ijkl} \partial_l u_k \in C^1(\bar{\Omega})$ ,

$1 \leq i, j, k, l \leq N$  and

$$a(\underline{u}, \underline{v}) + \int_{\Omega} (\operatorname{div} \underline{\sigma}(\underline{u})) \cdot \underline{v} \, dx = \langle \pi(\underline{u}), \underline{v} \rangle_{\Gamma} , \quad (3.19)$$



for every  $\underline{u} \in H_{\text{div}}(\Omega)$  and every  $\underline{v} \in (H^1(\Omega))^N$ , where  $\langle \cdot, \cdot \rangle_\Gamma$  denotes the duality pairing between  $(H^{\frac{1}{2}}(\Omega))^N$  and  $(H^{-\frac{1}{2}}(\Omega))^N$ .

Due to the above lemma, a generalized form of problem

(1.8)-(1.10) is:

Find  $\underline{u} \in (H^1(\Omega))^N$  such that

$$\text{div} \underline{u} + \underline{b} = \underline{0} \quad \text{in } \Omega, \quad (3.20)$$

with the boundary conditions

$$\pi(\underline{u}) = \underline{t} \quad \text{on } \Gamma_F, \quad (3.21)$$

$$\pi(\underline{u}) = -\tilde{\phi}(\underline{u}_n)\underline{n} \quad \text{on } \Gamma_C. \quad (3.22)$$

Note, however, that this formulation contains some ambiguity. Indeed,  $\pi(\underline{u})$  is merely in the space  $(H^{\frac{1}{2}}(\Omega))^N$  while  $\tilde{\phi}(\underline{u}_n)$  - hence,  $\tilde{\phi}(\underline{u}_n)\underline{n}$  - is only a measurable function. As  $\pi(\underline{u})$  is not a function in general, and a measurable function does not induce a distribution in a canonical sense, it is not clear how relation (3.22) must be understood. To circumvent this difficulty, we shall include, as a part of the problem, the condition

$$\pi(\underline{u}) \in (L^1(\Gamma))^N. \quad (3.23)$$

Such a condition does make sense in  $(D'(\Gamma))^N$ : It means that the action of the distribution  $\pi(\underline{u})$  on elements  $\underline{\xi} \in (D(\Gamma))^N$  is represented (in a necessarily unique way) by some element of  $(L^1(\Gamma))^N$ . As usual, the notation  $\pi(\underline{u})$  stands for both the distribution and its representative in  $(L^1(\Gamma))^N$ . Conditions (3.21) and (3.22) can then be understood in the sense of measurable functions, namely, almost

everywhere. We now give a first characterization of solutions to problem (3.20)-(3.23).

Lemma 3.2: An element  $\underline{u} \in (H^1(\Omega))^N$  is a solution to problem (3.20)-(3.23) if and only if  $\tilde{\phi}(\underline{u}_n) \in L^1(\Gamma_C)$  and

$$a(\underline{u}, \underline{v}) + \int_{\Gamma_C} \tilde{\phi}(\underline{u}_n) \underline{v}_n \, ds = \langle \underline{f}, \underline{v} \rangle_{\Omega} \quad \text{for every } \underline{v} \in (D(\bar{\Omega}))^N. \quad (3.24)$$

Proof: Let  $\underline{u} \in (H^1(\Omega))^N$  be a solution to problem (3.20)-(3.23). From (3.22) and (3.23), one has  $\tilde{\phi}(\underline{u}_n) \underline{n} \in (L^1(\Gamma_C))^N$  and hence  $\tilde{\phi}(\underline{u}_n) = \tilde{\phi}(\underline{u}_n) \underline{n} \cdot \underline{n} \in L^1(\Gamma_C)$ . Multiplying (3.20) by  $\underline{v} \in (D(\bar{\Omega}))^N$  and integrating over  $\Omega$ , the generalized Green's formula (3.19) of Lemma 3.1 yields

$$0 = \int_{\Omega} (\operatorname{div} \sigma(\underline{u}) + \underline{b}) \cdot \underline{v} \, dx = \langle \pi(\underline{u}), \underline{v} \rangle_{\Gamma} - a(\underline{u}, \underline{v}) + \int_{\Omega} \underline{b} \cdot \underline{v} \, dx. \quad (3.25)$$

The expression  $\langle \pi(\underline{u}), \underline{v} \rangle_{\Gamma}$  depends on the restriction of  $\underline{v}$  to the boundary  $\Gamma$  only, an element of  $(D(\Gamma))^N$ . Thus, applying (3.23), we get

$$\langle \pi(\underline{u}), \underline{v} \rangle_{\Gamma} = \int_{\Gamma} \pi(\underline{u}) \cdot \underline{v} \, ds. \quad (3.26)$$

Using a decomposition of the integral over  $\Gamma$  into integrals over  $\Gamma_C$  and  $\Gamma_F$  and from (3.21) and (3.22), (3.26) reads

$$\langle \pi(\underline{u}), \underline{v} \rangle_{\Gamma} = \int_{\Gamma_F} \underline{t} \cdot \underline{v} \, ds + \int_{\Gamma_C} \tilde{\phi}(\underline{u}_n) \underline{n} \cdot \underline{v} \, ds. \quad (3.27)$$

As  $\tilde{\phi}(u_n)\underline{n} \cdot \underline{v} = \tilde{\phi}(u_n)v_n$  by definition of  $v_n$ , it suffices to combine (3.25) and (3.27) and use the definition (3.14) of the external forces  $\underline{f}$  to see that  $\underline{u}$  is a solution to equation (3.24).

Conversely, let  $\underline{u} \in (H^1(\Omega))^N$  be a solution to equation (3.24) such that  $\tilde{\phi}(u_n) \in L^1(\Gamma_C)$ . Taking  $\underline{v}$  arbitrary in  $(D(\Omega))^N$  and by definition of  $\underline{f}$  (cf. (3.14)) it is immediate that  $\text{div} \underline{v}(\underline{u}) = \underline{b}$  in  $(D'(\Omega))^N$  and hence  $\underline{u}$  belongs to the space  $H_{\text{div} \underline{v}}$  (3.18). Together with the generalized Green's formula (3.19) of Lemma 3.1, we see for an arbitrary  $\underline{v} \in (D(\bar{\Omega}))^N$  that

$$\int_{\Gamma_C} \tilde{\phi}(u_n)v_n \, ds + \langle \pi(\underline{u}), \underline{v} \rangle_{\Gamma} = \int_{\Gamma_F} \underline{t} \cdot \underline{v} \, ds,$$

or, equivalently,

$$\langle \pi(\underline{u}), \underline{v} \rangle_{\Gamma} = - \int_{\Gamma_C} \tilde{\phi}(u_n)v_n \, ds + \int_{\Gamma_F} \underline{t} \cdot \underline{v} \, ds.$$

This relation involves restrictions of elements of  $(D(\bar{\Omega}))^N$  to the boundary  $\Gamma$  only, and hence can be equivalently stated for an arbitrary  $\underline{v} \in (D(\Gamma))^N$ . As  $\tilde{\phi}(u_n) \in L^1(\Gamma_C)$ , one has  $\tilde{\phi}(u_n)\underline{n} \in (L^1(\Gamma_C))^N$  and it follows that the distribution  $\pi(\underline{u})$  is represented by the element of  $(L^1(\Gamma))^N$  defined by  $\underline{t}$  on  $\Gamma_F$  and by  $\tilde{\phi}(u_n)\underline{n}$  on  $\Gamma_C$ . Hence,  $\underline{u}$  is a solution to problem (3.20)-(3.23).  $\square$

Let  $\underline{u} \in (H^1(\Omega))^N$  be a solution to problem (3.20)-(3.23). From relation (3.24), it is clear that the mapping  $\underline{v} \in (D(\bar{\Omega}))^N \rightarrow \int_{\Gamma_C} \tilde{\phi}(u_n)v_n \, ds$  extends as a linear continuous form over  $(H^1(\Omega))^N$ , say  $\langle \tilde{\phi}(u_n)\underline{n}, \underline{v} \rangle_{\Omega}$  (depending on the trace of  $\underline{v}$  on  $\Gamma$  only) and relation (3.24) remains valid with  $\langle \tilde{\phi}(u_n)\underline{n}, \underline{v} \rangle_{\Omega}$  replacing  $\int_{\Gamma_C} \tilde{\phi}(u_n)v_n \, ds$  for an arbitrary  $\underline{v} \in (H^1(\Omega))^N$ . On the other hand,

from Theorems 2.1 and 2.2, the expression  $\langle \tilde{\phi}(u_n)_n, \underline{v} \rangle_\Omega$  strongly resembles the derivative at  $\underline{u}$  of the functional

$$\underline{v} \in (H^1(\Omega))^N \mapsto j(\underline{v}_n), \quad (3.28)$$

where  $j$  is the functional (3.16). Strictly speaking, this is not true since the functional (3.28) is not differentiable (for instance, because it may take the value  $+\infty$ ). In some cases, lack of differentiability for convex functionals is not too serious a problem, but a standard assumption is that the functional at least have a domain with nonempty interior, i.e., be continuous on a nonempty open subset.

Here, this condition is not satisfied in general: For choices of  $N$  and  $\phi$  such that the Sobolev embedding theorems are not available, the functional (3.28) may perfectly be continuous at no point of  $(H^1(\Omega))^N$  since it may take the value  $+\infty$  near any point  $\underline{v}$  with  $j(\underline{v}_n) < +\infty$ . The idea of using Orlicz-like spaces is complicated by the fact that the function  $\phi$  is allowed to depend on the point  $\underline{x} \in \Gamma_C$ . Besides, it is not clear at all that changing the space  $(H^1(\Omega))^N$  into a smaller one, over which the functional (3.28) would have nicer properties, would not lead to later problems (as far as coerciveness is concerned for instance). Despite the fact that the functional (3.28) is convex, we have then no standard way of justifying the arguments with which it is formally easy to deduce that solutions to problem (3.20)–(3.23) are minimizers of the functional (3.15).

To make up for the lack of regularity of the functional (3.28), we shall adopt an approach based on convexity properties of the function

$\phi$  instead of convexity of the functional (3.28) directly. But, to do this, it is essential to obtain further information on the term  $\langle \tilde{\phi}(u_n)_n, y \rangle_\Omega$  for a general  $y \in (H^1(\Omega))^N$ : The next few results are devoted to proving (in Lemma 3.6) for every  $y \in (H^1(\Omega))^N$  and provided that  $u$  is a solution to (3.20)-(3.23) that  $\tilde{\phi}(u_n)_n v_n \in L^1(\Gamma_C)$  and  $\langle \phi(u_n)_n, y \rangle_\Omega = \int_{\Gamma_C} \phi(u_n) v_n \, ds$ , exactly as when  $y \in (D(\Omega))$ . A somewhat surprising assertion in which non-negativity of the function  $\phi$  is one of the two keys.

Lemma 3.3: Let  $T \geq 0$  be an element of  $L^1(\Gamma_C)$  and suppose that the mapping

$$v \in D(\bar{\Omega}) \rightarrow \int_{\Gamma_C} T v \, ds \quad (3.29)$$

extends as a linear continuous form  $\langle T, v \rangle_\Omega$  over the space  $H^1(\Omega)$ . Then, for every  $v \in H^1(\Omega)$ , one has  $T v \in L^1(\Gamma_C)$  and

$$\langle T, v \rangle_\Omega = \int_{\Gamma_C} T v \, ds \quad \text{for every } v \in H^1(\Omega). \quad (3.30)$$

Proof: Let  $v \in H^1(\Omega)$  be given. Suppose first  $0 \leq v \leq M$  for some constant  $M$ . Using the classical procedure of extension to  $H^1(\mathbb{R}^N)$  and regularization, it is easy to find a sequence  $(v^{(k)})$  of elements of  $D(\bar{\Omega})$  tending to  $v$  in  $H^1(\Omega)$  and verifying  $0 \leq v^{(k)} \leq M$ . After extracting a sub-sequence, we may assume that  $v^{(k)}$  tends to  $v$  almost everywhere on  $\Gamma_C$ . From the continuity of  $\langle T, \cdot \rangle_\Omega$  on the one hand and Lebesgue's dominated convergence theorem on the other hand, we get  $\langle T, v \rangle_\Omega = \lim \int_{\Gamma_C} T v^{(k)} \, ds$  and  $T v \in L^1(\Gamma_C)$

with  $\int_{\Gamma_C} Tv \, ds = \lim \int_{\Gamma_C} Tv^{(k)} \, ds$ . These relations prove (3.30) when  $0 \leq v \leq M$ .

Suppose next that  $v \geq 0$ . For every  $k \in N - \{0\}$  set

$$v^{(k)} = \inf(v, k).$$

Clearly,  $0 \leq v^{(k)} \leq k$  and  $v^{(k)} \in H^1(\Omega)$  for every  $k$  (cf. [11, Lemma 1.1, p. 313]). Arguing as in [11], it is easily seen that  $\|v^{(k)}\|_{1,\Omega} \leq \|v\|_{1,\Omega}$ . As  $v^{(k)}$  tends to  $v$  in  $L^2(\Omega)$ , it follows that  $v$  is the unique cluster point of the sequence  $(v^{(k)})$  in the weak topology of  $H^1(\Omega)$  and, hence,  $v^{(k)} \rightharpoonup v$  in  $H^1(\Omega)$ . As a result,  $\langle T, v \rangle_\Omega = \lim \langle T, v^{(k)} \rangle_\Omega$ . But  $\langle T, v^{(k)} \rangle_\Omega = \int_{\Gamma_C} Tv^{(k)} \, ds$  from the first part of the proof, so that

$$\langle T, v \rangle_\Omega = \lim \int_{\Gamma_C} Tv^{(k)} \, ds. \quad (3.31)$$

From the non-negativity of  $T$ , the sequence  $(Tv^{(k)})$  is non-negative and non-decreasing and tends to  $Tv$  almost everywhere. Applying the monotone convergence theorem, we find

$$\int_{\Gamma_C} Tv \, ds = \lim \int_{\Gamma_C} Tv^{(k)} \, ds. \quad (3.32)$$

The combination of (3.31) and (3.32) shows that  $Tv \in L^1(\Gamma_C)$  and (3.30) holds when  $v \geq 0$ .

Finally, let  $v$  be arbitrary in  $H^1(\Omega)$  and write  $v = v_+ - v_-$  with  $v_+ = \sup(v, 0)$ ,  $v_- = -\inf(v, 0)$ . From [11, Lemma 1.1, p. 313], we know that  $v_+$  and  $v_-$  belong to  $H^1(\Omega)$ . Thus,

$$\langle T, v \rangle_\Omega = \langle T, v_+ \rangle_\Omega - \langle T, v_- \rangle_\Omega.$$

From the above and since  $v_+$  and  $v_-$  are non-negative,  $Tv_+$  and  $Tv_-$  are in  $L^1(\Gamma_C)$  and this relation reads

$$\langle T, v \rangle_\Omega = \int_{\Gamma_C} Tv_+ \, ds - \int_{\Gamma_C} Tv_- \, ds = \int_{\Gamma_C} Tv \, ds ,$$

which completes the proof.  $\square$

The following result is a first extension of Lemma 3.3 to vector-valued functions.

Lemma 3.4: Let  $\underline{T} \in (L^1(\Gamma_C))^N$  be given and suppose that the components  $T_i$  of  $\underline{T}$  in the canonical basis of  $\mathbb{R}^N$  verify  $T_i \geq 0$ ,  $1 \leq i \leq N$ . Suppose also that the mapping

$$\underline{v} \in (D(\bar{\Omega}))^N \rightarrow \int_{\Gamma_C} \underline{T} \cdot \underline{v} \, ds$$

extends as a linear continuous form  $\langle \underline{T}, \underline{v} \rangle_\Omega$  over the space  $(H^1(\Omega))^N$ . Then, for every  $\underline{v} \in (H^1(\Omega))^N$ , one has  $\underline{T} \cdot \underline{v} \in L^1(\Gamma_C)$  and

$$\langle \underline{T}, \underline{v} \rangle_\Omega = \int_{\Gamma_C} \underline{T} \cdot \underline{v} \, ds .$$

Proof: Let  $1 \leq i \leq N$  be fixed and take  $v \in H^1(\Omega)$ . Denote by  $\underline{v} \in (H^1(\Omega))^N$  the vector-valued function whose components of order  $j \neq i$  are 0 and whose  $i^{\text{th}}$  component is  $v$ . For  $v \in D(\bar{\Omega})$ , one has  $\underline{v} \in (D(\bar{\Omega}))^N$  and

$$\langle \underline{T}, \underline{v} \rangle_\Omega = \int_{\Gamma_C} \underline{T} \cdot \underline{v} \, ds = \int_{\Gamma_C} T_i v \, ds .$$

As the mapping  $v \in H^1(\Omega) \rightarrow \underline{v} \in (H^1(\Omega))^N$  is obviously continuous, this shows that the mapping

$$v \in \mathcal{D}(\bar{\Omega}) \rightarrow \int_{\Gamma_C} T_1 v \, ds$$

extends as a linear continuous form  $\langle T_1, v \rangle_\Omega$  over  $H^1(\Omega)$ . Applying Lemma 3.3, it follows that  $T_1 v \in L^1(\Gamma_C)$  for every  $v \in H^1(\Omega)$  and

$$\langle T_1, v \rangle = \int_{\Gamma_C} T_t v \, ds.$$

From the denseness of  $(\mathcal{D}(\bar{\Omega}))^N$  in  $(H^1(\Omega))^N$ , the identity

$$\langle \underline{T}, \underline{v} \rangle_\Omega = \sum_{i=1}^N \langle T_i, v_i \rangle_\Omega$$

for  $\underline{v} = (v_i) \in (\mathcal{D}(\bar{\Omega}))^N$  remains valid for  $\underline{v} = (v_i) \in (H^1(\Omega))^N$  and thus reads

$$\langle \underline{T}, \underline{v} \rangle_\Omega = \sum_{i=1}^N \int_{\Gamma_C} T_i v_i \, ds = \int_{\Gamma_C} \underline{T} \cdot \underline{v} \, ds. \quad \square$$

Lemma 3.4 can be considerably generalized as follows:

Lemma 3.5: Let  $\underline{T} \in (L^1(\Gamma_C))^N$  be given and suppose that the mapping

$$\underline{v} \in (\mathcal{D}(\bar{\Omega}))^N \rightarrow \int_{\Gamma_C} \underline{T} \cdot \underline{v} \, ds$$

extends as a linear continuous form  $\langle \underline{T}, \underline{v} \rangle_\Omega$  over the space  $(H^1(\Omega))^N$ .

Let  $(\Gamma_k)$  be a finite covering of  $\Gamma$  by open subsets and suppose for every  $k$  that there is a system of coordinates in  $\mathbb{R}^N$  in



which  $T_i \geq 0$  on  $\Gamma_C \cap \Gamma_k$  <sup>(5)</sup>,  $1 \leq i \leq N$ . Then, for every  $\underline{v} \in (H^1(\Omega))^N$  one has  $\underline{T} \cdot \underline{v} \in L^1(\Gamma_C)$  and

$$\langle \underline{T}, \underline{v} \rangle_\Omega = \int_{\Gamma_C} \underline{T} \cdot \underline{v} \, ds.$$

Proof: Each open subset  $\Gamma_k$  of  $\Gamma$  is the intersection  $U_k \cap \Gamma$  of  $\Gamma$  with an open subset  $U_k$  of  $\bar{\Omega}$ . Let  $(\theta, \theta_k)$  be a partition of unity associated with the covering  $(\Omega, U_k)$  of  $\bar{\Omega}$ . For  $\underline{v} \in (D(\bar{\Omega}))^N$ , one has  $\theta_k \underline{v} \in (D(\bar{\Omega}))^N$  and

$$\int_{\Gamma_C} \underline{T} \cdot \theta_k \underline{v} \, ds = \int_{\Gamma_C} \theta_k \underline{T} \cdot \underline{v} \, ds.$$

The multiplication by  $\theta_k$  being continuous from  $(H^1(\Omega))^N$  into itself, this shows that the mapping

$$\underline{v} \in (D(\bar{\Omega}))^N \rightarrow \int_{\Gamma_C} \theta_k \underline{T} \cdot \underline{v} \, ds$$

extends as a linear continuous form  $\langle \theta_k \underline{T}, \underline{v} \rangle_\Omega$  over the space  $(H^1(\Omega))^N$ .

Let  $\chi_1, \dots, \chi_N$  be a basis of  $\mathbb{R}^N$  such that  $\underline{T} = \sum_{i=1}^N T_i \chi_i$  with  $T_i \geq 0$ ,  $1 \leq i \leq N$ , on  $\Gamma_C \cap \Gamma_k$  (such a basis exists by hypothesis). Denote by  $\underline{e}_1, \dots, \underline{e}_N$  the canonical basis of  $\mathbb{R}^N$  and by  $A \in \text{Isom}(\mathbb{R}^N)$  the linear mapping defined by

$$A \chi_i = \underline{e}_i, \quad 1 \leq i \leq N.$$

---

(5) A condition obviously fulfilled whenever  $\Gamma_C \cap \Gamma_k = \emptyset$ .

Set

$$\underline{S}_k = \sum_{i=1}^N \theta_k T_i \underline{e}_i \in (L^1(\Gamma_C))^N. \quad (3.33)$$

For  $\underline{v} \in (H^1(\Omega))^N$ , one has

$$\underline{S}_k \cdot \underline{v} = \sum_{i=1}^N \theta_k T_i \underline{e}_i \cdot \underline{v} = A(\theta_k \underline{T}) \cdot \underline{v} = \theta_k \underline{T} \cdot A^* \underline{v}, \quad (3.34)$$

where  $A^*$  is the adjoint of  $A$ . Obviously, the mapping  $\underline{v} \rightarrow A^* \underline{v}$  is an isomorphism of  $(H^1(\Omega))^N$  and  $A^*(D(\bar{\Omega}))^N = (D(\bar{\Omega}))^N$ . From (3.34), it then follows that the mapping

$$\underline{v} \in (D(\bar{\Omega}))^N \rightarrow \int_{\Gamma_C} \underline{S}_k \cdot \underline{v} \, ds \quad (= \int_{\Gamma_C} \theta_k \underline{T} \cdot A^* \underline{v} \, ds)$$

extends as a linear continuous form  $\langle \underline{S}_k, \underline{v} \rangle_{\Omega}$  over the space  $(H^1(\Omega))^N$ . In addition

$$\langle \underline{S}_k, \underline{v} \rangle_{\Omega} = \langle \theta_k \underline{T}, A^* \underline{v} \rangle_{\Omega} \quad (3.35)$$

for every  $\underline{v} \in (H^1(\Omega))^N$  since equality holds for  $\underline{v} \in (D(\bar{\Omega}))^N$ . On the other hand, the components  $\theta_k T_i$ ,  $1 \leq i \leq N$ , of  $\underline{S}_k$  in the canonical basis of  $\mathbb{R}^N$  verify  $\theta_k T_i \geq 0$  on  $\Gamma_k \cap \Gamma_C$  since  $\theta_k \geq 0$ . As  $\text{supp } \theta_k \subset \Gamma_k$ , one has  $\theta_k T_i \geq 0$  on  $\Gamma_C$  and Lemma 3.4 ensures for every  $\underline{v} \in (H^1(\Omega))^N$  that  $\underline{S}_k \cdot \underline{v} \in L^1(\Gamma_C)$  with

$$\langle \underline{S}_k, \underline{v} \rangle_{\Omega} = \int_{\Gamma_C} \underline{S}_k \cdot \underline{v} \, ds.$$

Using this result in conjunction with (3.34) and (3.35) in which  $(A^*)^{-1} \underline{v}$  replaces  $\underline{v}$  and since the mapping  $\underline{v} \rightarrow (A^*)^{-1} \underline{v}$  is

continuous from  $(H^1(\Omega))^N$  into itself, we deduce for every  $\underline{v} \in (H^1(\Omega))^N$  that  $\Theta_k \underline{T} \cdot \underline{v} \in L^1(\Gamma_C)$  with

$$\langle \Theta_k \underline{T}, \underline{v} \rangle_\Omega = \int_{\Gamma_C} \Theta_k \underline{T} \cdot \underline{v} \, ds. \quad (3.36)$$

Since  $\sum_k \Theta_k = 1$  on  $\Gamma$ , one has  $\underline{T} \cdot \underline{v} = \sum_k \Theta_k \underline{T} \cdot \underline{v} \in L^1(\Gamma_C)$  and the relation

$$\langle \underline{T}, \underline{v} \rangle_\Omega = \sum_k \langle \Theta_k \underline{T}, \underline{v} \rangle_\Omega, \quad (3.37)$$

obvious for  $\underline{v} \in (D(\bar{\Omega}))^N$ , remains valid for  $\underline{v} \in (H^1(\Omega))^N$  by denseness and continuity. The combination of (3.36) and (3.37) yields

$$\langle \underline{T}, \underline{v} \rangle_\Omega = \int_{\Gamma_C} \underline{T} \cdot \underline{v} \, ds,$$

for an arbitrary  $\underline{v} \in (H^1(\Omega))^N$  and the proof is complete.  $\square$

We are finally in position to prove

Lemma 3.6: Let  $T \geq 0$  be an element of  $L^1(\Gamma_C)$  and suppose that the mapping

$$\underline{v} \in (D(\bar{\Omega}))^N \rightarrow \int_{\Gamma_C} T v_n \, ds = \int_{\Gamma_C} T n \cdot \underline{v} \, ds$$

extends as a linear continuous form  $\langle T n, \underline{v} \rangle_\Omega$  over the space  $(H^1(\Omega))^N$ . Then, for every  $\underline{v} \in (H^1(\Omega))^N$ , one has  $T v_n \in L^1(\Gamma_C)$  and

$$\langle T n, \underline{v} \rangle_\Omega = \int_{\Gamma_C} T v_n \, ds.$$

Proof: The boundary  $\Gamma$  of  $\Omega$  being Lipschitz continuous, there is a covering  $(\Gamma_k)$  of  $\Gamma$  by open subsets such that  $\Gamma_k$  is the graph

of a Lipschitz-continuous function. This easily implies that there is  $\epsilon > 0$  such that the angle between two outer normal vectors  $\underline{n}(\underline{x})$  and  $\underline{n}(\underline{y})$ ,  $\underline{x}$  and  $\underline{y}$  in  $\Gamma_k$ , is less than or equal to  $180^\circ - \epsilon$ , or, equivalently, that all the vectors  $\underline{n}(\underline{x})$ ,  $\underline{x} \in \Gamma_k$ , are contained in a cone with angle less than  $180^\circ$ . Clearly, this leads to the conclusion that there is a system of coordinates in which  $n_i \geq 0$  on  $\Gamma_k$  (see Figure 3.1 below when  $N = 2$ : all the normal vectors have nonnegative components in the basis  $\gamma_1, \gamma_2$ )

As  $T \in L^1(\Gamma_C)$  one has  $T\underline{n} \in (L^1(\Gamma_C))^N$  and, in the appropriate system of coordinates exhibited above,  $Tn_i \geq 0$ ,  $1 \leq i \leq N$  on  $\Gamma_C \cap \Gamma_k$  since  $T \geq 0$ . Our assertion is then a simple application of Lemma 3.5 with  $\underline{T} = T\underline{n}$ .  $\square$

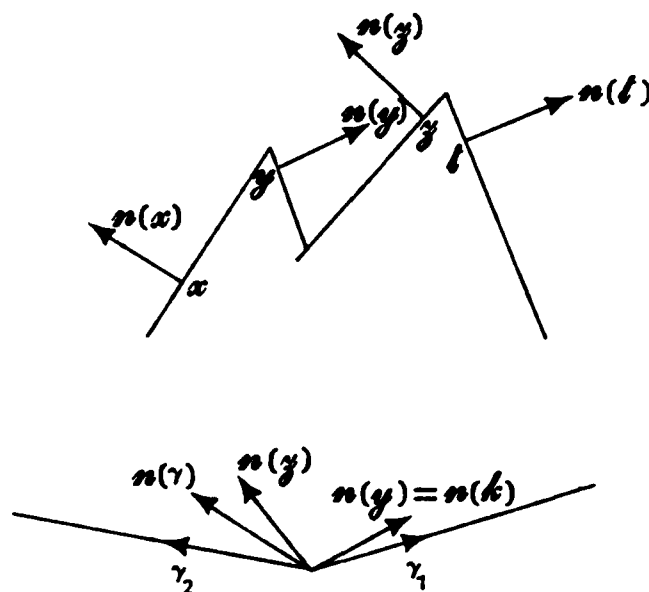


Fig. 3.1

Theorem 3.1: An element  $\underline{u} \in (H^1(\Omega))^N$  is a solution to (3.20)-(3.23) if and only if  $\phi(\underline{u}_n)\underline{v}_n \in L^1(\Gamma_C)$  for every  $\underline{v} \in (H^1(\Omega))^N$  and

$$a(\underline{u}, \underline{v}) + \int_{\Gamma_C} \tilde{\phi}(\underline{u}_n) v_n \, ds = \langle \underline{f}, \underline{v} \rangle_{\Omega} \quad \text{for every } \underline{v} \in (H^1(\Omega))^N. \quad (3.38)$$

Proof: Suppose that  $\tilde{\phi}(\underline{u}_n) v_n \in L^1(\Gamma_C)$  for every  $\underline{v} \in (H^1(\Omega))^N$ . Taking  $\underline{v}$  as the constant function equal to the  $i^{\text{th}}$  vector of the canonical basis of  $\mathbb{R}^N$ , we find

$$\tilde{\phi}(\underline{u}_n) n_i \in L^1(\Gamma_C), \quad 1 \leq i \leq N.$$

Thus,

$$\tilde{\phi}(\underline{u}_n) \sup_{1 \leq i \leq N} |n_i| \in L^1(\Gamma_C).$$

As  $\sup_{1 \leq i \leq N} |n_i(x)| \geq 1/\sqrt{N}$  for almost all  $x \in \Gamma_C$  (cf. (3.1)) we

deduce

$$0 \leq \tilde{\phi}(\underline{u}_n) \leq \sqrt{N} \tilde{\phi}(\underline{u}_n) \sup_{1 \leq i \leq N} |n_i|$$

and hence  $\tilde{\phi}(\underline{u}_n) \in L^1(\Gamma_C)$ . If, in addition, (3.38) holds, it is obvious from Lemma 3.2 that  $\underline{u}$  is a solution to problem (3.20)-(3.23).

Conversely, if  $\underline{u}$  is a solution to problem (3.20)-(3.23), Lemma 3.2 ensures that  $\tilde{\phi}(\underline{u}_n) \in L^1(\Gamma_C)$  and the mapping

$$\underline{v} \in (D(\bar{\Omega}))^N \rightarrow \int_{\Gamma_C} \tilde{\phi}(\underline{u}_n) v_n \, ds$$

extends as the linear continuous form over the space  $(H^1(\Omega))^N$

$$\underline{v} \in (H^1(\Omega))^N \rightarrow \langle \underline{f}, \underline{v} \rangle_{\Omega} - a(\underline{u}, \underline{v}).$$

The conclusion follows from Lemma 3.6 with  $T = \tilde{\phi}(\underline{u}_n)$ .  $\square$

With Theorem 3.1 as a starting point, we shall now be able to prove

Theorem 3.2: Let  $\underline{u} \in (H^1(\Omega))^N$  be a solution to problem (3.20)-(3.23). Then,  $\underline{u}$  is a minimizer of the functional

$$\underline{v} \in (H^1(\Omega))^N \rightarrow J(\underline{v}) = \frac{1}{2} a(\underline{v}, \underline{v}) + j(\underline{v}_n) - \langle \underline{f}, \underline{v} \rangle_{\Omega} \in \mathbb{R} \quad (3.39)$$

where  $j$  denotes the functional (3.16).

Proof: Let  $\underline{u} \in (H^1(\Omega))^N$  be a solution to problem (3.20)-(3.23). We first show that  $J(\underline{u}) < +\infty$ , or, equivalently, that  $j(\underline{u}_n) < +\infty$ . From (3.10), it follows that the mapping  $\phi(\underline{x}, t) = \int_0^t \phi(\underline{x}, \tau) d\tau$  verifies

$$0 \leq \phi(\underline{x}, t) \leq \frac{t}{2} \phi(\underline{x}, t)$$

for  $t > 0$  (a relation that was already used in the proof of Theorem 2.2). This inequality extends to  $t \in \mathbb{R}$  since  $\phi$  and  $\phi$  vanish for nonpositive values of  $t$ . In particular, taking  $t = u_n(\underline{x})$ , we get

$$0 \leq \tilde{\phi}(\underline{u}_n) \leq \frac{1}{2} \tilde{\phi}(\underline{u}_n) u_n. \quad (3.40)$$

As  $\tilde{\phi}(\underline{u}_n) u_n \in L^1(\Gamma_C)$  from Theorem 3.1, we find  $\tilde{\phi}(\underline{u}_n) \in L^1(\Gamma_C)$ , namely,  $j(\underline{u}_n) < +\infty$  (cf. (3.16)).

Now, let  $\underline{v} \in (H^1(\Omega))^N$  be given. We must prove that  $J(\underline{v}) \geq J(\underline{u})$ . Of course, this is satisfied if  $j(\underline{v}_n) = +\infty$ . Assume then  $j(\underline{v}_n) < +\infty$ , i.e.,  $\tilde{\phi}(\underline{v}_n) \in L^1(\Gamma_C)$ . One has

$$\begin{aligned} J(\underline{v}) - J(\underline{u}) &= \frac{1}{2} a(\underline{v} - \underline{u}, \underline{v} - \underline{u}) + a(\underline{u}, \underline{v} - \underline{u}) \\ &\quad + j(\underline{v}_n) - j(\underline{u}_n) - \langle \underline{f}, \underline{v} - \underline{u} \rangle_{\Omega}. \end{aligned} \quad (3.41)$$

From our assumptions, the mapping  $\phi(\underline{x}, \cdot)$  is convex for almost all  $\underline{x} \in \Gamma_C$  so that the inequality

$$\phi(\underline{x}, t) \geq \phi(\underline{x}, \tau) + \phi(\underline{x}, \tau)(t - \tau)$$

holds for every pair  $(t, \tau) \in \mathbb{R} \times \mathbb{R}$  and almost all  $\underline{x} \in \Gamma_C$ . Choosing  $t = v_n(\underline{x})$  and  $\tau = u_n(\underline{x})$  yields

$$\tilde{\phi}(v_n) \geq \tilde{\phi}(u_n) + \tilde{\phi}(u_n)(v_n - u_n) .$$

As the three terms  $\tilde{\phi}(v_n)$ ,  $\tilde{\phi}(u_n)$  and  $\tilde{\phi}(u_n)(v_n - u_n)$  are in  $L^1(\Gamma_C)$  (the latter from Theorem 3.1 with  $\underline{v} - \underline{u}$  replacing  $\underline{v}$ ), integrating both sides of the above inequality provides

$$j(v_n) \geq j(u_n) + \int_{\Gamma_C} \tilde{\phi}(u_n)(v_n - u_n) \, ds .$$

Applying (3.38) with  $\underline{v} - \underline{u}$  replacing  $\underline{v}$ , we obtain

$$j(v_n) \geq j(u_n) + \langle \underline{f}, \underline{v} - \underline{u} \rangle_{\Omega} - a(\underline{u}, \underline{v} - \underline{u}) .$$

Substituting into (3.41), we deduce

$$J(\underline{v}) - J(\underline{u}) \geq \frac{1}{2} a(\underline{v} - \underline{u}, \underline{v} - \underline{u}) \geq 0 ,$$

and the proof is complete.  $\square$

**Remark 3.1:** From the proof of Theorem 3.2, it also follows if  $\underline{u}$  and  $\underline{v}$  are two solutions of problem (3.20)-(3.23), and hence two minimizers of the functional (3.25), that  $a(\underline{v} - \underline{u}, \underline{v} - \underline{u}) = 0$ , which characterizes the difference  $\underline{v} - \underline{u}$  as an infinitesimal rigid motion (cf. §4).  $\square$

The converse of Theorem 3.2 is essentially based on the results of §2.

**Theorem 3.3:** Let  $\underline{u} \in (H^1(\Omega))^N$  be a minimizer of the functional  $J$  (3.39). Then,  $\underline{u}$  is a solution to problem (3.20)-(3.23).

**Proof:** Since the functional  $j$  (3.16) takes finite values for  $\xi = \underline{v}_n$  and  $\underline{v} \in (H^1(\Omega))^N$  (for instance, if  $\underline{v} \in (D(\bar{\Omega}))^N$ , because  $\underline{v}_n \in L^\infty(\Gamma_C)$  so that  $\tilde{\phi}(\underline{v}_n) \in L^1(\Gamma_C)$ , as it follows from Theorem 2.1 (ii) with  $\xi = 0$  and  $\eta = \underline{v}_n$ ) one has  $\tilde{\phi}(\underline{u}_n) \in L^1(\Gamma_C)$  when  $\underline{u}$  is a minimizer of the functional (3.39). From Theorem 2.1 (ii) in which  $\xi = \underline{u}_n$  and  $\eta = 0$ , we deduce that  $\tilde{\phi}(\underline{u}_n) \in L^1(\Gamma_C)$ . Next, for any given  $\underline{v} \in (D(\bar{\Omega}))^N$ , the normal component  $\underline{v}_n$  belongs to  $L^\infty(\Gamma_C)$ . Again, from Theorem 2.1 (ii) in which  $\xi = \underline{u}_n$  and  $\eta = t\underline{v}_n$ , the function

$$t \in \mathbb{R} \rightarrow j(\underline{u}_n + t\underline{v}_n)$$

is real-valued and differentiable at the origin with

$$\frac{d}{dt} j(\underline{u}_n + t\underline{v}_n) \Big|_{t=0} = \int_{\Gamma_C} \tilde{\phi}(\underline{u}_n) \underline{v}_n \, ds.$$

Hence, the function

$$t \in \mathbb{R} \rightarrow J(\underline{u} + t\underline{v}) \tag{3.42}$$

is real-valued and differentiable at the origin with

$$\frac{d}{dt} J(\underline{u} + t\underline{v}) \Big|_{t=0} = a(\underline{u}, \underline{v}) + \int_{\Gamma_C} \tilde{\phi}(\underline{u}_n) \underline{v}_n \, ds - \langle \underline{f}, \underline{v} \rangle.$$

Since  $t = 0$  is a minimum for the function (3.42), we obtain

$$a(\underline{u}, \underline{v}) + \int_{\Gamma_C} \tilde{\phi}(\underline{u}_n) \underline{v}_n \, ds - \langle \underline{f}, \underline{v} \rangle_\Omega = 0$$

for every  $\underline{v} \in (D(\bar{\Omega}))^N$  and the result follows from Lemma 3.2.  $\square$



The next section is devoted to proving the existence of minimizers of the functional (3.39) under suitable compatibility conditions between the applied forces and the geometry of  $\Gamma_C$  and to the study of uniqueness or non-uniqueness of solutions to problem (3.20)-(3.23).

#### 4. Existence and Uniqueness of Solutions to the Contact Problem.

On the basis of Theorems 3.1 and 3.2, existence of solutions to problem (3.20)-(3.23) is equivalent with existence of minimizers for the functional  $J$  (3.39). A classical approach consists in proving that the functional  $J$  is weakly sequentially lower semicontinuous and coercive over the space  $(H^1(\Omega))^N$ , both properties together providing existence of a minimizer for  $J$ . Convexity and continuity of the term

$$\underline{v} \in (H^1(\Omega))^N \rightarrow \frac{1}{2} a(\underline{v}, \underline{v}) - \langle \underline{f}, \underline{v} \rangle_{\Omega}$$

are sufficient to ensure its weak lower semicontinuity (see, e.g., [3]). By continuity of the trace:  $(H^1(\Omega))^N \rightarrow (H^{\frac{1}{2}}(\Omega))^N$  and the compactness of the embedding  $(H^{\frac{1}{2}}(\Omega))^N \rightarrow (L^1(\Gamma))^N$ , the mapping

$$\underline{v} \in (H^1(\Omega))^N \rightarrow v_n|_{\Gamma_C} \in L^1(\Gamma_C)$$

is weakly continuous. Together with Theorem 2.1(i), we then see that the functional

$$\underline{v} \in (H^1(\Omega))^N \rightarrow j(\underline{v}_n) = \int_{\Gamma_C} \tilde{\phi}(\underline{v}_n) ds \in \mathbb{R}$$

is weakly (sequentially) lower semicontinuous and so is then  $J$ . A result slightly more sophisticated than coerciveness of  $J$  over  $(H^1(\Omega))^N$  will be proved next under a condition expressing compatibility of the external forces with the geometry of  $\Gamma_C$ . From now on, we denote by  $R$  the  $N(N+1)/2$ -dimensional space of infinitesimal (or affine) rigid motions. We make the assumption

$$(C) \quad \begin{cases} \text{For every } \underline{R} \in R \text{ such that } R_n \leq 0 \text{ on } \Gamma_C \text{ and } \langle \underline{f}, \underline{R} \rangle_{\Omega} \geq 0, \\ \text{one has } R_n = 0 \text{ on } \Gamma_C \text{ and } \langle \underline{f}, \underline{R} \rangle_{\Omega} = 0. \end{cases}$$

In particular, condition (C) ("C" standing for "compatibility" or "coerciveness") requires the weaker assumption

$$(C') \quad \langle \underline{f}, \underline{R} \rangle_{\Omega} \leq 0 \quad \text{for every } \underline{R} \in R \text{ with } R_n \leq 0 \text{ on } \Gamma_C,$$

well known to play the role of compatibility condition in the Signorini's problem associated with the physical assumptions of this paper (see, e.g., [9]). A more complete relationship will be established in the next section. On the other hand, it is immediate from condition (C') that  $\langle \underline{f}, \underline{R} \rangle_{\Omega} = 0$  as soon as  $\underline{R} \in R$  and  $R_n = 0$  on  $\Gamma_C$ . For such an element  $\underline{R}$ , one then has  $J(\underline{v} + \underline{R}) = J(\underline{v})$  for

every  $\underline{y} \in (H^1(\Omega))^N$ . In other words, and with an obvious abuse of notation  $J(\underline{y}) = J(\dot{\underline{y}})$  where  $\dot{\underline{y}}$  denotes the equivalence class of  $\underline{y} \in (H^1(\Omega))^N$  in the space  $(H^1(\Omega))^N/N$  with

$$N = \{R \in R, R_n = 0 \text{ on } \Gamma_C\}. \quad (4.1)$$

The space  $(H^1(\Omega))^N/N$  identifies canonically with the space  $N^\perp$  (orthogonal in  $(H^1(\Omega))^N$ ) so that weak lower semicontinuity of  $J$  over  $(H^1(\Omega))^N$  implies weak lower semicontinuity of  $J$  over  $(H^1(\Omega))^N/N$ . Existence of a minimizer for  $J$  will then follow from the coerciveness of  $J$  over  $(H^1(\Omega))^N/N$ . This property, essentially based on condition (C), is proved in Theorem 4.1 below and closely follows [15, Theorem 1.1].

Theorem 4.1: Assume that condition (C) holds and that  $\phi(\underline{x}, t) > 0$  for every  $t > 0$  and almost all  $\underline{x} \in \Gamma_C$ . Then, the functional  $J$  is coercive over the space  $(H^1(\Omega))^N/N$ .

Proof: Applying Theorem 2.2, we see that the mapping

$$t \in (0, +\infty) \rightarrow \frac{1}{t^2} j(tv_n) \in \mathbb{R}^+ \quad (4.2)$$

is nondecreasing for every fixed  $y \in (H^1(\Omega))^N$  with

$$\omega_{\infty}(y) = 2 \lim_{t \rightarrow +\infty} \frac{1}{t^2} j(tv_n) = \int_{\Gamma_C} \ell(v_n)_+^2 ds, \quad (4.3)$$

where, for almost all  $x \in \Gamma_C$ , we have set

$$\ell(x) = \lim_{t \rightarrow +\infty} \frac{\phi(x, t)}{t} \geq 0. \quad (4.4)$$

Note from the hypothesis  $\phi(x, t) > 0$  and the monotonicity of  $\phi(x, t)/t$  that the stronger conclusion

$$\ell > 0 \quad \text{on } \Gamma_C \quad (4.5)$$

holds.

Assume by contradiction that the functional  $J$  is not coercive over the space  $(H^1(\Omega))^N$ , namely that there is a sequence  $(y^{(k)})$  of elements in  $N^\perp$  such that  $J(y^{(k)}) \leq M$  for some constant  $M$  and  $\lim \|y^{(k)}\|_{1, \Omega} = +\infty$ . Setting  $y^{(k)} = t_k e^{(k)}$ ,  $t_k = \|y^{(k)}\|_{1, \Omega}$ ,  $\|e^{(k)}\|_{1, \Omega} = 1$  and dividing by  $t_k^2$  we find

$$a(e^{(k)}, e^{(k)}) + \frac{1}{t_k^2} j(t_k e_n^{(k)}) - \frac{1}{t_k} \langle f, e^{(k)} \rangle_\Omega \leq \frac{M}{t_k^2}. \quad (4.6)$$

Let  $e \in N^\perp$  be a cluster point of the sequence  $(e^{(k)})$  in the weak topology of  $(H^1(\Omega))^N$ . After extracting a sub-sequence, we may assume  $e^{(k)} \rightharpoonup e$ . As  $j$  is non-negative, (4.6) yields

$$a(\underline{e}^{(k)}, \underline{e}^{(k)}) - \frac{1}{t_k} \langle f, \underline{e}^{(k)} \rangle_{\Omega} \leq \frac{M}{t_k^2}.$$

Since  $\lim t_k = +\infty$ , one then has

$$\lim a(\underline{e}^{(k)}, \underline{e}^{(k)}) = 0, \quad (4.7)$$

whereas  $a(\underline{e}, \underline{e}) \leq \lim a(\underline{e}^{(k)}, \underline{e}^{(k)})$ . Hence,  $a(\underline{e}, \underline{e}) = 0$ , namely,  $\underline{e}$  is an infinitesimal rigid motion. Further, due to the ellipticity of the bilinear form  $a(\cdot, \cdot)$  over the space  $(H^1(\Omega))^N/R$  (a consequence of Korn's inequality; see, e.g., [1]), (4.7) means that the sequence of orthogonal projections of  $\underline{e}^{(k)}$  onto  $R^\perp$  tends strongly to 0. Since  $R$  is finite dimensional, weak convergence of  $\underline{e}^{(k)}$  to  $\underline{e}$  implies strong convergence of the orthogonal projections of  $\underline{e}^{(k)}$  onto  $R$  (to  $\underline{e} \in R$ ). Hence, strong convergence of  $\underline{e}^{(k)}$  to  $\underline{e}$  in  $(H^1(\Omega))^N$  follows. In particular,  $\|\underline{e}\|_{1,\Omega} = 1$ .

Now, observe that (4.6) also yields

$$\frac{1}{t_k^2} j(t_k \underline{e}_n^{(k)}) - \frac{1}{t_k} \langle f, \underline{e}^{(k)} \rangle_{\Omega} \leq \frac{M}{t_k^2}.$$

As  $j$  is non-negative, we infer

$$\lim_{t_k} \frac{1}{t_k^2} j(t_k \underline{e}_n^{(k)}) = 0. \quad (4.8)$$

Let us then fix  $t > 0$ . As  $\underline{e}^{(k)}$  tends to  $\underline{e}$ ,  $t \underline{e}^{(k)}$  tends to  $t \underline{e}$  and from the (weak) lower semicontinuity of  $j$ , one has  $j(t \underline{e}) \leq \lim j(t \underline{e}^{(k)})$ . Multiplying by  $1/t^2$ , we get

$$\frac{1}{t^2} j(te_n) \leq \liminf_t \frac{1}{t^2} j(te_n^{(k)}) . \quad (4.9)$$

On the other hand,  $t_k \geq t$  for  $k$  large enough: From the monotonicity of the mapping (4.2) for fixed  $\underline{v}$  and taking  $\underline{v} = \underline{e}^{(k)}$  we deduce

$$\frac{1}{t^2} j(te_n^{(k)}) \leq \frac{1}{t_k^2} j(t_k e_n^{(k)}) .$$

Thus,

$$\liminf_t \frac{1}{t^2} j(te_n^{(k)}) \leq \liminf_{t_k} \frac{1}{t_k^2} j(t_k e_n^{(k)}) . \quad (4.10)$$

From (4.8)-(4.10) and since  $j$  is non-negative, we find

$$\frac{1}{t^2} j(te_n) = 0 \quad \text{for every } t > 0 .$$

Thus, in notation (4.3)

$$\omega_\infty(\underline{e}) = 2 \lim_{t \rightarrow +\infty} \frac{1}{t^2} j(te_n) = \int_{\Gamma_C} \ell(e_n)_+^2 ds = 0 .$$

Back to (4.5), this shows that  $(e_n)_+ = 0$ , i.e.,  $e_n \leq 0$ , on  $\Gamma_C$ .

Finally, note that  $\langle \underline{f}, \underline{e} \rangle_\Omega \geq 0$ . Indeed, if  $\langle \underline{f}, \underline{e} \rangle_\Omega < 0$ , one has  $\langle \underline{f}, \underline{e}^{(k)} \rangle_\Omega < 0$  for  $k$  large enough and (4.6) provides

$$0 \leq -\frac{1}{t_k} \langle \underline{f}, \underline{e}^{(k)} \rangle_\Omega \leq \frac{M}{t_k^2} .$$

Multiplying by  $t_k > 0$  and taking the limit, we obtain  $\langle \underline{f}, \underline{e} \rangle_\Omega = 0$ , a contradiction.

To sum up, the element  $\underline{e}$  has been shown to verify the conditions  $\underline{e} \in R$ ,  $\underline{e} \in N^{\perp 1}$ ,  $\|\underline{e}\|_{1,\Omega} = 1$ ,  $\underline{e}_n \leq 0$  on  $\Gamma_C$  and  $\langle \underline{f}, \underline{e} \rangle_{\Omega} \geq 0$ . Using condition (C), we must have  $\underline{e}_n = 0$ , namely,  $\underline{e} \in R$ . This obviously requires  $\underline{e} = 0$ , contradicting the fact that  $\|\underline{e}\|_{1,\Omega} = 1$ .  $\square$

Remark 4.1: The condition  $\phi(\underline{x}, t) > 0$  for every  $t > 0$  and almost all  $\underline{x} \in \Gamma_C$  is not merely physically acceptable, but it is the only physically acceptable assumption. Indeed, it takes into account the fact that at each point  $\underline{x} \in \Gamma_C$  such that  $\underline{n}(\underline{x})$  is defined, any positive normal displacement produces a positive normal response (see §1). Nevertheless, the proof of Theorem 4.1 relies on the weaker property  $\lambda > 0$  on  $\Gamma_C$ : Due to our assumptions on the growth of  $\phi(\underline{x}, t)/t$ , this is equivalent to assuming that  $\phi(\underline{x}, t) > 0$  for almost all  $\underline{x} \in \Gamma_C$  and  $t > 0$  large enough (possibly depending on  $\underline{x}$ ).  $\square$

Remark 4.2: An interesting particular case when condition (C) is fulfilled is when

$$(S) \left\{ \begin{array}{l} \text{For every } \underline{R} \in R - \{0\}, \text{ the set } \{\underline{x} \in \Gamma_C, R_n(\underline{x}) > 0\} \\ \text{has a positive measure.} \end{array} \right.$$

Indeed, if condition (S) is satisfied,  $\underline{R} = 0$  is the sole element of  $R$  such that  $R_n \leq 0$  on  $\Gamma_C$ . It follows that condition (C) is satisfied with any choice of external forces  $\underline{f}$ . Condition (S) has a very simple interpretation: As we shall see later on (cf. Corollary 4.1), it means that problem (3.20)-(3.23) with no external forces

(i.e.,  $\underline{f} = 0$ ) has no nonzero solution. Since solutions to this problem must be infinitesimal rigid motion, this strikingly relates to the intuitive idea that the body is stuck (whence "(S)" for the condition) because of its contact along  $\Gamma_C$ .  $\square$

As an immediate corollary to Theorem 4.1, we can state

Theorem 4.2: Assume that condition (C) holds and that  $\phi(\underline{x}, t) > 0$  for every  $t > 0$  and almost all  $\underline{x} \in \Gamma_C$ . Then, problem (3.20)-(3.23) has at least one solution.  $\square$

To complete this section, we shall now examine questions related to the uniqueness of the solution to problem (3.20)-(3.23). We begin with the essential

Lemma 4.1: Let  $\underline{u}$  and  $\hat{\underline{u}}$  be two solutions to problems (3.20)-(3.23). Then,  $\hat{\underline{u}} - \underline{u} = \underline{R} \in R$  and

$$\tilde{\phi}_t(\underline{u}_n + t\underline{R}_n)\underline{R}_n = 0 \quad \text{on } \Gamma_C, \quad 0 \leq t \leq 1. \quad (4.11)$$

Proof: Applying Theorem 3.1 with  $\underline{u}$  and  $\hat{\underline{u}}$  successively, we find for every  $\underline{v} \in (H^1(\Omega))^N$  that  $(\tilde{\phi}(\hat{\underline{u}}_n) - \tilde{\phi}(\underline{u}_n))\underline{v}_n$  belongs to  $L^1(\Gamma_C)$  with

$$a(\hat{\underline{u}} - \underline{u}, \underline{v}) + \int_{\Gamma_C} (\tilde{\phi}(\hat{\underline{u}}_n) - \tilde{\phi}(\underline{u}_n))\underline{v}_n \, ds = 0.$$

With the choice  $\underline{v} = \hat{\underline{u}} - \underline{u}$ , we get

$$a(\hat{\underline{u}} - \underline{u}, \hat{\underline{u}} - \underline{u}) + \int_{\Gamma_C} (\tilde{\phi}(\hat{\underline{u}}_n) - \tilde{\phi}(\underline{u}_n))(\hat{\underline{u}}_n - \underline{u}_n) \, ds = 0 \quad (4.12)$$



From the convexity of the function  $\phi(x, \cdot)$  for almost all  $x \in \Gamma_C$ , the inequality

$$(\phi(x, t) - \phi(x, \tau))(t - \tau) \geq 0,$$

holds for every pair  $(t, \tau) \in \mathbb{R} \times \mathbb{R}$ . Setting  $t = \hat{u}_n(x)$  and  $\tau = u_n(x)$ , it follows that

$$\int_{\Gamma_C} (\tilde{\phi}(\hat{u}_n) - \tilde{\phi}(u_n))(\hat{u}_n - u_n) ds \geq 0.$$

Since the bilinear form  $a(\cdot, \cdot)$  is positive semidefinite, this relation shows that (4.12) holds if and only if

$$a(\hat{u} - u, \hat{u} - u) = 0 \quad (4.13)$$

and

$$\int_{\Gamma_C} (\tilde{\phi}(\hat{u}_n) - \tilde{\phi}(u_n))(\hat{u}_n - u_n) ds = 0. \quad (4.14)$$

Relation (4.13) characterizes the difference  $\hat{u} - u$  as an element  $R \in R$  and relation (4.14) thus reads

$$\int_{\Gamma_C} (\tilde{\phi}(u_n + R_n) - \tilde{\phi}(u_n))R_n ds = 0. \quad (4.15)$$

Now, as Theorem 3.2 characterizes the solutions to problem (3.20)-(3.23) as minimizers of the convex functional (3.39), each element of the form  $u + t(\hat{u} - u)$ ,  $0 \leq t \leq 1$ , is a solution to problem (3.20)-(3.23) as well. Replacing then  $R_n$  by  $tR_n$  in (4.15), we obtain

$$\frac{1}{t} \int_{\Gamma_C} (\tilde{\phi}(u_n + tR_n) - \tilde{\phi}(u_n))R_n ds = 0, \quad 0 < t \leq 1. \quad (4.16)$$

As  $\tilde{\phi}(u_n) \in L^1(\Gamma_C)$  since  $u$  is a solution to problem (3.20)-(3.23) (see the proof of Theorem 3.3) and  $R_n \in L^\infty(\Gamma_C)$ , we can apply Theorem 2.1 (ii) with  $\xi = u_n$  and  $\eta = tR_n$ : On the one hand, we see that (4.16) coincides with the expression (cf. relation (2.39))

$$\frac{1}{t} (j'_{u_n}(tR_n) - j'_{u_n}(0)) \cdot R_n = 0, \quad 0 < t \leq 1,$$

and, in the limit as  $t$  tends to 0, we find on the other hand

$$0 = j''_{u_n}(0) \cdot (R_n)^2 = \int_{\Gamma_C} \tilde{\phi}_t(u_n) R_n^2 ds.$$

As  $\phi_t \geq 0$ , one has  $\tilde{\phi}_t(u_n) R_n^2 = 0$  on  $\Gamma_C$  and hence  $\tilde{\phi}_t(u_n) R_n = 0$  on  $\Gamma_C$ . Replacing  $u$  by  $u + tR$  and  $R$  by  $(1-t)R$  yields (4.11) for  $0 \leq t < 1$ . The result for  $t = 1$  follows by continuity of  $\phi_t(x, \cdot)$  for almost all  $x \in \Gamma_C$ .  $\square$

Theorem 4.3: Assume that  $\phi(x, t) > 0$  for almost all  $x \in \Gamma_C$  and every  $t > 0$  and that problem (3.20)-(3.23) has a solution  $u$ . Then, all the solutions to this problem are of the form  $u + R$  with  $R \in R$  such that  $u_n \leq -(R_n)_+ \leq 0$  on the set  $\{x \in \Gamma_C, R_n(x) \neq 0\}$  (a vacuous condition if and only if  $R \in N$ ).<sup>(6)</sup>

Proof: From Lemma 4.1, non-uniqueness of the solution  $u$  requires the existence of an element  $R \in R - \{0\}$  such that  $u + R$  is also a solution and  $\tilde{\phi}_t(u_n + R_n) R_n = 0$ ,  $0 \leq t \leq 1$ , on  $\Gamma_C$ . It is then clear that  $\tilde{\phi}_t(u_n + R_n) = 0$  when  $R_n \neq 0$ . From (3.10) and

<sup>(6)</sup> And such an element  $R$  verifies  $\langle f, R \rangle_\Omega = 0$ ; see the proof of Corollary 4.3.

the assumption  $\phi(\underline{x}, t) > 0$  for almost all  $\underline{x} \in \Gamma_C$  and every  $t > 0$ , one has  $\phi(\underline{x}, t) > 0$  for the same choices of  $\underline{x}$  and  $t$ . Hence, on  $\Gamma_C$ ,  $u_n + tR_n \leq 0$ ,  $0 \leq t \leq 1$ , whenever  $R_n \neq 0$ . But this is clearly equivalent to saying that  $u_n \leq \min(0, -R_n) = -(R_n)_+$  when  $R_n \neq 0$ .

Conversely, let  $\underline{R}$  be as in Theorem 4.3. Using the same equivalence as above, it is immediate that  $\tilde{\phi}_t(u_n + R_n) = \tilde{\phi}_t(u_n)$  so that  $\underline{u} + \underline{R}$  is a solution to problem (3.20)-(3.23) since  $g(\underline{u} + \underline{R}) = g(\underline{u})$  regardless of the element  $\underline{R} \in R$ .  $\square$

Corollary 4.1 (an equivalent form of condition (S)): Assume that  $\phi(\underline{x}, t) > 0$  for almost all  $\underline{x} \in \Gamma_C$  and every  $t > 0$ . Then, condition (S) is equivalent to the uniqueness of the solution  $\underline{u} = \underline{0}$  to problem (3.20)-(3.23) with no external forces (i.e.,  $\underline{f} = \underline{0}$ ).

Proof: From Theorem 4.3, uniqueness of the solution  $\underline{u} = \underline{0}$  means that  $N = \{0\}$  and for every  $\underline{R} \in R - \{0\}$  that  $0(=u_n) > -(R_n)_+$  on a subset of  $\Gamma_C$  with positive measure. Hence, the conclusion.  $\square$

A first uniqueness question worthy of examination is that of the area of contact and normal stress along  $\Gamma_C$ .

Corollary 4.2: Assume that  $\phi(\underline{x}, t) > 0$  for almost all  $\underline{x} \in \Gamma_C$  and every  $t > 0$  and that problem (3.20)-(3.23) has at least one solution. Then, the area of physical contact

$$A = A(\underline{u}) = \{\underline{x} \in \Gamma_C, u_n(\underline{x}) > 0\}$$

and the normal stress  $\tilde{\phi}(u_n)$  are independent of the solution  $\underline{u}$ .

Proof: This is an easy consequence from Theorem 4.3. Indeed, let  $\underline{u}$  and  $\underline{u} + \underline{R}$ ,  $\underline{R} \in R$ , be two solutions of problem (3.20)-(3.23) and let  $\underline{x} \in \Gamma_C$  be given. If  $R_n(\underline{x}) = 0$ , one has  $u_n(\underline{x}) = u_n(\underline{x}) + R_n(\underline{x})$ . If  $R_n(\underline{x}) \neq 0$ , the relation  $u_n(\underline{x}) \leq - (R_n)_+(\underline{x})$  yields  $u_n(\underline{x}) \leq 0$  and  $u_n(\underline{x}) + R_n(\underline{x}) \leq 0$ . Hence,  $u_n(\underline{x}) > 0$  if and only if  $u_n(\underline{x}) + R_n(\underline{x}) > 0$  (and, in this case,  $R_n(\underline{x}) = 0$ ) so that  $A(\underline{u}) = A(\underline{u} + \underline{R})$  and  $\tilde{\phi}(\underline{u}_n)(\underline{x}) = \tilde{\phi}(\underline{u}_n + \underline{R}_n)(\underline{x}) (= 0 \text{ if } R_n(\underline{x}) \neq 0)$ .  $\square$

Remark 4.3: We emphasize that the area of physical contact cannot be replaced by the area of geometrical contact:

$$\{\underline{x} \in \Gamma_C, u_n(\underline{x}) \geq 0\} \quad (4.18)$$

in Corollary 4.2. Indeed, the set (4.18) may greatly vary from one solution to another. This is easily seen by taking  $\underline{u}$  as a solution to the linear problem

$$\operatorname{div} \underline{\sigma}(\underline{u}) + \underline{b} = 0 \quad \text{in } \Omega,$$

$$\pi(\underline{u}) = \underline{t} \quad \text{on } \Gamma_F,$$

$$\pi(\underline{u}) = 0 \quad \text{on } \Gamma_C,$$

verifying  $u_n \leq -\epsilon < 0$  on  $\Gamma_C$ . Such a choice is obviously possible by taking  $\underline{b}$  and  $\underline{t}$  accordingly and  $\underline{u}$  is also a solution to problem (3.20)-(3.23). It suffices then to "move"  $\underline{u}$  through translations to observe modifications of the area of geometrical contact (cf. Figure 4.1).

Given a solution  $\underline{u}$  to problem (3.20)-(3.23), every element of the form  $\underline{u} + \underline{R}$ ,  $\underline{R} \in N$ , is a solution too. Thus, uniqueness of the

solution can be established to within elements of  $N$  only. With this restriction, it is easy to derive from Theorem 4.3 several uniqueness statements reducing to actual uniqueness when  $N = \{0\}$ . For instance, if  $\phi(\underline{x}, t) > 0$  for almost all  $\underline{x} \in \Gamma_C$  and every  $t > 0$ , condition (C) holds (so that existence is ensured by Theorem 4.2), and the solution  $\underline{u}$  is known to verify  $u_n > 0$  on  $\Gamma_C$  (i.e., the area of physical contact  $A$  verifies  $A = \Gamma_C$ ). Indeed, let  $\underline{R} \in R \setminus N$  be given. By definition of the space  $N$ , one has

$$\text{meas}(\{\underline{x} \in \Gamma_C, R_n(\underline{x}) \neq 0\}) > 0.$$

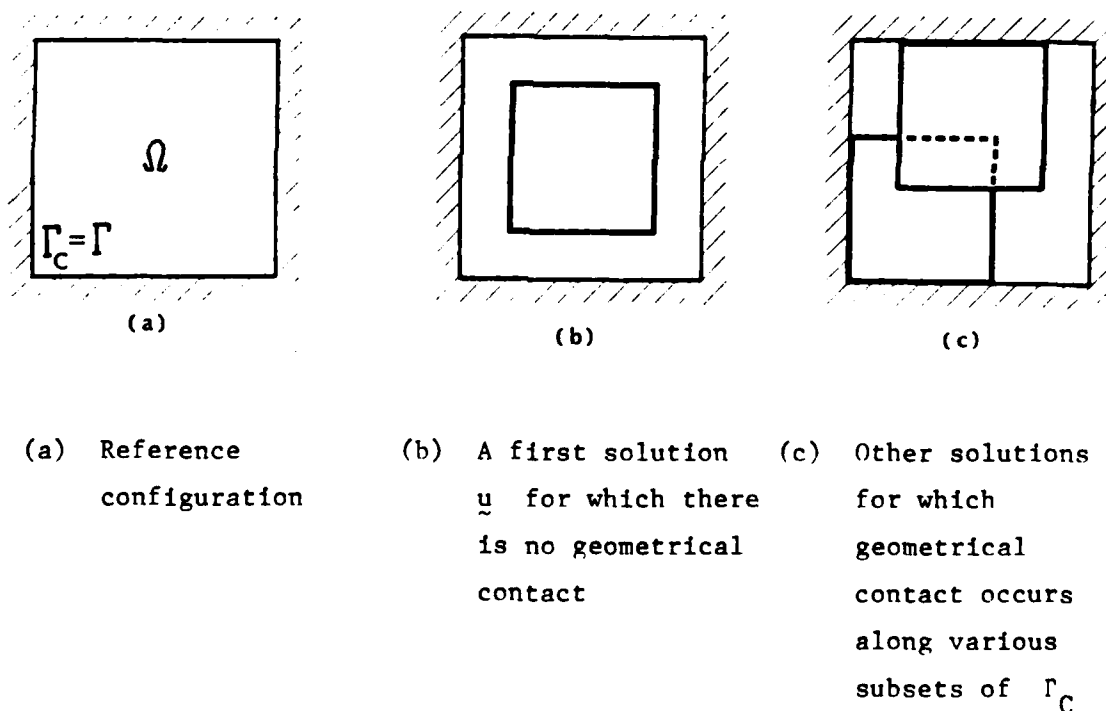


Figure 4.1

From Theorem 4.3, it follows that  $u_n \leq 0$  on a subset of  $\Gamma_C$  with positive measure, an obvious contradiction. This result suggests that uniqueness might be closely related to the fact that the area of physical contact (independent of the solution from Corollary 4.2) has a positive measure. Indeed, Corollaries 4.3 and 4.4 below do express this property under the following compatibility condition (U) (for "uniqueness") between the applied external forces and the geometry of  $\Gamma_C$ :

$$(U) \left\{ \begin{array}{l} \text{For every } \underline{R} \in R \text{ with } \langle \underline{f}, \underline{R} \rangle_{\Omega} = 0, \text{ one has either } \underline{R} \in N \\ \text{(i.e., } R_n = 0 \text{ on } \Gamma_C) \text{ or } R_n(x) \neq 0 \text{ for almost all } x \in \Gamma_C. \end{array} \right.$$

How general condition (U) is will be examined in §5 in the simple but significant case  $N = 2$ . To the best of our knowledge, it does not relate to any classical assumption in the associated Signorini's problem.

Corollary 4.3: Assume  $\phi(\underline{x}, t) > 0$  for almost all  $\underline{x} \in \Gamma_C$  and every  $t > 0$  and that conditions (C) and (U) hold. Then, problem (3.20)-(3.23) has a unique solution to within elements of the space  $N$  provided that the area of physical contact (independent of the solution from Corollary 4.2) has a positive measure.

Proof: Let  $u$  be a solution to problem (3.20)-(3.23), the existence of which is ensured by Theorem 4.2. By hypothesis

$$\text{meas}(\{\underline{x} \in \Gamma_C, u_n(\underline{x}) > 0\}) > 0. \quad (4.19)$$

We shall make repeated use of Theorem 4.3. First, let  $\underline{R} \in R$  be such that  $\underline{u} + \underline{R}$  is a solution too. Since  $u_n \leq 0$  on  $\Gamma_C$  whenever  $R_n \neq 0$ , one has  $\tilde{\phi}(u_n)R_n = 0$  on  $\Gamma_C$ . Theorem 3.1 with  $\underline{v} = \underline{R}$  then yields

$$\langle \underline{f}, \underline{R} \rangle_{\Omega} = a(\underline{u}, \underline{R}) + \int_{\Gamma_C} \tilde{\phi}(u_n) R_n \, ds = 0. \quad (4.20)$$

Assume that  $\underline{R} \notin N$ . Then, from condition (U), one has  $R_n(\underline{x}) \neq 0$  for almost all  $\underline{x} \in \Gamma_C$ . Theorem 4.3 then shows that  $u_n \leq 0$  a.e. on  $\Gamma_C$ , contradicting (4.19).  $\square$

Remark 4.4: All the assumptions of Corollary 4.3 can be checked without knowing any solution to problem (3.20)-(3.23). This is clear except for the condition  $\text{meas}(A) > 0$  ( $A$  = area of physical contact). However, an immediate verification shows that an equivalent formulation of the condition  $\text{meas}(A) > 0$  is that the linear problem

$$\text{div } \underline{\sigma}(\underline{v}) + \underline{b} = 0 \quad \text{in } \Omega, \quad (4.21)$$

$$\pi(\underline{v}) = \underline{t} \quad \text{on } \Gamma_F, \quad (4.22)$$

$$\pi(\underline{v}) = 0 \quad \text{on } \Gamma_C \quad (4.23)$$

has no solution  $\underline{v}$  with  $v_n \leq 0$  on  $\Gamma_C$  (such a solution would indeed be a solution to problem (3.20)-(3.23) with  $\text{meas}(A) = \text{meas}(A(\underline{v})) = 0$  and conversely).  $\square$

Closely related to Remark 4.4 is the following:

Corollary 4.4: Assume that  $\phi(\underline{x}, t) > 0$  for almost all  $\underline{x} \in \Gamma_C$  and every  $t > 0$  and that conditions (C) and (U) hold. Assume further that there is  $\underline{R} \in R$  such that

$$\langle \underline{f}, \underline{R} \rangle_{\Omega} \neq 0 . \quad (4.24)$$

Then, problem (3.20)-(3.23) has a unique solution to within elements of the space  $\mathcal{H}$  .

Proof: It suffices to apply Corollary 4.3 and Remark 4.4 since (4.24) means that the external forces do not verify the Fredholm alternative, and hence the linear problem (4.21)-(4.23) has no solution.  $\square$

## 5. Concluding Remarks

In this section, we examine the meaning of conditions (C), (S) and (U). For the sake of brevity, we limit ourselves to the simpler case when  $N = 2$  . We shall also make precise the relationship to Signorini's problem and discuss some generalizations and extensions of our results, notably to the contact problem with friction.

More on the Conditions (C), (S) and (U). Suppose  $N = 2$  and the boundary  $\Gamma$  is connected and piecewise  $C^1$  so that there is a counterclockwise parameterization  $\underline{x}(\lambda) = (x_1(\lambda), x_2(\lambda))$  of  $\Gamma$  which is continuously differentiable except at a finitely many points, with  $\|\underline{dx}/d\lambda\| = 1$  (euclidian norm). The outward normal vector  $\underline{n}(\underline{x})$  has then components

$$\begin{aligned} n_1(\underline{x}(\lambda)) &= (dx_2/d\lambda)(\lambda) , \\ n_2(\underline{x}(\lambda)) &= -(dx_1/d\lambda)(\lambda) . \end{aligned} \quad (5.1)$$

The three-dimensional space  $\mathcal{V}$  of infinitesimal rigid motions consists of mappings of the form



$$\underline{x} = (x_1, x_2) \in \mathbb{R}^2 \rightarrow R(\underline{x}) = (\gamma x_2 - \beta, -\gamma x_1 + \alpha) \in \mathbb{R}^2, \quad (5.2)$$

with  $(\alpha, \beta, \gamma) \in \mathbb{R}^3$ . From (5.1) and (5.2),

$$R_n(\underline{x}(\lambda)) = \frac{d}{d\lambda} \left[ \frac{\gamma}{2} (x_1^2(\lambda) + x_2^2(\lambda)) - \alpha x_1(\lambda) - \beta x_2(\lambda) \right].$$

More precisely, if  $\gamma = 0$  (so that  $R$  is a translation)

$$R_n(\underline{x}(\lambda)) = -\frac{d}{d\lambda} (\alpha x_1(\lambda) + \beta x_2(\lambda)) \quad (5.3)$$

and, if  $\gamma \neq 0$ ,

$$R_n(\underline{x}(\lambda)) = \frac{\gamma}{2} \frac{d}{d\lambda} \left[ \left( x_1(\lambda) - \frac{\alpha}{\gamma} \right)^2 + \left( x_2(\lambda) - \frac{\beta}{\gamma} \right)^2 \right] \quad (5.4)$$

Among conditions (C), (S) and (U), only (S) is purely geometrical, i.e., does not require any compatibility condition with the applied forces. In what follows, we make the physically realistic assumption  $\text{meas}(\Gamma_C \setminus \overset{\circ}{\Gamma}_C) = 0$ . From (5.3) and (5.4) and assuming that  $\underline{x}$  runs over  $\Gamma_C$  counterclockwise, it is easily seen that condition (S) is equivalent to saying that

(1) There is no nonzero vector  $\underline{e} \in \mathbb{R}^2$  such that the mapping

$$\underline{x} \in \overset{\circ}{\Gamma}_C \rightarrow \underline{x} \cdot \underline{e} \in \mathbb{R}, \quad (5.5)$$

is nonincreasing (resp. nondecreasing) on all the connected components of  $\overset{\circ}{\Gamma}_C$ .<sup>(7)</sup> This condition is conveniently viewed by saying that no component of  $\underline{x}$  along any line is nonincreasing (resp. nondecreasing) as  $\underline{x}$  runs over each connected component of  $\overset{\circ}{\Gamma}_C$  counterclockwise.

---

<sup>(7)</sup> Monotonicity makes sense since  $\Gamma_C$  is one-dimensional.

(ii) There is no point  $\underline{x}_0 \in \mathbb{R}^2$  such that the mapping

$$\underline{x} \in \overset{\circ}{\Gamma}_C \rightarrow \|\underline{x} - \underline{x}_0\| \in \mathbb{R} \text{ (euclidian norm)} \quad (5.6)$$

is nonincreasing (resp. nondecreasing) on each connected component of  $\overset{\circ}{\Gamma}_C$ .<sup>(8)</sup> On the basis of this characterization, it is easy to see that Figure 5.1 below exemplifies two cases when condition (S) holds

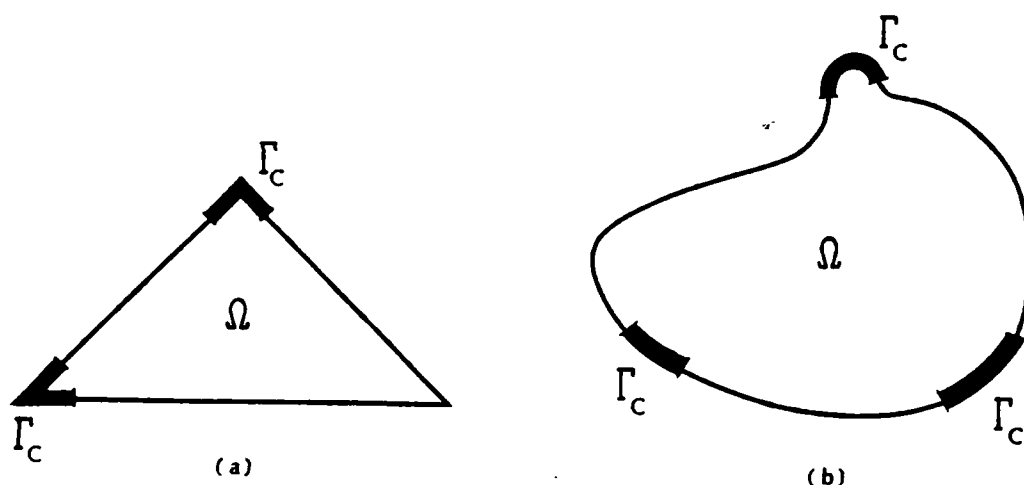


Figure 5.1

We shall now give an interpretation of condition (U) in the case  $N = \{0\}$  (observe in passing that condition (U) is never vacuous since  $N = \mathbb{R}$  is impossible). If so, condition (U) reads: For every  $R \in \mathbb{R} - \{0\}$  such that  $\langle \underline{f}, \underline{R} \rangle_{\Omega} = 0$ , one has  $R_n(\underline{x}) \neq 0$  almost everywhere on  $\Gamma_C$ . Owing to (5.3) and (5.4), condition (U) can be viewed by saying that  $\overset{\circ}{\Gamma}_C$  contains no interval and no arc of a circle of a special kind. More precisely, set

$$\underline{r}(\underline{f}) = \int_{\Omega} \underline{b} \, dx + \int_{\Gamma_F} \underline{t} \, ds \in \mathbb{R}^2$$

with components  $r_1(\underline{f})$  and  $r_2(\underline{f})$  and

$$m(\underline{f}) = \int_{\Omega} \det(\underline{b}(\underline{x}), \underline{x}) d\underline{x} + \int_{\Gamma_F} \det(\underline{s}(\underline{x}), \underline{x}) d\underline{s} \in \mathbb{R}.$$

Then,  $\overset{\circ}{\Gamma}_C$  should contain

- a) If  $\underline{r}(\underline{f}) \neq 0$ : no interval colinear with the line orthogonal with  $\underline{r}(\underline{f})$  and no arc of circle with centre on the line generated by  $\underline{r}(\underline{f})$ .
- b) If  $\underline{r}(\underline{f}) = 0$ : no interval if  $m(\underline{f}) \neq 0$  and no interval and no arc of circle if  $m(\underline{f}) = 0$ .

Conditions (a) and (b) above are easily seen to be necessary. Strictly speaking, they are not sufficient to ascertain that condition (U) holds (when  $N = \{0\}$ ) if  $\Gamma$  is only piecewise  $C^1$ . Nevertheless, they are sufficient if  $\overset{\circ}{\Gamma}_C$  is contained in a piecewise analytical submanifold of  $\Gamma$ . In this last assumption, the interpretation of condition (U) when  $N \neq \{0\}$  is trivial since it is always satisfied. Indeed, from (5.3) and (5.4) we infer that the condition  $N \neq \{0\}$  amounts to assuming that  $\overset{\circ}{\Gamma}_C$  is a union of intervals parallel to a given direction or a union of arcs of circles with the same center (in any case, the space  $N$  is one-dimensional). If, for a given  $\underline{R} \notin N$  the set  $\{\underline{x} \in \Gamma_C, R_n(\underline{x}) = 0\}$  did not have measure zero,  $\overset{\circ}{\Gamma}_C$  would contain an interval parallel to a different direction or an arc of a circle with a different center. All the possible combinations are contradictory so that  $R_n(\underline{x}) \neq 0$  for almost all  $\underline{x} \in \Gamma_C$  when  $\underline{R} \notin N$ . Condition (U) trivially follows. These considerations show that the two situations described on Figure 5.1 (a) and (b) correspond with the case  $N = \{0\}$  (note that  $N = \{0\}$  as soon as condition (S) holds) and condition (U) holds for "most" choices of  $\underline{f}$  on Figure 5.1(a) and for every choice

of  $\underline{f}$  on Figure 5.1(b). Figure 5.2 below represents situations in which

- $N = \{0\}$  and condition (U) holds provided  $r_1(\underline{f}) \neq 0$  and  $r_2(\underline{f}) \neq 0$  (on Fig. 5.2(a));
- $N \neq \{0\}$  so that condition (U) holds for every  $\underline{f}$  (on Fig. 5.2(b), (c) and (d)).

On the other hand, condition (S) is violated in each of the four cases of Figure 5.2, but condition (C) holds with a varying generality. More precisely, condition (C) holds if and only if

- $r_1(\underline{f}) < 0$  on Figure 5.2(a)
- $r_1(\underline{f}) = 0$  on Figure 5.2(b)
- $m(\underline{f}) = 0$  on Figure 5.2(c)
- $r_1(\underline{f}) = 0$  and  $0 < m(\underline{f}) < -r_2(\underline{f})$  on Figure 5.2(d).

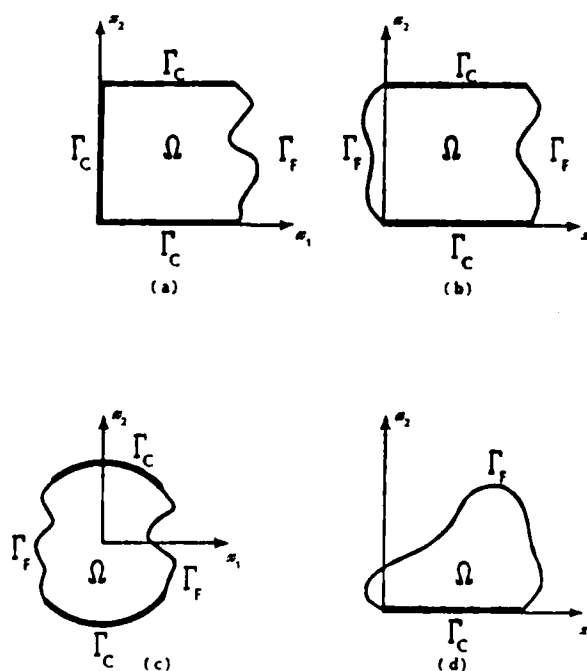


Figure 5.2

The above comments carry on to the case when  $\Gamma$  is not connected but  $\Gamma_C$  is contained in a connected component of  $\Gamma$ . In the general case, the only difference is that  $\eta$  must run clockwise (instead of counterclockwise) over the components of  $\Gamma$  not contained in the unbounded component of  $\mathbb{R}^2 \setminus \Omega$ .

Other Boundary Conditions. Boundary conditions of various other types can be considered instead of (3.2)-(3.22). For instance, the body occupying the domain  $\Omega$  may be clamped along a subset  $\Gamma_D$  of  $\Gamma$  with  $\text{meas}(\Gamma_D) > 0$  and/or action of linear springs on some subset  $\Gamma_E$  of  $\Gamma$  with  $\text{meas}(\Gamma_E) > 0$  can be taken into account. Such problems involve appropriate modifications of the technical results of §§2 and 3. In this case, coerciveness and uniqueness of a minimizer follow from the coerciveness of the quadratic part over the space of admissible displacements. These situations have already been considered in [10] with a simple choice of normal response  $\phi$  allowing the use of Sobolev's embedding theorems, thus avoiding the technicalities of §§2-4.

Relationship to Signorini's Problem. All the properties of the function  $\phi$  are obviously unchanged when  $\phi$  is replaced by  $\lambda\phi$ ,  $\lambda > 0$  a given real number. In this process, the function  $\phi$  is changed into  $\lambda\phi$ . Assuming  $\phi(\underline{x}, t) > 0$  for almost all  $\underline{x} \in \Gamma_C$  and every  $t > 0$  and that condition (C) holds, problem (3.20)-(3.23) with  $\lambda\phi$  replacing  $\phi$  has always a solution. Besides, from the proof of Theorems 4.1 and 4.2, it has always a solution (not necessarily unique) in the space  $N^\perp$ .

Theorem 5.1: Assume that  $\phi(\underline{x}, t) > 0$  for almost all  $\underline{x} \in \Gamma_C$  and every  $t > 0$  and that condition (C) holds. Then, for every  $\varepsilon > 0$ , there is  $\Lambda > 0$  such that for every  $\lambda \geq \Lambda$  and every solution  $\underline{u}(\lambda) \in N^\perp$  of problem (3.20)-(3.23) with  $\lambda\phi$  replacing  $\phi$ , there is  $\underline{u} \in N^\perp$  (possibly depending on  $\lambda$ ) solution to the Signorini's problem: Minimize

$$\frac{1}{2} a(\underline{v}, \underline{v}) - \langle \underline{f}, \underline{v} \rangle_\Omega, \quad (5.7)$$

over the closed convex subset of  $(H^1(\Omega))^N$

$$K = \{ \underline{v} \in (H^1(\Omega))^N, v_n \leq 0 \text{ on } \Gamma_C \}, \quad (5.8)$$

such that

$$\| \underline{u}(\lambda) - \underline{u} \|_{1, \Omega} \leq \varepsilon. \quad (5.9)$$

Proof: We argue by contradiction: If Theorem 5.1 is not true, there is  $\varepsilon > 0$  and a sequence  $(\lambda_k)$  tending to  $+\infty$  such that

$$\| \underline{u}(\lambda_k) - \underline{u} \|_{1, \Omega} > \varepsilon, \quad (5.10)$$

for every index  $k$  and every solution  $\underline{u}$  to the Signorini problem. Existence of at least one solution to it in  $(H^1(\Omega))^N$  is ensured by condition (C), a weaker form of which, already encountered, is

$$(C') \quad \langle \underline{f}, \underline{R} \rangle_\Omega \leq 0 \quad \text{for every } \underline{R} \in R \text{ with } R_n \leq 0$$

(see, e.g., [4,9]). Existence of a solution in  $N^\perp$  trivially follows (note that  $K + N = K$  and that (C') implies  $\langle \underline{f}, \underline{R} \rangle = 0$  for every  $\underline{R} \in N$ ). It is not restrictive to assume  $\lambda_k \geq 1$  for every index  $k$ ,

which will henceforth be done without further mention. Denote by  $J_\lambda$  the functional

$$\underline{v} \in (H^1(\Omega))^N \rightarrow J_\lambda(\underline{v}) = \frac{1}{2} a(\underline{v}, \underline{v}) + \lambda \int_{\Gamma_C} \tilde{\phi}(\underline{v}_n) ds - \langle \underline{f}, \underline{v} \rangle_\Omega \in \mathbb{R}. \quad (5.11)$$

Clearly,  $J_\lambda \geq J_1 = J$  for  $\lambda \geq 1$ . Hence,

$$J_{\lambda_k}(\underline{u}(\lambda_k)) \geq J(\underline{u}(\lambda_k)) \quad \text{for every index } k. \quad (5.12)$$

On the other hand, we know that  $\underline{u}(\lambda_k)$  is characterized by (cf. Theorem 3.1)

$$a(\underline{u}(\lambda_k), \underline{v}) + \lambda_k \int_{\Gamma_C} \tilde{\phi}(\underline{u}_n(\lambda_k)) \underline{v}_n ds = \langle \underline{f}, \underline{v} \rangle_\Omega$$

for every  $\underline{v} \in (H^1(\Omega))^N$ . (5.13)

Taking  $\underline{v} = \underline{u}(\lambda_k)$ , we get

$$a(\underline{u}(\lambda_k), \underline{u}(\lambda_k)) + \lambda_k \int_{\Gamma_C} \tilde{\phi}(\underline{u}_n(\lambda_k)) \underline{u}_n(\lambda_k) ds = \langle \underline{f}, \underline{u}(\lambda_k) \rangle_\Omega. \quad (5.14)$$

Now, recall (cf. (3.40) with  $\lambda_k \tilde{\phi}$  and  $\lambda_k \tilde{\phi}$  instead of  $\tilde{\phi}$  and  $\tilde{\phi}$ )

$$\lambda_k \tilde{\phi}(\underline{u}_n(\lambda_k)) \leq \frac{\lambda_k}{2} \tilde{\phi}(\underline{u}_n(\lambda_k)) \underline{u}_n(\lambda_k).$$

Together with (5.14) and the definition of the functional  $J_{\lambda_k}$ , this inequality yields

$$J_{\lambda_k}(\underline{u}(\lambda_k)) \leq -\frac{1}{2} \langle \underline{f}, \underline{u}(\lambda_k) \rangle_\Omega. \quad (5.15)$$

With (5.12), we obtain

$$J(\underline{u}(\lambda_k)) + \frac{1}{2} \langle \underline{f}, \underline{u}(\lambda_k) \rangle_{\Omega} = \frac{1}{2} a(\underline{u}(\lambda_k), \underline{u}(\lambda_k)) + \int_{\Gamma_C} \tilde{\phi}(\underline{u}_n(\lambda_k)) ds$$

$$- \frac{1}{2} \langle \underline{f}, \underline{u}(\lambda_k) \rangle_{\Omega} \leq 0. \quad (5.16)$$

But it is obvious that condition (C) holds with  $\underline{f}/2$  replacing  $\underline{f}$ . The coerciveness result proved in Theorem 4.1 shows that (5.16) requires the sequence  $(\underline{u}(\lambda_k))$  to be bounded in  $N^{\perp}$ . After extracting a sub-sequence, we may assume that there is  $\underline{u} \in N^{\perp}$  such that  $\underline{u}(\lambda_k) \rightharpoonup \underline{u}$ . Let then  $\underline{v} \in K$ . As  $\tilde{\phi}(\underline{u}_n(\lambda_k)) \geq 0$ , relation (5.13) shows that  $a(\underline{u}(\lambda_k), \underline{v}) \geq \langle \underline{f}, \underline{v} \rangle_{\Omega}$ . In the weak limit, we then find

$$a(\underline{u}, \underline{v}) \geq \langle \underline{f}, \underline{v} \rangle_{\Omega} \quad \text{for every } \underline{v} \in K. \quad (5.17)$$

Next, as  $\tilde{\phi}(\underline{u}_n(\lambda_k)) \underline{u}_n(\lambda_k) \geq 0$ , we infer from (5.14) that

$$a(\underline{u}(\lambda_k), \underline{u}(\lambda_k)) \leq \langle \underline{f}, \underline{u}(\lambda_k) \rangle_{\Omega}. \quad (5.18)$$

A classical argument of weak lower semicontinuity thus provides

$$a(\underline{u}, \underline{u}) \leq \langle \underline{f}, \underline{u} \rangle_{\Omega}. \quad (5.19)$$

From (5.15) and (5.11), the boundedness of the sequence  $(\underline{u}(\lambda_k))$  in  $N^{\perp}$  shows that the sequence  $\left\{ \lambda_k \int_{\Gamma_C} \tilde{\phi}(\underline{u}_n(\lambda_k)) ds \right\}$  is bounded. Therefore,

$$\lim \int_{\Gamma_C} \tilde{\phi}(\underline{u}_n(\lambda_k)) ds = 0. \quad (5.20)$$

With the Sobolev embedding theorem, we see that  $\underline{u}_n(\lambda_k)$  tends to  $\underline{u}_n$  in the strong topology of  $L^1(\Gamma_C)$ . Applying Theorem 2.1(1) and (5.20), we deduce that  $\phi(\underline{u}_n) \in L(\Gamma_C)$  with  $\int_{\Gamma_C} \phi(\underline{u}_n) ds = 0$ .



Hence,  $\tilde{\phi}(u_n) = 0$  on  $\Gamma_C$  since  $\phi$  is non-negative. The assumption  $\phi(x, t) > 0$  for almost all  $x \in \Gamma_C$  and every  $t > 0$  shows that  $\phi(x, t) > 0$  for the same choice of  $x$  and  $t$ . Thus,  $\tilde{\phi}(u_n) = 0$  on  $\Gamma_C$  if and only if  $u_n \leq 0$  on  $\Gamma_C$ , namely  $u \in K$ . From (5.19) and (5.17), with  $v = u$ , we arrive at

$$a(u, u) = \langle f, u \rangle_{\Omega} \quad (5.21)$$

Besides, with (5.21), (5.17) can be rewritten as

$$a(u, v - u) \geq \langle f, v - u \rangle_{\Omega} \quad \text{for every } v \in K.$$

It is well known that this relation characterizes  $u$  as a minimizer of the quadratic functional (5.7) over the set  $K$ , i.e.,  $u$  is a solution to Signorini's problem. To obtain the desired contradiction with (5.10), it remains to show that

$$\lim \|u(\lambda_k) - u\|_{1, \Omega} = 0 \quad (5.22)$$

Actually, the above relation reduces to showing that

$$\lim a(u(\lambda_k), u(\lambda_k)) = a(u, u) \quad (5.23)$$

Indeed, denoting by  $P$  the orthogonal projection from  $(H^1(\Omega))^N$  onto the space  $R$ , the mapping

$$v \in (H^1(\Omega))^N \rightarrow [a(v, v) + \|Pv\|_{1, \Omega}^2]^{\frac{1}{2}}, \quad (5.24)$$

is a norm equivalent to  $\|\cdot\|_{1, \Omega}$  (since the bilinear form  $a(\cdot, \cdot)$  induces a norm equivalent to the quotient norm over the space  $((H^1(\Omega))^N / R)$ . As  $u(\lambda_k)$  tends weakly to  $u$ , the sequence of

projections  $P_{\underline{u}}(\lambda_k)$  tends to  $P_{\underline{u}}$  in the strong topology of  $(H^1(\Omega))^N$  since the space  $R$  is finite dimensional. Hence, if (5.23) holds, the sequence  $(\underline{u}(\lambda_k))$  tends to  $\underline{u}$  in the weak topology of  $(H^1(\Omega))^N$  and the sequence of its norms (5.24) tends to the norm (5.24) of  $\underline{u}$ , proving (5.22) by a standard argument. To establish (5.23), recall that we already know that

$$a(\underline{u}, \underline{u}) \leq \liminf a(\underline{u}(\lambda_k), \underline{u}(\lambda_k)) . \quad (5.25)$$

on the other hand, due to (5.21), relation (5.18) also reads

$$a(\underline{u}(\lambda_k), \underline{u}(\lambda_k)) \leq a(\underline{u}, \underline{u}) + \langle \underline{f}, \underline{u}(\lambda_k) - \underline{u} \rangle_{\Omega} .$$

Thus,

$$\overline{\lim} a(\underline{u}(\lambda_k), \underline{u}(\lambda_k)) \leq a(\underline{u}, \underline{u}) . \quad (5.26)$$

Relation (5.23) is immediate from (5.25) and (5.26), which completes the proof.  $\square$

**Remark 5.1:** The result stated in Theorem 5.1 is rather strong since it means that provided  $\lambda$  is large enough, any solution  $\underline{u}(\lambda)$  to problem (3.20)-(3.23) with  $\lambda\phi$  replacing  $\phi$  is arbitrarily close to some solution to Signorini's problem in the space  $(H^1(\Omega))^N$ . Indeed, this result is exactly what Theorem 5.1 states if  $\underline{u}(\lambda)$  belongs to  $N^{\perp}$ . The general case is immediate since solutions are defined to within elements of  $N$  (recall that  $\langle \underline{f}, \underline{R} \rangle_{\Omega} = 0$  for  $\underline{R} \in N$ ). Note that the conclusion is independent of the normal response  $\phi$ . Its physical significance is clear: It means that the Signorini problem is the limiting case of an infinite normal response along  $\Gamma_C$ .  $\square$

Remark 5.2: Using the boundedness of the sequence  $\{\underline{u}(\lambda_k)\}$  and taking  $\underline{v}$  to be the  $i$ th vector of the canonical basis in (5.13), one sees that the sequence  $\left\{ \lambda_k \int \tilde{\phi}(\underline{u}_n(\lambda_k)) \underline{v}_n \right\}$  is bounded in  $L^1(\Gamma_C)$  by repeating arguments in Theorem 3.1. From relations (3.21) and (3.22) with  $\lambda_k \phi$  replacing  $\phi$ , it follows that the sequence  $\left\{ \pi(\underline{u}(\lambda_k)) \right\}$  is bounded in  $L^1(\Gamma)$ . With this observation, one infers when  $\underline{u} = \lim \underline{u}(\lambda_k)$ , and hence when  $\underline{u}$  is any solution to Signorini's problem, that  $\pi(\underline{u})$  is defined as a (vector-valued) Random measure on  $\Gamma$ . As  $\pi(\underline{u})$  represents a generalization of the surface traction  $\underline{\sigma}(\underline{u}) \cdot \underline{n}$ , the formal interpretation of  $\underline{u}$  as a solution to problem (1.3)-(1.7) ignores that this measure may have a singular part with respect to Lebesgue's measure. Assuming -- but there seems to be no mathematical justification of this assumption -- that the singular part does not exist, it is not difficult to deduce from Theorem 5.1 that conditions (1.3)-(1.7) are fulfilled by the solutions to Signorini's problem (upon replacing  $\underline{\sigma}(\underline{u}) \cdot \underline{n}$  by  $\pi(\underline{u})$ ) .  $\square$

Admissibility of an Initial Gap. Instead of assuming that geometrical contact occurs along  $\Gamma_C$  in the reference configuration (i.e., when no external forces are present), it is possible to allow some initial gap  $g$  between the candidate contact surface  $\Gamma_C$  and the body with which contact should occur. Such an initial gap can be taken into account through a function  $g \in L^\infty(\Gamma_C)$  verifying  $g \geq 0$  on  $\Gamma_C$  and the normal response can be modified by replacing  $\phi$  by

$$\phi_g(\underline{x}, t) = \phi(\underline{x}, t - g(\underline{x})) . \quad (5.27)$$

However, serious limitations to the use of this model are imposed by the physical requirement that the normal response be evaluated in the deformed configuration of  $\Gamma_C$ , thus modifying the direction of the normal vector  $\underline{n}$ . When  $g = 0$ , this is without importance since the normal response vanishes at those points at which physical contact does not occur and the actual displacement is very small at those points at which contact occurs (so that the modification of the normal is not significant). The problem is different when  $g \neq 0$  since points originally located at a nonzero distance may come in contact after a significant variation of the normal and at points unknown in advance. This closely relates to the question of actually measuring the initial gap  $g$ , which cannot be satisfactorily answered in a static framework. In other words,  $\phi_g(\underline{x}, u_n(\underline{x}))$  has in general nothing to do with the actual normal response due to contact at the points  $\underline{x} + u(\underline{x})$  for an arbitrary  $u$ . Such a relation as (5.27) should then not be used unless there is physical evidence that the actual displacement along  $\Gamma_C$  due to the action of the applied external forces occurs (nearly) in the direction normal to  $\Gamma_C$  (so that  $g(\underline{x})$  can be measured as the distance from  $\underline{x} \in \Gamma_C$  to the obstacle in the direction  $\underline{n}(\underline{x})$ ), at least at those points located at a nonzero distance from the obstacle. In practice, this requires  $g$  computed as above to be "small" while the body occupying the domain  $\Omega$  has a sufficiently rigid behavior under the action of the applied external forces.

From a mathematical standpoint, and with the assumptions  $g \in L^\infty(\Gamma_C)$ ,  $g \geq 0$ , it can be shown that all the properties stated with  $\phi$  are true with  $\phi_g$  given by (5.27) replacing  $\phi$  with the

only obvious exception that  $\phi_g(\underline{x}, t)$  is not positive for every positive  $t$  whenever  $\phi(\underline{x}, t)$  is. This, however, does not modify the existence result (Theorem 4.2) which actually relies on the fact that  $\phi(\underline{x}, t)$  be positive for  $t$  large enough (cf. Remark 4.1), unaffected by changing  $\phi$  into  $\phi_g$ . Differences merely take place in the uniqueness statements, with simple modifications: for instance, the area of physical contact must be defined by  $\{\underline{x} \in \Gamma_C, u_n(\underline{x}) > g(\underline{x})\}$  and Corollary 4.4 is unchanged.

The Contact Problem with Friction. In [10], we have considered a similar contact problem with friction, with boundary conditions involving a quadratic form coercive over the space of admissible displacements and a normal response of the form  $\phi(\underline{x}, t) = c_n(\underline{x})(t_+)^{m_n}$  where  $c_n \in L^\infty(\Gamma_C)$ ,  $c_n \geq 0$  and  $m_n > 1$  such that  $H^{\frac{1}{2}}(\Gamma) \hookrightarrow L^{m_n+1}(\Gamma)$ . The tangential friction force was supposed to be proportional to  $c_T(\underline{x})(t_+)^{m_T}$  with  $c_T \in L^\infty(\Gamma_C)$ ,  $c_T \geq 0$  and  $m_T > 1$  such that  $H^{\frac{1}{2}}(\Gamma) \hookrightarrow L^{m_T+1}(\Gamma)$ , and collinear with a vector field  $\underline{\tau}(\underline{x})$  of unitary vectors tangent to (part of)  $\Gamma_C$ . This model allows recovery of the usual Coulomb's law when  $m_n = m_T$  and  $c_T = \mu c_n$  where  $\mu$  is the coefficient of friction. As a physical example of this situation, consider a belt rubbing along (part of)  $\Gamma_C$  with velocity proportional to  $\underline{\tau}$ . Existence and local uniqueness was established either for sufficiently small external forces or for sufficiently small coefficient  $c_T$  (i.e., sufficiently small coefficient of friction if  $m_n = m_T$  and  $c_T = \mu c_n$ ). These results rely on the inverse mapping theorem and, in the latter case, all amounts to proving that

the quadratic form associated with the second derivative of the energy<sup>(8)</sup> at the solution of the problem with no friction (i.e.,  $c_T = 0$ ) is elliptic over the space of admissible displacements.

With the boundary conditions of this paper and with the normal response and tangential friction force described above, the same method is available: Denoting by  $\underline{u}$  a solution (supposed to exist) of the problem with no friction and applied external forces  $\underline{f}$ , the quadratic form associated with the second derivative at  $\underline{u}$  of the energy functional  $J$  (3.39) is

$$\underline{v} \in (H^1(\Omega))^N \rightarrow a(\underline{v}, \underline{v}) + m_n \int_{\Gamma_C} c_n(u_n)_+^{m_n-1} v_n^2 ds. \quad (5.28)$$

This quadratic form is not coercive if and only if there is a sequence  $(v^{(k)}) \in (H^1(\Omega))^N$  such that  $\|v^{(k)}\|_{1,\Omega} = 1$  and

$$\lim \left| a(v^{(k)}, v^{(k)}) + m_n \int_{\Gamma_C} c_n(u_n)_+^{m_n-1} (v_n^{(k)})^2 ds \right| = 0.$$

Hence,  $\lim a(v^{(k)}, v^{(k)}) = 0$  and  $\lim \int_{\Gamma_C} c_n(u_n)_+^{m_n-1} (v_n^{(k)})^2 ds = 0$ .

Considering a sub-sequence, we may assume that  $(v^{(k)})$  tends weakly to  $\underline{v}$  in  $(H^1(\Omega))^N$ . From the weak lower semicontinuity of  $a(\cdot, \cdot)$ , we find  $a(\underline{v}, \underline{v}) = 0$ , so that  $\underline{v}$  is an infinitesimal rigid motion  $\underline{R}$ . As the space  $R$  is finite dimensional, the sequence of orthogonal projections of  $v^{(k)}$  onto  $R$  tends strongly to  $\underline{R}$  while, due to the

---

(8) But the problem with friction does not reduce to finding the critical points of some energy functional, i.e., the problem is no longer variational.

ellipticity of  $a(\cdot, \cdot)$  over the quotient space  $(H^1(\Omega))^N / R$ , the sequence of orthogonal projections of  $\underline{v}^{(k)}$  onto  $R^\perp$  tends strongly to zero. As a result,  $(\underline{v}^{(k)})$  tends strongly to  $\underline{R}$  in the space  $(H^1(\Omega))^N$  and  $\underline{R} \neq 0$  since  $\|\underline{v}^{(k)}\|_{1,\Omega} = 1$ . From the continuity of the embedding  $H^{\frac{1}{2}}(\Gamma) \hookrightarrow L^{\frac{m_n+1}{m_n}}(\Gamma)$ , this yields

$$\int_{\Gamma_C} c_n(u_n)_+^{m_n-1} R_n^2 ds = \lim \int_{\Gamma_C} c_n(u_n)_+^{m_n-1} (v_n^{(k)})^2 ds = 0.$$

Provided that  $c_n > 0$  on  $\Gamma_C$ , this clearly requires  $u_n(x) \leq 0$  for almost all  $x \in \Gamma_C$  such that  $R_n(x) \neq 0$ . In particular,

$$c_n(u_n)_+ R_n = 0 \quad \text{on } \Gamma_C. \quad (5.29)$$

As  $\underline{u}$  is a solution to the problem with no friction, one has

$$a(\underline{u}, \underline{v}) + \int_{\Gamma_C} c_n(u_n)_+^{m_n} v_n ds = \langle \underline{f}, \underline{v} \rangle_\Omega \quad \text{for every } \underline{v} \in (H^1(\Omega))^N. \quad (5.30)$$

Setting  $\underline{v} = \underline{R}$  in (5.30) and using (5.29), we find

$$\langle \underline{f}, \underline{R} \rangle_\Omega = 0.$$

The above relation shows that a contradiction with  $\underline{R} \neq 0$  is reached if, for instance,  $N = \{0\}$ ,  $u_n$  is known to verify  $u_n > 0$  on  $\Gamma_C$  and condition (C) holds (which also ensures the existence of  $\underline{u} : \phi(x, t) = c_n(x)(t_+)^{m_n}$  with  $c_n > 0$  on  $\Gamma_C$  and  $m_n > 1$  fulfills all the assumptions necessary in this paper). Another case is when

$N = \{0\}$ , physical contact occurs (i.e.,  $\text{meas}(\{x \in \Gamma_C, u_n(x) > 0\}) > 0$ ) and condition (U) holds. If we drop the condition  $N = \{0\}$ , ellipticity of the quadratic form (5.38) over the space  $(H^1(\Omega))^N$  is obviously impossible but ellipticity is recovered over the space  $(H^1(\Omega))^N / N$ . This weaker result is nevertheless sufficient to prove existence and local uniqueness to within elements of the space  $N$  of the problem with friction when  $c_T$  is small enough (in  $L^\infty(\Gamma_C)$ ).

Remark 5.3: Roughly speaking, the above considerations can be summarized as follows: Existence and local uniqueness to within elements of the space  $N$  of the problem with friction is ensured as soon as  $c_T$  is small enough and physical contact does occur in the problem with no friction (for instance, if the external forces do not verify the Fredholm alternative; see Remark 4.4). If physical contact does not occur, the problems with or without friction have trivial solutions, namely, those of the linear problem (4.21)–(4.23).  $\square$

#### REFERENCES FOR THIS APPENDIX

1. Deimling, K., Nonlinear Functional Analysis. Berlin: Springer-Verlag (1985).
2. Duvaut, G. and Lions, J. L., Inequalities in Mechanics and Physics. New York: Springer-Verlag, (1976).
3. Ekeland, I. and Temam R., Analyse Convexe et Problèmes Variationnels. Paris: Dunod, Gauthiers-Villars, (1974).
4. Fichera, G., "Problemi elastostatici con vincoli unilaterali: il problema di Signorini con condizioni ambigue al contorno," Atti Accad. Naz. Lincei, 8, pp. 91-140 (1963-64).
5. Jarusek, J., "Contact Problems with Bounded Friction, Coercive Case," Czechoslovak Math J., 33 (108), pp. 337-361 (1983).



6. Kikuchi, N. and Oden, J. T., Contact Problems in Elasticity, SIAM, Philadelphia (1985).
7. Kinderlehrer, D., "A Note on the Variational Method in Contact Problems," in Free Boundary Problems: Theory and Applications, A. Fasano and M. Primicerio (Eds.), Res. Notes in Math., 79. London: Pitman, pp. 539-548, (1983).
8. Krasnoselskii, M. A., Topological Methods in the Theory of Nonlinear Integral Equations. New York: Pergamon Press, (1964).
9. Lions, J. L. and Stampacchia, G., "Variational Inequalities," Comm. Pure Appl. Math., 20, pp. 493-519 (1967).
10. Martins, J. A. C., Oden, J. T., Rabier, P. and Campos, L., "Existence and Local Uniqueness of Solutions to Contact Problems in Elasticity with Nonlinear Friction Laws," Int'l. J. of Eng. Sc. (to appear).
11. Necas, J., Les Méthodes Directes en Théorie des Equations Elliptiques. Paris: Masson, (1967).
12. Necas, J., Jarusek, J. and Haslinger, J., "On the Solution of the Variational Inequality to the Signorini Problem with Small Friction," Bolletino UMI, 5, 17-13, pp. 796-811 (1980).
13. Oden, J. T. and Martins, J. A. C., "Models and Computational Methods for Dynamic Friction Phenomena," Comp. Methods in Appl. Mech. and Eng., 52, pp. 527-634 (1985).
14. Oden, J. T., Qualitative Methods in Nonlinear Mechanics. Englewood Cliffs: Prentice Hall (1986).
15. Rabier, P., "A Necessary and Sufficient Condition for the Coerciveness of Certain Functionals," SIAM J. Math. Anal., 15, No. 2, pp. 367-388 (1984).
16. Rabier, P., "Definition and Properties of a Particular Notion of Convexity," J. Num. Funct. Anal. Opt., 7(4), pp. 279-302 (1984-85).
17. Sanchez-Palencia, E. and Suquet, P., "Friction and Homogenization of a Boundary," in Free Boundary Problems: Theory and Applications, A. Fasano and M. Primicerio (Eds.), Res. Notes in Meth., 79, pp. 561-571. London: Pitman, (1983).
18. Stampacchia, G., "Formes bilinéaires coercitives sur les ensembles convexes," CRAS, Paris, Serie A, 258, pp. 4413-4416 (1964).
19. Whitehouse, D. J. and Archard, J. F., "The Properties of Random Surfaces of Significance in their Contact," Proc. Roy. Soc. Lond., A316, pp. 97-121 (1970).

END

12-86

DTIC